

Characterization of B cell and antibody responses
induced by vaccination against the human coronaviruses
MERS-CoV and SARS-CoV-2

Cumulative Dissertation

to obtain the doctoral degree of the natural sciences

Dr. rer. nat.

University of Hamburg
Faculty of Mathematics, Informatics and Natural Sciences
Department of Biology

submitted by

Leonie Marie Weskamm

Hamburg 2023

This work was performed between February 2020 and January 2023 at the University Medical Center Hamburg-Eppendorf (UKE, Hamburg, Germany) at the Institute for Infection Research and Vaccine Development (IIRVD, former working group *Emerging Infections*), associated with the Department of Clinical immunology of Infectious Diseases at the Bernhard Nocht Institute for Tropical Medicine (BNITM, Hamburg, Germany).

Date of the disputation:

07.07.2023

Evaluators of the dissertation:

Prof. Dr. med. Marylyn M. Addo

Prof. Dr. Thomas Dobner

Persistent Identifier:

urn:nbn:de:gbv:18-ediss-110424

Declaration on oath

I hereby declare, on oath, that I have written the present dissertation on my own and have not used further resources and aids than those stated in the dissertation.

Eidesstattliche Erklärung

Hiermit erkläre ich an Eides statt, dass ich die vorliegende Dissertationsschrift selbst verfasst und keine anderen als die angegebenen Quellen und Hilfsmittel benutzt habe.

Hamburg, 17.01.2023



Leonie Marie Weskamm

Abstract

Over the past decades, numerous viruses of zoonotic origin have newly emerged in the human population, including three coronaviruses (CoV) causing respiratory diseases in the human host: The severe acute respiratory syndrome (SARS)-CoV, the Middle East respiratory syndrome (MERS)-CoV, and most recently SARS-CoV-2 which caused a worldwide pandemic. Vaccines are one of the most important countermeasures in the fight against viral spread and the related disease, and vaccine platforms such as mRNA and viral vectors have the potential to accelerate vaccine development in response to newly emerging pathogens. One promising viral vector is the recombinant Modified Vaccinia virus Ankara (rMVA), which has been shown to be safe and immunogenic in multiple studies. Binding and neutralizing antibody titers are considered correlates of protection against many pathogens, but additional immune parameters may show statistical association with protection from infection and/or disease and may be useful to predict vaccine efficacy.

The aim of this thesis was a comprehensive analysis of antibodies and B cells induced by vaccination against MERS and COVID-19, the respiratory diseases caused by MERS-CoV and SARS-CoV-2. The major focus was the characterization of the immune responses elicited by the rMVA-based vaccine candidates tested in phase 1 clinical trials at the University Medical Center Hamburg-Eppendorf, including the MERS vaccine MVA-MERS-S and the two COVID-19 vaccines MVA-SARS-2-S and MVA-SARS-2-ST. For this purpose, a repertoire of techniques was developed, allowing for an antigen-specific analysis of antibody isotypes, subclasses and non-neutralizing functionality, as well as frequency and phenotype of memory B cells. Additionally, the immunogenicity of the rMVA-based COVID-19 vaccine candidates was compared to control cohorts of healthy individuals and immunocompromised patients vaccinated with licensed COVID-19 vaccines based on mRNA and ChAd vaccine platforms.

MVA-MERS-S, based on the full-length native MERS-CoV spike protein, had been shown to be safe and immunogenic in a previous study. As part of this thesis, the impact of a late booster vaccination was investigated and revealed substantial increases in the frequency of spike-specific B cells and titers of IgG antibodies. Additionally, antibody persistence as well as neutralizing and non-neutralizing antibody functionality were strongly enhanced following the booster vaccination. MVA-SARS-2-ST, encoding for a pre-fusion stabilized version of the SARS-CoV-2 spike protein with an inactivated S1/2 cleavage site, elicited enhanced immunogenicity compared to MVA-SARS-2-S, a vaccine based on the native spike protein. A late booster vaccination with MVA-SARS-2-ST elicited stronger immune responses in individuals with lower baseline immunity. In direct comparison to licensed COVID-19 vaccines, both rMVA-based candidates induced lower antibody levels. Notably, all three rMVA-based vaccines induced the pro-inflammatory and highly functional IgG1 and IgG3 subclasses, whereas an atypical induction of the IgG2 and IgG4 subclasses was observed after repeated mRNA vaccination.

Overall, these findings underline the complexity and provide important insights into the factors influencing vaccine-induced immune responses. The immune signatures identified for the specific vaccines indicate that the quality of immune responses may be dependent on the vaccine platform and antigen, as well as the antigen-specific immunity prior to vaccination. Additionally, the obtained findings highlight the potential of late booster vaccinations to induce recall responses that may result in enhanced persistence and functionality of antibodies. The here developed techniques provide a tool to comprehensively analyze magnitude and phenotype of antigen-specific antibody and memory B cell responses, which may contribute to a better understanding of vaccine-induced immune mechanisms and specific immune markers that correlate with protection.

Zusammenfassung

In den letzten Jahrzehnten traten in der menschlichen Bevölkerung vermehrt zoonotische Viren auf, darunter drei Coronaviren (CoV), die im Menschen zu schweren Atemwegserkrankungen führen können: Das *Severe acute respiratory syndrome* (SARS)-CoV, das *Middle East respiratory syndrome* (MERS)-CoV, und zuletzt SARS-CoV-2, das eine weltweite Pandemie verursachte. Impfstoffe sind eine der wichtigsten Maßnahmen gegen die Ausbreitung von Viren und die damit assoziierten Erkrankungen. Insbesondere Impfstoff-Plattformen wie mRNA und virale Vektoren haben das Potential, die Impfstoffentwicklung gegen neuauftretende Pathogene zu beschleunigen. Ein vielversprechender viraler Vektor ist das rekombinante *Modified Vaccinia virus Ankara* (rMVA), welches sich in verschiedenen Studien als sicher und immunogen erwiesen hat. Bindende und neutralisierende Antikörpertiter gelten als Korrelat für den Schutz vor vielen Pathogenen, aber auch andere Immunparameter können wichtig für die Protektion vor Infektion und/oder Erkrankung sein.

Das Ziel dieser Arbeit war eine umfassende Analyse der durch Impfung gegen MERS und COVID-19 induzierten Antikörper und B-Zellen. Der Fokus lag dabei auf der Charakterisierung der Immunantworten nach Impfung mit rMVA-basierten Impfstoffkandidaten, die in Phase 1 klinischen Studien am Universitätsklinikum Hamburg-Eppendorf getestet wurden: der MERS-Impfstoff MVA-MERS-S und die zwei COVID-19-Impfstoffe MVA-SARS-2-S und MVA-SARS-2-ST. Zu diesem Zweck wurde eine Reihe von Methoden etabliert, die die Antigen-spezifische Analyse von Antikörper-Isotypen, -Subklassen und nicht-neutralisierender Funktionalität, sowie der Frequenz und dem Phänotyp von B-Gedächtniszellen ermöglichen. Zusätzlich wurde die Immunogenität der rMVA-basierten COVID-19 Impfstoffe zu Kontrollkohorten gesunder Proband:innen und immungeschwächter Patient:innen verglichen, die mit zugelassenen mRNA- und ChAd-basierten COVID-19 Impfstoffen geimpft wurden.

MVA-MERS-S, basierend auf dem nativen MERS-CoV Spike-Protein, hatte sich bereits in einer früheren Studie als sicher und immunogen erwiesen. Als Teil dieser Doktorarbeit wurde der Einfluss einer späten Auffrischungsimpfung untersucht, welche einen beträchtlichen Anstieg der Spike-spezifischen B-Zellen und IgG-Antikörpertiter hervorrief. Zusätzlich zeigten die Antikörper eine erhöhte Persistenz, sowie neutralisierende und nicht-neutralisierende Funktionalität. Der Impfstoff MVA-SARS-2-ST, der für ein stabilisiertes SARS-CoV-2 Spike-Protein mit inaktivierter S1/2-Spaltungsstelle kodiert, zeigte eine verstärkte Immunogenität im Vergleich zu MVA-SARS-2-S, der auf dem nativen Spike-Protein basiert. Eine späte Auffrischungsimpfung mit MVA-SARS-2-ST löste in Individuen mit geringerer vorheriger Immunität eine stärkere Immunantwort aus. Im Vergleich zu zugelassenen COVID-19-Impfstoffen induzierten beide rMVA-basierten Kandidaten geringere Antikörpertiter. Alle drei rMVA-Impfstoffe induzierten die pro-inflammatorischen und funktionellen Antikörpersubklassen IgG1 und IgG3, während nach wiederholter mRNA-Impfung eine atypische Induktion von IgG2 und IgG4 auftrat.

Insgesamt liefern diese Ergebnisse wichtige Einblicke in die Faktoren, die die impfinduzierte Immunantwort beeinflussen und heben deren Komplexität hervor. Die identifizierten Immunsignaturen weisen auf eine Abhängigkeit der Immunantwort von Impfstoff-Plattform und -Antigen hin sowie von der vor einer Impfung vorhandenen Immunität. Zusätzlich unterstreichen die hier gewonnenen Erkenntnisse das Potential später Auffrischungsimpfungen zur Reaktivierung von B-Gedächtniszellen, die in der Produktion von Antikörpern mit erhöhter Persistenz und Funktionalität resultieren kann. Die hier entwickelten Methoden bieten ein Hilfsmittel zur umfassenden Analyse der Stärke und Funktionalität von Antikörper- und B-Gedächtniszell-Antworten, die zu einem besseren Verständnis impfinduzierter Immunmechanismen und spezifischer Immunkorrelate beitragen können.

Table of Contents

| | |
|--|------------|
| Declaration on oath | II |
| Abstract | III |
| Zusammenfassung | IV |
| Table of Contents | V |
| 1 Introduction | 1 |
| 1.1 Emerging infectious diseases | 1 |
| 1.1.1 Human coronaviruses (HCoV) | 1 |
| 1.2 Vaccine development against emerging viruses | 4 |
| 1.2.1 Platform approaches for vaccine development | 5 |
| 1.2.2 Innate and adaptive immune responses to infection and vaccination | 7 |
| 1.2.3 Correlates of vaccine-induced protection | 8 |
| 1.3 B cell immune responses..... | 10 |
| 1.3.1 B cell development and maturation..... | 11 |
| 1.3.2 Primary B cell activation by protein antigens..... | 11 |
| 1.3.3 The germinal center reaction | 12 |
| 1.3.4 B cell memory and recall responses..... | 13 |
| 1.4 Antibodies – structure and functionality..... | 13 |
| 1.4.1 Antibody isotypes and subclasses | 14 |
| 1.4.2 Non-neutralizing antibody functions against viruses | 16 |
| 1.5 Aim of the study | 17 |
| 2 Publications | 19 |
| 2.1 Persistence of MERS-CoV-spike-specific B cells and antibodies after late third immunization with the MVA-MERS-S vaccine | 20 |
| 2.2 Flow cytometric protocol to characterize human memory B cells directed against SARS-CoV-2 spike protein antigens | 49 |
| 2.3 Humoral and cellular immunogenicity of two MVA-based COVID-19 vaccine candidates compared to ChAd and mRNA platforms | 66 |
| 2.4 Stabilized recombinant SARS-CoV-2 spike antigen enhances vaccine immunogenicity and protective capacity | 96 |
| 2.5 SARS-CoV-2 specific cellular response following COVID-19 vaccination in patients with chronic lymphocytic leukemia | 116 |
| 2.6 SARS-CoV-2-specific cellular response following third COVID-19 vaccination in patients with chronic lymphocytic leukemia | 121 |

| | | |
|----------|---|------------|
| 3 | Unpublished Data | 127 |
| 3.1 | ADCP capacity induced by MVA-MERS-S vaccination | 127 |
| 3.2 | ADNKA capacity induced by MVA-MERS-S vaccination | 128 |
| 4 | Discussion..... | 130 |
| 4.1 | Background and study design | 130 |
| 4.1.1 | rMVA as a vaccine platform | 130 |
| 4.1.2 | The MVA-MERS-S vaccine candidate..... | 131 |
| 4.1.3 | The MVA-SARS-2-S and MVA-SARS-2-ST vaccine candidates | 132 |
| 4.2 | The spike protein as a vaccine antigen for emerging HCoVs | 132 |
| 4.3 | Influence of platform and dosing on vaccine immunogenicity | 135 |
| 4.3.1 | MERS vaccine candidates | 136 |
| 4.3.2 | COVID-19 vaccine candidates and licensed vaccines | 136 |
| 4.4 | Booster strategies and MBC recall responses | 137 |
| 4.4.1 | Homologous versus heterologous prime-boost vaccination | 138 |
| 4.4.2 | The impact of the time interval between prime-boost vaccination | 139 |
| 4.4.3 | The potential of a late booster vaccination | 139 |
| 4.5 | Route of vaccine administration | 141 |
| 4.6 | Impact of host factors on vaccine immunogenicity | 142 |
| 4.7 | Systems vaccinology and systems serology | 144 |
| 4.7.1 | Antibody isotypes and subclasses | 144 |
| 4.7.2 | Antibody functionality | 145 |
| 4.8 | CoPs against MERS and COVID-19..... | 146 |
| 4.9 | Conclusions and future perspectives | 147 |
| 4.9.1 | Techniques to study antigen-specific B cells and antibodies | 147 |
| 4.9.2 | The MVA-MERS-S vaccine candidate..... | 147 |
| 4.9.3 | COVID-19 vaccines..... | 148 |
| 4.9.4 | The rMVA vaccine platform..... | 149 |
| 5 | References..... | 150 |
| 6 | Abbreviations | 182 |
| 7 | Acknowledgements..... | 185 |

1 Introduction

1.1 Emerging infectious diseases

Emerging infectious diseases have been a threat to human health since recorded history and have caused millions of deaths over the past centuries. Most of them are caused by pathogens that originate from animal reservoirs and are transmitted to humans in a process termed “zoonotic spillover”. These pathogens may then rapidly spread within the human population, as there is often only limited or no pre-existing immunity (Woolhouse et al., 2005, Woolhouse and Gowtage-Sequeria, 2005, Morens and Fauci, 2013, Afrough et al., 2019). Ancient zoonotic diseases include smallpox, malaria, measles, plague, and the H1N1 “Spanish” influenza, and have killed substantial parts of the human population (Morens and Fauci, 2020, Acuna-Soto et al., 2002, Potter, 2001).

Many zoonotic viruses have newly emerged or re-emerged in the last decades, most of them highly pathogenic to humans. This was likely enhanced by factors such as population growth and urbanization, international travel and commerce, as well as climate change (Morens and Fauci, 2013, Bloom et al., 2017, Sands et al., 2016). Some examples are the human immunodeficiency virus (HIV), Ebola and Marburg filoviruses, the H1N1 “swine” influenza A virus, *Chikungunya virus*, *Zika virus*, Lassa virus, Rift Valley and Crimean-Congo haemorrhagic fever viruses, as well as three viruses of the coronavirus (CoV) family: The severe acute respiratory syndrome (SARS)-CoV, the Middle East respiratory syndrome (MERS)-CoV, and most recently SARS-CoV-2 that caused a worldwide pandemic (Afrough et al., 2019, Graham and Sullivan, 2018, Sharma et al., 2021).

1.1.1 Human coronaviruses (HCoV)

The family of *coronaviridae* represents a group of enveloped, positive-sense, single-stranded RNA viruses within the order *nidovirales*. There are four endemic strains of HCoVs, namely HCoV-OC43, HCoV-229E, HCoV-NL63 and HCoV-HKU1, that mainly cause asymptomatic or mild respiratory and gastrointestinal infections and account for 5-30 % of the common colds (Li and Lin, 2013, Corman et al., 2019, Zhu et al., 2020). During the last two decades, three pathogenic HCoVs newly emerged and caused outbreaks of different dimensions: SARS-CoV, MERS-CoV, and SARS-CoV-2 (Li and Lin, 2013, Zhu et al., 2020, Meo et al., 2020) (Figure 1). All three are zoonotic viruses, causing respiratory diseases of different severities in the human host. Manifestations include unspecific, influenza-like symptoms such as fever, cough and shortness of breath, but can rapidly progress to more severe illness with pneumonia, multiple organ failure, and death (WHO, 2022a, de Wit et al., 2016, WHO, 2022b, Peiris, 2003, Naqvi et al., 2020).

The first case of human SARS-CoV infection was reported in Guangdong, China, in 2002, and the virus was later identified to originate from civet cats (Zhu et al., 2020). Being transmitted by aerosols/droplets in human-to-human contact, the respiratory disease rapidly spread worldwide, causing 8422 cases in 30 countries with a case fatality rate (CFR) of approximately 10 % (Chan-Yeung and Xu, 2003, Li and Lin, 2013, Peiris, 2003). The outbreak was contained within a year after emergence and no cases of human SARS-CoV infection have been reported since 2004 (Corman et al., 2019, Memish et al., 2020).

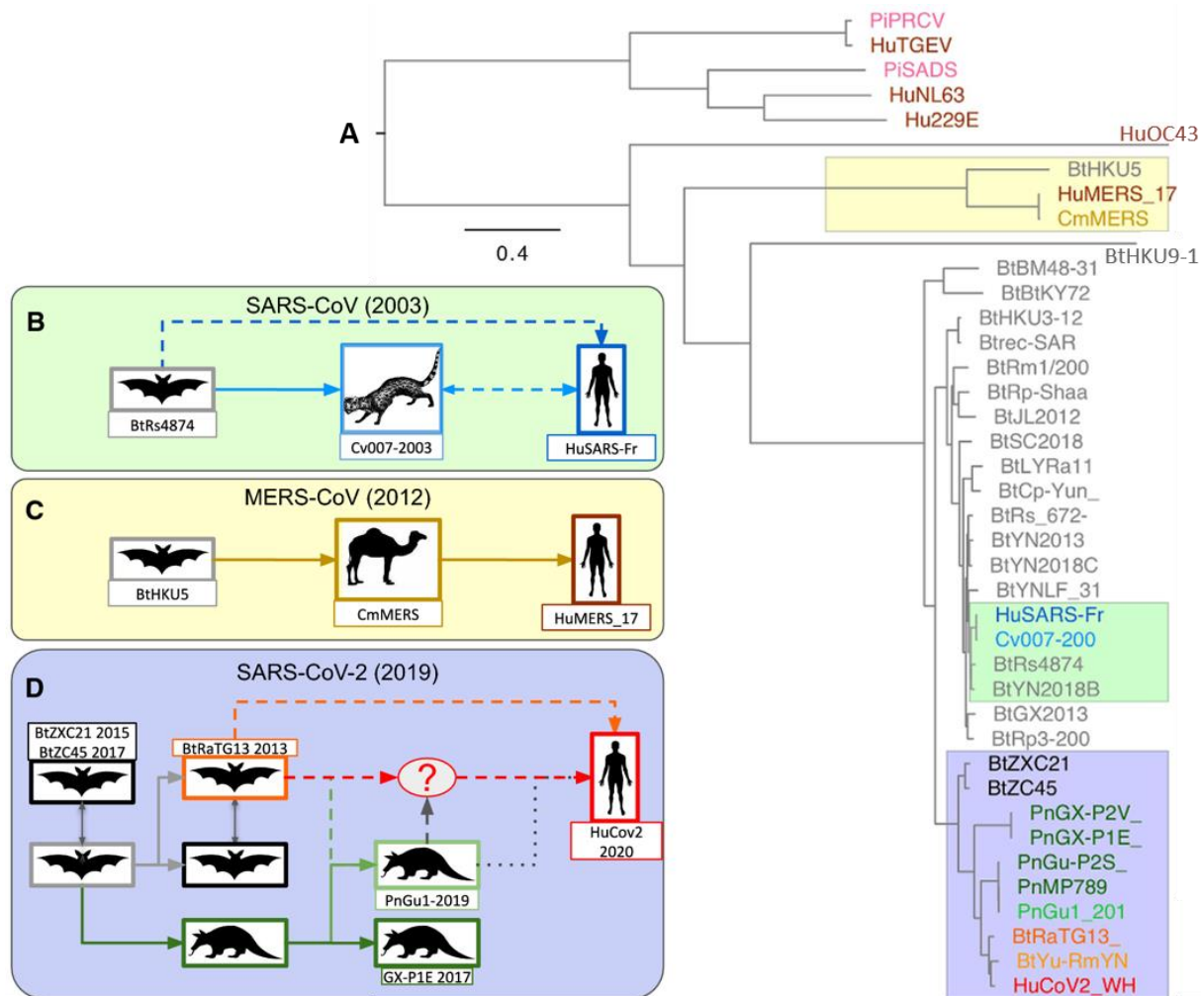


Figure 1: Phylogeny and animal reservoirs of epidemic human coronaviruses. A) Phylogenetic tree of coronaviruses, based on multiple alignment of the complete coronavirus genomes, followed by maximum likelihood inference (Sallard et al., 2021). The prefixes of virus names indicate the host species. Bt: bat, Hu: human, Pn: pangolin, Cv: civet, Cm: camel, Pi: pig. **B-D)** Hypotheses for transmission of the epidemic coronaviruses SARS-CoV, MERS-CoV and SARS-CoV-2 from bats to humans via intermediate animal hosts, based on the molecular phylogeny of the viral genomes. The civet cat has been suggested as an intermediate host for SARS-CoV and dromedary camels have been shown to be the animal reservoir for MERS-CoV transmission to humans, whereas the intermediate animal host for transmission of SARS-CoV-2 to humans is still unknown. Figure adjusted from Sallard et al. (2021).

The second epidemic HCoV, MERS-CoV, first appeared in 2012. It was isolated from a patient in Saudi Arabia (Zaki et al., 2012) and dromedary camels were identified as the critical animal reservoir of the virus, responsible for primary transmission (Gossner et al., 2014, Hui et al., 2018). A secondary, human-to-human transmission of the virus requires close contact and has been particularly reported from household settings and health-care facilities (Hui et al., 2018, Cauchemez et al., 2013). Unlike SARS-CoV, MERS-CoV continues to sporadically appear in the human population, with most cases reported from the Arabian Peninsula. Health-care-associated outbreaks occurred several times in Saudi Arabia (2014, 2015, 2016, and 2018) and the United Arab Emirates (2013, 2014) (Memish et al., 2020, Hunter et al., 2016, Rabaan et al., 2021). The largest outbreak outside the Middle East occurred in South Korea in 2015, with 186 cases and 38 associated deaths resulting from a single imported case of MERS-CoV

infection (Memish et al., 2020, Kim et al., 2017). As of December 2022, the WHO has reported 2602 laboratory-confirmed cases of MERS in 27 countries, with a CFR of about 36 % (WHO, 2022c).

The third highly pathogenic HCoV, SARS-CoV-2, was first detected in 2019 in Wuhan, China, and is the causative agent of the Coronavirus Disease-2019 (COVID-19) (Wang et al., 2020). Bats have been suggested as the primary source of SARS-CoV-2, however, the intermediate animal host responsible for transmission to the human species has not yet been identified (Sharma et al., 2021, Holmes et al., 2021, Sallard et al., 2021). Exceeding SARS-CoV and MERS-CoV in terms of transmissibility, SARS-CoV-2 rapidly spread within the human population (Sharma et al., 2021). The SARS-CoV-2 outbreak was declared a public health emergency of international concern (PHEIC) on the 30th of January 2020 and a pandemic on the 11th of March 2020 (WHO, 2020a, WHO, 2020c). As of September 2022, 610 million cases of SARS-CoV-2 infection have been reported in 214 countries, with 6.5 million associated deaths, resulting in a CFR of approximately 1 % (WHO, 2022d, Sharma et al., 2021). Beyond severe short- and long-term consequences on public health, the COVID-19 pandemic and the associated containment measures also had serious economic, social, and political effects (Allain-Dupré et al., 2020).

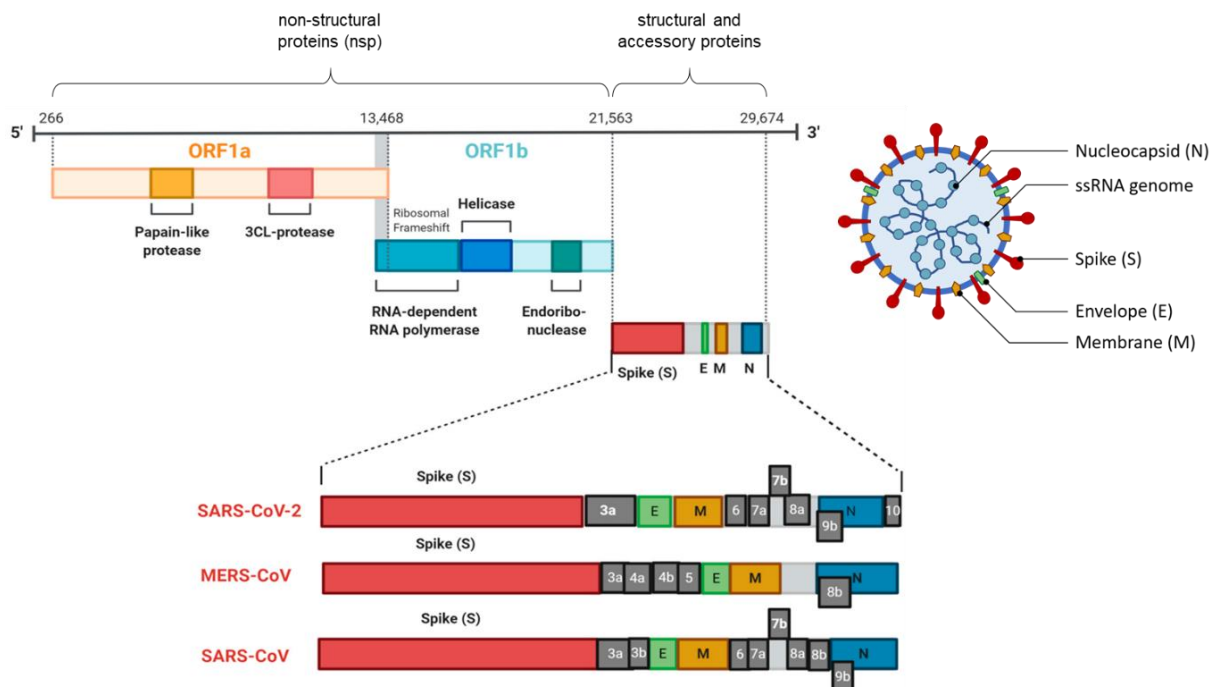


Figure 2: Coronavirus genome organization and particle structure. The coronavirus genome (left panel, adjusted from Zhand et al. (2020)) consists of the two open reading frames (ORFs) 1a and 1b encoding 16 non-structural proteins (nsp) and the genes encoding the four structural proteins spike (S), envelope (E), membrane (M) and nucleocapsid (N) as well as several accessory proteins. SARS-CoV, MERS-CoV and SARS-CoV-2 share sequence similarities in many genes. The 26-32 kb single stranded RNA genome is organized in a helical structure by interaction with the N protein and surrounded by the 100-160 nm diameter lipid envelope containing the structural proteins S, E and M (right panel).

SARS-CoV, MERS-CoV and SARS-CoV-2 belong to the genus of betacoronaviruses. Their genome consists of the genes encoding four structural proteins (nucleocapsid, spike, envelope, and membrane), as well as the open reading frames (ORFs) 1a and 1b, encoding 16 non-structural proteins involved e.g. in viral replication (Gorbalenya et al., 1989, Ziebuhr, 2004, Rabaan et al., 2021, Naqvi et al., 2020) (Figure 2). Phylogenetic analyses have revealed highly conserved sequences of many genes

including ORF1ab, spike, nucleocapsid, and envelope protein genes, but not the gene encoding for the membrane protein. The overall sequence similarities of the viruses' genomes are approximately 79 % between SARS-CoV and SARS-CoV-2, and 50 % between MERS-CoV and SARS-CoV-2 (Lu et al., 2020, Borrega et al., 2021, Hu et al., 2021).

The spike protein is responsible for virus entry into the host cell, which it mediates by binding to different host cell receptors: The dominant entry receptor for SARS-CoV and SARS-CoV-2 is the angiotensin-converting enzyme 2 (ACE2), whereas MERS-CoV entry is mediated via binding to the dipeptidyl peptidase 4 (DPP4, also termed cluster of differentiation (CD) 26) (Medina-Enríquez et al., 2020, Wang et al., 2013, Li et al., 2003, Lu et al., 2013). These entry receptors are expressed in a broad range of tissues, including the respiratory and gastrointestinal tract, and kidneys (ACE2 and DPP4), but also the heart and olfactory neuroepithelium for ACE2, as well as the liver, thymus, prostate and bone marrow for DPP4 (Fodoulian et al., 2020, Imai et al., 2010, Memish et al., 2020, Raj et al., 2013, Beyerstedt et al., 2021). Due to its crucial role in virus entry, the spike protein is an important target for vaccine development, as will be discussed below (section 4.2).

1.2 Vaccine development against emerging viruses

Vaccines are one of the most important achievements in the fight against infectious diseases. One remarkable example of vaccine effectiveness is the global eradication of smallpox accomplished in 1977, following an intense and internationally coordinated vaccination campaign. Additionally, vaccination has massively contributed to the reduction of morbidity and mortality caused by viral pathogens including polio, measles, rubella and mumps viruses (Roush and Murphy, 2007, Mokhort et al., 2018, Mao and Chao, 2020, Delany et al., 2014). It has been specified as an important tool to achieve the Sustainable Development Goals (SDGs) defined by the United Nations (UN). In this context, immunization has been listed with a critical role for SDG number 3 – to ensure healthy lives and promote well-being for all at all ages – but is also suggested to contribute directly or indirectly to 13 others of the 17 SDGs (WHO, 2020b, UN, 2015, Gavi, 2020). Vaccination is a powerful strategy for preventing and controlling infections with emerging viruses. However, some challenges have to be overcome: In the context of newly emerged viruses, detailed biological information is often missing, including knowledge about the virus structure, antigen variability or immunodominance, and correlates of protection (CoPs) (Trovato et al., 2020, Afrough et al., 2019). As there are often no therapeutics available, high levels of bio-safety are required for the handling of emerging viruses, which adds to the challenges of the research in this field. Another limitation is the lack of funding for research on rare pathogens that are unlikely to provide an effective payback on investment (Afrough et al., 2019, Bloom et al., 2017). Importantly, new infrastructures for vaccine development and funding have been established in the last decade, which was accelerated in response to the Ebola virus outbreak in 2014 in West Africa with its unpredicted size, speed and reach (Plotkin, 2017, Afrough et al., 2019).

In May 2015, the World Health Organization (WHO) established an initiative aiming to reduce the time between the declaration of a public health emergency and the availability of effective diagnostic tests, vaccines, and treatments: the research and development (R&D) Blueprint for Action to Prevent Epidemics (Mehand et al., 2018, WHO, 2016). Focusing on severe emerging diseases with the potential to evoke public health emergencies, the WHO developed a list of priority diseases to specify R&D needs including vaccine development and to address funding strategies, as well as logistical and social

challenges of epidemics (Graham and Sullivan, 2018). Multiple proposals to establish an international fund to develop vaccines against emerging pathogens with epidemic potential led to the foundation of the Coalition for Epidemic Preparedness Innovations (CEPI) in January 2017 (Røttingen et al., 2017, Sands et al., 2016). CEPI is funded by multiple governments and philanthropic organizations and aims to establish a system to accelerate the development of vaccines and thereby be better prepared for epidemics, allowing for a rapid response to an outbreak situation. Funded by CEPI, vaccine candidates can be taken through phase 1 and 2 clinical trials to provide first evidence for safety and immunogenicity, followed by the production of a stockpile for emergency use and efficacy testing in case of a potential future outbreak (Plotkin et al., 2015, Plotkin, 2017, Gouglas et al., 2019, Samarasekera, 2021).

1.2.1 Platform approaches for vaccine development

An important approach to rapidly develop vaccines against emerging pathogens are platform technologies: they are based on modules such as recombinant viral vectors, DNA plasmids or nanoparticles containing mRNA, and deliver a synthetic gene encoding for an antigen (Figure 3). In contrast to traditional approaches such as subunit vaccines, killed or live attenuated viruses, they have the advantage that manufacturing processes and safety profile, as well as general characteristics of the elicited immune response, are predominantly determined by the platform instead of the specific antigen (Afrough et al., 2019, Sasso et al., 2020, Ewer et al., 2016b, Bloom et al., 2017, Brisse et al., 2020, Pardi et al., 2018, Liu, 2019). Therefore, platform-based vaccines can be comprehensively studied in preparedness for outbreaks, allowing for rapid development upon emergence of a new pathogen. The relevance of platform approaches was recently illustrated by the SARS-CoV-2 pandemic: the first four COVID-19 vaccines to be licensed for emergency use by the European Medicines Agency (EMA) and/or the U.S. Food and Drug Administration (FDA) were based on mRNA and the chimpanzee adenovirus Y25 (ChAd) and adenovirus type 26 (Ad26) viral vectors (EMA, 2020a, EMA, 2021c, EMA, 2021a, EMA, 2021b, FDA, 2020b, FDA, 2020a, FDA, 2021). All these platforms had been previously studied in the context of other pathogens (Zhang et al., 2019, Ewer et al., 2017, Custers et al., 2021), and could thus be rapidly adjusted to encode the SARS-CoV-2 spike protein.

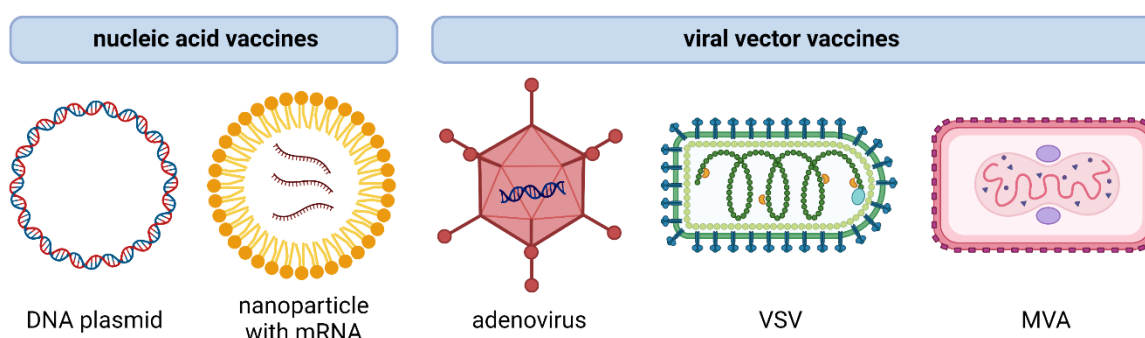


Figure 3: Vaccine platforms. Platform technologies are a promising approach for the rapid vaccine development against emerging pathogens. Based on modules such as DNA plasmids, nanoparticles containing mRNA, or viral vectors, they deliver a synthetic gene encoding for a pathogen-specific antigen. Viral vector vaccine platforms have been developed based on different viruses, including adenoviruses, the vesicular stomatitis virus (VSV), as well as the Modified Vaccinia virus Ankara (MVA). Figure created with BioRender.

Protein delivery systems based on mRNA technologies have been investigated since the 1990s, and over the past decade many technological innovations have enabled them to become a promising platform in the fields of vaccine development and protein replacement therapy, as reviewed by Pardi et al. (2018) and Dolgin (2021). The mRNA platform is noninfectious and non-integrating with no potential risk of host infection or insertional mutagenesis, and various modifications can be used to modulate the mRNA's stability and immunogenicity (Pardi et al., 2018, Szabó et al., 2022). For example, the incorporation of pseudouridine into the mRNA has been shown to reduce innate immune responses such as the activation of Toll-like receptors (TLRs), and to enhance the translation capacity by improving the overall stability of the mRNA (Van Lint et al., 2015, Devoldere et al., 2016, Szabó et al., 2022, Karikó et al., 2008). mRNA-based vaccines have been studied against viral diseases caused by *Respiratory syncytial virus* (RSV), HIV-1, *Zika virus*, influenza viruses, and Ebola virus (Feldman et al., 2019, Espeseth et al., 2020, Zhang et al., 2019), and recently the first mRNA vaccines were approved for medical use in humans by the FDA and EMA: the COVID-19 vaccines BNT162b2 (Comirnaty, BioNTech/Pfizer) and mRNA-1273 (Spikevax, Moderna) (Szabó et al., 2022).

The concept of viral vectors was first introduced in 1972 based on the simian virus 40 (SV40) and since then many types of viruses have been used for the development of vaccine platforms, including adenoviruses, herpesviruses, lentiviruses, *Vaccinia virus* mutants such as the recombinant Modified Vaccinia virus Ankara (rMVA), as well as the vesicular stomatitis virus (VSV) and the *Measles virus* (Ura et al., 2014, Jackson et al., 1972, Plotkin, 2017, Humphreys and Sebastian, 2018). During the last decades, genetic alterations have improved safety and immunogenicity of viral vectors, and enabled large scale manufacturing which typically involves propagation in suitable cell lines (Ura et al., 2014). Replication-deficient viral vectors are generally safer than replication-competent vectors, but may require a higher dose or a prime-boost regimen to elicit sufficient immunity, which might be operationally disadvantageous in outbreak situations (Travieso et al., 2022, Maslow, 2017, Henao-Restrepo et al., 2015). An advantage of viral vector vaccines is the robust induction of both humoral and cellular immunity, including cytotoxic T cells which are crucial to eliminate pathogen-infected cells (Coughlan et al., 2018, Ura et al., 2022, Ramezanzpour et al., 2016, Gilbert, 2012). In addition, viral vector vaccines are capable of eliciting strong immunogenicity without the use of adjuvants; mimicking a natural virus infection, they result in the induction of innate cytokines and co-stimulatory molecules that are needed to efficiently induce adaptive immune responses (Afrough et al., 2019, Akira et al., 2006, Travieso et al., 2022, Ura et al., 2014, Sasso et al., 2020, Zhong et al., 2021). One obstacle in the development of viral vector-based vaccines is the potentially pre-existing immunity against the virus used as a viral vector, which might negatively influence immunogenicity elicited by the vaccine (Saxena et al., 2013, Ura et al., 2014). This phenomenon has for instance been reported for the adenovirus type 5 (Ad5), which has a seroprevalence of up to 90 % in the human population (Barouch et al., 2011, Fausther-Bovendo and Kobinger, 2014, Li et al., 2017), and led to increased investigation of the less seroprevalent Ad26 as well as simian adenoviruses such as ChAd (Pollard and Bijker, 2021, Rollier et al., 2011). Anti-vector immunity can also be an issue in the context of repeated vaccination with the same viral vector, and may be overcome by the use of heterologous prime-boost regimens (Travieso et al., 2022, Pollard and Bijker, 2021, Ura et al., 2014). However, homologous booster vaccinations with viral vector vaccines have also been shown to be immunogenic in multiple studies (Fathi et al., 2022, Kreijtz et al., 2014, Voysey et al., 2021, Li et al., 2017).

Viral vector vaccines have been tested against a variety of infectious diseases in numerous pre-clinical and clinical trials (Travieso et al., 2022, Plotkin, 2017, Ura et al., 2021), and as of November 2022 four viral vector vaccines have been approved for use in humans by the EMA and/or FDA: two vaccination regimens against Ebola virus disease (EVD) and two against COVID-19. Those against EVD include a single dose of the VSV-based vaccine rVSV-ZEBOV (Ervebo, Merck Sharp & Dohme, licensed in 2019) and a heterologous two-dose vaccination regimen with Ad26.ZEBOV and MVA-BN-Filo (Zabdeno and Mvabea, Janssen-Cilag GmbH, licensed in 2020), based on Ad26 and rMVA platforms, respectively (Anywaine et al., 2019, Mutua et al., 2019, Clarke et al., 2020, EMA, 2019, EMA, 2020b, FDA, 2019a). Against COVID-19, two viral vector vaccines based on ChAd and Ad26 platforms were approved for emergency use in 2021: The ChAdOx1-S vaccine (Vaxzevria, AstraZeneca), and the Ad26.COV2.S vaccine (Jcovden, Janssen-Cilag GmbH) (Folegatti et al., 2020b, Hardt et al., 2022, EMA, 2021b, EMA, 2021a, FDA, 2021).

1.2.2 Innate and adaptive immune responses to infection and vaccination

Immune responses to infection or vaccination are mediated by different kinds of immune cells and can be divided into innate and adaptive immune mechanisms. Innate immune responses are generally induced within hours after antigen exposure and act against a broad range of pathogen structures, whereas adaptive immune responses need several days or weeks to develop and are specifically directed against the respective antigen (Turvey and Broide, 2010, Chaplin, 2010, Dempsey et al., 2003) (Figure 4). Vaccine-mediated protection relies mainly on the induction of effector mechanisms of the adaptive immune system that persist in the body and can rapidly act to control invading pathogens (Siegrist, 2018). Nevertheless, innate and adaptive immune responses are tightly linked and can contribute to the activation of one another (Jain and Pasare, 2017).

Cells of the innate immune system include natural killer (NK) cells, granulocytes (neutrophils, eosinophils, and basophils), monocytes, macrophages and dendritic cells (DCs), that are involved in different immune functions. For instance, NK cells are capable of recognizing and killing virus-infected cells and producing cytokines (Abel et al., 2018, Cerwenka and Lanier, 2001). Neutrophils, monocytes and macrophages are phagocytes that recognize conserved structures of pathogens (pathogen-associated molecular patterns, PAMPs) or signals secreted by infected cells (damage-associated molecular patterns, DAMPs) via their pattern recognition receptors (PRRs) (Medzhitov and Janeway, 2000, Dempsey et al., 2003). Additionally, monocytes and macrophages secrete pro-inflammatory cytokines and are involved in antigen presentation. The most specialized antigen-presenting cells are DCs; they capture and process antigens, migrate to the secondary lymphoid organs (SLOs) and present the antigen on their surface via major histocompatibility complex (MHC) class I and class II proteins. As such, dendritic cells form a crucial link between the innate and the adaptive immune response (Murphy, 2012, Wiczorek et al., 2017, Dempsey et al., 2003).

The key components of the adaptive immune system are B lymphocytes (B cells) and T lymphocytes (T cells). They are equipped with a large repertoire of antigen-specific B or T cell receptors (BCRs, TCRs), capable of recognizing approximately 10^7 to 10^9 different antigens. Each single B or T cell bears only one kind of antigen-specific receptor on its surface and circulates through the body as a so-called naïve lymphocyte prior to the first encounter with its specific antigen. Upon antigen encounter, B and T cells further differentiate into fully functional effector lymphocytes with distinct immune functions. The main function of B cells is the secretion of antibodies, also referred to as immunoglobulins (Igs). These

molecules represent a secreted form of the BCR and are capable of recognizing a specific pathogen, leading to the neutralization or recruitment of effector cells (Cooper, 1984, Siegrist, 2018, Lu et al., 2018). As they are secreted into extracellular fluids (e.g. blood, mucous secretions), antibody-mediated immunity is also referred to as humoral immunity. T cells can exhibit multiple functions that are mediated by differential expression of surface molecules and cytokines. For instance, cytotoxic T cells recognize and kill virus-infected cells, whereas T helper cells secrete cytokines and provide support for the generation and maintenance of B and cytotoxic T cell responses. Regulatory T cells control the activity of different immune cell populations and contribute to the maintenance of immunologic tolerance (Geginat et al., 2014, Beňová et al., 2020, Wan et al., 2020). A unique feature of the adaptive immune system is the capability of generating immunological memory. During the course of an immune response, some of the activated B and T cells become memory cells that can persist for a long time in the absence of the respective antigen and are capable of rapid reactivation upon secondary antigen exposure (Abbas, 2017, Murphy, 2012).

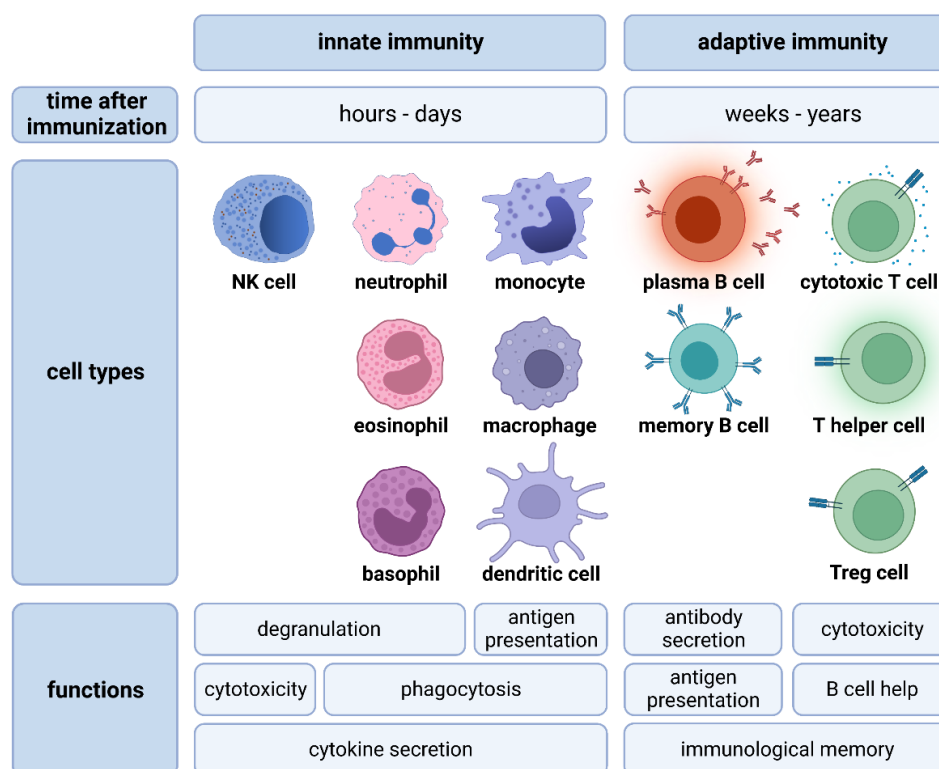


Figure 4: Innate and adaptive immune cell functions. Innate immune cells are activated within hours to days after immunization and act against a broad range of pathogens via recognition of conserved pathogen structures, whereas cells of the adaptive immune system act very specifically against one pathogen. Adaptive immune cells develop within a few days or weeks after immunization and can persist for years or decades, providing pathogen-specific immune memory. Figure created with BioRender.

1.2.3 Correlates of vaccine-induced protection

CoPs are defined as immune markers that are statistically associated with and may or may not be a mechanistic causal agent of protection induced by infection or vaccination (Plotkin and Gilbert, 2012). Multiple pathways are involved in the immune responses against pathogens, and it is often not known whether vaccine-induced antibodies or specific immune cell subsets correlate with protection or vaccine efficacy. Firstly, the magnitude of antibody or cellular immune responses does not necessarily

predict their functionality, and secondly, mechanisms of protection may be multifaceted and can strongly differ between distinct pathogens using different routes or mechanisms of infection (Siegrist, 2018, Plotkin, 2001, Goldblatt et al., 2022a, Jang and Seong, 2021). To determine the susceptibility of an individual or a population and enable the choice of the vaccine antigen and/or platform, it is important to define specific CoPs for individual pathogens. CoPs provide an important tool to predict vaccine efficacy from immunogenicity endpoints which may be used to evaluate the consistency of vaccine production, license combination vaccines or enable immune bridging to license second-generation vaccines. Additionally, mechanistic CoPs may increase the understanding of basic immunology (Edwards, 2001, Plotkin, 2010, Qin et al., 2007).

CoPs can be determined by the analysis of immune responses in protected and unprotected subjects in efficacy trials, by observations made in immunosuppressed individuals, in human challenge studies or by extrapolation from animal challenge studies (Medetgul-Ernar and Davis, 2022, Callegaro and Tibaldi, 2019, Nguipdop-Djomo et al., 2013, Qin et al., 2007). However, animal models have been shown to provide only limited prediction of human disease or vaccine efficacy, underlining the importance of systems biology approaches to extend the insights that can be derived from human studies (Pulendran and Ahmed, 2011, Davis, 2008, Pulendran et al., 2010, Querec et al., 2009). Importantly, CoPs can differ between protection from detectable infection (also referred to as sterilizing immunity), symptomatic infection and severe disease or hospitalization. Prevention of infection may be achieved only by vaccine-induced antibodies, whereas protection against severe disease can be supported by T cells, even in the absence of antibodies (Siegrist, 2018, Plotkin, 2008).

Antibodies have been described as CoPs for many of the currently licensed vaccines, including those against the viral diseases smallpox, influenza, hepatitis A, hepatitis B, varicella, measles, rubella, polio, rabies, and COVID-19 (Plotkin, 2008, Siegrist, 2018, Goldblatt et al., 2022a, Meyer et al., 2021, Houry et al., 2021). Based on the titers of binding (or sometimes neutralizing) antibodies, absolute correlates can be defined for some diseases (e.g. measles and rubella), meaning that a certain titer of antibodies almost guarantees protection. For many other viral diseases there are only relative correlates available: In these cases, a correlation exists between antibody titer and protection, but no protective threshold can be defined for breakthrough infections (Plotkin, 2008). During the last years, non-neutralizing antibody functions have increasingly been recognized as important drivers of protection, as underlined by several studies using system serology approaches to comprehensively profile humoral immunity in humans. For example, complement activity has been suggested to be part of the protective immunity against the diseases caused by influenza viruses, *West Nile virus*, Ebola virus, *Vaccinia virus* and SARS-CoV-2 (Lu et al., 2018, Lamerton et al., 2022, Meyer et al., 2021). Antiviral activity mediated via antibody-dependent activation of innate immune mechanisms has been described e.g. against HIV-1, influenza viruses, Ebola virus, herpesviruses, RSV and SARS-CoV-2 (Liu et al., 2017, Von Holle and Moody, 2019, Bournazos et al., 2014, Hagemann et al., 2022, Chung et al., 2014, He et al., 2016, Zohar et al., 2020, Tay et al., 2019, Meyer et al., 2021, Bartsch et al., 2022). Despite the importance of antibodies as CoPs, other immune parameters may also contribute substantially to protection. T cell-mediated immune functions are for example critical in protection against intracellular infections, and to support efficient B cell activation. Memory B cells (MBCs) are an important determinant of vaccine-induced long-term protection, and have been shown to be a CoP against hepatitis B virus infection, even in the absence of persisting serum antibodies (Plotkin, 2010, Tuaille et al., 2006, West and Calandra, 1996).

To develop safe and efficacious vaccines against existing pathogens and be able to rapidly react upon outbreaks with newly emerging ones, it is important to gain a better understanding of the exact immune mechanisms induced by different vaccine platforms and to find more specific CoPs for individual pathogens. This thesis focusses on a comprehensive analysis of vaccine-induced B cell and antibody responses, which are described in more detail in the following sections.

1.3 B cell immune responses

Originating from the bone marrow, B cells undergo several differentiation steps, resulting in the generation of mature, naïve B cells which traffic through peripheral blood and SLOs. The primary activation of naïve B cells is dependent on their cognate antigen, recognized by the specific BCR, and support by antigen-specific T cells. B cell activation can result in the differentiation into antibody-secreting plasma cells or MBCs, and initiates several maturation processes leading to enhanced quality of secreted antibodies (Cyster and Allen, 2019, Wishnie et al., 2021). A secondary antigen encounter upon reinfection or booster vaccination can reactivate MBCs generated by the first infection or vaccination, leading to so-called recall responses. In comparison to naïve B cells, the activation of MBCs requires lower amounts of antigen and is independent of T cells, often leading to a more rapid and stronger increase in antibody plasma levels upon recall responses (Siegrist, 2018, Palm and Henry, 2019). The different steps of B cell differentiation and activation are visualized in Figure 5 and will be discussed in more detail below.

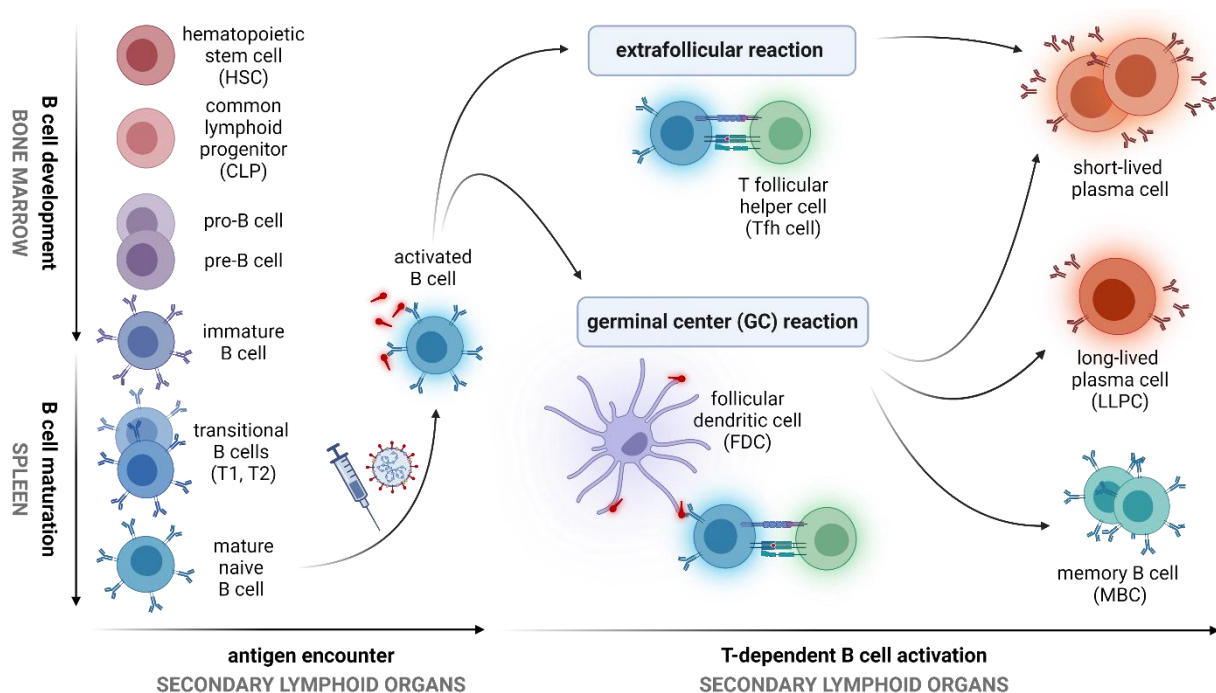


Figure 5: B cell development and T-dependent activation. B cells develop from hematopoietic stem cells in the bone marrow which they leave as immature B cells to further mature in the spleen. Mature, naïve B cells reside mainly in secondary lymphoid organs (SLOs), where they encounter their specific antigen upon vaccination or infection. Antigen binding leads to B cell receptor signaling and subsequent migration to the T cell zone of the SLOs, where the activated B cell interacts with T follicular helper (Tfh) cells. Tfh cell stimulation can lead to a rapid extrafollicular B cell reaction with limited class switch recombination (CSR), resulting mainly in the differentiation into short-lived plasma cells, or in the formation of germinal centers (GCs). The GC reaction requires the involvement of follicular dendritic cells (FDCs) and results in pronounced CSR and somatic hypermutation (SHM) of antibodies. It gives rise to memory B cells (MBCs) as well as short- and long-lived plasma cells producing antibodies of increased affinity towards the antigen. Figure created with BioRender.

1.3.1 B cell development and maturation

Like all blood cells, B cells are derived from hematopoietic stem cells (HSCs) that reside in the bone marrow. In response to signals provided by specific bone marrow niches and stromal cells, HSCs differentiate into common lymphoid precursor cells and further into the earliest committed B-lineage cell, the pro-B cell. B cell development proceeds with the V(D)J rearrangement of the Ig heavy chain locus, followed by the light chain genes. V(D)J recombination produces increased diversity of the antibody repertoire, but also results in many unsuccessful rearrangements. Therefore, several checkpoints have to be passed by a developing B cell: Successful rearrangement of the heavy chain locus results in the formation of a functional pre-B cell receptor that induces cell proliferation and initiates the transition of the pro- to the pre-B cell stage. Here, light chain rearrangement occurs and, if successful, leads to the generation of an immature B cell expressing a BCR of IgM isotype on its surface. Unsuccessful rearrangement of heavy or light chain genes leads to apoptosis of pro- and pre-B cells, respectively (Murphy, 2012, LeBien, 2000, LeBien and Tedder, 2008, Nagasawa, 2006, Bendall et al., 2014, Morgan and Tergaonkar, 2022).

After clonal deletion of autoreactive cells, immature B cells leave the bone marrow and enter the blood circulation to migrate to SLOs, i.e. spleen, lymph nodes or mucosa-associated lymphoid tissues (MALT). The homing of B cells to specific regions (B cell follicles) of the SLOs is mediated by chemokines like C-X-C motif ligand 13 (CXCL13), which is expressed mainly by follicular dendritic cells (FDCs) and binds to the C-X-C chemokine receptor type 5 (CXCR5) on the B cell surface. Newly formed B cells compete for the entry to SLOs and if they do not succeed they die within a few days in the peripheral blood circulation. If they are able to enter the lymphoid follicles, they receive survival signals that are needed for further maturation through two transitional states (T1 and T2) to mature, naïve B cells. In this stage, B cells downregulate their expression of IgM, whereas expression of IgD, CXCR5 and CD21 is increased (Murphy, 2012, Batten et al., 2000, Martin et al., 2016, Tangye and Mackay, 2006, Morgan and Tergaonkar, 2022).

1.3.2 Primary B cell activation by protein antigens

Resting B cells of a mature, naïve phenotype mostly reside in the SLOs, with a minor portion trafficking through the peripheral blood. Antigen encounter occurs most likely in the B cell follicles of lymph nodes draining the vaccine injection site. Binding of an antigen to a BCR on a naïve B cell results in receptor signaling as well as internalization, processing and presentation of the antigen via MHC class II molecules (Kwak et al., 2019, Phan et al., 2009). BCR signaling results in upregulation of the C-C chemokine receptor type 7 (CCR7), leading to migration of B cells to the border of the T cell zone (Reif et al., 2002, Cyster and Allen, 2019). Here, they encounter antigen-specific T follicular helper (Tfh) cells that have previously been primed by DCs presenting the respective antigenic peptides (Garside et al., 1998). Depending on different factors including the BCR's affinity for the antigen, Tfh stimuli can result in a rapid extrafollicular B cell reaction or in the formation of GCs, where B cells undergo further affinity maturation (Zotos et al., 2010, Akkaya et al., 2020, Wishnie et al., 2021).

The extrafollicular reaction results in the differentiation of naïve B cells into plasma cells secreting low-affinity germline antibodies, that can be of both unswitched (IgM) and switched isotypes (IgG, IgA, IgE). These responses are rapid, leading to appearance of IgM and low-level IgG antibodies in the blood as early as a few days after primary immunization. Although important to provide a first line of defense,

these responses are of limited sustainability, as the plasma cells emerging from the extrafollicular reaction are short-lived and the generation of MBCs is very limited (MacLennan et al., 2003, Bortnick and Allman, 2013, Taylor et al., 2012).

As opposed to the extrafollicular reaction, a primary GC reaction takes a few weeks, with the first hypermutated IgG antibodies appearing in the blood around 10 to 14 days and the peak levels observed around four weeks after immunization. However, the GC reaction is important to improve the quality and persistence of antigen-specific antibodies. It gives rise to plasma cells producing isotype-switched antibodies of increased affinity, and, importantly, to two long-living B cell populations that are crucial to confer long-term protection against a pathogen: Long-lived plasma cells (LLPCs) and MBCs (Akkaya et al., 2020, Siegrist, 2018, De Silva and Klein, 2015, Goodnow et al., 2010).

Both plasma cells and (to a lesser extent) MBCs can also be generated by mechanisms independent of GCs and T helper cells. However, these T-independent antibody responses are of lower affinity and are mainly induced by bacterial polysaccharides, whereas viral protein antigens typically elicit T-dependent responses, as described above (Siegrist, 2018, Akkaya et al., 2020). T-independent immune responses are comprehensively reviewed by Allman et al. (2019) and Obukhanych and Nussenzweig (2006) and will not be discussed in detail here.

1.3.3 The germinal center reaction

In the GC reaction, naïve B cells proliferate and undergo further maturation steps, receiving stimuli from two specific cell populations: Tfh cells and follicular dendritic cells (FDCs) (Goodnow et al., 2010, De Silva and Klein, 2015). Tfh cells differ from other T helper cell subsets regarding chemokine receptors, transcription factors, surface markers and interleukins (IL) and have a unique capacity of providing efficient B cell help by different costimulatory molecules, including CD40 ligand (CD40L), inducible T-cell costimulator (ICOS), IL-10 and IL-21 (Linterman and Vinuesa, 2010, Crotty, 2015). Notably, FDCs are a distinct cell type from the DCs described above. They are not derived from HSCs and neither have phagocytic activity nor present antigens via MHC class II proteins. Instead, they are specialized to capture antigens that are part of immune complexes and retain them on their surface without prior internalization or processing steps, for presentation to B cells (Murphy, 2012, Cyster and Allen, 2019).

The GC formation is dependent on FDCs, that attract antigen-specific B and Tfh cells by secretion of CXCL13 and present antigens for extended periods (Siegrist, 2018). Initiated by activation and survival signals from FDCs and Tfh cells, antigen-specific B cells undergo clonal proliferation, accompanied by two mechanisms of BCR maturation that are mediated by the activation-induced cytidine deaminase: Ig class switch recombination (CSR) and affinity maturation. CSR switches BCRs of the IgM isotype into IgG, IgA and IgE isotypes that – once secreted as antibodies – differ in localization and functionality (Kracker and Durandy, 2011, Schroeder and Cavacini, 2013). Affinity maturation is the result of a process called somatic hypermutation (SHM), in which mutations are introduced into the variable-region segment of the Ig gene. These random mutations increase the affinity of the BCRs in only a small portion of B cells, which subsequently have an advantage in the competition for antigens presented by FDCs. Upon binding, antigens are internalized by B cells, processed into small peptides and presented on the cell surface via MHC class II proteins, allowing for an interaction with Tfh cells. The interaction of B cells, Tfh cells and FDCs favors the proliferation, survival and selection of B cells with

the highest affinity for the vaccine antigen and eventually leads to the differentiation of GC B cells into MBCs and plasma cells producing BCRs and antibodies of enhanced affinity (Goodnow et al., 2010, Siegrist, 2018, Linterman and Vinuesa, 2010).

1.3.4 B cell memory and recall responses

Both LLPCs and MBCs can persist for several months or even decades in the human body and use different mechanisms to mediate long-term protection. LLPCs reside in bone marrow niches and continuously secrete antibodies to maintain a first line of defense against invading pathogens, whereas MBCs provide a second level of immunity against (variant) pathogens that escape the LLPC-mediated defense (Akkaya et al., 2020, Brynjolfsson et al., 2017, Khodadadi et al., 2019, Radbruch et al., 2006, Sallusto et al., 2010, Purtha et al., 2011, Amanna et al., 2007). Unlike LLPCs, MBCs do not produce antibodies but persist in a quiescent state in spleen and lymph nodes. Upon secondary exposure to an antigen by either booster vaccination or infection, the MBCs generated in the primary response are rapidly reactivated. They proliferate and differentiate into plasma cells or they can re-enter the GC reaction, leading to enhanced magnitude and persistence of the subsequent antibody responses and providing the opportunity to adapt to variant pathogens (Suan et al., 2015, Burton et al., 2018, Purtha et al., 2011, Kotaki et al., 2022, Kurosaki et al., 2015). As opposed to naïve B cells, MBCs are reactivated by lower amounts of antigen and do not require T cell help for differentiation. Therefore, MBC recall responses exceed primary responses in rapidity, magnitude and antigen specificity (Palm and Henry, 2019, Good-Jacobson and Shlomchik, 2010). Compared to a primary GC reaction that takes a few weeks, high-affinity antibodies appear as early as 4 to 7 days after a secondary immunization and are maintained by short-lived plasma cells for a few weeks. Afterwards, antibody levels start to decline, but with slower dynamics than after the primary response, due to increased numbers of LLPCs residing in the bone marrow (Siegrist, 2018).

1.4 Antibodies – structure and functionality

Antibodies or Igs are glycoproteins that are secreted by B cells and play an important role in vaccine-mediated protection. One important mechanism of action is the recognition and specific binding of pathogens, preventing their host cell entry and/or replication. Further, antibodies can act against pathogens via a variety of other effector mechanisms, including the activation of complement system and innate effector cells, as well as the regulation of B cell activity and survival. The different antibody functions are mediated by two distinct domains, namely the fragments antigen binding (Fab) and crystallizable (Fc), that are defined based on early experiments investigating antibody structure by protease cleavage. In each antibody molecule, two identical Fab domains are linked to one Fc domain via a flexible hinge region (Schroeder and Cavacini, 2013) (Figure 6).

The Fab domain contains the variable regions of Ig heavy and light chains which are combined to build the antigen binding site. Variable antibody regions are generated by V(D)J recombination during B cell development and can be further adapted by SHM upon antigen encounter, to increase the affinity for their cognate antigen. The main function of the Fab fragment is the binding and consequential neutralization of pathogens, considered an important mechanism to prevent entry into host cells and control replication and dissemination of the pathogen (Schroeder and Cavacini, 2013, Chiu et al., 2019). Specificity and affinity of the Fab region are the major determinants of the antibodies' neutralizing capacity. However, there is growing evidence that neutralization activity can also be

affected by the Fc domain (Bournazos et al., 2014, Hessel et al., 2007, Lu et al., 2018, Torres and Casadevall, 2008).

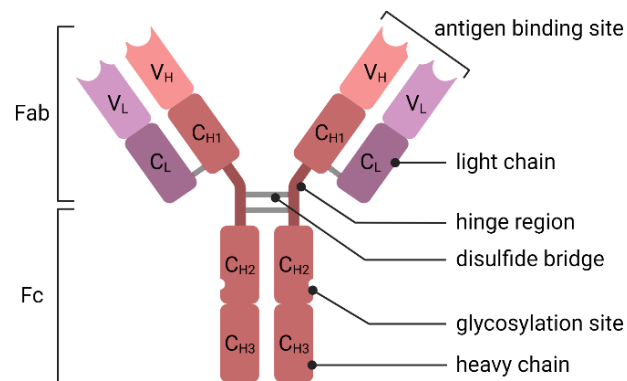


Figure 6: Antibody structure. Antibodies are composed of two identical heterodimers, each consisting of a heavy chain (HC) and a light chain (LC), that are linked via disulfide bonds. Both HCs and LCs contain variable (V_H, V_L) and constant regions (C_{H1-H3}, C_L). The variable domains of both HCs and LCs are generated by V(D)J recombination and somatic hyper-mutation and are paired to form the antigen binding site. The HC constant domains are subject to class switch recombination and define the isotype and subclass of an antibody. Two distinct functional domains are defined: the fragment antigen binding (Fab) responsible for specific binding and neutralization of an antigen, and the fragment crystallizable (Fc) which mediates non-neutralizing effector functions. Figure created with BioRender.

The Fc domain is composed of the constant regions of two Ig heavy chains and mediates non-neutralizing antibody functions via binding to different receptors and sensor molecules. Based on the heavy chain constant domains, different antibody isotypes and subclasses are defined, that differ in their abundance, receptor affinity, and functional capacity (Schroeder and Cavacini, 2013, Lu et al., 2018). An additional structural feature strongly influencing the Fc domain's functional capacity are post-translational modifications with glycan structures. The extent of glycosylation varies between the different isotypes, has been shown to impact antibody stability and represents a key regulator of non-neutralizing antibody functions (Arnold et al., 2007, Irvine and Alter, 2020, Schroeder and Cavacini, 2013, Reusch and Tejada, 2015).

1.4.1 Antibody isotypes and subclasses

Based on the constant domain of the Ig heavy chains, human antibodies are classified into five isotypes which result from CSR during B cell activation: IgA, IgD, IgE, IgG, IgM. IgA and IgM possess an additional joining chain, allowing for the formation of dimers and pentamers, respectively, whereas the other isotypes circulate as monomers (Figure 7).

IgM is the first BCR isotype expressed during B cell development and also the first type of antibody to be secreted in primary responses induced by vaccination or infection. Usually, IgM antibodies are more poly-reactive than other isotypes and bind their antigen with relatively low affinity, as they have not undergone extensive SHM. They are therefore also referred to as natural antibodies. Despite their low affinity, IgM antibodies are important to provide a first line of defense against primary infections. They can attain high avidity by formation of pentamers and function in fixing of the complement system and opsonization of pathogens (Schroeder and Cavacini, 2013).

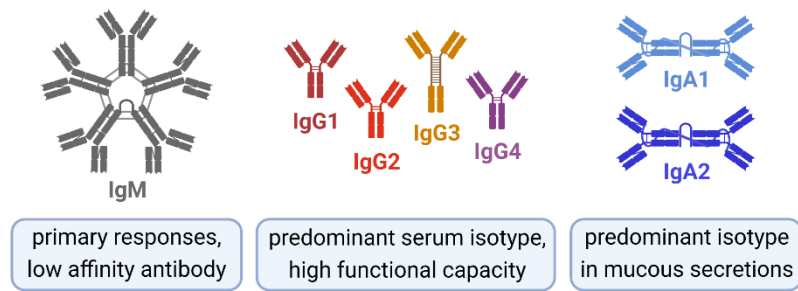


Figure 7: Antibody isotypes and subclasses involved in immune responses to vaccination and infection. Antibodies can be classified into different isotypes and subclasses based on their Fc fragment. IgM antibodies are mainly involved in primary responses and are usually of relatively low affinity. IgG is the predominant antibody isotype in human serum and can be subdivided into the four subclasses IgG1 to IgG4 that are numbered according to their abundance and have distinct functional capacities. The IgA isotype is predominantly found in mucous secretions and plays an important role in the protection against mucosal infections. It consists of the two subclasses IgA1 and IgA2. Figure created with BioRender.

IgG is the predominant antibody isotype found in the human body and especially the blood. It has the longest serum half-life (one to three weeks, depending on subclass) and is the only isotype capable of transplacental transport to a fetus (Firan et al., 2001, Schroeder and Cavacini, 2013, Morell et al., 1970, Grevys et al., 2022). Compared to IgM, IgG antibodies generally show a higher antigen affinity and potency to induce effector functions, and are especially involved in secondary immune responses. IgG antibodies can be subdivided into four subclasses, that are numbered according to their abundance in human serum: IgG1 (60-70 %), IgG2 (20-30 %), IgG3 (5-8 %) and IgG4 (1-3 %). The four subclasses exhibit different functional activities, with IgG1 and IgG3 typically involved in responses towards viral protein antigens, whereas IgG2 is associated with bacterial polysaccharide antigens. IgG4 has been observed in response to allergens and following repeated or long-term exposure to antigens in a non-infectious setting (Vidarsson et al., 2014, Lefranc and Lefranc, 2001). IgG3 is a potent pro-inflammatory antibody that activates complement system and effector cells with the highest efficiency of all four subclasses. This high functional capacity might be linked to additional glycosylation sites and an elongated hinge region resulting in greater molecular flexibility (Lee et al., 2017, Vidarsson et al., 2014). In terms of functionality, IgG3 is closely followed by IgG1, whereas IgG2 and IgG4 are less potent in activating effector cells. IgG4 is the only IgG subclass not capable of activating the complement system (Schroeder and Cavacini, 2013).

IgA displays lower serum levels than IgG, but is the most abundant isotype in mucous secretions like saliva and breast milk (Woof and Mestecky, 2005). In serum, IgA circulates as a monomer, whereas in secretions the majority of IgA is present in the form of dimers and tetramers. There are two subclasses of IgA: IgA1 which makes up the largest portion of serum IgA, and IgA2 which predominates in mucosal secretions. IgA plays an important role in the protection from viruses and bacteria at mucosal surfaces, where it acts by direct neutralization but also by mediation of Fc-dependent effector cell functions (Schroeder and Cavacini, 2013, Russell, 2007).

IgD and IgE have a short half-life and are present at very low levels in human serum. The function of circulating IgD is not fully understood, whereas IgE is associated with hypersensitivity and allergic reactions as well as the response to parasitic worm infections (Schroeder and Cavacini, 2013).

1.4.2 Non-neutralizing antibody functions against viruses

Besides virus neutralization, non-neutralizing antibody functions are increasingly recognized as important mediators of protection against viruses. Non-neutralizing antibody functions include the activation of the complement system and innate effector cells as well as the regulation of B cell activity and survival, and are mediated via binding of the Fc antibody region to different receptors and sensor molecules (Vidarsson et al., 2014, Chung et al., 2015, Tay et al., 2019, Lu et al., 2018, Zhang et al., 2022a) (Figure 8).

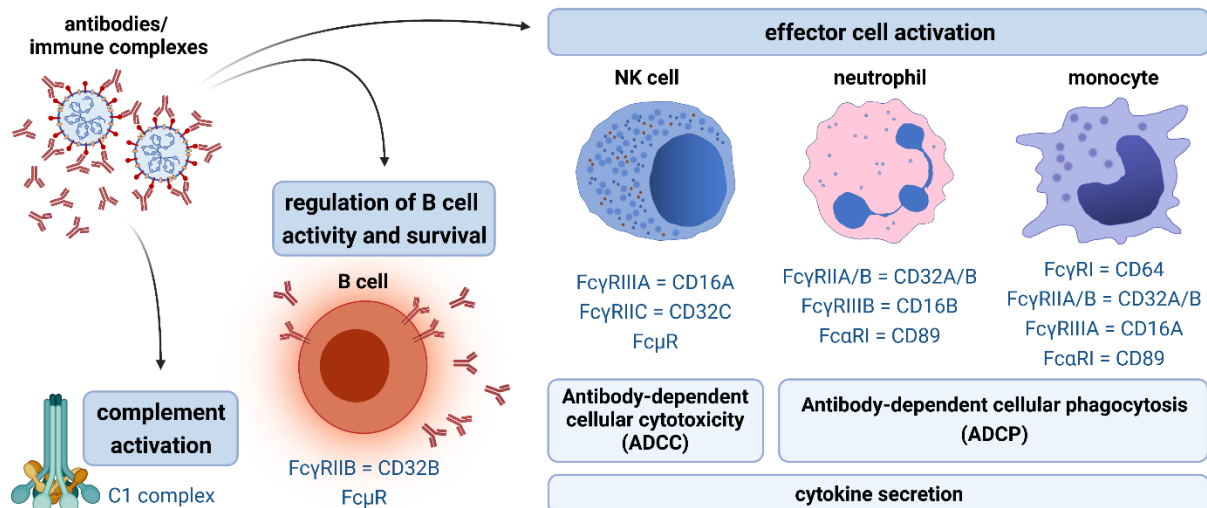


Figure 8: Non-neutralizing antibody functions. Besides neutralization of pathogens, antibodies can mediate different non-neutralizing effector functions. These are mediated via binding of the Fc fragment to different sensor molecules and receptors (indicated in blue script), and include the activation of the complement system via binding to the C1 complex, as well as the regulation of B cells and activation of innate effector cells via binding to Fc receptors expressed on the cell surface. Effector cell functions induced by antibodies include antibody-dependent cellular cytotoxicity (ADCC) elicited by NK cells, and antibody-dependent cellular phagocytosis (ADCP), elicited by neutrophils and monocytes. Figure created with BioRender.

Activation of the complement system is initiated by binding of antibodies in immune complexes to C1q, with pentameric IgM and aggregated IgG antibodies being the most potent inducers. Complement fixation leads e.g. to the production of pro-inflammatory peptides and to the phagocytosis by monocytes, macrophages, neutrophils and dendritic cells expressing complement receptors (Merle et al., 2015a, Merle et al., 2015b, Gunn and Alter, 2016). Complement activation can also facilitate B cell maturation: Complement-opsonized immune complexes bound by complement receptors on naïve non-cognate B cells have been shown to be transferred to FDCs in GCs, where they are captured and processed by antigen-specific B cells, resulting in enhanced stimulation by Tfh cells (Gonzalez et al., 2010). Many other effector functions are mediated via binding of antibodies or immune complexes to Fc receptors that are differentially expressed on the surface of distinct immune cell subsets (Figure 8). Isotypes and subclasses differ in their specificities and affinities for Fc receptors, which is one of the underlying mechanisms for their distinct functional capacities. FcμR, the Fc receptor for IgM, is expressed on B, T and NK cells and is mainly involved in the regulation of B cell development, maturation and activation, as well as immunological tolerance (Lu et al., 2018).

Innate effector cell functions are mainly mediated by antibody binding to the Fc receptors for IgG and IgA, termed Fc γ R and Fc α R, respectively, (Liu et al., 2019, Vidarsson et al., 2014). Most extensively studied are the Fc γ Rs which consist of three different classes with distinct expression patterns: Fc γ RI (CD64), Fc γ RII (CD32) A/B/C and Fc γ RIII (CD16) A/B, with A, B and C representing different isoforms. CD64 is only expressed by monocytic cells (including macrophages and some subsets of DCs), whereas CD32 and CD16 isoforms show a broader expression pattern on the surface of monocytes, granulocytes and NK cells (Bournazos et al., 2016). Among the three classes, CD64 has the highest affinity for IgG and is therefore the only class capable of binding monomeric IgG, while CD32 and CD16 are only activated by aggregated IgG or immune complexes. There are also differences in the affinities of the IgG subclasses: IgG1 and IgG3 bind to all three classes of Fc γ Rs with relatively high affinity, whereas IgG4 and IgG2 show weaker overall binding capacities (Schroeder and Cavacini, 2013). Fc α R (CD89), the Fc receptor for IgA, is found on neutrophils and monocyte-derived cells and binds polymeric IgA with higher affinity than serum IgA (Russell, 2007, Schroeder and Cavacini, 2013, Hamre et al., 2003).

Upon Fc binding, most of the Fc receptors (CD64, CD32A/C, CD16A and CD89) induce activating signaling pathways via an immunoreceptor tyrosine-based activation motif (ITAM). CD32B is the only inhibitory Fc γ R and functions via an immunoreceptor tyrosine-based inhibitory motif (ITIM) (Schroeder and Cavacini, 2013). Depending on the cell type and the receptors involved, Fc receptor signaling can lead to different effector mechanisms, including antibody-dependent cellular cytotoxicity (ADCC) or phagocytosis (ADCP), the secretion of cytokines and other pro-inflammatory molecules, as well as antigen presentation (Monteiro and Van De Winkel, 2001).

ADCC is induced by antigen-specific antibodies on the surface of e.g. virus-infected cells, that bind to CD16 on NK cells via their Fc region. CD16 signaling subsequently results in the degranulation of NK cells and release of cytotoxic molecules such as perforin and granzyme, leading to lysis of the target cells and clearance of pathogens (Trapani and Smyth, 2002, Vivier et al., 2011).

ADCP, also referred to as opsonophagocytosis, describes the clearance of immune complexes and antibody-opsonized pathogens, but also virus-infected cells by mononuclear phagocytes (monocytes, macrophages and DCs) and granulocytes (mainly neutrophils, but also eosinophils, basophils and mast cells). The mechanism of ADCP is induced by binding of FcRs on innate immune cells to the Fc region of antibodies that are part of an immune complex and may be accompanied by the secretion of antimicrobial peptides, proteases, cytokines, reactive oxygen and nitrogen species, as well as the presentation of antigens, facilitating downstream adaptive immune responses (Lu et al., 2018, van Egmond et al., 2015, Tay et al., 2019). Differential FcR signaling via ITAM and ITIM determines the fate of the endocytosed immune complex; ITAM signaling leads to the transport of pathogens to lysosomes for degradation and antigen processing for presentation to T cells, whereas ITIM signaling results in retention of the intact antigens for subsequent transfer to B cells for the induction of humoral immunity (Lu et al., 2018, Boross et al., 2014, Bergtold et al., 2015).

1.5 Aim of the study

Binding antibody titers and neutralization capacity are considered CoPs against many infectious diseases and are assessed in most clinical vaccine trials to assess immunogenicity. However, they provide an incomplete picture, as antibody-mediated protection depends on many additional parameters, such as non-neutralizing functionality and B cell memory (Chung et al., 2015, Pulendran

and Ahmed, 2011, Ackerman et al., 2017, Lu et al., 2018, Sallusto et al., 2010). During the last decades, systems serology approaches have emerged, aiming at a more comprehensive analysis of antibody structure and (non-) neutralizing functionality, to gain a better understanding of the specific antibody features that contribute to protection against infection or disease. Besides the analysis of antibody responses, the characterization of antigen-specific B cells may provide important insights into vaccine-induced protection. LLPCs and MBCs can persist in the human body for years or even decades and are responsible for conferring long-term immunity (Akkaya et al., 2020, Siegrist, 2018, Nishio et al., 2022, West and Calandra, 1996, Goldblatt et al., 2022a).

The aim of this thesis was the comprehensive analysis of antibody structure and functionality, as well as frequencies and phenotype of B cells induced by vaccination against HCoV. For this purpose, several antigen-specific assays were developed, and applied to study the immune responses induced by rMVA-based vaccine candidates against MERS and COVID-19, that were investigated in phase 1 clinical trials at the University Medical Center Hamburg-Eppendorf (UKE). In order to put these results into clinical perspective, the abovementioned analyses were also performed on samples of healthy and immunocompromised patients vaccinated with licensed COVID-19 vaccines.

2 Publications

Briefly, this cumulative doctoral thesis is based on the following publications: The first one, *“Persistence of MERS-CoV-spike-specific B cells and antibodies after late third immunization with the MVA-MERS-S vaccine”*, was published in the journal *Cell Reports Medicine* (Weskamm et al., 2022b) and describes the immunogenicity of the MVA-MERS-S vaccine, investigating the impact of a late booster vaccination and focusing on antibody and B cell responses assessed by different techniques. Additional data on non-neutralizing antibody functions elicited by the MVA-MERS-S vaccine are shown in the *Unpublished data* section. Subsequently, the methods established for analysis of MERS-CoV spike-specific antibodies and B cells were adjusted to the spike protein of SARS-CoV-2. A detailed description for the characterization of antigen-specific MBCs using multi-color flow cytometry was published in the journal *STAR protocols* under the title *“Flow cytometric protocol to characterize human memory B cells directed against SARS-CoV-2 spike protein antigens”* (Weskamm et al., 2022a). Different assays were then applied to study humoral and B cell responses elicited by MVA-SARS-2-S and MVA-SARS-2-ST, in direct comparison to licensed COVID-19 vaccines based on mRNA and ChAd vaccine platforms. Together with data on T cell responses investigated by Leonie Mayer based on the same study cohorts, these data led to the joint manuscript *“Humoral and cellular immunogenicity of two MVA-based COVID-19 vaccine candidates compared to ChAd and mRNA platforms”*, which has been submitted to the journal *Nature Communications* on the 16th of December 2022 (Mayer and Weskamm, submitted to *Nature Communications*).

In addition to the three first author publications described above, the experimental work of this thesis contributed to additional publications from different collaborations, resulting in three co-authorships: Meyer Zu Natrup et al. (2022) report the results from the pre-clinical studies of the MVA-SARS-2-S/ST vaccines in the publication *“Stabilized recombinant SARS-CoV-2 spike antigen enhances vaccine immunogenicity and protective capacity”* in the *Journal of Clinical Investigation*. Mellinghoff et al. (2022a, 2022b) describe humoral and cellular responses elicited by a second and third COVID-19 vaccination in chronic lymphocytic leukemia (CLL) patients in the two publications *“SARS-CoV-2 specific cellular response following COVID-19 vaccination in patients with chronic lymphocytic leukemia”* and *“SARS-CoV-2-specific cellular response following third COVID-19 vaccination in patients with chronic lymphocytic leukemia”*, in the journals *Leukemia* and *Haematologica*, respectively.

2.1 Persistence of MERS-CoV-spike-specific B cells and antibodies after late third immunization with the MVA-MERS-S vaccine

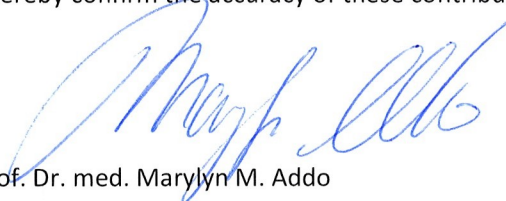
Leonie M. Weskamm, Anahita Fathi, Matthijs P. Raadsen, Anna Z. Mykytyn, Till Koch, Michael Spohn, Monika Friedrich, MVA-MERS-S Study Group, Bart L. Haagmans, Stephan Becker, Gerd Sutter, Christine Dahlke* and Marylyn M. Addo*

*These authors contributed equally

Published in *Cell Reports Medicine*, DOI: 10.1016/j.xcrm.2022.100685

Leonie Marie Weskamm established the bead-based multiplex ELISA for analysis of MERS-CoV spike-specific antibody isotypes and subclasses, as well as the IgG ELISpot and the flowcytometric assay for analysis of MERS-CoV spike-specific B cells, and planned and conducted all related experiments and data analysis. She was also responsible for data visualization and created Figures 1 to 6 as well as Supplementary Figures S2 to S4. She wrote the major part of the original manuscript draft and was involved in the communication with the collaboration partners who conducted the analysis of binding IgG and neutralizing antibodies, as well as the correlation analysis shown in Figure 7. During the publication process, she was involved in the revision of the manuscript and the communication with the journal editors.

I hereby confirm the accuracy of these contributions

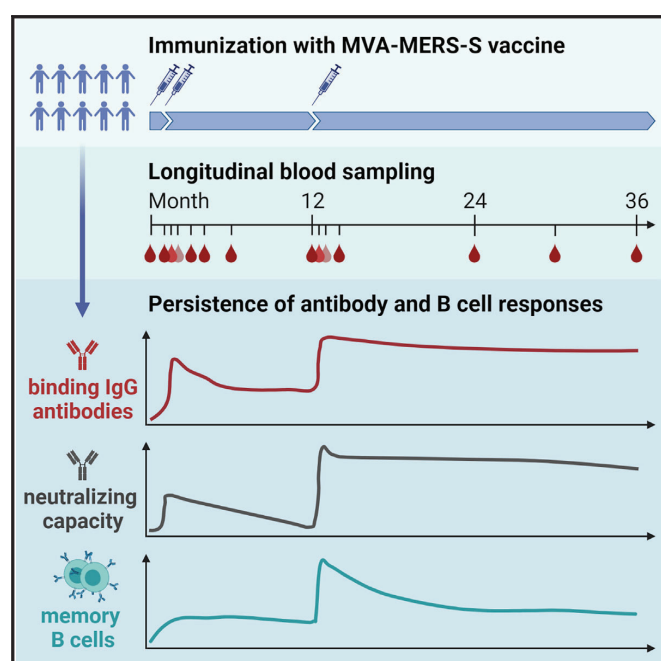


Prof. Dr. med. Marylyn M. Addo

17.1.2023

Persistence of MERS-CoV-spike-specific B cells and antibodies after late third immunization with the MVA-MERS-S vaccine

Graphical abstract



Authors

Leonie M. Weskamm, Anahita Fathi, Matthijs P. Raadsen, ..., Gerd Sutter, Christine Dahlke, Marylyn M. Addo

Correspondence

m.weskamm@uke.de (L.M.W.),
c.dahlke@uke.de (C.D.)

In brief

Weskamm et al. longitudinally describe B and T cell responses as well as antibody subclasses and neutralization capacity induced by three homologous immunizations with the MVA-MERS-S vaccine candidate. A late booster vaccination significantly enhances the frequency and persistence of memory B cells, binding IgG1 and neutralizing antibodies.

Highlights

- A late boost with the MVA-MERS-S vaccine enhances frequency of antibodies and B cells
- Binding IgG and neutralizing antibodies persist for 2 years after the late boost
- Responses specific to MERS-CoV-spike S1 and S2 subunits show distinct dynamics
- Vaccine-induced antibodies predominantly belong to IgG1 and IgG3 subclasses



Weskamm et al., 2022, Cell Reports Medicine 3, 100685
July 19, 2022 © 2022 The Author(s).
<https://doi.org/10.1016/j.xcrm.2022.100685>





Article

Persistence of MERS-CoV-spike-specific B cells and antibodies after late third immunization with the MVA-MERS-S vaccine

Leonie M. Weskamm,^{1,2,3,*} Anahita Fathi,^{1,2,3,6} Matthijs P. Raadsen,⁷ Anna Z. Mykytyn,⁷ Till Koch,^{1,2,3,6} Michael Spohn,^{8,9,10} Monika Friedrich,^{1,2,3} MVA-MERS-S Study Group, Bart L. Haagmans,⁷ Stephan Becker,^{4,11} Gerd Sutter,^{5,12} Christine Dahlke,^{1,2,3,13,14,*} and Marylyn M. Addo^{1,2,3,6,13}

¹Institute for Infection Research and Vaccine Development (IIRVD), University Medical Centre Hamburg-Eppendorf, Hamburg, Germany

²Department for Clinical Immunology of Infectious Diseases, Bernhard Nocht Institute for Tropical Medicine, Hamburg, Germany

³German Centre for Infection Research, Hamburg-Lübeck-Borstel-Riems, Germany

⁴German Centre for Infection Research, Gießen-Marburg-Langen, Germany

⁵German Centre for Infection Research, München, Germany

⁶First Department of Medicine, Division of Infectious Diseases, University Medical Centre Hamburg-Eppendorf, Hamburg, Germany

⁷Department of Virology, Erasmus Medical Centre, Rotterdam, the Netherlands

⁸Research Institute Children's Cancer Centre Hamburg, Hamburg, Germany

⁹Department of Pediatric Hematology and Oncology, University Medical Centre Hamburg-Eppendorf, Hamburg, Germany

¹⁰Bioinformatics Core Unit, Hamburg University Medical Centre, Hamburg, Germany

¹¹Institute for Virology, Philipps University Marburg, Marburg, Germany

¹²Division of Virology, Institute for Infectious Diseases and Zoonoses, Department of Veterinary Sciences, LMU Munich, Munich, Germany

¹³These authors contributed equally

¹⁴Lead contact

*Correspondence: m.weskamm@uke.de (L.M.W.), c.dahlke@uke.de (C.D.)

<https://doi.org/10.1016/j.xcrm.2022.100685>

SUMMARY

The Middle East respiratory syndrome (MERS) is a respiratory disease caused by MERS coronavirus (MERS-CoV). In follow up to a phase 1 trial, we perform a longitudinal analysis of immune responses following immunization with the modified vaccinia virus Ankara (MVA)-based vaccine MVA-MERS-S encoding the MERS-CoV-spike protein. Three homologous immunizations were administered on days 0 and 28 with a late booster vaccination at 12 ± 4 months. Antibody isotypes, subclasses, and neutralization capacity as well as T and B cell responses were monitored over a period of 3 years using standard and bead-based enzyme-linked immunosorbent assay (ELISA), 50% plaque-reduction neutralization test (PRNT50), enzyme-linked immunospot (ELISpot), and flow cytometry. The late booster immunization significantly increases the frequency and persistence of spike-specific B cells, binding immunoglobulin G1 (IgG1) and neutralizing antibodies but not T cell responses. Our data highlight the potential of a late boost to enhance long-term antibody and B cell immunity against MERS-CoV. Our findings on the MVA-MERS-S vaccine may be of relevance for coronavirus 2019 (COVID-19) vaccination strategies.

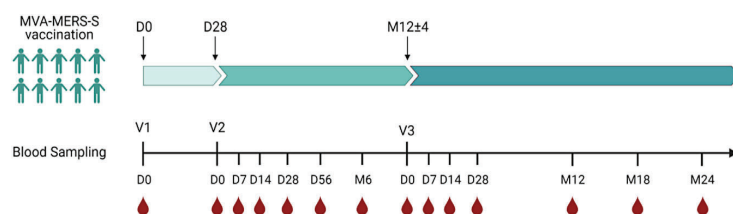
INTRODUCTION

The Middle East respiratory syndrome (MERS) is a viral respiratory disease caused by MERS-coronavirus (MERS-CoV),^{1,2} which was first identified in a patient in Saudi Arabia in 2012.³ As a disease of the lower respiratory tract, MERS can progress rapidly from unspecific, influenza-like symptoms to severe pneumonia, multiple organ failure, and death. Primary transmission of MERS-CoV infections is linked to exposure to dromedary camels.^{4,5} Secondary infections can occur via human-to-human transmission, with nosocomial and household outbreaks accounting for most cases.^{6,7} As of February 2022, 2,585 cases, including 890 associated deaths, were reported in 27 countries with a case fatality rate of 34.4%.⁸ There are no licensed vac-

cines or specific therapeutic options available to prevent or treat MERS-CoV infection. However, effective countermeasures are crucial to avoid potential future outbreaks and to prevent infections of persons at risk.

In general, vaccine-induced immune responses include activation and priming of naive T and B cells. With regard to the B cell population, vaccination induces short living plasmablasts and plasma cells secreting high amounts of antibodies. Furthermore, B cell activation can result in the generation of two long-lasting cell populations, namely long-lived plasma cells (LLPCs) and memory B cells (MBCs). Both can be maintained for a long time in the absence of the specific antigen^{9,10} and contribute to the maintenance of immunological memory. Antibodies can exhibit neutralizing activity via their fragment




Figure 1. Study design

Study participants ($n = 10$) received two vaccinations with MVA-MERS-S (V1 and V2) 28 days apart and a late third vaccination (V3) at 12 ± 4 months after prime. Blood was frequently sampled for up to 2 years after V3 at indicated time points (see also Table S1). Figure was created with BioRender.com.

antigen-binding (Fab) region, whereas structural properties of the fragment crystallizable (Fc) region classify antibodies into immunoglobulin (Ig) isotypes (e.g., IgA, IgG, IgM) and subclasses (IgA1–2, IgG1–4) that differ in their abundance and non-neutralizing functional capacities. While the exact vaccine-induced correlates of protection against MERS have not been identified thus far, humoral immune responses are considered to be critical in mediating protection against infection and severe disease.

A variety of MERS vaccines have been developed and tested in preclinical stages.^{2,11} Most of them are based on the MERS-CoV-spike (S) protein, which is the primary inducer of the host immune response. MERS-CoV-S is composed of an N-terminal S1 subunit and a C-terminal S2 subunit and can be cleaved at the junction between the two subunits either during viral biogenesis or upon encounter of target cells.^{12,13} The S protein acquires different conformations while mediating the entry of the virus into the host cell. To initiate infection, the receptor-binding domain (RBD) contained in the S1 subunit recognizes its host cell receptor dipeptidylpeptidase 4 (DPP4), followed by the fusion of viral and host cell membrane mediated by the S2 subunit.^{14,15} Neutralizing antibodies that target the S protein can therefore block virus attachment and entry into the host cell. Thus far, only three vaccine candidates have reported their results from early-phase clinical trials showing safety and immunogenicity.^{16–19} One of them is the viral vector vaccine MVA-MERS-S, which is based on the recombinant modified vaccinia virus Ankara (rMVA) vector platform and encodes the full-length S protein (GenBank: JX869059).²⁰ Between 2017 and 2019, we evaluated MVA-MERS-S at two dose levels (low dose: 1×10^7 plaque-forming units [PFUs], high dose: 1×10^8 PFU) for safety and immunogenicity in a first-in-human phase 1 clinical trial in 23 participants¹⁶ (ClinicalTrials.gov: NCT03615911).

A homologous prime-boost immunization using a 28-day interval revealed a benign safety profile and was effective in inducing humoral and cell-mediated immune responses against MERS-CoV-S1.¹⁶ Seroconversion was detected in 87% of all participants and in 100% of the high-dose cohort. However, antibodies waned within 6 months. A follow-up study was initiated to assess safety and immunogenicity of a late third immunization with MVA-MERS-S (1×10^8 PFU) at 12 ± 4 months after prime vaccination in a subgroup of 10 participants.²¹ Seven of these individuals were included in a long-term observational study and followed up with for another 2 years.

We here analyzed antibody as well as T and B cell responses specific to the S1 and S2 subunit of MERS-CoV-S to gain comprehensive insights into adaptive immunity induced by three vaccinations with MVA-MERS-S. A specific focus of our study is

the induction and longevity of MBCs as well as the distribution of antibody isotypes and subclasses. Antibody analysis was conducted using a standard and a bead-based multiplex enzyme-linked immunosorbent assay (ELISA) as well as a 50% plaque-reduction neutralization test (PRNT50), whereas T and B cell responses were assessed by enzyme-linked immunospot (ELISpot) and flow cytometry assays. Our findings highlight the benefits of a late third vaccination, demonstrating for the first-time persistence of MERS-CoV-specific vaccine-induced humoral immunity over a 2-year period.

RESULTS

Being part of a phase 1 trial initiated in December 2017, a subgroup of ten study participants received three doses of the viral vector vaccine MVA-MERS-S encoding the MERS-CoV-S protein. The first two immunizations were administered 28 days apart with a late third immunization 12 ± 4 months after prime vaccination. Immune responses were monitored after each vaccination and followed up on for another 2 years (Figure 1).

Late third immunization with MVA-MERS-S resulted in robust and long-lasting binding IgG and neutralizing antibodies but less pronounced T cell responses

In a first step, we monitored MERS-CoV-S-specific antibodies and T cells to gain a broad overview on adaptive immune responses following three vaccinations with MVA-MERS-S (Figure 2).

Binding IgG antibody responses were evaluated using an in-house ELISA based on a full-length recombinant MERS-CoV-S protein (Figure 2A). Both the second and third immunization (V2 and V3, respectively) induced S-specific IgG antibody levels above the cutoff in all ten vaccinees. The IgG responses induced by V2 peaked at V2:day 14 and declined during the next months but stayed above the cutoff (optical density [OD] 0.1) in 100% of the study participants ($n = 10/10$) for approximately 12 months after prime immunization (V3:day 0). Following V3, antibody levels rapidly increased and were maintained above cutoff throughout the entire study period for all analyzed vaccinees ($n = 7/7$; V3:months 18–24). IgG responses induced by V2 reached a median OD of 0.8 at V2:day 14 and showed a broad range in magnitude (min–max: 0.3–1.8 OD). In comparison, V3 induced a very strong and homogenous response of S-specific IgG in all vaccinees, resulting in a median OD value of 1.8 (min–max: 1.6–2.3 OD) and a fold change of 2.6 at V3:day 14 compared with V2:day 14.

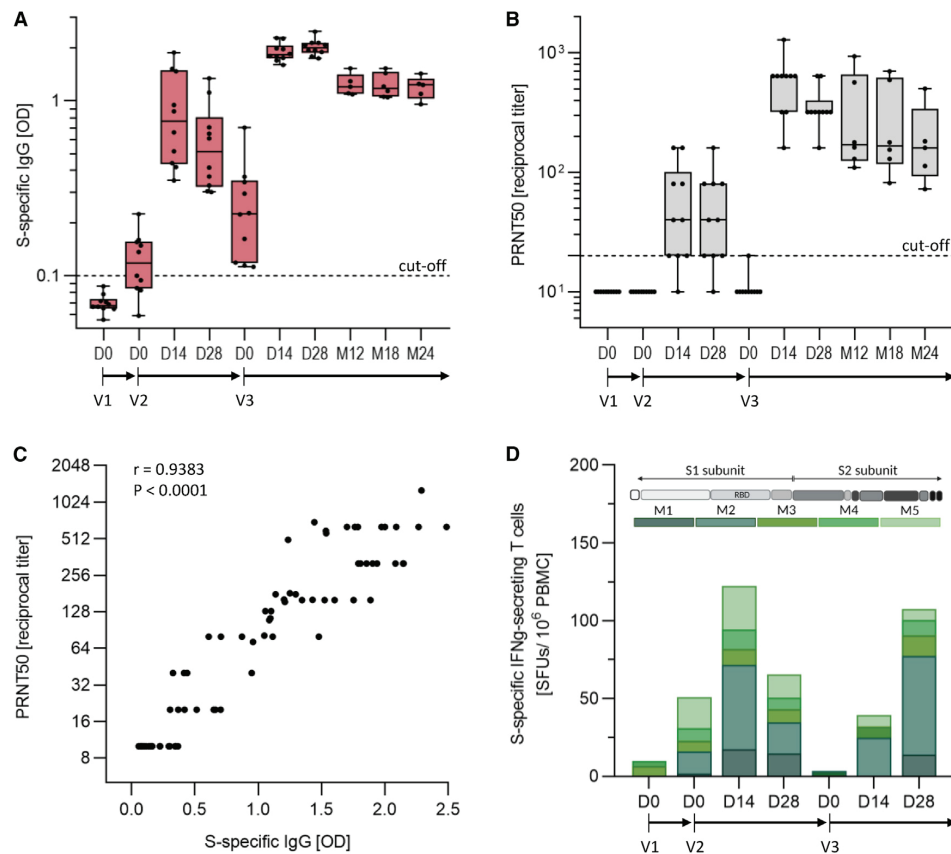


Figure 2. MERS-CoV-S-specific humoral and T cell responses induced by three vaccinations with MVA-MERS-S

(A) Longitudinal dynamics of S-specific IgG antibodies. Shown are the optical density (OD) values measured at 450–620 nm by ELISA. Data are represented as individual data points (mean of technical duplicates) and median \pm interquartile range (IQR).

(B) Neutralization activity of serum antibodies as measured by 50% plaque-reduction neutralization test (PRNT50). Data are represented as individual data points and median \pm IQR.

(C) Spearman correlation between S-specific IgG antibodies and serum neutralization activity.

(D) T cell responses as measured by IFN γ ELISpot after stimulation with five overlapping peptide (OLP) pools (M1–M5), spanning the entire MERS-CoV-S amino acid sequence. Shown are the median values of spot forming units (SFUs; mean of technical triplicates) across all vaccinees ($n = 10$) for each OLP pool. Number of samples, median, and p values for each time point and all three assays are shown in Table S2.

Serum neutralization capacity was assessed by PRNT50 (Figure 2B). While V1 did not induce neutralizing antibodies, V2 led to an increased titer in 90% of participants ($n = 9/10$) with a median reciprocal titer of 40 (min–max: 10–160) at V2:day 14. Neutralizing antibody titers declined during the following year, resulting in titers below the cutoff in 90% ($n = 9/10$) of the study participants. Upon V3, all participants generated neutralizing antibody responses, showing a strong increase compared with V2 with a median reciprocal titer of 640 (min–max: 160–1,280) at V3:day 14. During the following 12–24 months, the titer of neutralizing antibodies continuously decreased but stayed above the threshold in 100% of the analyzed study participants ($n = 7/7$). Two years after the late boost immunization, 80% of the partic-

ipants ($n = 4/5$) showed neutralizing antibody titers persisting at levels at least 3-fold higher (min–max: 3- to 16-fold) compared with the peak response induced by the second vaccination (V2:day 14), whereas one vaccinee showed a titer similar to V2:day 14.

S-specific IgG antibody titers measured by ELISA showed a positive correlation with the serum neutralization capacity measured by PRNT50, as shown in Figure 2C ($r = 0.9383$, $p < 0.0001$).

Besides antibodies, T cell responses also represent a key element of the adaptive immune system and were evaluated by interferon- γ (IFN γ) ELISpot in this study. Peripheral blood mononuclear cells (PBMCs) were stimulated with five

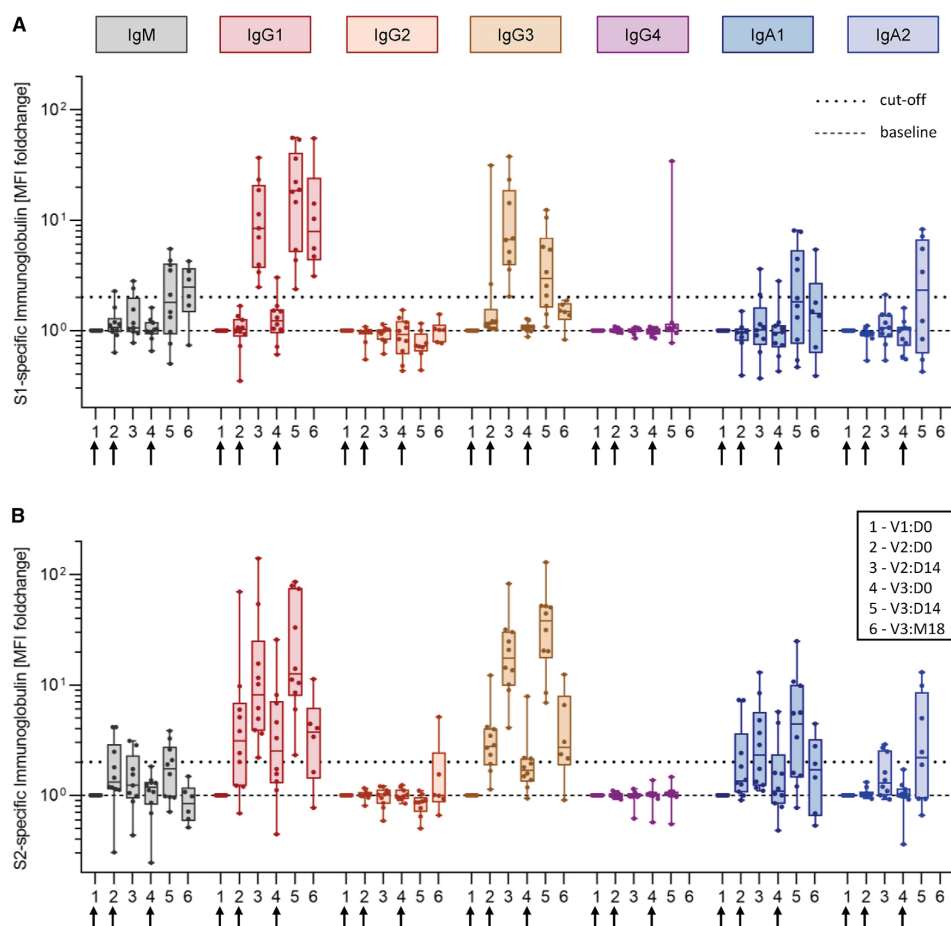


Figure 3. Isotype and subclass distribution within vaccine-induced MERS-CoV-S-specific antibodies

S1- (A) and S2- (B) specific responses of IgM, IgG1–4, and IgA1–2 at different time points after vaccination, displayed as fold changes of median fluorescence intensities (MFIs; measured by bead-based ELISA) compared with baseline values at V1:day 0. Data are represented as individual data points (mean of technical duplicates) and median \pm IQR. Number of samples and median fold changes are shown in [Table S3](#).

overlapping peptide (OLP) pools (M1–M5) spanning the entire MERS-CoV-S protein. S-specific T cell responses first emerged after a single shot of MVA-MERS-S in 40% of the vaccinees ($n = 4/10$; V2:day 0) and were further enhanced after the V2, with peak responses observed at V2:day 14 ([Figure 2D](#); see also [Figure S1](#) and [Koch et al. ¹⁶](#)). Overall, MERS-CoV-S-specific $IFN\gamma$ secretion was detected in 80% (8/10) of all participants at one or more time points throughout the first two vaccinations until V3:day 0. Following the third vaccination, 50% of the participants ($n = 5/10$) showed an $IFN\gamma$ secretion at the analyzed time points. Across all study participants, T cell responses were observed to all five OLP pools, but responses to pool M2, which covers the RBD sequence, were most frequently detected ($n = 7/10$). Depicting the median value of $IFN\gamma$ responses across all ten vaccinees for each OLP pool, [Figure 2D](#) demonstrates the

peak response at V2:day 14 as well as the predominant responses to M2 after both V2 and V3.

Taken together, these data demonstrate that V2 induced detectable humoral and T cell responses in 100% ($n = 10/10$) and 80% ($n = 8/10$) of vaccinees, respectively, which declined during the following months. The late V3 homogeneously induced anti-S IgG levels in 100% ($n = 10/10$) of the vaccinees, exceeding the levels induced by V2 and showing enhanced persistence. In comparison, T cell responses after V3 were more diverse and less pronounced than after V2.

Antibodies induced by MVA-MERS-S predominantly belong to IgG1 and IgG3 subclasses

To gain insight into the distribution of antibody isotypes and subclasses induced by MVA-MERS-S vaccination, we longitudinally

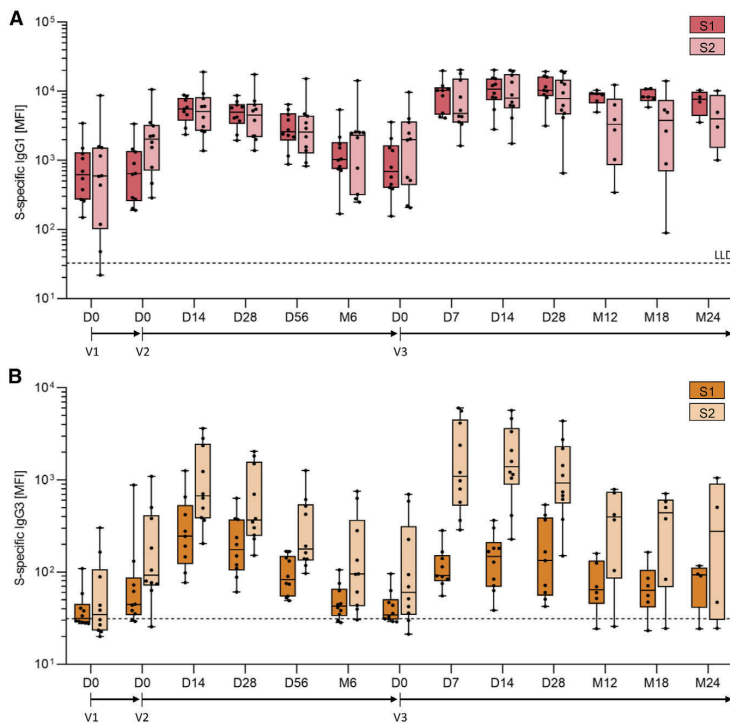


Figure 4. Longitudinal dynamics of MERS-CoV-S-specific IgG1 and IgG3 antibodies

Vaccine-induced S1/S2-specific IgG1 (A) and IgG3 (B) are displayed as MFI, measured by bead-based multiplex ELISA. Data are represented as individual data points (mean of technical duplicates) and median \pm IQR. LLD, lower limit of detection. Number of samples, median, and p values for each time point are shown in Table S4.

after prime at V2:day 0 in 70% ($n = 7/10$) of the study participants. In comparison, S1-specific IgG3 was only detectable in 20% ($n = 2/10$) of the participants, and no vaccinee showed S1-specific IgG1 at this early time point (Figures 3A and 3B).

Individual levels of S1/S2-specific IgG1 and IgG3 are depicted in Figures 4A and 4B, highlighting that IgG1 was homogeneously and strongly induced in all participants after both V2 and V3, while the magnitude of IgG3 responses showed a broader distribution within the cohort. Comparing peak responses induced by V2 and V3, S1-specific IgG1 showed a 2.3-fold increase after V3 compared with V2. S2-specific responses resulted in a fold change of 1.7. Comparing the median of MFI values, S1- and S2-specific IgG1 reached similar levels at V2:day 14 (S1:

analyzed plasma samples using a bead-based multiplex ELISA. The median fluorescence intensity (MFI) was used as a relative measure for antibody responses. An induction of 2-fold above baseline (V1:day 0) was defined as a positive assay response. For IgM and IgA antibodies, we observed only a slight induction that was not consistent throughout the cohort (Figures 3A and 3B). With regard to IgG subclasses, MERS-CoV-S-specific IgG1 and IgG3 showed vaccine-induced responses with peak levels observed 14 days after V2 and V3. By contrast, only one of the participants reached the threshold values for IgG2 and IgG4, respectively (Figures 3A and 3B).

At V2:day 14, 100% of the study participants showed a positive assay response for S1- and S2-specific IgG1 and IgG3 (S1: $n = 9/9$; S2: $n = 10/10$). Plasma levels of both subclasses waned during the following months until V3:day 0, resulting in levels above cutoff in 10% (S1/IgG1, $n = 1/10$), 0% (S1/IgG3, $n = 0/10$), 50% (S2/IgG1, $n = 5/10$), and 30% (S2/IgG3, $n = 3/10$) of the study participants, respectively. V3 reinduced S1-specific IgG1 and S2-specific IgG1 and IgG3 in 100% ($n = 10/10$) as well as S1-specific IgG3 in 70% ($n = 7/10$) of participants. Notably, the antibody responses induced by V3 persisted for a longer period of time than those induced by V2. At the late time point V3:month 18, antibody levels persisted above the cutoff in 100% (S1/IgG1, $n = 6/6$), 0% (S1/IgG3, $n = 0/6$), 66.7% (S2/IgG1, $n = 4/6$), and 83.3% (S2/IgG3, $n = 5/6$) of participants.

S2-specific antibodies were induced earlier than those specific to S1, with S2-specific IgG1 and IgG3 responses detected 28 days

5,483; S2: 5,079), whereas S1- exceeded S2-specific IgG1 at V3:day 14 (S1: 10,714; S2: 7,894). In comparison, S1-specific IgG3 responses decreased at V3:day 14 compared with V2:day 14, whereas IgG3 responses toward S2 increased 1.6-fold. As opposed to IgG1, IgG3 responses resulted in higher MFIs for S2- than for S1-specific responses both after V2 (S1: 244; S2: 671) and V3 (S1: 147; S2: 1,401). Although peak responses after V3 were observed at V3:day 7, S1- and S2-specific IgG1 and IgG3 were already elevated at V3:day 7, indicating a rapid response of antibody secretion following the late immunization. The peak antibody level was prolonged until V3:day 28.

MERS-CoV-S-specific B cells were induced by MVA-MERS-S vaccination and persisted for up to 2 years

We here investigated the frequency of antigen-specific B cells (ASBCs) induced by MVA-MERS-S vaccination using an IgG ELISpot with pre-stimulated PBMCs. MERS-CoV-S1/S2-specific ASBCs were quantified as spot-forming units (SFUs) per million PBMCs (Figures 5A–5C). ASBCs showed a first peak 14 days after the second vaccination (V2:day 14), but their numbers declined during the following 8–14 months. Notably, they were again rapidly induced after V3 at numbers significantly higher than after V2.

Comparing responses against the two MERS-CoV-S subunits, S2-specific ASBCs were already induced by V1 in 50% of vaccinees (V2:day 0: $n = 5/10$, median SFU = 8), while S1-specific ASBCs were not detectable at this early time point. V2 induced

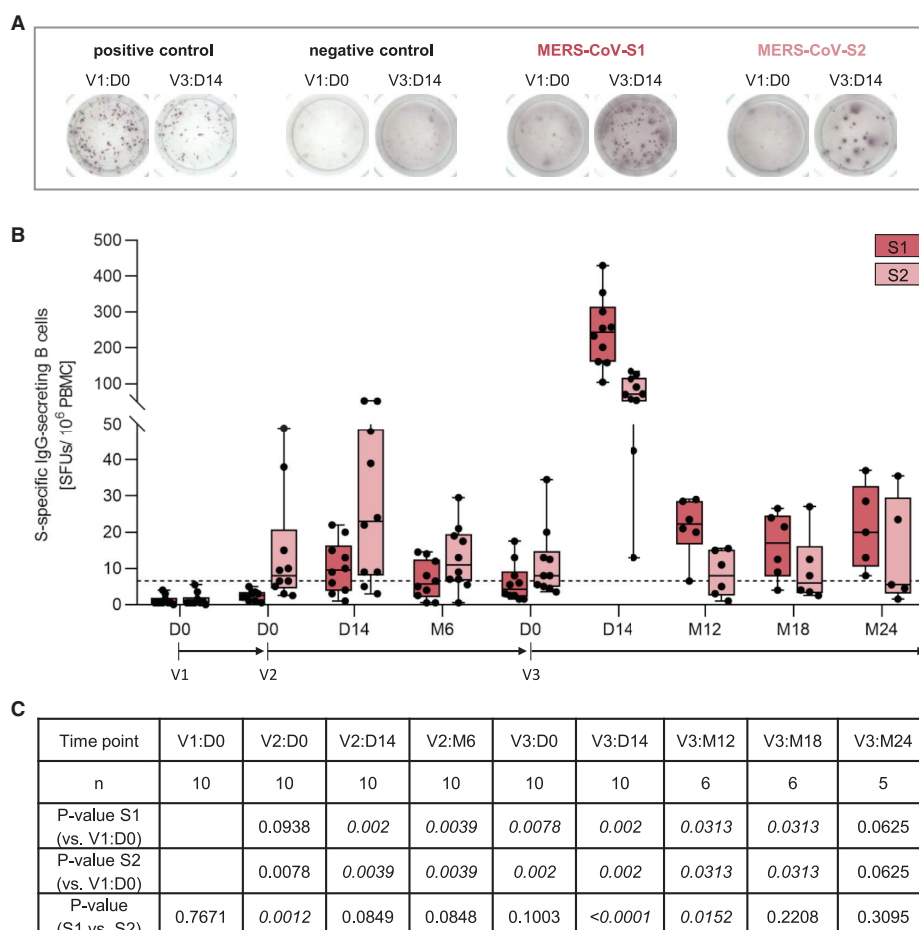


Figure 5. Antigen-specific B cell responses induced by MVA-MERS-S vaccination

(A) Representative IgG ELISpot images of antigen-specific and control wells for PBMCs taken before the first (V1:day 0) and after the third vaccination (V3:day 14). (B) Frequencies of vaccine-induced S1/S2-specific B cells displayed as SFUs/ 10^6 PBMCs as determined by IgG ELISpot. Data are represented as individual data points (mean of technical duplicates) and median \pm IQR. The dotted line indicates the cutoff value (6.6 SFUs/ 10^6 PBMCs). (C) p values as determined by Wilcoxon signed rank test (between time points) and Mann Whitney U test (between S1 and S2 responses). Number of samples, median, and p values for each time point are shown in [Table S5](#).

higher numbers of S2- than S1-specific ASBCs (median SFUs: S2 = 23, S1 = 9.5), with 80% of the participants ($n = 8/10$) showing responses above the cutoff for S2 and 60% ($n = 6/10$) for S1 at the time point V2:day 14. Prior to late V3 (V3:day 0), S2-specific ASBCs were still present above the cutoff in 60% ($n = 6/10$) of participants compared with 30% ($n = 3/10$) for S1-specific B cells. V3 increased the frequency of both S1- and S2-specific ASBCs, resulting in peak responses at day 14 (V3:day 14). All vaccinees ($n = 10/10$) showed responses above the cutoff for both S subunits at this time point but with higher frequencies of S1- compared with S2-specific ASBCs (median values: S1: 243.8 SFUs, S2: 70.5 SFUs). Comparing peak responses of ASBCs induced by V2 and V3, the number of both

S1- and S2-specific ASBCs was significantly higher at V3:day 14 compared with V2:day 14 (Wilcoxon signed rank test: S1: $p = 0.002$, S2: $p = 0.0059$), with median fold changes of 24.9 and 2.8 for S1 and S2, respectively. The number of ASBCs decreased following V3:day 14 but persisted above the cutoff throughout the whole study period in 85.7% of all analyzed participants ($n = 6/7$) for S1 and 28.6% of participants ($n = 2/7$) for S2 (V3:months 12–24). Notably, the numbers of S1-specific ASBCs detected 12 to 24 months after V3 were higher than those of the peak response after V2, with median values of 22, 17, and 20 SFUs (V3:month 12, V3:month 18, V3:month 24) compared with 9.5 SFUs (V2:day 14). Overall, the number of S2-specific ASBCs was higher following V1 and V2, but S1-specific

ASBCs showed a rapid and strong increase after V3 and remained detectable until the end of the study.

MERS-CoV-S-specific MBCs predominantly belong to the IgG isotype and showed an activated phenotype after late third vaccination

To specifically analyze the induction and phenotype of antigen-specific MBCs, we performed a flow cytometric assay using a combination of fluorescently labeled antigen probes for recognition of MERS-CoV-S-specific B cells (Figures 6A and S2).

The percentage of the total MBC compartment stayed constant over time and was not influenced by vaccinations (Figure S3). However, a detailed analysis of MERS-CoV-S-specific MBCs revealed an increase following MVA-MERS-S vaccination, showing distinct dynamics for each isotype (Figures 6B and S3). For S-specific MBCs of the IgM isotype, no significant changes in the median frequency (MFR) were observed at any time point after V1, V2, or V3 compared with baseline (p values for all time points are shown in Table S6). In comparison, the population of S-specific IgG⁺ MBCs showed a first significant increase at V2:day 7 (MFR = 0.15%) with a fold change of 1.9 compared with V1:day 0 (MFR = 0.075%). From this time point on, the population of S-specific IgG⁺ MBCs stayed elevated at a significant level until V3:month 18. The frequency of S-specific IgG⁺ MBCs ranged from 0.11% to 0.17% between V2:day 7 and V3:day 0 and was strongly enhanced after the late boost, resulting in a fold change of 11.3 for the peak response at V3:day 14 (MFR = 0.89%). Alongside peak responses at V3:day 14, an induction of S-specific MBCs was already observed at V3:day 7 (MFR = 0.36%; fold change = 5.2) and prolonged until V3:day 28 (MFR = 0.885%; fold change = 10.8). Notably, frequencies declined to 0.19% at V3:month 12 but stayed 2.5-fold above baseline until the end of study (V3:month 24). For the IgA isotype, S-specific MBCs revealed no significant changes following V1 and V2, whereas V3 induced significant increases at V3:day 14 (MFR = 0.4%; fold change = 3.8) and V3:day 28 (MFR = 0.17%; fold change = 2.2) compared with V1:day 0 (MFR = 0.09%). The levels declined but stayed above baseline at late time points (V3:month 12 to V3:month 24; fold changes ranging from 1.1 to 1.5).

Since the IgG⁺ MBC population showed the strongest induction upon vaccination, we further characterized this subset for activation phenotypes, using the markers CD27 and CD21 (Figure 6C). At V1:day 0, the largest proportion (71.7%) of S-specific IgG⁺ MBCs showed a resting phenotype (CD27⁺CD21⁺), whereas activated (CD27⁺CD21⁻), intermediate (CD27⁻CD21⁻), and atypical (CD27⁻CD21⁺) MBCs were less frequent with MFRs of 12.9%, 5.3%, and 9.5%, respectively. Frequencies of activated MBCs were increased at days 7, 14, and 28 following both V2 and V3. Nevertheless, only V3 induced a significant enrichment of the activated MBC compartment with frequencies of 45.2%, 48.9%, and 36.2% at V3:day 7, V3:day 14, and V3:day 28, respectively.

Positive correlations were observed between early and late S2-specific IgG antibody and B cell responses

Correlation analysis was performed between IgG1, IgG3, and ASBC responses at different time points using correlograms

specific for S1 and S2 responses. Note that S-specific MBCs were included in both correlograms. Correlations of S1-specific antibody and B cell responses revealed a rather heterogeneous picture (Figure 7A) compared with S2-specific responses showing several clusters of positive correlations (Figure 7B). S1-specific responses showed positive correlations between single time points, with the strongest correlations observed for IgG1 (V2:day 14 versus V3:month 18) and IgG3 (V1:day 0 versus V3:month 18) as well as between IgG1 (V1:day 0) versus MBCs (V2:day 14). In comparison, the S2 correlogram revealed positive correlations for all three types of S2-specific responses: IgG1, IgG3, and ASBCs. With regard to IgG1, all time points correlated strongly with each other, while IgG3 responses correlated strongly after V2 and V3 but less so with baseline levels. For IgG1, IgG3, and ASBCs, the responses induced at V3:day 14 correlated with those persisting at V3:month 18. Early responses of both S2-specific ASBCs and S-specific MBCs correlated with S2-specific IgG1 and IgG3 antibody responses at all time points, with the strongest association observed between MBCs and IgG1.

DISCUSSION

The present study aimed at investigating vaccine-induced immunogenicity following V1, V2, and late V3 with the MERS vaccine candidate MVA-MERS-S. Here, we report on the immunogenic potential of a late boost vaccination, providing insight into T and B cell responses and describing for the first time long-term persistence of vaccine-induced MERS-CoV-S1- and -S2-specific antibodies and B cells.

The first two immunizations with MVA-MERS-S (V1 and V2) induced T cell and antibody responses, demonstrating a seroconversion of 100% (n = 11/11) in the high-dose cohort.¹⁶ Besides MVA-MERS-S, two other MERS vaccine candidates have been investigated in phase 1 clinical trials: the DNA-based candidate GLS-5300¹⁸ and the chimpanzee adenoviral vector ChAdOx1 MERS.^{17,19} Using a three-dose schedule over 12 weeks and a single shot, the vaccine candidates GLS-5300 and ChAdOx1 MERS induced seroconversion in 94% (n = 61/65) and 100% (high dose, n = 9/9) of the study participants, respectively.¹⁷⁻¹⁹ A recent phase 1b trial testing ChAdOx1 MERS completed the first MERS vaccine trial in Saudi Arabia underscoring an acceptable safety and immunogenicity profile in healthy Middle Eastern adults.¹⁹ Here, seroconversion occurred in 100% (n = 9/9) of participants who received the high dose. All three MERS vaccine candidates were shown to be safe and immunogenic, with antibody levels declining after vaccination but remaining above baseline until 6–12 months post prime immunization.¹⁶⁻¹⁹ T cell responses measured by IFN γ ELISpot were examined in all four studies and showed responses above the cutoff value in the majority of study participants throughout the study period.¹⁶⁻¹⁹

We extended our original trial by a late V3.²¹ While T cell responses following V3 were rather diverse, MERS-CoV-S-specific B cells and antibodies of the IgG isotype as well as neutralizing antibodies were rapidly and homogeneously induced in all vaccinees. In addition, the population of S-specific MBCs not only increased in frequency but was also enriched for activated

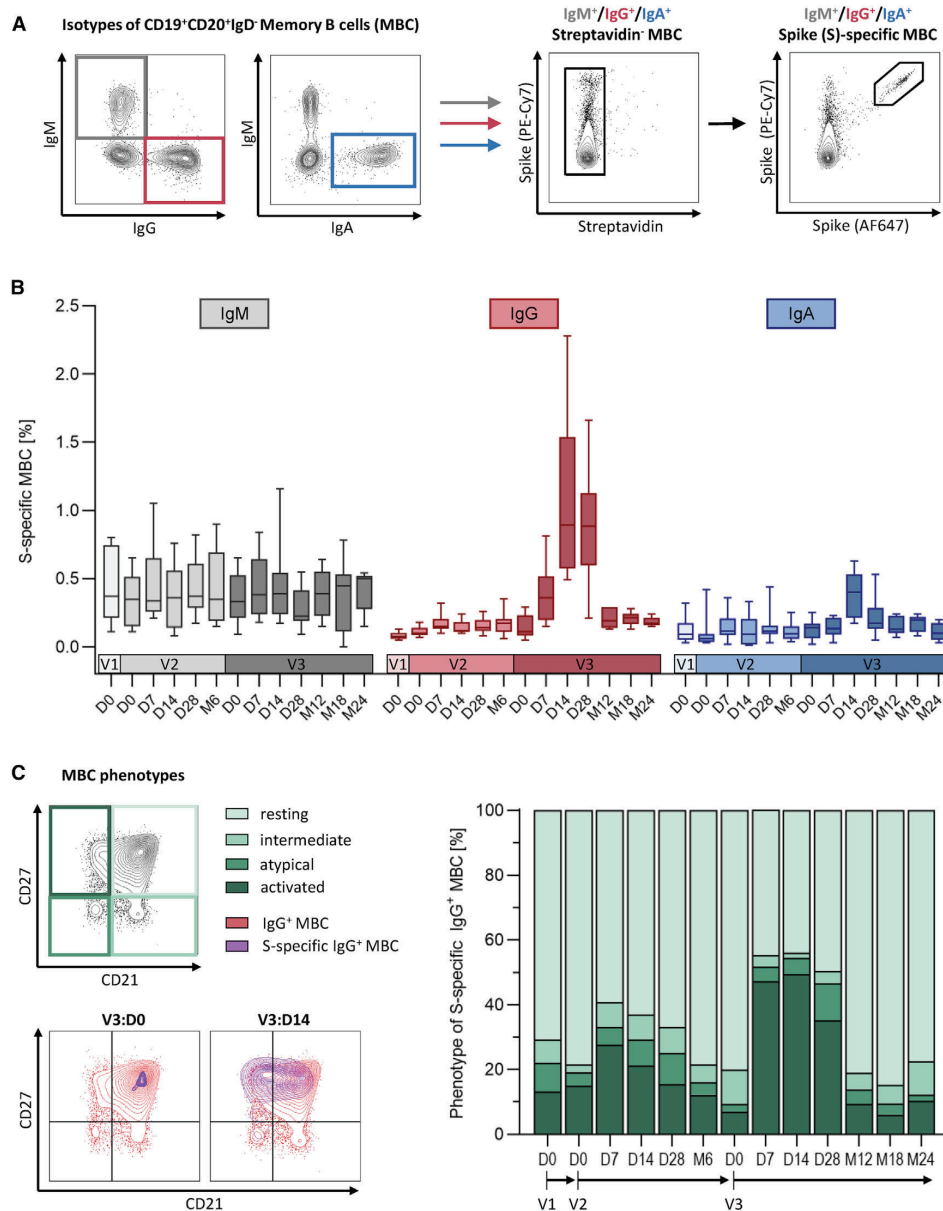


Figure 6. Characterization of vaccine-induced memory B cells

(A) Gating strategy for analysis of isotypes and MERS-CoV-S-specific cells within the memory B cell (MBC) population (representative contour plots belong to time point V3:day 14 from one study participant; gating strategy for identification of MBCs within whole PBMCs shown in Figure S2).

(B) Longitudinal dynamics of antigen-specific MBCs induced by three vaccinations with MVA-MERS-S (V1, V2, and V3). Data are displayed as frequencies of S-specific cells within IgM⁺/IgG⁺/IgA⁺ MBCs. Boxplots indicate median \pm IQR. Number of samples, median, and p values compared with V1:day 0 are shown in Table S6.

(C) Resting, intermediate, atypical, and activated MBC phenotypes as identified by expression of CD21 and CD27 (top left panel). Representative plots are shown for one study participant at V3:day 0 and V3:day 14 and depict overlaid contour plots of total IgG⁺ MBCs and S-specific IgG⁺ MBCs (bottom left panel). Longitudinal distributions of phenotypes within the S-specific IgG⁺ MBC compartment are shown as mean values of all study participants.

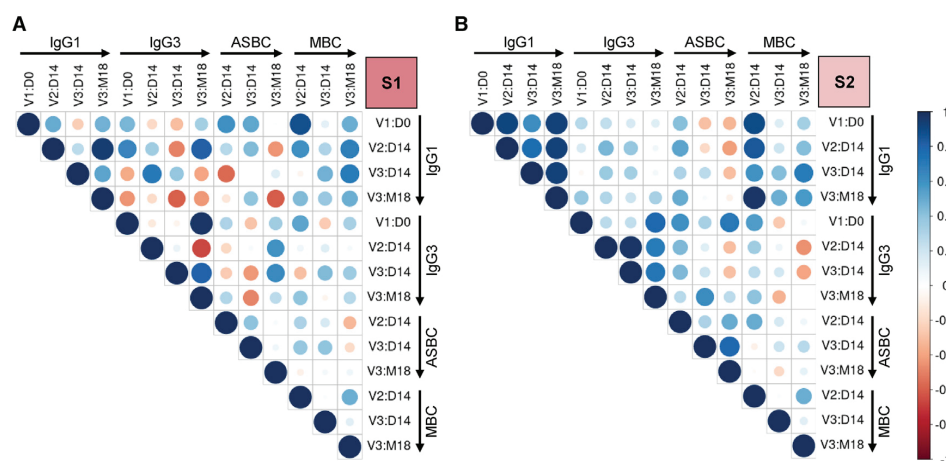


Figure 7. Correlation between vaccine-induced antibody and B cell responses

Correlation analysis of MERS-CoV-S1- (A) and -S2- (B) specific IgG1, IgG3, and ASBC responses at different time points after vaccinations 1, 2, and 3 (V1, V2, and V3). S-specific MBC responses were included into correlograms of both the S1 and S2 antigen. Positive correlations are shown in blue and negative correlations in red, as indicated by the color bar. Sample numbers included into correlation analysis are provided in Table S7.

MBCs (CD27⁺CD21⁻) resembling plasma cell precursors.²² This finding, together with antibody responses emerging early after V3 (V3:day 7), provides evidence for the generation of MBCs following V1 and V2, which were then reactivated upon V3. The observed long-lasting S-specific MBCs and ASBCs, but in particular, S1-specific IgG1 and neutralizing antibody responses, in all analyzed participants indicate enhanced induction of not only MBCs but also LLPCs after V3. LLPCs are responsible for maintaining plasma antibody levels, whereas MBCs can rapidly differentiate into antibody-secreting cells upon antigen re-exposure.²³ The strong and robust induction of MERS-CoV-S-specific B cells and antibodies detectable during the entire study period may contribute to preventing infection and shaping the disease course upon MERS-CoV infection. These findings emphasize the relevance of the late boost.

Several factors influence vaccine-induced immune responses, which are often multilayered and can be different for specific vaccine candidates. For example, vector immunity, innate immune responses,²⁴ and the developmental stage of MBCs²⁵ can impact the magnitude and quality of boost immune responses. It has been shown that a prolonged interval between prime and boost immunization can be a key element to enhance immunogenicity, as recently demonstrated for the coronavirus 2019 (COVID-19) adenovirus vector vaccine Vaxzevria (AstraZeneca, ChAdOx1 nCoV-19). The vaccine showed stronger immune responses and efficacy when the prime-boost interval was extended from 28 to 84 days.^{26,27} The impact of late boosting had been shown previously for the HIV vaccine RV144, where it led to higher IgG titers associated with higher neutralizing capacity,²⁸ and for an rMVA vaccine against H5N1 (MVA-H5-sfMR), which elicited the highest antibody responses when the boost was administered 1 year after prime immunization.²⁹ In the latter study, antibody-secreting cells were effi-

ciently induced after the late boost, whereas antigen-specific T cell responses varied considerably within the cohort,³⁰ a finding comparable to our observations. A recent publication by Munro et al. evaluated the impact of a V3 in a large COVID-19 vaccine trial, in which different prime and boost combinations based on a variety of vaccine platforms were investigated.³¹ Different magnitudes of humoral and cellular responses were revealed, depending on the type of vaccine administered for prime and boost immunization. These data highlight the complexity of vaccine-induced immune responses and that specific platforms and intervals might play a critical role for efficient boosting of the humoral, cellular, or both types of immune responses.

In the context of MERS-CoV-S subunits, studies evaluating immune responses to SARS-CoV, SARS-CoV-2, and MERS-CoV have emphasized the importance of responses to the S1 subunit, as they can comprise RBD-specific antibodies capable of blocking interactions with the host cell receptor DPP4. In previous clinical trials testing MERS vaccines, only S1-specific responses were monitored,^{16–18} whereas the impact of S2 has been understudied to date. However, a recent murine study emphasized its importance, as two monoclonal antibodies against an S2 epitope showed protection against MERS-CoV in mice.³² Here, we addressed vaccine-induced MERS-CoV-S2-specific responses in humans for the first time and observed that S2-specific antibodies and ASBCs were already detected following prime immunization in contrast to S1-specific responses, which were earliest detected after the V2. Due to its high conservation among betacoronaviruses, the S2 subunit has been discussed as a target for cross-reactive antibodies resulting from previous infections with different species of human CoVs (HCoVs). Particularly in the case of SARS-CoV-2 infection or vaccination, it is currently discussed that the conserved S2 subunit may trigger S2-specific responses early after antigen

encounter, and cross-reactivity was especially reported toward HCoV-OC43.³³ The isolated MERS-CoV-S2-specific monoclonal antibodies from the above-mentioned mouse study were also cross-reactive to HCoV-OC43.³² Our study participants were screened for pre-existing antibodies against the HCoVs HCoV-OC43, HCoV-229E, HCoV-HKU1, and HCoV-NL63 prior to the V1 with MVA-MERS-S.²¹ Pre-existing antibodies against HCoV-OC43 correlated with S2-specific ASBC responses after V1 and V2 and, to a lesser extent, with S1-specific ASBCs induced by V2 (Figure S4), whereas no correlations with other HCoVs were observed. Comparing antibodies and B cells induced by MVA-MERS-S, positive correlations were specifically observed between early and late time points of S2-specific responses, further underlining a potentially higher dependence of S2-specific responses on pre-existing levels of immunity compared with S1-specific responses, which may result in stronger S2-specific responses after V1. However, the role of early, cross-reactive S2-specific responses in preventing infection and modulating disease progression warrants further investigation.

The comprehensive analysis of antibody isotypes and subclasses may contribute to a better understanding of vaccine-induced protection, as they differ in their capacity to induce non-neutralizing effector functions whose relevance has been shown for a variety of infections and vaccinations.^{34–38} While neutralizing antibodies are critical for the prevention of virus entry into the host cell, non-neutralizing antibody functions are increasingly recognized as important mediators of virus control. The antibodies induced by MVA-MERS-S predominantly belong to the IgG1 and IgG3 subclasses, which are known to bind human Fc receptors with high affinity and to be potent activators of effector cells.³⁹ Notably, a similar pattern of IgG1 and IgG3 induction has also been observed following immunization with the adenoviral vector vaccine Vaxzevria.⁴⁰ IgG3 is a pro-inflammatory antibody subclass that has been associated with enhanced protection against viruses, e.g., in a trial of the RV144 HIV vaccine,^{35,41,42} and the here-observed robust IgG3 responses against the conserved S2 subunit may represent a critical element in the context of non-neutralizing functions. Future studies should include investigations on the functionality of antibodies by using systems serology approaches to better understand the full impact of MVA-MERS-S prime and boost immunizations on the quality of vaccine-induced antibodies.

Important aspects that need to be addressed in future trials are the exact contribution of dosing intervals, distinct boosting strategies, and heterologous prime-boost regimens to immunogenicity of MERS vaccines. While data on correlates of protection (CoPs) are still very limited for MERS-CoV, we can gain first insights into CoPs from SARS-CoV-2 infection. Here, neutralizing antibodies are suggested to be critical for protection against infection,^{43,44} while protection against severe disease is assumed to be at least partially driven by T cell responses.⁴⁵ The importance of neutralizing antibodies against MERS has been recently emphasized by Kim and colleagues. Using passive transfer of neutralizing antibodies from MERS survivors to mice, they observed significantly reduced viral loads and increased survival rates, suggesting a protective effect of neutralizing antibodies.⁴⁶ Whether MBCs can be used as a CoP, analogous to

the hepatitis B context,⁴⁷ remains unknown to date but was recently suggested in a publication on SARS-CoV-2 Delta-variant breakthrough infections. In this study, a lower frequency of virus-specific MBCs was detected in patients with breakthrough infection, providing first evidence that MBCs might be used as a CoP.⁴⁸ Our data on MVA-MERS-S highlight its potential to induce robust and long-lasting antibody and B cell responses and represent a promising basis for future studies. Whether these factors mediate protection against infection and/or disease severity and death is not addressable with the data presented here.

The here-observed kinetics of antibody persistence show similarities to those observed in MERS survivors, as reported by three studies monitoring their adaptive immune responses.^{46,49,50} Sustained antibody titers were observed for 3 to 5 years, especially in individuals that suffered from severe MERS. In comparison, survivors with mild or asymptomatic disease revealed a more variable response with lower titers. In the study by Cheon et al., binding antibodies were detected for up to 4 years after infection and significantly dropped in the 5th year, whereas the neutralizing antibody titers against MERS-CoV decreased more rapidly and were significantly reduced at 4 years after infection.⁴⁹

Taken together, our study demonstrates that MVA-MERS-S induced robust MERS-CoV-S-specific B cells and antibodies in a homologous vaccination regimen, whereas T cell responses displayed a more heterogeneous pattern within the cohort. Magnitude and persistence of both MERS-CoV-S-specific B cells and antibodies were strongly enhanced by the late third vaccination. Antibody levels and neutralization capacity seemed to be stabilized after the late boost. This work adds evidence to a growing number of reports, demonstrating that late boosting could be an important tool for improving vaccine-induced immunogenicity against CoVs. A vaccination schedule using a long interval could be of particular interest in a pre-pandemic situation to establish long-lasting S-specific antibodies in the target population, e.g., healthcare and camel workers, while a short interval or even single-shot immunizations are crucial in outbreak situations. This pilot study using MVA-MERS-S forms the basis for future studies and may also provide translatable insights into long-term immune responses to COVID-19 vaccines and the application of late-boosting strategies.

Limitations of the study

In our study, we longitudinally evaluate adaptive immune responses after immunization with the MVA-MERS-S vaccine candidate. One limitation of our study is the small size of the study cohort, which consists of ten study participants who received three vaccinations and were subsequently monitored until 28 days after the last vaccination. During the long-term follow up (12–24 months after the third vaccination), seven of the ten study participants continued with further visits. A second limitation of our study is the usage of PBMCs to study MBC responses. While peripheral blood provides first insights into the induction of antigen-specific cells following vaccination, analyses of lymphoid tissue and bone marrow would be additionally important to investigate vaccine-induced B and T cell populations.

Furthermore, we did not evaluate the induction of vaccine-induced mucosal responses as we did not sample biopsies from the pharyngeal mucosa. In addition, the impact of the observed immune responses on protection against MERS-CoV infection and disease remains an open question that cannot be addressed with our study.

CONSORTIA

The members of the MVA-MERS-S Study group are Etienne Bartels, Swantje Gundlach, Thomas Hestekamp, Verena Krähling, Susan Lassen, My Linh Ly, Joseph H. Pötsch, Stefan Schmiedel, Anisa Volz, and Madeleine E. Zinser.

STAR★METHODS

Detailed methods are provided in the online version of this paper and include the following:

- **KEY RESOURCES TABLE**
- **RESOURCE AVAILABILITY**
 - Lead contact
 - Materials availability
 - Data and code availability
- **EXPERIMENTAL MODEL AND SUBJECT DETAILS**
 - Vaccine construct
 - Study design and participants
 - Blood sampling
- **METHOD DETAILS**
 - ELISA
 - PRNT50
 - IFN γ ELISpot assay
 - Bead-based multiplex ELISA
 - IgG ELISpot assay
 - Flowcytometry
- **QUANTIFICATION AND STATISTICAL ANALYSIS**
- **ADDITIONAL RESOURCES**

SUPPLEMENTAL INFORMATION

Supplemental information can be found online at <https://doi.org/10.1016/j.xcrm.2022.100685>.

ACKNOWLEDGMENTS

We thank all volunteers for their participation in this first-in-human phase 1 vaccine trial and their commitment and dedication to research against emerging CoVs. We would also like to express our sincere gratitude to all trial center members for their extraordinary work (Clinical Trial Center North GmbH & Co. KG, Hamburg), especially Saskia Borregaard, Alen Jambrecina, and Laura Kaltenberg. We also thank Keith Chappell (University of Queensland) for providing MERS-CoV-S clamp antigen. This work was funded by the DFG grant AD171/3-1 and the DZIF infrastructure “Clinical management and epidemiology of emerging infections” [01.702] and FKZ8009801908, FKZ8009701702, and FKZ80095CLANF.

AUTHOR CONTRIBUTIONS

Conceptualization, M.M.A., S.B., G.S., A.F., T.K., and C.D.; methodology, L.M.W., C.D., M.P.R., and B.L.H.; investigation: L.M.W., M.F., M.P.R., A.Z.M., and the MVA-MERS-S Study Group; formal analysis and visualization,

L.M.W. and M.S.; writing – original draft, L.M.W. and C.D.; writing – review & editing, L.M.W., C.D., M.M.A., A.F., T.K., G.S., and B.L.H.; supervision, C.D. and M.M.A.

DECLARATION OF INTERESTS

The authors declare no competing interests.

Received: October 8, 2020

Revised: February 25, 2022

Accepted: June 16, 2022

Published: July 19, 2022

REFERENCES

1. WHO (2021). MERS Situation Update. <http://www.emro.who.int/health-topics/mers-cov/mers-outbreaks.html>.
2. Modjarrad, K., Moorthy, V.S., Ben Embarek, P., Van Kerkhove, M., Kim, J., and Kieny, M.P. (2016). A roadmap for MERS-CoV research and product development: report from a World Health Organization consultation. *Nat. Med.* 22, 701–705. <https://doi.org/10.1038/nm.4131>.
3. Zaki, A.M., van Boheemen, S., Bestebroer, T.M., Osterhaus, A.D., and Fouchier, R.A. (2012). Isolation of a novel coronavirus from a man with pneumonia in Saudi Arabia. *N. Engl. J. Med.* 367, 1814–1820. <https://doi.org/10.1056/NEJMoa1211721>.
4. Gossner, C., Danielson, N., Gervelmeyer, A., Berthe, F., Faye, B., Kaasik Aaslav, K., Adlhoch, C., Zeller, H., Penttinen, P., and Coulombier, D. (2016). Human-dromedary camel interactions and the risk of acquiring zoonotic Middle East respiratory syndrome coronavirus infection. *Zoonoses Public Health* 63, 1–9. <https://doi.org/10.1111/zph.12171>.
5. Hui, D.S., Azhar, E.I., Kim, Y.J., Memish, Z.A., Oh, M.D., and Zumla, A. (2018). Middle East respiratory syndrome coronavirus: risk factors and determinants of primary, household, and nosocomial transmission. *Lancet Infect. Dis.* 18, e217–e227. [https://doi.org/10.1016/S1473-3099\(18\)30127-0](https://doi.org/10.1016/S1473-3099(18)30127-0).
6. Cauchemez, S., Fraser, C., Van Kerkhove, M.D., Donnelly, C.A., Riley, S., Rambaut, A., Enouf, V., van der Werf, S., and Ferguson, N.M. (2014). Middle East respiratory syndrome coronavirus: quantification of the extent of the epidemic, surveillance biases, and transmissibility. *Lancet Infect. Dis.* 14, 50–56. [https://doi.org/10.1016/S1473-3099\(13\)70304-9](https://doi.org/10.1016/S1473-3099(13)70304-9).
7. Cauchemez, S., Nouvellet, P., Cori, A., Jombart, T., Garske, T., Clapham, H., Moore, S., Mills, H.L., Salje, H., Collins, C., et al. (2016). Unraveling the drivers of MERS-CoV transmission. *Proc. Natl. Acad. Sci. USA* 113, 9081–9086. <https://doi.org/10.1073/pnas.1519235113>.
8. WHO (2022). <https://www.who.int/emergencies/mers-cov/en/>. <https://www.who.int/emergencies/mers-cov/en/>.
9. West, D.J., and Calandra, G.B. (1996). Vaccine induced immunologic memory for hepatitis B surface antigen: implications for policy on booster vaccination. *Vaccine* 14, 1019–1027. [https://doi.org/10.1016/0264-410x\(96\)00062-x](https://doi.org/10.1016/0264-410x(96)00062-x).
10. Bauer, T., and Jilg, W. (2006). Hepatitis B surface antigen-specific T and B cell memory in individuals who had lost protective antibodies after hepatitis B vaccination. *Vaccine* 24, 572–577. <https://doi.org/10.1016/j.vaccine.2005.08.058>.
11. Yong, C.Y., Ong, H.K., Yeap, S.K., Ho, K.L., and Tan, W.S. (2019). Recent advances in the vaccine development against Middle East respiratory syndrome-coronavirus. *Front. Microbiol.* 10, 1781. <https://doi.org/10.3389/fmicb.2019.01781>.
12. Park, B.K., Maharjan, S., Lee, S.I., Kim, J., Bae, J.Y., Park, M.S., and Kwon, H.J. (2019). Generation and characterization of a monoclonal antibody against MERS-CoV targeting the spike protein using a synthetic peptide epitope-CpG-DNA-liposome complex. *BMB Rep.* 52, 397–402. <https://doi.org/10.5483/bmbrep.2019.52.6.185>.

13. Li, F. (2016). Structure, function, and evolution of coronavirus spike proteins. *Annu. Rev. Virol.* *3*, 237–261. <https://doi.org/10.1146/annurev-virology-110615-042301>.
14. Lu, L., Liu, Q., Zhu, Y., Chan, K.H., Qin, L., Li, Y., Wang, Q., Chan, J.F.W., Du, L., Yu, F., et al. (2014). Structure-based discovery of Middle East respiratory syndrome coronavirus fusion inhibitor. *Nat. Commun.* *5*, 3067. <https://doi.org/10.1038/ncomms4067>.
15. Zhang, N., Jiang, S., and Du, L. (2014). Current advancements and potential strategies in the development of MERS-CoV vaccines. *Expert Rev. Vaccines* *13*, 761–774. <https://doi.org/10.1586/14760584.2014.912134>.
16. Koch, T., Dahlke, C., Fathi, A., Kupke, A., Krähling, V., Okba, N.M.A., Halwe, S., Rohde, C., Eickmann, M., Volz, A., et al. (2020). Safety and immunogenicity of a modified vaccinia virus Ankara vector vaccine candidate for Middle East respiratory syndrome: an open-label, phase 1 trial. *Lancet Infect. Dis.* *20*, 827–838. [https://doi.org/10.1016/s1473-3099\(20\)30248-6](https://doi.org/10.1016/s1473-3099(20)30248-6).
17. Folegatti, P.M., Bittaye, M., Flaxman, A., Lopez, F.R., Bellamy, D., Kupke, A., Mair, C., Makinson, R., Sheridan, J., Rohde, C., et al. (2020). Safety and immunogenicity of a candidate Middle East respiratory syndrome coronavirus viral-vectored vaccine: a dose-escalation, open-label, non-randomised, uncontrolled, phase 1 trial. *Lancet Infect. Dis.* *20*, 816–826. [https://doi.org/10.1016/S1473-3099\(20\)30160-2](https://doi.org/10.1016/S1473-3099(20)30160-2).
18. Modjarrad, K., Roberts, C.C., Mills, K.T., Castellano, A.R., Paolino, K., Muthumani, K., Reuschei, E.L., Robb, M.L., Racine, T., Oh, M.D., et al. (2019). Safety and immunogenicity of an anti-Middle East respiratory syndrome coronavirus DNA vaccine: a phase 1, open-label, single-arm, dose-escalation trial. *Lancet Infect. Dis.* *19*, 1013–1022. [https://doi.org/10.1016/S1473-3099\(19\)30266-X](https://doi.org/10.1016/S1473-3099(19)30266-X).
19. Bosaeeed, M., Balkhy, H.H., Almaziad, S., Aljami, H.A., Alhatmi, H., Alanazi, H., Alahmadi, M., Jawhary, A., Alenazi, M.W., Almasoud, A., et al. (2022). Safety and immunogenicity of ChAdOx1 MERS vaccine candidate in healthy Middle Eastern adults (MERS002): an open-label, non-randomised, dose-escalation, phase 1b trial. *Lancet Microbe.* *3*, e11–e20. [https://doi.org/10.1016/S2666-5247\(21\)00193-2](https://doi.org/10.1016/S2666-5247(21)00193-2).
20. Song, F., Fux, R., Provacia, L.B., Volz, A., Eickmann, M., Becker, S., Osterhaus, A.D., Haagmans, B.L., and Sutter, G. (2013). Middle East respiratory syndrome coronavirus spike protein delivered by modified vaccinia virus Ankara efficiently induces virus-neutralizing antibodies. *J. Virol.* *87*, 11950–11954. <https://doi.org/10.1128/JVI.01672-13>.
21. Fathi, A., Dahlke, C., Krahling, V., Kupke, A., Okba, N.M.A., Raadsen, M.P., Heidepriem, J., Muller, M.A., Paris, G., Lassen, S., et al. (2022). Increased neutralization and IgG epitope identification after MVA-MERS-S booster vaccination against Middle East respiratory syndrome. Preprint at medRxiv. <https://doi.org/10.1101/2022.02.14.22270168>.
22. Sanz, I., Wei, C., Jenks, S.A., Cashman, K.S., Tipton, C., Woodruff, M.C., Hom, J., and Lee, F.E. (2019). Challenges and opportunities for consistent classification of human B cell and plasma cell populations. *Front. Immunol.* *10*, 2458. <https://doi.org/10.3389/fimmu.2019.02458>.
23. Slifka, M.K., Antia, R., Whitmire, J.K., and Ahmed, R. (1998). Humoral immunity due to long-lived plasma cells. *Immunity* *8*, 363–372. [https://doi.org/10.1016/s1074-7613\(00\)80541-5](https://doi.org/10.1016/s1074-7613(00)80541-5).
24. Palgen, J.L., Tchitchek, N., Rodriguez-Pozo, A., Jouhault, Q., Abdelhouthab, H., Dereuddre-Bosquet, N., Contreras, V., Martinon, F., Cosma, A., Lévy, Y., et al. (2020). Innate and secondary humoral responses are improved by increasing the time between MVA vaccine immunizations. *NPJ Vaccines* *5*, 24. <https://doi.org/10.1038/s41541-020-0175-8>.
25. Sallusto, F., Lanzavecchia, A., Araki, K., and Ahmed, R. (2010). From vaccines to memory and back. *Immunity* *33*, 451–463. <https://doi.org/10.1016/j.immuni.2010.10.008>.
26. Voysey, M., Costa Clemens, S.A., Madhi, S.A., Weckx, L.Y., Folegatti, P.M., Aley, P.K., Angus, B., Baillie, V.L., Barnabas, S.L., Borhat, Q.E., et al. (2021). Single-dose administration and the influence of the timing of the booster dose on immunogenicity and efficacy of ChAdOx1 nCoV-19 (AZD1222) vaccine: a pooled analysis of four randomised trials. *Lancet* *397*, 881–891. [https://doi.org/10.1016/S0140-6736\(21\)00432-3](https://doi.org/10.1016/S0140-6736(21)00432-3).
27. Voysey, M., and Pollard, A.J. (2021). ChAdOx1 nCoV-19 vaccine: asymptomatic efficacy estimates - authors' reply. *Lancet* *397*, 2248. [https://doi.org/10.1016/S0140-6736\(21\)00976-4](https://doi.org/10.1016/S0140-6736(21)00976-4).
28. Pitisuttithum, P., Nitayaphan, S., Chariyalertsak, S., Kaewkungwal, J., Dawson, P., Dhitavat, J., Phonrat, B., Akapirat, S., Karasavvas, N., Wiczorek, L., et al. (2020). Late boosting of the RV144 regimen with AIDS VAX B/E and ALVAC-HIV in HIV-uninfected Thai volunteers: a double-blind, randomised controlled trial. *Lancet HIV* *7*, e238–e248. [https://doi.org/10.1016/S2352-3018\(19\)30406-0](https://doi.org/10.1016/S2352-3018(19)30406-0).
29. Kreijtz, J.H., Goeijenbier, M., Moesker, F.M., van den Dries, L., Goeijenbier, S., De Gruyter, H.L., Lehmann, M.H., Mutsert, G., van de Vijver, D.A., Volz, A., et al. (2014). Safety and immunogenicity of a modified-vaccinia-virus-Ankara-based influenza A H5N1 vaccine: a randomised, double-blind phase 1/2a clinical trial. *Lancet Infect. Dis.* *14*, 1196–1207. [https://doi.org/10.1016/S1473-3099\(14\)70963-6](https://doi.org/10.1016/S1473-3099(14)70963-6).
30. de Vries, R.D., Altenburg, A.F., Nieuwkoop, N.J., de Bruin, E., van Trierum, S.E., Pronk, M.R., Lamers, M.M., Richard, M., Nieuwenhuijse, D.F., Koopmans, M.P.G., et al. (2018). Induction of cross-clade antibody and T-cell responses by a modified vaccinia virus ankara-based influenza A(H5N1) vaccine in a randomized phase 1/2a clinical trial. *J. Infect. Dis.* *218*, 614–623. <https://doi.org/10.1093/infdis/jiy214>.
31. Munro, A.P.S., Janani, L., Cornelius, V., Aley, P.K., Babbage, G., Baxter, D., Bula, M., Cathie, K., Chatterjee, K., Dodd, K., et al. (2021). Safety and immunogenicity of seven COVID-19 vaccines as a third dose (booster) following two doses of ChAdOx1 nCoV-19 or BNT162b2 in the UK (COV-BOOST): a blinded, multicentre, randomised, controlled, phase 2 trial. *Lancet* *398*, 2258–2276. [https://doi.org/10.1016/S0140-6736\(21\)02717-3](https://doi.org/10.1016/S0140-6736(21)02717-3).
32. Wang, C., van Haperen, R., Gutiérrez-Álvarez, J., Li, W., Okba, N.M.A., Albuлесcu, I., Widjaja, I., van Dieren, B., Fernandez-Delgado, R., Sola, I., et al. (2021). A conserved immunogenic and vulnerable site on the coronavirus spike protein delineated by cross-reactive monoclonal antibodies. *Nat. Commun.* *12*, 1715. <https://doi.org/10.1038/s41467-021-21968-w>.
33. Nguyen-Contant, P., Embong, A.K., Kanagaiah, P., Chaves, F.A., Yang, H., Branche, A.R., Topham, D.J., and Sangster, M.Y. (2020). S protein-reactive IgG and memory B cell production after human SARS-CoV-2 infection includes broad reactivity to the S2 subunit. *mBio* *11*, e01991–20. <https://doi.org/10.1128/mBio.01991-20>.
34. Zohar, T., Loos, C., Fischinger, S., Atyeo, C., Wang, C., Slein, M.D., Burke, J., Yu, J., Feldman, J., Hauser, B.M., et al. (2020). Compromised humoral functional evolution tracks with SARS-CoV-2 mortality. *Cell* *183*, 1508–1519.e12. <https://doi.org/10.1016/j.cell.2020.10.052>.
35. Fischinger, S., Dolatshahi, S., Jennewein, M.F., Rerks-Ngarm, S., Pitisuttithum, P., Nitayaphan, S., Michael, N., Vasani, S., Ackerman, M.E., Streeck, H., and Alter, G. (2020). IgG3 collaborates with IgG1 and IgA to recruit effector function in RV144 vaccinees. *JCI Insight* *5*, 140925. <https://doi.org/10.1172/jci.insight.140925>.
36. Arnold, K.B., and Chung, A.W. (2018). Prospects from systems serology research. *Immunology* *153*, 279–289. <https://doi.org/10.1111/imm.12861>.
37. Rowntree, L.C., Chua, B.Y., Nicholson, S., Koutsakos, M., Hensen, L., Douros, C., Selva, K., Mordant, F.L., Wong, C.Y., Habel, J.R., et al. (2021). Robust correlations across six SARS-CoV-2 serology assays detecting distinct antibody features. *Clin. Transl. Immunol.* *10*, e1258. <https://doi.org/10.1002/cti2.1258>.
38. Selva, K.J., van de Sandt, C.E., Lemke, M.M., Lee, C.Y., Shoffner, S.K., Chua, B.Y., Davis, S.K., Nguyen, T.H.O., Rowntree, L.C., Hensen, L., et al. (2021). Systems serology detects functionally distinct coronavirus antibody features in children and elderly. *Nat. Commun.* *12*, 2037. <https://doi.org/10.1038/s41467-021-22236-7>.
39. Boudreau, C.M., and Alter, G. (2019). Extra-neutralizing FcR-mediated antibody functions for a universal influenza vaccine. *Front. Immunol.* *10*, 440. <https://doi.org/10.3389/fimmu.2019.00440>.



40. Barrett, J.R., Belji-Rammerstorfer, S., Dold, C., Ewer, K.J., Folegatti, P.M., Gilbride, C., Halkerston, R., Hill, J., Jenkin, D., Stockdale, L., et al. (2021). Author Correction: phase 1/2 trial of SARS-CoV-2 vaccine ChAdOx1 nCoV-19 with a booster dose induces multifunctional antibody responses. *Nat. Med.* 27, 1113. <https://doi.org/10.1038/s41591-021-01372-z>.
41. Damelang, T., Rogerson, S.J., Kent, S.J., and Chung, A.W. (2019). Role of IgG3 in infectious diseases. *Trends Immunol.* 40, 197–211. <https://doi.org/10.1016/j.it.2019.01.005>.
42. Chung, A.W., Ghebremichael, M., Robinson, H., Brown, E., Choi, I., Lane, S., Dugast, A.S., Schoen, M.K., Rolland, M., Suscovich, T.J., et al. (2014). Polyfunctional Fc-effector profiles mediated by IgG subclass selection distinguish RV144 and VAX003 vaccines. *Sci. Transl. Med.* 6, 228ra38. <https://doi.org/10.1126/scitranslmed.3007736>.
43. Khoury, D.S., Cromer, D., Reynaldi, A., Schlub, T.E., Wheatley, A.K., Juno, J.A., Subbarao, K., Kent, S.J., Triccas, J.A., and Davenport, M.P. (2021). Neutralizing antibody levels are highly predictive of immune protection from symptomatic SARS-CoV-2 infection. *Nat. Med.* 27, 1205–1211. <https://doi.org/10.1038/s41591-021-01377-8>.
44. Earle, K.A., Ambrosino, D.M., Fiore-Gartland, A., Goldblatt, D., Gilbert, P.B., Siber, G.R., Dull, P., and Plotkin, S.A. (2021). Evidence for antibody as a protective correlate for COVID-19 vaccines. *Vaccine* 39, 4423–4428. <https://doi.org/10.1016/j.vaccine.2021.05.063>.
45. Moss, P. (2022). The T cell immune response against SARS-CoV-2. *Nat. Immunol.* 23, 186–193. <https://doi.org/10.1038/s41590-021-01122-w>.
46. Kim, Y.S., Agerim, A., Park, U., Kim, Y., Park, H., Rhee, J.Y., Choi, J.P., Park, W.B., Park, S.W., Kim, Y., et al. (2021). Sustained responses of neutralizing antibodies against Middle East respiratory syndrome coronavirus (MERS-CoV) in recovered patients and their therapeutic applicability. *Clin. Infect. Dis.* 73, e550–e558. <https://doi.org/10.1093/cid/ciaa1345>.
47. Plotkin, S. (2014). History of vaccination. *Proc. Natl. Acad. Sci. USA* 111, 12283–12287. <https://doi.org/10.1073/pnas.1400472111>.
48. Tay, M.Z., Rouers, A., Fong, S.W., Goh, Y.S., Chan, Y.H., Chang, Z.W., Xu, W., Tan, C.W., Chia, W.N., Torres-Ruesta, A., et al. (2022). Decreased memory B cell frequencies in COVID-19 delta variant vaccine breakthrough infection. *EMBO Mol. Med.* 14, e15227. <https://doi.org/10.15252/emmm.202115227>.
49. Cheon, S., Park, U., Park, H., Kim, Y., Nguyen, Y.T.H., Agerim, A., Rhee, J.Y., Choi, J.P., Park, W.B., Park, S.W., et al. (2022). Longevity of seropositivity and neutralizing antibodies in recovered MERS patients: a 5-year follow-up study. *Clin. Microbiol. Infect.* 28, 292–296. <https://doi.org/10.1016/j.cmi.2021.06.009>.
50. Alshukairi, A.N., Khalid, I., Ahmed, W.A., Dada, A.M., Bayumi, D.T., Malic, L.S., et al. (2016). Antibody Response and Disease Severity in Healthcare Worker MERS Survivors. *Emerg Infect Dis* 22, 1113–1115.
51. Brown, E.P., Licht, A.F., Dugast, A.S., Choi, I., Bailey-Kellogg, C., Alter, G., and Ackerman, M.E. (2012). High-throughput, multiplexed IgG subclassing of antigen-specific antibodies from clinical samples. *J. Immunol. Methods* 386, 117–123. <https://doi.org/10.1016/j.jim.2012.09.007>.



STAR★METHODS

KEY RESOURCES TABLE

| REAGENT or RESOURCE | SOURCE | IDENTIFIER |
|--|---|---|
| Antibodies | | |
| Mouse Anti-Human IgM-PE | SouthernBiotech | Cat#9020-09; RRID:AB_2796586 |
| Mouse Anti-Human IgA1-PE | SouthernBiotech | Cat#9130-09; RRID:AB_2796656 |
| Mouse Anti-Human IgA2-PE | SouthernBiotech | Cat#9140-09; RRID:AB_2796664 |
| Mouse Anti-Human IgG1 Hinge-PE | SouthernBiotech | Cat#9052-09; RRID:AB_2796621 |
| Mouse Anti-Human IgG2 Fc-PE | SouthernBiotech | Cat#9070-09; RRID:AB_2796639 |
| Mouse Anti-Human IgG3 Hinge-PE | SouthernBiotech | Cat#9210-09; RRID:AB_2796701 |
| Mouse Anti-Human IgG4 Fc-PE | SouthernBiotech | Cat#9200-09; RRID:AB_2796693 |
| PerCP anti-human CD3 Antibody | Biolegend | Cat#344813; RRID:AB_10641841 |
| PerCP anti-human CD14 Antibody | Biolegend | Cat#301847; RRID:AB_2564058 |
| Alexa Fluor® 700 anti-human CD56 (NCAM) Antibody | Biolegend | Cat#318316; RRID:AB_604104 |
| Brilliant Violet 650™ anti-human CD20 Antibody | Biolegend | Cat#302335; RRID:AB_11218609 |
| Brilliant Violet 785™ anti-human IgD Antibody | Biolegend | Cat#348241; RRID:AB_2629808 |
| Brilliant Violet 570™ anti-human IgM Antibody | Biolegend | Cat#314517; RRID:AB_10913816 |
| BD OptiBuild™ BUV805 Mouse Anti-Human IgG | BD | Cat#742041; RRID:AB_2871333 |
| BUV563 Mouse Anti-Human CD19 | BD | Cat#612917; RRID:AB_2870202 |
| BD Horizon™ BUV737 Mouse Anti-Human CD21 | BD | Cat#612788; RRID:AB_2870115 |
| BD Horizon™ BB515 Mouse Anti-Human CD27 | BD | Cat#564643; RRID:AB_2744354 |
| IgA Antibody anti-human, APC-Vio 770 | Miltenyi Biotec | Cat#130-113-999; RRID:AB_2733153 |
| Rabbit anti-MERS-CoV Nucleoprotein antibody | Genetex | Cat#GTX134868; RRID:AB_2887364 |
| Goat anti-Rabbit IgG antibody, Alexa Fluor 488 | Invitrogen | Cat#A32731; RRID:AB_2633280 |
| Bacterial and virus strains | | |
| MERS-CoV, EMC/2012 isolate | | GenBank accession no. NC_019843.3 |
| Biological samples | | |
| Cryopreserved PBMC from MVA-MERS-S vaccinees | University Clinical Center Hamburg-Eppendorf, Germany | N/A |
| Cryopreserved plasma from MVA-MERS-S vaccinees | University Clinical Center Hamburg-Eppendorf, Germany | N/A |
| Cryopreserved serum from MVA-MERS-S vaccinees | University Clinical Center Hamburg-Eppendorf, Germany | N/A |
| Chemicals, peptides, and recombinant proteins | | |
| Recombinant clamp MERS-CoV-spike protein | Keith Chappell, The School of Chemistry and Molecular Biosciences, University of Queensland, Brisbane, QLD, Australia | N/A |
| MERS peptide pool 1-5 | JPT Peptide Technologies | Customized; Sequences indicated in Table S8 |
| CEF Pool (extended) | JPT Peptide Technologies | Cat#PM-CEF-E-3 |
| Phytohemagglutinin (PHA) (1 mg/mL) | Sigma | Cat#L8902-5MG |
| MERS-CoV Spike Protein (S1 Subunit, aa 1-725, His Tag) | Sino Biological | Cat#40069-V08B1 |
| MERS-CoV Spike Protein (S2 Subunit, aa 726-1296, His Tag) | Sino Biological | Cat#40070-V08B |
| MERS-CoV Spike S1+S2 Protein (ECD, aa 1-1297, His Tag), Biotinylated | Sino Biological | Cat#40069-V08B-B |

(Continued on next page)

Continued

| REAGENT or RESOURCE | SOURCE | IDENTIFIER |
|---|----------------------------|---|
| LIVE/DEAD™ Fixable Blue Dead Cell Stain Kit | Thermo Fisher | Cat#L23105 |
| Streptavidin, (PE-Cy5.5) | Thermo Fisher | Cat#SA1018 |
| AF647 Streptavidin | Biolegend | Cat#405237 |
| PE-Cy7 Streptavidin | Biolegend | Cat#405206 |
| BIO200 - BIO-200 biotin solution | Avidity | Cat#BIO200 |
| Critical commercial assays | | |
| CTL Human IFN-g Single colour 384- well Enzymatic ELISpot Kit | ImmunoSpot | Cat#hlFNg-3M/5 |
| Human IgG ELISpot BASIC kit (ALP) | Mabtech | Cat#3850-2A |
| Software and algorithms | | |
| FlowJo v10.8.0 | FlowJo, LLC | https://www.flowjo.com/ |
| GraphPad Prism v8.0.1 | GraphPad | https://www.graphpad.com |
| R v4.0.2 | R Foundation | https://www.r-project.org/foundation/ |
| RStudio | RStudio | https://www.rstudio.com/ |
| Elispot Reader v7.0 (build 16577) | AID GmbH | https://www.elispot.com/ |
| Bio-Plex Manager™ Software v6.2 (build 175) | Bio-Rad Laboratories, Inc. | https://www.bio-rad.com/ |
| SpectroFlo® v3.0.1 | Cytek Biosciences | https://cytekbio.com/ |

RESOURCE AVAILABILITY

Lead contact

Further information and requests for resources and reagents should be directed to and will be fulfilled by the lead contact, Christine Dahlke (c.dahlke@uke.de).

Materials availability

This study did not generate new unique reagents.

Data and code availability

- All data reported in this paper will be shared by the [lead contact](#) upon request.
- This paper does not report original code.
- Any additional information required to reanalyze the data reported in this paper is available from the [lead contact](#) upon request.

EXPERIMENTAL MODEL AND SUBJECT DETAILS

Vaccine construct

MVA-MERS-S is based on a rMVA vector encoding for the full-length MERS-CoV-S-glycoprotein, based on the sequence of EMC/2012 (GenBank accession no. JX869059). MVA-MERS-S expresses the full-length S protein of MERS-CoV with a molecular mass closely corresponding to the mass predicted from the S gene nucleotide sequence and evidence for an S1 and S2 cleavage of full-length S.²⁰ The cDNA sequence was not codon-optimized in the classical sense. It was obtained by gene synthesis and modified by introducing silent codon alterations to inactivate three signal sequences (TTTTNT) for termination of vaccinia virus-specific early transcription. This modification allows for optimized gene expression when using early-late promoters for MVA-specific transcription of recombinant genes. The vaccine was manufactured by IDT Biologika GmbH (Dessau, Germany) in primary chicken embryo fibroblasts (CEF).

Study design and participants

NCT03615911 was a phase 1 clinical trial to address safety and immunogenicity of the vaccine candidate MVA-MERS-S in healthy adults. The study was conducted in Hamburg (Germany) at the University Medical Center Hamburg-Eppendorf (UKE). Eligible adults were males or females aged between 18 and 55 without previous MVA-immunization. Study participants were divided into two dose groups that received either 1×10^7 plaque-forming units (PFU, low dose) or 1×10^8 PFU (high dose) on days 0 and 28¹⁶. A subgroup of participants (3 male, 7 female) from the low dose ($n = 3$) and the high dose ($n = 7$) groups received a late booster immunization of 1×10^8 PFU MVA-MERS-S 12 ± 4 months after prime immunization²¹ and represents the core study population of this manuscript. The study design of the clinical trial was reviewed and approved by the Competent National Authority (Paul-Ehrlich-Institut, PEI).



Langen, Germany) and the Ethics Committee of the Hamburg Medical Association and is registered at [ClinicalTrials.gov](https://www.clinicaltrials.gov) (NCT03615911). The observational study was approved by the Ethics Committee of the Hamburg Medical Association and is registered under Protocol No. PV6079. All studies were performed in accordance with the Declaration of Helsinki in its version of Fortaleza 2013. All participants provided written informed consent prior to enrollment in the studies.

Blood sampling

Serum and EDTA blood were sampled from all study participants ($n = 10$) before vaccination 1 (V1:D0), at days 0, 7, 14, 28 and 152 (= 6 months) after vaccination 2 (V2:D0, V2:D7, V2:D14, V2:D28, V2:M6) and at days 0, 7, 14 and 28 after vaccination 3 (V3:D0, V3:D7, V3:D14, V3:D28). Additionally, blood was sampled at 12, 18 and 24 months after V3 from some of the participants (V3:M12, V3:M18, V3:M24). For the exact days of blood sampling and the number of participants sampled late after V3 see [Table S1](#). PBMC were isolated from EDTA blood via Ficoll separation and cryopreserved in liquid nitrogen. Plasma and serum samples were stored at -80°C .

METHOD DETAILS

ELISA

Total anti-MERS-CoV-S IgG was measured using a standardized in-house indirect ELISA. High binding 96-well microplates were coated at 4°C overnight with $100\ \mu\text{L}$ of full-length recombinant clamp MERS-CoV-S protein ($1\ \mu\text{g}/\text{mL}$, supplied by Keith Chappell, University of Queensland). Plates were blocked using $100\ \mu\text{L}$ blotto in TBS (ThermoFisher Scientific) per well for 60 min at 37°C . Plates were washed three times after each incubation step, using PBS with 0.05% (v/v) Tween 20. Sera were diluted 1:100 in blocking buffer and $100\ \mu\text{L}$ of diluted serum was incubated on the coated plates at 37°C for 60 min. Antibody staining was performed using $100\ \mu\text{L}$ of horseradish peroxidase (HRP)-conjugated rabbit-anti-human IgG secondary antibody ($1.3\ \text{mg}/\text{mL}$, Dako) in 1:6000 dilution in PBS for 60 min at 37°C . Enzymatic reaction was initiated by adding $100\ \mu\text{L}$ 3,3',5,5'-Tetramethylbenzidine (TMB) substrate for 5 min at room temperature. The reaction was stopped by adding $100\ \mu\text{L}$ of 0.25 M sulfuric acid. Photometry was performed using a microplate reader (Tecan Infinite F200) at a measurement wavelength of 450 nm with a reference wavelength of 620 nm. Results were reported as optical density (OD) values of the measurement wavelength, subtracted by the reference wavelength. The cut-off OD value for positivity was set at > 0.1 , above the geometric mean OD value of negative control sera +3 standard deviations (0.094).

PRNT50

Serum samples were heat inactivated at 56°C for 30 min. $50\ \mu\text{L}$ of serum were serially diluted by 2-fold in Opti-MEM I ($1\times$) + GlutaMAX (Gibco), mixed 1:1 with 400 PFU of MERS-CoV (EMC/2012 isolate; GenBank accession no. NC_019843.3) and incubated at 37°C for 1 h. The mixture was then transferred to Calu-3 cell monolayers maintained in Opti-MEM I ($1\times$) + GlutaMAX (Gibco) supplemented with 10% Fetal Bovine Serum (FBS), penicillin ($100\ \text{IU}/\text{mL}$), and streptomycin ($100\ \text{IU}/\text{mL}$). Cells were incubated at 37°C and 5% CO_2 for 8 h and subsequently fixed and permeabilized with formalin and 70% ethanol, respectively. Cells were washed with phosphate buffered saline (PBS) and blocked in 0.6% bovine serum albumin (BSA). Stainings were performed using rabbit anti-MERS-CoV nucleocapsid antibody (Genetex, 1:2000 in 0.1% BSA in PBS) followed by goat anti-rabbit Alexa Fluor 488 antibody (Invitrogen, 1:4000 in 0.1% BSA in PBS). Stained plates were scanned on the Amersham Typhoon Biomolecular Imager (GE Healthcare) and infection was quantified using ImageQuantTL 8.2 image analysis software (GE Healthcare). The PRNT50 titer was quantified using non-linear regression analysis in Graphpad Prism 9.

IFN γ ELISpot assay

IFN γ secretion by T cells was analyzed using a CTL Human IFN- γ Single color 384-well Enzyme-linked Immuno Spot Assay (ELISpot, ImmunoSpot $\text{\textcircled{R}}$). Cryopreserved PBMC were thawed, rested overnight and plated at 5×10^5 PBMCs per well in serum-free medium (CTL medium, ImmunoSpot $\text{\textcircled{R}}$). PBMC were stimulated with OLP pools M1-M5, spanning the entire amino acid sequence of MERS-CoV-S protein (final concentration: $1\ \mu\text{g}/\text{mL}$; for peptide sequences see [Table S8](#)) for 16 h at 37°C and 9% CO_2 . While incubation with phytohemagglutinin (PHA) and a CMV/EBV/Influenza (CEF) peptide pool (JPT Peptide Technologies) served as positive controls, negative controls were incubated with CTL medium plus Dimethyl sulfoxide (DMSO) at the same concentration used for the reconstitution of the MERS-CoV-S peptide pools. Spot detection, ELISpot image acquisition and analyses were performed using the AID EliSpot Reader System (AID GmbH). Spot forming units (SFU) were calculated using the geometric mean of triplicates. DMSO controls were used to normalize the data. A positive response was defined using two criteria: first, a response >50 SFU per 1 M PBMCs and secondly, a four-fold value above baseline (V1:D0).

Bead-based multiplex ELISA

A bead-based multiplex ELISA was used to determine the proportion of isotypes and subclasses within MERS-CoV-S-specific antibodies. Two regions of carboxylated microspheres (Luminex) were covalently coupled with either the S1 or S2 subunit of MERS-CoV-S (SinoBiological) as described previously.⁵¹ Microspheres of both regions were diluted to 50,000/mL in PBS containing 0.1% BSA and added to a black, clear-bottom 96 well microplate at $50\ \mu\text{L}$ (Greiner Bio-One). $50\ \mu\text{L}$ of plasma sample diluted 1:50 in 0.1% BSA/PBS were added and incubated overnight at 4°C and 850 rpm on an orbital shaker. The microspheres were washed with 0.1% BSA/PBS containing 0.5% Triton X-(3 \times) and with 0.1% BSA/PBS (1 \times). PE-conjugated detection antibodies specific for



human IgM, IgG1, IgG2, IgG3, IgG4, IgA1 and IgA2 (Southern Biotech) were added to individual wells for detection of microsphere-bound plasma antibodies. Plates were incubated for 2 h at room temperature and 850 rpm, washed and read out on a Bio-Plex 200 System. The cut-off value was defined as 2-fold above baseline. All measurements were performed in duplicates and the mean of both wells was used for further analysis. Microspheres incubated with detection antibodies in absence of plasma sample (blank wells) were measured as a control for unspecific background signal and used for calculation of the lower limit of detection (LLD) of each analyte: $LLD = \text{mean (normalized blank)} + 3 \times \text{standard deviation (normalized blank)}$.

IgG ELISpot assay

MERS-CoV-S-specific B cells were analyzed using an antigen-specific IgG ELISpot. Cryopreserved PBMC were thawed, resuspended to 2×10^6 cells/mL and stimulated in R10 containing 1% Hepes (Thermo Fisher Scientific), 0.5 $\mu\text{g/mL}$ resiquimod (R848, Mabtech) and 5 ng/mL interleukin-2 (IL-2, Mabtech) for 75 h at 37°C and 5% CO_2 . PVDF-Multi-Screen-IP plates (Millipore) were treated with 15 $\mu\text{L/well}$ 35% ethanol and washed with sterile water. Plates were coated overnight at 4°C with 100 $\mu\text{L/well}$ of either PBS containing anti-IgG capture antibody (15 $\mu\text{g/mL}$, Mabtech), MERS-CoV-S protein S1 or S2 subunit (10 $\mu\text{g/mL}$, SinoBiological), or PBS only. Plates were washed and after 30 min blocking with R10 containing 1% Hepes, pre-stimulated PBMC were added to two replicate wells of each coating condition and incubated for 16 h at 37°C and 5% CO_2 . For detection of spots, biotinylated anti-IgG detection antibody, streptavidin-ALP and BCIP/NBT-plus substrate solution (Mabtech) were used according to the manufacturer's protocol. Plates were analyzed using an AID EliSpot Reader System (AID GmbH). The cut-off value was set at 6.6 SFU, calculated as the geometric mean of blank wells +2 standard deviations.

Flowcytometry

Multiparametric flow cytometry was used to analyze the isotype and activation phenotype of MERS-CoV-S-specific memory B cells. Antigen probes for detection of antigen-specific B cells were prepared in advance by multimerization of biotinylated MERS-CoV-S antigen (SinoBiological) with fluorescently labeled streptavidin (SA). To be able to exclude B cells binding to SA and the respective fluorophore, SA-PE/Cy5.5 (Thermo Fisher) was added as a decoy probe and MERS-CoV-S was separately multimerized with SA labeled with two different fluorophores. For multimerization, MERS-CoV-S protein was mixed with SA-PE/Cy7 and SA-AF647 (Biolegend), respectively, at a molar ratio of 4:1 (mass ratio 11:1) and incubated for 60 min at 4°C. Cryopreserved PBMC were thawed and distributed in a 96 well V-bottom plate at $5\text{--}10 \times 10^6$ PBMC per sample. Cells were first stained with FcR blocking reagent (Miltenyi Biotec, 1:20) and LIVE/DEAD Fixable Blue (Thermo Fisher, 1:1000) in 100 μL of FACS Buffer (PBS containing 2% FBS and 2 mM EDTA) for 15 min at 4°C. Cells were then washed and stained with 50 μL of Brilliant Stain Buffer (BD) containing 5 μM free d-biotin (Avidity), 165 ng spike-PE/Cy7, 165 ng spike-AF647 and 20 ng SA-PE/Cy5.5 decoy probe for 60 min at 4°C. Cells were washed again and subsequently stained with 100 μL of FACS Buffer/Brilliant Stain Buffer (1:1) mixed with 2.5 μL of antibodies against human CD3, CD14, CD56, CD19, CD20, CD21, CD27, IgD, IgM, IgG and IgA (see [key resource table](#)) for 30 min at 4°C. After surface staining, cells were washed and fixed with 4% PFA for 15 min at room temperature. Cells were washed again, resuspended in 100 μL of FACS Buffer and acquired using a Cytex® Aurora (Cytex Biosciences).

QUANTIFICATION AND STATISTICAL ANALYSIS

Flowcytometry data was analyzed using FlowJo software v.10. Statistical analysis was performed using GraphPad Prism (v8.0.1). Statistical testing was conducted by using two-tailed Wilcoxon signed-rank and Mann-Whitney U tests for paired and unpaired samples, respectively, and the level of significance was set to 0.05. The number of study participants (n), median and p values for all experiments are shown in [Tables S2–S7](#). The number of study participants differs between experiments at some time points because samples were not always sufficient to perform all experiments. Correlations between ELISA and PRNT50 data ([Figure 2C](#)) as well as between B cells and HCoV antibodies ([Figure S4](#)) were calculated with GraphPad Prism using non-parametric Spearman's correlation. Correlations within MERS-CoV datasets and the plots based on them were rendered with R (v4.0.2) and R package corrplot (v0.84) (using Visualization of a Correlation Matrix (v0.84), available from <https://github.com/taiyun/corrplot>).

ADDITIONAL RESOURCES

ClinicalTrials.gov Identifier: NCT03615911. <https://clinicaltrials.gov/ct2/show/NCT03615911>.

Cell Reports Medicine, Volume 3

Supplemental information

**Persistence of MERS-CoV-spike-specific B cells
and antibodies after late third immunization
with the MVA-MERS-S vaccine**

Leonie M. Weskamm, Anahita Fathi, Matthijs P. Raadsen, Anna Z. Mykytyn, Till Koch, Michael Spohn, Monika Friedrich, MVA-MERS-S Study Group, Bart L. Haagmans, Stephan Becker, Gerd Sutter, Christine Dahlke, and Marylyn M. Addo

Supplementary Information

MVA-MERS-S Study group members and affiliations

Etienne Bartels (Institute for Infection Research and Vaccine Development UKE (IIRVD)), German Centre for Infection Research (DZIF), Swantje Gundlach (IIRVD, DZIF), Thomas Hestekamp (DZIF), Verena Krähling (Philipps University Marburg), Susan Lassen (IIRVD, DZIF), My Linh Ly (IIRVD, DZIF), Joseph H. Pötsch (IIRVD, DZIF), Stefan Schmiedel (Division of Infectious Diseases UKE), Asisa Volz (TiHo Hannover), Madeleine E. Zinser (IIRVD, DZIF)

Supplemental Figures

10

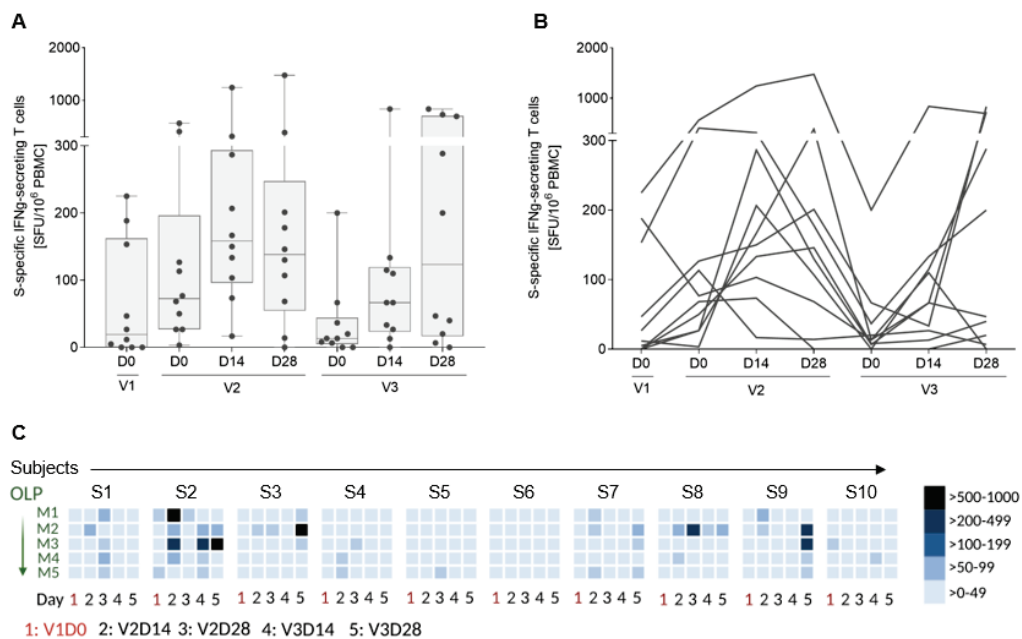


Figure S1. IFN γ T cell responses induced by MVA-MERS-S vaccination, related to Figure 2. T-cell responses were assessed using a CTL-Human IFN γ ELISpot. PBMCs were stimulated with five overlapping peptide (OLP) pools (M1-M5) spanning the entire MERS-CoV-S amino acid sequence (technical triplicates). A response was defined as positive when two criteria were met: i) >50 spot forming units (SFU)/1x10⁶ PBMCs; ii) four-fold value over baseline (day 0). **(A)** IFN γ responses to all five OLP pools (sum) underlines induction at V2:D0 and V2:D14. A third vaccination induced T cell responses in some of the vaccinees. Each dot represents one participant and the sum of SFU to all five pools. **(B)** Sum of SFU to all five pools per participant. **(C)** Heatmap of selected time points indicating number of SFU per peptide pool.

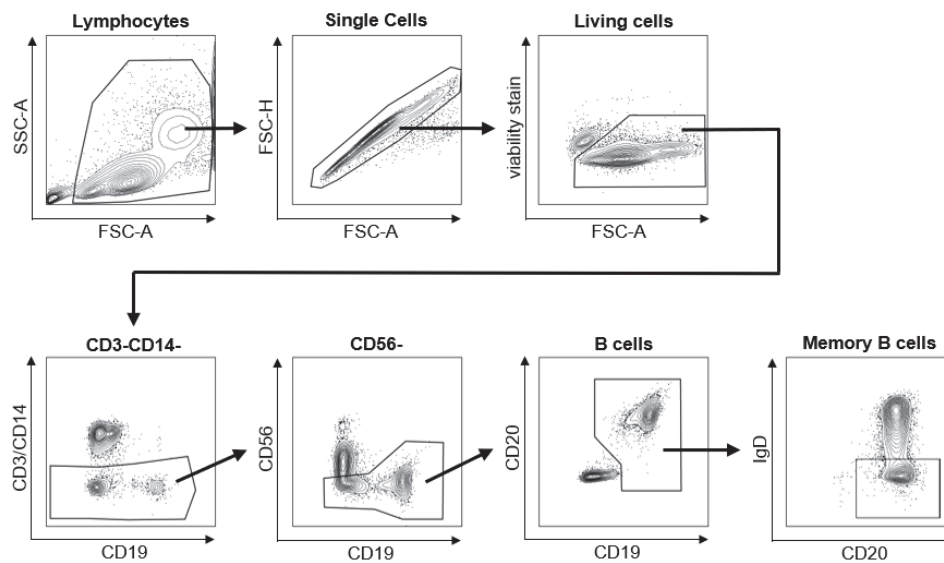


Figure S2. Gating strategy for flowcytometric analysis of memory B cells within PBMC, related to Figure 6. Using the forward scatter (FSC) and sideward scatter (SSC) signal, lymphocytes were first identified based on their size and granularity, followed by exclusion of doublets and dead cells. Subsequently, T cells, monocytes and NK cells were excluded based on their expression of CD3, CD14 and CD56, respectively, and B cells were identified by their expression of CD19. Memory B cells (MBC) were then gated as IgD⁻CD20⁺ cells as opposed to IgD⁺ naïve B cells and IgD⁻CD20⁻ antibody-secreting cells. Further identification of MBC phenotypes, isotypes and spike-specific B cells was achieved as shown in Fig. 6.

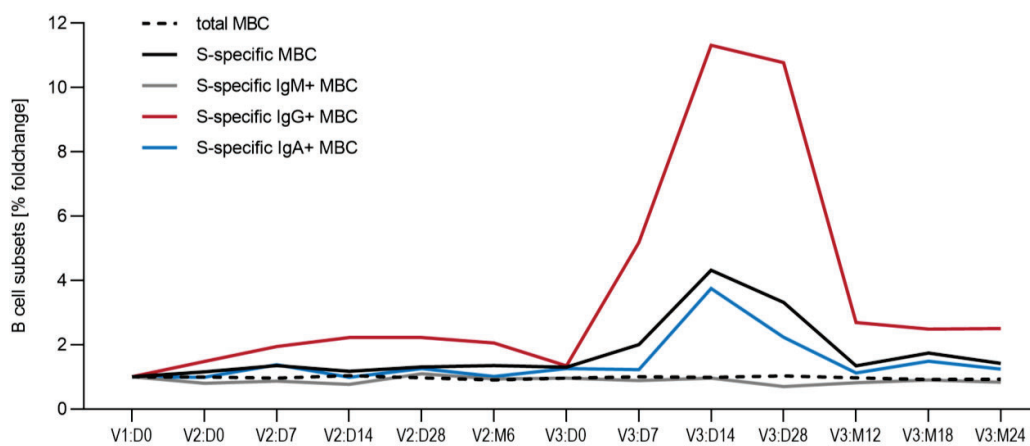


Figure S3. Longitudinal dynamics of the total and S-specific MBC compartment, related to Figure 6. Percentages of S-specific cells refer to the populations of MBC and IgM⁺/IgG⁺/IgA⁺ MBC, respectively. Total MBC frequencies were calculated referring to all single, living lymphocytes.

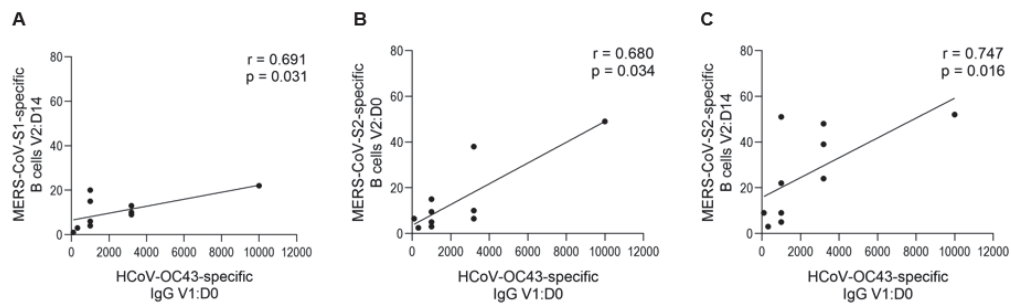


Figure S4. Correlation between vaccine-induced MERS-CoV-S-specific B cells and pre-existing HCoV-OC43 antibodies, related to Figure 5. Pre-existing HCoV-OC43 were correlated with MERS-CoV-S1-specific B cells at V2:D14 (A) and MERS-CoV-S2-specific B cells at V2:D0 (B) and V2:D14 (C). r - and p -values were calculated using non-parametric Spearman's correlation.

Supplemental Tables

Table S1. Time points of blood sampling late after V3, related to Figure 1 and STAR Methods.

| | Time point after late boost (V3) | | |
|-------------------------------|----------------------------------|-----------|-----------|
| Time point [months (M)] | V3:M12 | V3:M18 | V3:M24 |
| Time period [days (D)] | D325-D347 | D477-D514 | D603-D672 |
| Study participants (n) | 6 | 6 | 5 |
| 1 | D347 | D487 | D672 |
| 2 | D345 | D514 | x |
| 3 | D332 | D477 | D603 |
| 4 | x | x | D603 |
| 5 | D327 | 477 | D608 |
| 6 | D325 | D491 | x |
| 7 | D334 | D492 | D629 |

Blood samples were collected between 12 and 24 months after the late boost vaccination (V3) from 7 of the 10 study participants and included into our study. The exact days of blood donation for each study participant are shown above and were assigned to the time points V3:M12, V3:M18 and V3:M24.

Table S2. Statistical analysis of MERS-CoV-S-specific IgG binding and neutralizing antibodies as well as T cell responses, related to Figure 2.

| Time point | V1:D0 | V2:D0 | V2:D14 | V2:D28 | V3:D0 | V3:D14 | V3:D28 | V3:M12 | V3:M18 | V3:M24 |
|------------|-------------------------|---------|---------------|---------------|---------------|--------------|---------------|---------------|---------------|--------|
| IgG | n | 10 | 10 | 10 | 10 | 10 | 10 | 5 | 6 | 5 |
| | Median OD | 0.06732 | 0.1182 | 0.7663 | 0.5123 | 0.2258 | 2.014 | 1.205 | 1.174 | 1.235 |
| | p-value | | 0.0039 | 0.002 | 0.002 | 0.002 | 0.002 | 0.0625 | 0.0313 | 0.0625 |
| PRNT50 | n | 10 | 10 | 10 | 10 | 10 | 10 | 6 | 6 | 5 |
| | Median reciprocal titre | 10.00 | 10.00 | 40.00 | 40.00 | 10.00 | 320.0 | 170.0 | 166.5 | 160.4 |
| | p-value | | - | 0.0039 | 0.0039 | >0.9999 | 0.002 | 0.0313 | 0.0313 | 0.0625 |
| T cells | n | 10 | 10 | 10 | 10 | 10 | 10 | N/A | N/A | N/A |
| | Median SFU | 19.17 | 72.5 | 158.3 | 138 | 13.33 | 123.3 | N/A | N/A | N/A |
| | p-value | | 0.0645 | 0.0137 | 0.0391 | 0.4258 | 0.0488 | N/A | N/A | N/A |

P-values were calculated for the given time point in comparison to V1:D0, using Wilcoxon signed rank test. P-values <0.05 are displayed in italic and bold letters. T cells were not analyzed for time points V3:M12 to V3:M24.

Table S3. Number of samples and median foldchanges of MERS-CoV-S-specific antibody isotypes and subclasses, related to Figure 3.

| Time point | S1 | | | | | | S2 | | | | | |
|------------|-------------------|-------|--------|-------|--------|--------|-------|-------|--------|-------|--------|--------|
| | V1:D0 | V2:D0 | V2:D14 | V3:D0 | V3:D14 | V3:M18 | V1:D0 | V2:D0 | V2:D14 | V3:D0 | V3:D14 | V3:M18 |
| IgM | n | 10 | 10 | 10 | 10 | 6 | 10 | 10 | 10 | 10 | 10 | 6 |
| | median foldchange | 1,00 | 1,07 | 1,06 | 1,00 | 1,78 | 1,00 | 1,32 | 1,23 | 1,18 | 1,73 | 0,84 |
| IgG1 | n | 10 | 10 | 9 | 10 | 6 | 10 | 10 | 10 | 10 | 10 | 6 |
| | median foldchange | 1,00 | 1,02 | 8,42 | 1,22 | 18,47 | 1,00 | 2,41 | 10,17 | 1,73 | 11,15 | 3,40 |
| IgG2 | n | 10 | 10 | 10 | 10 | 8 | 10 | 10 | 10 | 10 | 9 | 6 |
| | median foldchange | 1,00 | 0,98 | 0,98 | 0,84 | 0,72 | 1,00 | 1,00 | 1,01 | 0,97 | 0,87 | 0,99 |
| IgG3 | n | 10 | 10 | 9 | 10 | 6 | 10 | 10 | 10 | 10 | 10 | 6 |
| | median foldchange | 1,00 | 1,15 | 6,58 | 1,07 | 3,37 | 1,00 | 2,85 | 20,85 | 1,58 | 44,44 | 3,05 |
| IgG4 | n | 10 | 10 | 10 | 9 | - | 10 | 10 | 10 | 10 | 8 | - |
| | median foldchange | 1,00 | 1,00 | 1,03 | 1,00 | 1,04 | 1,00 | 1,00 | 0,99 | 1,02 | 1,02 | - |
| IgA1 | n | 10 | 10 | 10 | 10 | 6 | 10 | 10 | 10 | 10 | 10 | 6 |
| | median foldchange | 1,00 | 0,96 | 1,01 | 0,95 | 1,82 | 1,00 | 1,34 | 2,30 | 1,09 | 4,44 | 1,69 |
| IgA2 | n | 10 | 10 | 10 | 10 | - | 10 | 10 | 10 | 10 | 10 | - |
| | median foldchange | 1,00 | 0,94 | 1,05 | 1,01 | 2,31 | 1,00 | 1,01 | 1,28 | 1,01 | 2,18 | - |

Table S4. Statistical analysis of MERS-CoV-S-specific IgG1 and IgG3 responses as measured by bead-based ELISA, related to Figure 4.

| Time point | | V1:D0 | V2:D0 | V2:D14 | V2:D28 | V2:D56 | V2:M6 | V3:D0 | V3:D7 | V3:D14 | V3:D28 | V3:M12 | V3:M18 | V3:M24 | |
|------------|------------|---|---------------|---------------|--------------|--------------|---------------|---------------|---------------|--------------|---------------|---------------|---------------|--------|--|
| IgG1 | n | 10 | 10 | 9 | 10 | 10 | 10 | 10 | 9 | 10 | 9 | 6 | 6 | 4 | |
| | Median MFI | 619.7 | 636.6 | 5483 | 4992 | 2580 | 1024 | 680.2 | 10230 | 10714 | 10345 | 9020 | 8228 | 7583 | |
| | p-value | | 0.6953 | 0.0039 | 0.002 | 0.002 | 0.0039 | 0.0645 | 0.0039 | 0.002 | 0.0039 | 0.0313 | 0.0313 | 0.125 | |
| IgG3 | n | 10 | 10 | 10 | 10 | 10 | 10 | 10 | 10 | 10 | 10 | 6 | 6 | 4 | |
| | Median MFI | 592.5 | 2030 | 5079 | 4505 | 2545 | 2295 | 2000 | 4805 | 7894 | 7831 | 3320 | 3799 | 4002 | |
| | p-value | | 0.0098 | 0.002 | 0.002 | 0.002 | 0.0137 | 0.0195 | 0.002 | 0.002 | 0.002 | 0.0625 | 0.0938 | 0.25 | |
| IgG1 | n | 10 | 10 | 9 | 10 | 10 | 10 | 10 | 9 | 10 | 9 | 6 | 6 | 4 | |
| | Median MFI | 31.38 | 44.25 | 244.3 | 174.7 | 82.69 | 42.78 | 34.21 | 91.11 | 147.5 | 133.6 | 64.62 | 63.43 | 93.32 | |
| | p-value | | 0.002 | 0.0039 | 0.002 | 0.002 | 0.0098 | 0.1641 | 0.0039 | 0.002 | 0.0039 | 0.0625 | 0.0625 | 0.25 | |
| IgG3 | n | 10 | 10 | 10 | 10 | 10 | 10 | 10 | 10 | 10 | 10 | 6 | 6 | 4 | |
| | Median MFI | 34.52 | 92.57 | 671.1 | 365.2 | 176.9 | 95.22 | 60.37 | 1094 | 1401 | 930.6 | 394.9 | 440.8 | 275.6 | |
| | p-value | | 0.002 | 0.002 | 0.002 | 0.002 | 0.002 | 0.0039 | 0.002 | 0.002 | 0.002 | 0.0625 | 0.0625 | 0.25 | |
| | | P-values were calculated for the given time point in comparison to V1:D0, using Wilcoxon signed rank test. P-values <0.05 are displayed in italic and bold letters. | | | | | | | | | | | | | |

Table S5. Statistical analysis of MERS-CoV-S-specific B cell responses as measured by IgG ELISpot, related to Figure 5.

| Time point | V1:D0 | V2:D0 | V2:D14 | V2:M6 | V3:D0 | V3:D14 | V3:M12 | V3:M18 | V3:M24 |
|--|------------------------|--------|---------------|---------------|---------------|-------------------|---------------|---------------|--------|
| | n | 10 | 10 | 10 | 10 | 10 | 10 | 6 | 6 |
| S1 | Median SFU | 0.5 | 9.5 | 5.75 | 4.25 | 243.8 | 22.25 | 17 | 20 |
| | p-value (vs. V1:D0) | 0.0938 | 0.002 | 0.0039 | 0.0078 | 0.002 | 0.0313 | 0.0313 | 0.0625 |
| S2 | Median SFU | 0.5 | 23 | 11 | 8 | 70.5 | 8 | 6 | 5.5 |
| | p-value (vs. V1:D0) | | 0.0039 | 0.0039 | 0.002 | 0.002 | 0.0313 | 0.0313 | 0.0625 |
| S1 vs. S2 | p-value (S1 vs. S2) | 0.7671 | 0.0849 | 0.0848 | 0.1003 | <0.0001 | 0.0152 | 0.2208 | 0.3095 |
| P-values were calculated using Mann-Whitney U (S1 vs. S2) and Wilcoxon signed rank test (given time point vs. V1:D0). P-values <0.05 are displayed in italic and bold letters. | | | | | | | | | |

Table S6. Statistical analysis of MERS-CoV-S-specific MBC responses as measured by flowcytometry, related to Figure 6.

| Time point | V1:D0 | V2:D0 | V2:D7 | V2:D14 | V2:D28 | V2:M6 | V3:D0 | V3:D7 | V3:D14 | V3:D28 | V3:M12 | V3:M18 | V3:M24 |
|--|-------|--------|---------------|---------------|---------------|---------------|---------------|---------------|---------------|---------------|---------------|---------------|---------|
| n | 10 | 10 | 10 | 6 | 10 | 10 | 10 | 10 | 10 | 10 | 6 | 6 | 5 |
| MFR | 0.37 | 0.345 | 0.335 | 0.36 | 0.37 | 0.345 | 0.33 | 0.38 | 0.39 | 0.225 | 0.39 | 0.445 | 0.5 |
| p-value | | 0.1211 | 0.3594 | 0.0625 | 0.6055 | 0.6016 | 0.4160 | 0.4844 | 0.9043 | 0.1055 | 0.6875 | 0.8438 | 0.8125 |
| MFR | 0.075 | 0.1 | 0.15 | 0.12 | 0.14 | 0.17 | 0.11 | 0.36 | 0.89 | 0.885 | 0.19 | 0.215 | 0.17 |
| p-value | | 0.0859 | 0.0039 | 0.0313 | 0.0098 | 0.0078 | 0.0469 | 0.0020 | 0.0020 | 0.0020 | 0.0313 | 0.0313 | 0.0625 |
| MFR | 0.09 | 0.06 | 0.115 | 0.09 | 0.115 | 0.095 | 0.14 | 0.135 | 0.4 | 0.17 | 0.13 | 0.195 | 0.1 |
| p-value | | 0.5801 | 0.2891 | >0.9999 | 0.1992 | 0.9023 | 0.6719 | 0.4258 | 0.0039 | 0.0391 | >0.9999 | 0.4063 | >0.9999 |
| Median Frequencies (MFR) refer to the frequencies of antigen-specific cells within IgM+/IgG+/IgA+ memory B cells. P-values were calculated for the given time point in comparison to V1:D0, using Wilcoxon signed rank test. P-values <0.05 are displayed in italic and bold letters. | | | | | | | | | | | | | |

Table S7. Number of samples included into correlation analysis, related to Figure 7.

| Time point | | V1:D0 | V2:D14 | V3:D14 | V3:M18 |
|------------|------|-------|--------|--------|--------|
| n (S1) | IgG1 | 10 | 9 | 10 | 6 |
| | IgG3 | 10 | 9 | 10 | 6 |
| | ASBC | - | 9 | 10 | 6 |
| | MBC | - | 9 | 10 | 6 |
| n (S2) | IgG1 | 10 | 10 | 10 | 6 |
| | IgG3 | 10 | 10 | 10 | 6 |
| | ASBC | - | 10 | 10 | 6 |
| | MBC | - | 10 | 10 | 6 |

2.2 Flow cytometric protocol to characterize human memory B cells directed against SARS-CoV-2 spike protein antigens

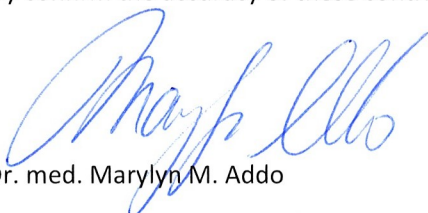
Leonie M. Weskamm, Christine Dahlke* and Marylyn M. Addo*

*These authors contributed equally

Published in *STAR Protocols*, DOI: 10.1016/j.xpro.2022.101902

Leonie Marie Weskamm established the protocol and designed the antibody panel for the flowcytometric characterization of SARS-CoV-2 spike-specific memory B cells and conducted all related experiments. She was responsible for analysis and visualization of all data shown in the manuscript and wrote the original manuscript draft. During the review process she revised the manuscript and was responsible for the communication with the journal editors.

I hereby confirm the accuracy of these contributions

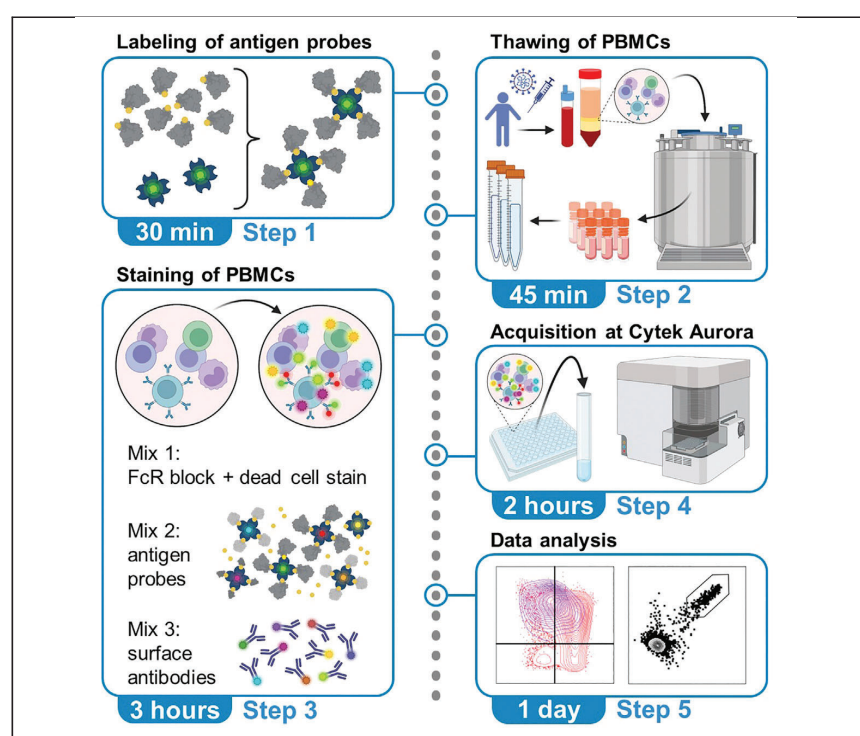

Prof. Dr. med. Marylyn M. Addo

17.1.2023

STAR Protocols

Protocol

Flow cytometric protocol to characterize human memory B cells directed against SARS-CoV-2 spike protein antigens



Memory B cells (MBCs), part of the immune response elicited by infection or vaccination, can persist in lymphoid organs and peripheral blood and are capable of rapid reactivation upon secondary antigen exposure. Here, we describe a flow cytometric assay to identify antigen-specific MBCs from peripheral blood mononuclear cells and characterize their isotypes and activation status. We detail steps to use fluorescently labeled antigen probes derived from the SARS-CoV-2 spike protein. These can be adapted to detect MBCs against other antigens.

Publisher's note: Undertaking any experimental protocol requires adherence to local institutional guidelines for laboratory safety and ethics.

Leonie M.
Weskamm, Christine
Dahlke, Marylyn M.
Addo

m.weskamm@uke.de

Highlights

Characterization of memory B cell isotypes and activation status

Simultaneous identification of three antigen specificities: spike S1, S2, RBD

Protocol can easily be adjusted to other protein-based antigens

Detailed information on staining, acquisition (Cytex Aurora), and gating strategy

Weskamm et al., STAR
Protocols 3, 101902
December 16, 2022 © 2022
The Author(s).
<https://doi.org/10.1016/j.xpro.2022.101902>



STAR Protocols

CellPress
OPEN ACCESS



Protocol

Flow cytometric protocol to characterize human memory B cells directed against SARS-CoV-2 spike protein antigens

Leonie M. Weskamm,^{1,2,3,6,7,*} Christine Dahlke,^{1,2,3,5} and Marylyn M. Addo^{1,2,3,4,5}

¹Institute for Infection Research and Vaccine Development (IIRVD), University Medical Centre Hamburg-Eppendorf, 20251 Hamburg, Germany

²Department for Clinical Immunology of Infectious Diseases, Bernhard Nocht Institute for Tropical Medicine, 20359 Hamburg, Germany

³German Centre for Infection Research, Partner Site Hamburg-Lübeck-Borstel-Riems, Hamburg, Germany

⁴First Department of Medicine, Division of Infectious Diseases, University Medical Centre Hamburg-Eppendorf, 20251 Hamburg, Germany

⁵These authors contributed equally

⁶Technical contact

⁷Lead contact

*Correspondence: m.weskamm@uke.de
<https://doi.org/10.1016/j.xpro.2022.101902>

SUMMARY

Memory B cells (MBCs), part of the immune response elicited by infection or vaccination, can persist in lymphoid organs and peripheral blood and are capable of rapid reactivation upon secondary antigen exposure. Here, we describe a flow cytometric assay to identify antigen-specific MBCs from peripheral blood mononuclear cells and characterize their isotypes and activation status. We detail steps to use fluorescently labeled antigen probes derived from the SARS-CoV-2 spike protein. These can be adapted to detect MBCs against other antigens.

For complete details on the use and execution of this protocol, please refer to Weskamm et al. (2022).¹

BEFORE YOU BEGIN

Here we describe a multiparametric flow cytometric assay to identify antigen-specific memory B cells (MBCs) from human peripheral blood mononuclear cells (PBMCs). Besides antigen specificity, MBCs are further characterized to identify their antibody isotype and activation status. We provide here detailed information about the staining procedure, a basic workflow for acquisition of samples on a spectral flow cytometer (Cytek Aurora) and a proposed gating strategy.

The protocol below describes the specific steps for detection of MBCs directed against SARS-CoV-2. Several fluorophores are used to differentiate between 3 different antigen specificities: the spike protein subunits S1 and S2, as well the receptor binding domain (RBD). We here used proteins from the SARS-CoV-2 Wuhan-Hu-1 strain, but the protocol could easily be adapted to other variants of SARS-CoV-2. The examples provided in this protocol are based on the staining of cryopreserved PBMCs from healthy donors, collected before and at different time points after vaccination against SARS-CoV-2. Notably, the protocol could also be used to analyze spike-specific B cells in convalescent individuals or be adapted to stain B cells with specificity towards other antigens or pathogens. The protocol has also been established for staining of MERS-CoV spike-specific B cells in MERS vaccinees.¹



STAR Protocols 3, 101902, December 16, 2022 © 2022 The Author(s).
This is an open access article under the CC BY-NC-ND license (<http://creativecommons.org/licenses/by-nc-nd/4.0/>).

1



Institutional permissions

The cryopreserved PBMCs used in this study were isolated from EDTA blood obtained from healthy donors. Blood donations were approved by the Competent National Authority (Paul-Ehrlich-Institut, Langen, Germany) and the ethic committee of the Medical Association Hamburg, Germany (reference numbers: 2020-10376-BO-ff, PV4780), and conducted at the University Medical Centre Hamburg-Eppendorf, Germany. All participants provided written informed consent prior to enrollment in the study.

Preparation of reagents and buffers

⌚ Timing: 30 min

1. Prepare staining buffer.
 - a. Mix 500 mL 1× PBS with 10 mL heat-inactivated Fetal Bovine Serum (FBS) and 2 mL 0.5 M EDTA (see also [materials and equipment](#) section).
2. Reconstitute biotinylated SARS-CoV-2 spike antigens.
 - a. Reconstitute lyophilized proteins with 80 µL of sterile water to obtain a stock concentration of 0.25 mg/mL.
 - b. Use immediately or store in aliquots at –20°C to –80°C for up to three months.
 - c. Avoid repeated freeze and thaw cycles.
3. Aliquot Bio-200 biotin solution for long-term storage (several years) at –20°C or –80°C.
 - a. At 4°C Bio-200 biotin solution is stable for up to 2 months.

KEY RESOURCES TABLE

| REAGENT or RESOURCE | SOURCE | IDENTIFIER |
|---|--|-----------------------------------|
| Antibodies | | |
| PerCP anti-human CD3 Antibody (final dilution 1:54) | Biologend | Cat#344813; RRID: AB_10641841 |
| PerCP anti-human CD14 Antibody (final dilution 1:54) | Biologend | Cat#301847; RRID: AB_2564058 |
| Alexa Fluor® 700 anti-human CD56 (NCAM) Antibody (final dilution 1:54) | Biologend | Cat#318316; RRID: AB_604104 |
| Brilliant Violet 650™ anti-human CD20 Antibody (final dilution 1:54) | Biologend | Cat#302335; RRID: AB_11218609 |
| Brilliant Violet 785™ anti-human IgD Antibody (final dilution 1:54) | Biologend | Cat#348241; RRID: AB_2629808 |
| Brilliant Violet 570™ anti-human IgM Antibody (final dilution 1:54) | Biologend | Cat#314517; RRID: AB_10913816 |
| BD OptiBuild™ BUV805 Mouse Anti-Human IgG (final dilution 1:54) | BD | Cat#742041; RRID: AB_2871333 |
| BUV563 Mouse Anti-Human CD19 (final dilution 1:54) | BD | Cat#612917; RRID: AB_2870202 |
| BD Horizon™ BUV737 Mouse Anti-Human CD21 (final dilution 1:54) | BD | Cat#612788; RRID: AB_2870115 |
| BD Horizon™ BB515 Mouse Anti-Human CD27 (final dilution 1:54) | BD | Cat#564643; RRID: AB_2744354 |
| IgA Antibody anti-human, APC-Vio 770 (final dilution 1:54) | Miltenyi Biotec | Cat#130-113-999; RRID: AB_2733153 |
| Biotinylated detection mAbs (MT78/145) (final dilution 1:100) | Mabtech | Cat#3850-6-250; PRID: AB_10666158 |
| Biological samples | | |
| Cryopreserved PBMCs from healthy volunteers vaccinated against SARS-CoV-2 | University Medical Center Hamburg-Eppendorf, Germany | N/A |

(Continued on next page)

STAR Protocols

Protocol



Continued

| REAGENT or RESOURCE | SOURCE | IDENTIFIER |
|---|-------------------|---|
| Chemicals, peptides, and recombinant proteins | | |
| SARS-CoV-2 (2019-nCoV) Spike S1-His Recombinant Protein, Biotinylated | Sino Biological | 40591-V08H-B |
| SARS-CoV-2 (2019-nCoV) Spike S2 ECD-His Recombinant Protein, Biotinylated | Sino Biological | 40590-V08B-B |
| SARS-CoV Spike/RBD Protein (RBD, His Tag), Biotinylated | Sino Biological | 40150-V08B2-B |
| FcR Blocking Reagent human | Miltenyi Biotec | Cat#130-059-901 |
| LIVE/DEAD™ Fixable Blue Dead Cell Stain Kit | Thermo Fisher | Cat#L23105 |
| PE-Cy5.5 Streptavidin | Thermo Fisher | Cat#SA1018 |
| AF647 Streptavidin | Biolegend | Cat#405237 |
| PE-Cy7 Streptavidin | Biolegend | Cat#405206 |
| PE Streptavidin | Biolegend | Cat#405203 |
| BV711 Streptavidin | Biolegend | Cat#405241 |
| BV421 Streptavidin | Biolegend | Cat#405225 |
| BIO200 - BIO-200 biotin solution | Avidity | Cat#BIO200 |
| Brilliant Stain Buffer | BD | 566349 |
| UltraComp eBeads™ Compensation Beads | Thermo Fisher | 01-2222-41 |
| SpectroFlo® QC Beads | Cytek Biosciences | SKU B7-10001 |
| Software and algorithms | | |
| SpectroFlo® v3.0.1 | Cytek Biosciences | https://cytekbio.com/ |
| FlowJo v10.8.0 | FlowJo, LLC | https://www.flowjo.com/ |

MATERIALS AND EQUIPMENT

Staining buffer

| Reagent | Final concentration | Amount |
|----------------------|---------------------|--------------|
| DPBS | N/A | 500 mL |
| Heat-inactivated FBS | 2% (v/v) | 10 mL |
| EDTA (0.5 M) | 2 mM | 2 mL |
| Total | N/A | 50 mL |

Store at 4°C up to two months.

Optical configuration of the S laser Cytek Aurora (Cytek Biosciences, Fremont, California)

| Laser | Excitation wavelength | Channels for detection |
|--------------|-----------------------|------------------------|
| Ultraviolet | 355 nm | UV1-UV16 |
| Violet | 405 nm | V1-V16 |
| Blue | 488 nm | B1-B14 |
| Yellow Green | 561 nm | YG1-YG10 |
| Red | 640 nm | R1-R8 |

STEP-BY-STEP METHOD DETAILS

Preparation of antigen probes

- ⌚ Timing: 30 min preparation + 60 min incubation

In this step, antigen probes for detection of SARS-CoV-2 spike-specific B cells are prepared by multi-merization of biotinylated antigens with fluorescently labeled streptavidin (SA).

1. Dilute SA conjugates to a concentration of 50 ng/μL in staining buffer.

Table 1. Preparation of antigen probes

| | Concentration [mg/mL] | Amount [ng/sample] | Volume [μL/sample] |
|---------------------------------------|--------------------------|-----------------------|-----------------------|
| SA-AF647/SARS-CoV-2-S1-biotin | | | |
| SA-AF647 (52 kDa) | 0.05 | 15 | 0.3 |
| SARS-CoV-2-S1-biotin (76.5 kDa) | 0.25 | 90 | 0.36 |
| Staining buffer | N/A | N/A | 0.34 |
| SA-PE-Cy7/SARS-CoV-2-S1-biotin | | | |
| SA-PE-Cy7 (52 kDa) | 0.05 | 15 | 0.3 |
| SARS-CoV-2-S1-biotin (76.5 kDa) | 0.25 | 90 | 0.36 |
| Staining buffer | N/A | N/A | 0.34 |
| SA-PE/SARS-CoV-2-S2-biotin | | | |
| SA-PE (52 kDa) | 0.05 | 15 | 0.3 |
| SARS-CoV-2-S2-biotin (59.37 kDa) | 0.25 | 75 | 0.3 |
| Staining buffer | N/A | N/A | 0.3 |
| SA-BV711/SARS-CoV-2-S2-biotin | | | |
| SA-BV711 (52 kDa) | 0.05 | 15 | 0.3 |
| SARS-CoV-2-S2-biotin (59.37 kDa) | 0.25 | 75 | 0.3 |
| Staining buffer | N/A | N/A | 0.3 |
| SA-BV421/SARS-CoV-2-RBD-biotin | | | |
| SA-BV421 (52 kDa) | 0.05 | 15 | 0.3 |
| SARS-CoV-2-RBD-biotin (26.5 kDa) | 0.25 | 33 | 0.13 |
| Staining buffer | N/A | N/A | 0.17 |

- Mix SA conjugates (15 ng/ sample) with the respective biotinylated antigens at a molar ratio of 1:4 and add staining buffer according to [Table 1](#). Mass ratios were calculated as 1:6 for SA/SARS-CoV-2-S1, 1:5 for SA/SARS-CoV-2-S2 and 1:2.2 for SA/SARS-CoV-2-RBD.
- Incubate for 60 min at 4°C and use the incubation time to thaw cryopreserved PBMCs.

Note: As antigen-specific B cells are very rare, bright fluorophores are used for labeling of antigen probes. To exclude B cells binding to the respective fluorophores, each antigen is separately multimerized with SA labeled with two different fluorophores. Only double positive cells are classified as spike-specific. Note that only one fluorophore is used for the RBD, as it is part of the S1 subunit and can be plotted against one of the S1 antigen probes.

Alternatives: In this step, the antigens can be exchanged to adjust the protocol to detect B cells specific to other variants of the spike protein or other antigens of SARS-CoV-2, as well as antigens of other pathogens. For adjustment to other SARS CoV-2 variants, the amounts of S1, S2, and RBD can be adopted from [Table 1](#), as they have the same molecular weight. For different proteins, the mass ratio to be used for labeling with fluorophore-conjugated SA has to be calculated based on a molar ratio of 1:4 (SA: protein), as described above. If there is only one antigen of interest, the other antigen probes/ fluorophores can be excluded from the staining protocol.

Thawing of cryopreserved PBMC

⌚ **Timing:** 45 min, depending on number of samples

In this step, cryopreserved human PBMCs are thawed and counted for subsequent staining.

- Prepare a 15 mL conical tube with 9 mL of ice-cold staining buffer for each sample and cool down centrifuge to 4°C.

STAR Protocols

Protocol



5. Thaw cells.
 - a. Place cryotube with frozen PBMCs in a 37°C water bath until partially thawed.
 - b. Rapidly transfer vial into sterile working bench and decant cells into 15 mL conical tube containing staining buffer.
 - c. Use 1 mL of fresh staining buffer to collect remaining cells from cryotube and transfer them into the same 15 mL conical tube.

△ **CRITICAL:** Rapidly conduct steps 5a–c. Subsequently place samples on ice until continuation with step 6 to reduce toxicity of DMSO contained in the freezing medium.

6. Wash and count PBMCs.
 - a. Centrifuge samples for 8 min at 600 g and 4°C.
 - b. Discard the supernatant and resuspend cells using a 200 µL pipette.
 - c. Fill tube up to 10 mL with ice-cold staining buffer and resuspend directly before counting.
 - d. Mix 20 µL of cell suspension with 20 µL of Trypan Blue, transfer 10 µL into counting slide and count cells manually or using an automated cell counter.
 - e. Centrifuge samples for 8 min at 600 g and 4°C.
 - f. Discard the supernatant and resuspend cells in a maximum volume of 200 µL of staining buffer.
7. Transfer 5 to 10 million PBMCs to a 96 well V-bottom plate for staining.

Note: This protocol was established for staining of 5–10 million PBMCs per sample, but can also be used for staining lower or higher amounts of cells. Note that lower cell numbers may reduce the sensitivity of the assay due to the low frequency of antigen-specific B cells within PBMCs.

Staining of PBMCs for flow cytometric analysis

⌚ **Timing:** 3 h

This section describes the procedure of staining PBMCs for flow cytometric analysis and consists of three staining steps and subsequent fixation. At first, the PBMCs are stained with an amine-reactive dye for detection of dead cells, in combination with an Fc receptor (FcR) blocking reagent to prevent non-specific binding of antibodies via their Fc region. The subsequent staining of antigen-specific cells is performed using the antigen probes prepared in steps 1–3. Additionally, SA labeled with PE/Cy5.5 is added as a decoy probe to distinguish B cells specific to the spike antigens from those binding to SA. Brilliant Stain Buffer containing free d-biotin is used to minimize potential cross-reactivity between the antigen probes. In a third staining step, different surface markers are stained using fluorophore-conjugated antibodies, followed by fixation with the cross-linking agent paraformaldehyde (PFA).

8. Prepare staining mixes 1 to 3 according to [Table 2](#) and store them at 2°C–8°C until needed.

△ **CRITICAL:** For staining mix 2, free biotin has to be added prior to the sequential addition of SA-labeled antigen probes. This way, any possible free binding sites of SA resulting from the individual labeling reactions are occupied by the free biotin before adding the next antigen probe.

Note: Volumes are indicated for staining of a single sample and can be scaled up depending on sample number. Some excess volume should be included into staining mixes.

9. Perform blocking of Fc receptors and staining of dead cells.
 - a. Centrifuge samples in 96 well plate for 3 min at 500 g and 4°C.
 - b. Decant supernatant.


Table 2. Preparation of staining mixes 1–3

| Reagent | Volume [μ L/sample] |
|--|--------------------------|
| Mix 1: Dead cell staining and FcR blocking | 105 |
| Staining buffer | 100 |
| LIVE/DEAD™ Fixable Blue Dead Cell Stain | 0.1 |
| FcR Blocking Reagent | 5 |
| Mix 2: Antigen-specific staining | 55 |
| Brilliant Stain Buffer | 50 |
| BIO-200 biotin solution | 0.5 |
| Streptavidin-PE-Cy5.5, diluted 1:10 in staining buffer | 0.2 |
| SA-AF647/SARS-CoV-2-S1-biotin | 1 |
| SA-PE-Cy7/SARS-CoV-2-S1-biotin | 1 |
| SA-PE/SARS-CoV-2-S2-biotin | 0.9 |
| SA-BV711/SARS-CoV-2-S2-biotin | 0.9 |
| SA-BV421/SARS-CoV-2-RBD-biotin | 0.6 |
| Mix 3: Antibody surface staining | 135 |
| Staining buffer | 50 |
| Brilliant Stain Buffer | 50 |
| BUV563 α -CD19 | 2.5 |
| BUV737 α -CD21 | 2.5 |
| BUV805 α -IgG | 2.5 |
| BV480 α -CD71 | 2.5 |
| BV570 α -IgM | 2.5 |
| BV650 α -CD20 | 2.5 |
| BV785 α -IgD | 2.5 |
| BB515 α -CD27 | 2.5 |
| PerCP α -CD3 | 2.5 |
| PerCP α -CD14 | 2.5 |
| AF700 α -CD56 | 2.5 |
| APC-Vio770 α -IgA | 2.5 |
| APC/Fire810 α -CD38 | 2.5 |

- c. Resuspend cells in 105 μ L per well of staining mix 1 as prepared in step 8.
- d. Incubate for 15 min at 4°C.
10. Wash cells.
 - a. Add 100 μ L of staining buffer and centrifuge samples for 3 min at 500 g and 4°C.
 - b. Decant supernatant.
 - c. Resuspend cells in 200 μ L staining buffer and centrifuge for 3 min at 500 g and 4°C.
 - d. Decant supernatant.
11. Perform staining of antigen-specific B cells.
 - a. Resuspend cells in 55 μ L of staining mix 2 as prepared in step 8.
 - b. Incubate for 60 min at 4°C.
12. Wash cells as described in steps 10a–d.
13. Stain surface markers.
 - a. Resuspend cells in 135 μ L of mix 3 as prepared in step 8.
 - b. Incubate for 30 min at 4°C.
14. Wash cells as described in steps 10a–d.
15. Fix cells using 4% paraformaldehyde (PFA).
 - a. Resuspend cells in 100 μ L of 4% PFA.
 - b. Incubate for 15 min at 20°C–25°C.
16. Wash cells as described in steps 10a–d.
17. Resuspend cells in 100 μ L of staining buffer and store at 4°C until acquisition.

△ CRITICAL: For incubation steps and storage, samples and staining mixes should be placed in the dark, as the fluorophores are sensitive to light exposure.



Table 3. Panel overview and preparation of single stained controls

| Peak emission channel | Fluorophore | Antibody/ Antigen | Sample type used for reference control | Reagent for single cell staining | Volume [μ L] |
|-----------------------|--------------|----------------------|--|-------------------------------------|-------------------|
| UV | fixable BLUE | dead cell stain | killed PBMCs | fixable BLUE | 0.1 |
| | BUV563 | α -CD19 | PBMCs | BUV563/ α -CD19 | 2.5 |
| | BUV737 | α -CD21 | PBMCs | BUV737/ α -CD21 | 2.5 |
| | BUV805 | α -IgG | PBMCs | BUV805/ α -IgG | 2.5 |
| Violet | BV421 | SARS-CoV-2-RBD | beads | biotin/ α -IgG + SA-BV421 | 1 + 1 |
| | BV480 | α -CD71 | beads | BV480/ α -CD71 | 1 |
| | BV570 | α -IgM | PBMCs | BV570/ α -IgM | 2.5 |
| | BV650 | α -CD20 | PBMCs | BV650/ α -CD20 | 2.5 |
| | BV711 | SARS-CoV-2-S2 | beads | biotin/ α -IgG + SA-BV711 | 1 + 1 |
| | BV785 | α -IgD | PBMCs | BV785/ α -IgD | 2.5 |
| Blue | BB515 | α -CD27 | PBMCs | BB515/ α -CD27 | 2.5 |
| | PerCP | α -CD3 | PBMCs | PerCP/ α -CD3 | 2.5 |
| | | α -CD14 | beads | PerCP/ α -CD14 | 1 |
| Yellow/Green | PE | SARS-CoV-2-S2 | beads | biotin/ α -IgG + SA-PE | 1 + 1 |
| | PE-Cy5.5 | Streptavidin | beads | biotin/ α -IgG + SA-PE-Cy5.5 | 1 + 1 |
| | PE-Cy7 | SARS-CoV-2-S1 | beads | biotin/ α -IgG + SA-PE-Cy7 | 1 + 1 |
| | AF647 | SARS-CoV-2-S1 | beads | biotin/ α -IgG + SA-AF647 | 1 + 1 |
| Red | AF700 | α -CD56 | beads | AF700/ α -CD56 | 1 |
| | APC-Vio770 | α -IgA | beads | APC-Vio770/ α -IgA | 1 |
| | APC-Fire810 | α -CD38 | PBMCs | APC-Fire810/ α -CD38 | 2.5 |

▮▮▮ Pause point: Samples can be acquired directly or stored at 4°C to be measured the next day.

Single stained controls for Cytex Aurora

⌚ Timing: 90 min (or in parallel with regular staining protocol)

This section describes the preparation of single stained reference controls, which have to be prepared for each fluorophore included in the assay. Reference controls are needed for unmixing of raw data files, as they define the signature of each fluorophore across the full emission spectrum. If possible, reference controls should be prepared using the same cell type and staining protocol as for the regular staining procedure. However, it might be more feasible to use compensation beads (e.g., UltraComp eBeads, Thermo Fisher) for antibodies directed against rare antigens, to obtain sufficient events in the fluorophore-positive population. To provide reference controls for the fluorophores used in the antigen probes, compensation beads can be coated with any biotinylated antibody of host species mouse, rat or hamster, and subsequently labeled with the respective fluorophore-conjugated SA. Staining of reference controls for dead cell stains can be performed on killed PBMCs (e.g., by heat shocking, as described below).

Note: Reference controls only have to be prepared and acquired once and can then be saved and re-used for all subsequent measurements.

18. Kill PBMCs for dead cell stain reference control.
 - a. Transfer approximately 2 million PBMCs into a 1.5 mL tube and incubate in the water bath at 65°C for 10 min.
19. Distribute PBMCs and compensation beads in 96 well plate, as needed for reference controls (see Table 3). Include two additional wells for unstained PBMCs and beads, respectively.
 - a. Killed PBMCs: add approximately 2 million cells per well.



- b. PBMCs: add approximately 2 million cells per well.
 - c. Beads: add one drop of beads per well.
 - 20. Wash samples.
 - a. Fill up wells to approximately 200 μ L with staining buffer.
 - b. Centrifuge samples for 3 min at 500 g and 4°C.
 - c. Discard supernatant.
 - 21. Perform single stain of dead cells.
 - a. Dilute LIVE/DEAD™ Fixable Blue Dead Cell Stain 1:1000 in staining buffer.
 - i. Add 100 μ L of diluted fixable BLUE to killed PBMCs.
 - ii. Add 100 μ L of staining buffer to all other samples.
 - b. Resuspend samples and incubate for 15 min at 4°C.
 - 22. Wash samples.
 - a. Add 100 μ L of staining buffer and centrifuge samples for 3 min at 500 g and 4°C.
 - b. Decant supernatant.
 - c. Resuspend samples in 200 μ L staining buffer and centrifuge for 3 min at 500 g and 4°C.
 - d. Decant supernatant.
 - 23. Perform single stains on PBMCs and beads according to [Table 3](#).
 - a. Resuspend all samples in 100 μ L of staining buffer.
 - i. PBMCs: add 2.5 μ L of the respective antibody.
 - ii. Beads: add 1 μ L of the respective antibody or 1 μ L of biotinylated anti-IgG antibody plus 1 μ L of fluorescently labeled SA.
 - b. Incubate for 30 min at 4°C.
- Alternatives:** Instead of biotinylated anti-IgG antibody, a biotinylated antibody directed against any antigen can be used, as the compensation beads capture any mouse, rat, or hamster antibody.
- 24. Wash samples as described in steps 22a–d.
 - 25. Fix cells using 4% paraformaldehyde (PFA).
 - a. Resuspend cells in 100 μ L of 4% PFA.
 - b. Resuspend beads in 100 μ L of staining buffer.
 - c. Incubate for 15 min at 20°C–25°C.
 - 26. Wash samples as described in steps 22a–d.
 - 27. Resuspend samples in 100 μ L of staining buffer and store at 4°C in the dark until acquisition.

Note: Fixation with PFA is only required for cellular samples, and steps 25 to 26 may be skipped for the wells containing compensation beads. However, it may be more feasible to stain cells and beads in the same plate and to resuspend beads in staining buffer during fixation of cellular samples, as described above.

Acquisition at Cytek Aurora

⌚ **Timing:** 2–5 h, depending on number of samples

Warm-up of lasers and running of Quality Control (QC): 60 min.

Setting up experiment and reference controls: 30 min.

Acquisition: approximately 5 min per sample.

This section describes the process of starting up the Cytek Aurora, setting up a new experiment and acquiring reference controls as well as samples. Parts of this section are adopted from the Cytek® Aurora Quick Reference Guide (available from <https://cytekbio.com/pages/user-guides>).

STAR Protocols

Protocol



28. Start-up Cytex Aurora.
 - a. Start SpectroFlo software and switch on Cytex Aurora.
 - b. Perform "Clean Flow Cell" and run ddH₂O for 30 min.
 - c. After at least 45 min of laser warm-up, run QC with SpectroFlo® QC Beads.
29. Set up experiment.
 - a. Create a new experiment.
 - b. Select fluorescent tags used in your experiment (see [Table 3](#) for complete panel).
 - c. Add groups.
 - i. Create a reference group and select control type (Cells or Beads) for each single-stained control.
 - ii. Create groups for your samples. Add tubes and label them with sample IDs (tubes and labels can be edited at any time during the experiment).
 - d. Enter labels for markers associated with each fluorescent tag.
 - e. Define acquisition settings. For groups containing samples (not reference controls), adjust stopping criteria to high thresholds to make sure that the whole sample is acquired, as an example:
 - i. Events to Record: 1,000,000.
 - ii. Stopping Volume (μL): 3,000.
 - iii. Stopping Time (sec): 10,000.
 - f. Save and open experiment.
30. Acquire reference controls.
 - a. Select the Default Raw Worksheet (Raw) for the reference controls.
 - b. Adjust SSC and FSC gains to be on scale for cells or beads, respectively.
 - c. Record unstained and single stained controls of the reference group.
 - d. Select live unmixing.
31. Acquire samples.
 - a. Select the Default Unmixed Worksheet for the samples.
 - b. Create plots resembling the basic gating strategy to be able to monitor cell populations while recording.
 - c. Adjust SSC and FSC gains for the lymphocyte population to be on scale.
 - d. Transfer each sample from the 96 well plate to a 5 mL flow cytometry tube. Pass through a cell strainer cap to ensure single cell suspension and wash out with 50–100 μL of staining buffer. The volume of buffer can be adjusted to change the event rate.
 - e. Vortex each tube prior to acquisition to resuspend cells.
 - f. Acquire samples.
32. Export unmixed fcs files.

EXPECTED OUTCOMES

For identification and quantification of cell populations, the fcs data files can be analyzed using FlowJo or comparable software packages. An exemplary analysis using the FlowJo software is provided in [Figures 1](#) and [2](#), based on samples from four healthy donors obtained before and at different time points after vaccination against SARS-CoV-2. Donor characteristics and type of vaccinations are indicated in [Table 4](#).

Our proposed gating strategy for identification of B cell subsets within the PBMC population is shown in [Figure 1A](#). Lymphocytes are first identified based on their size and granularity using the forward scatter (FSC) and sideward scatter (SSC) signals, followed by exclusion of doublets and dead cells. Subsequently, T cells, monocytes and NK cells are excluded based on their expression of CD3, CD14 and CD56, respectively, and B cells are identified by their expression of CD19. MBCs are then gated as IgD⁺CD20⁺ cells as opposed to IgD⁺ naïve B cells and IgD⁺CD20⁻ antibody-secreting cells (ASCs). The majority of the ASC population is short-lived and only transiently present after vaccination or infection, whereas MBCs can persist for years or even decades after immunization.²⁻⁴

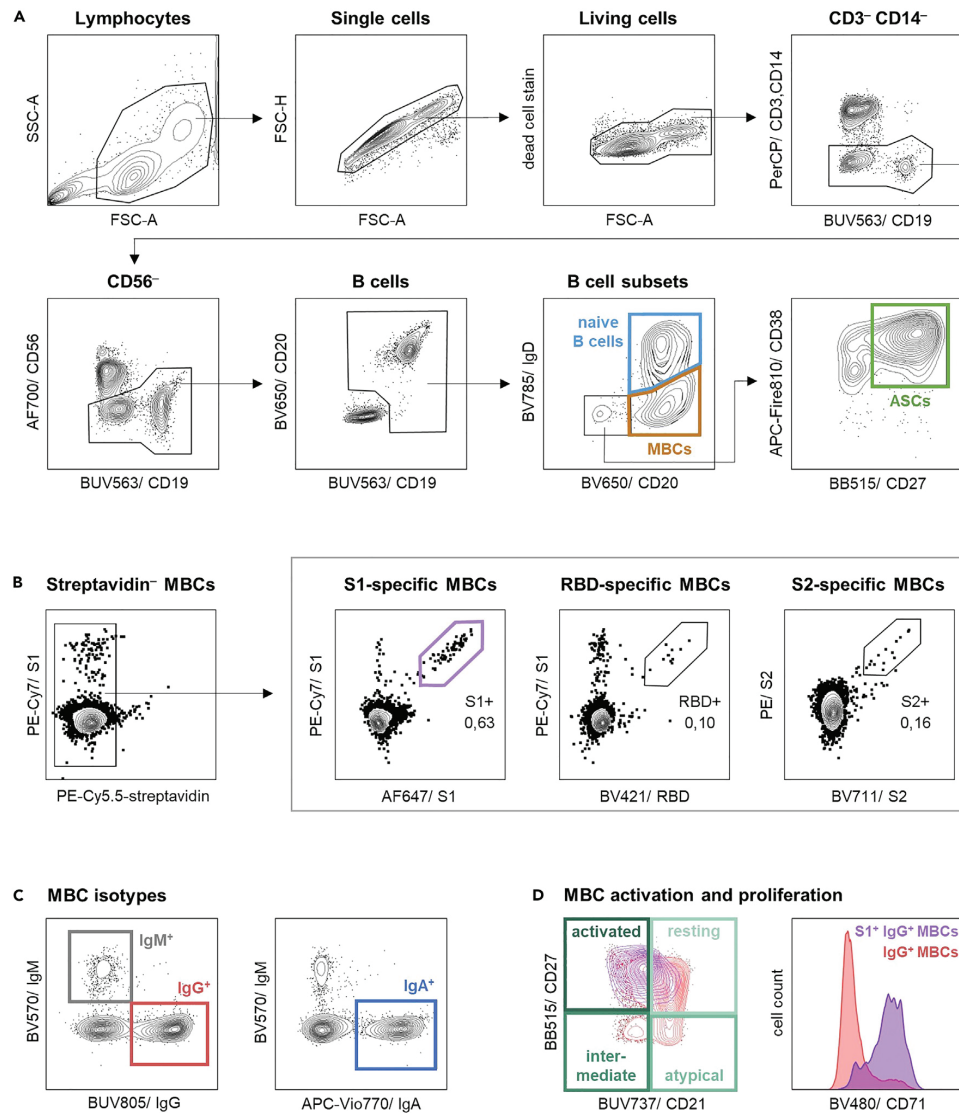


Figure 1. Gating strategy for identification of B cell subsets and characterization of memory B cells (MBCs)

(A) Identification of B cell subsets from PBMCs. Lymphocytes are first identified based on their size and granularity as indicated by the forward scatter (FSC) and sideward scatter (SSC) signals. Subsequently, doublets and dead cells are excluded from the analysis, as well as T cells, monocytes and NK cells, based on expression of CD3, CD14 and CD56, respectively. B cells are identified by expression of CD19 and/or CD20 and subsequently further divided into B cell subsets. Memory B cells (MBCs) are identified as IgD⁻CD20⁺ cells as opposed to IgD⁺ naive B cells and IgD⁻CD20⁺ antibody-secreting cells.

(B) Identification of antigen-specific MBCs. After exclusion of streptavidin-binding MBCs, antigen-specific cells are identified as double positive for the respective antigen probes (S1, RBD, S2).

(C) Identification of isotypes IgM, IgG and IgA within the MBC population.

(D) MBC activation and proliferation status, depicted as overlaid contour plots and histograms of total IgG⁺ MBCs (red) and S1-specific IgG⁺ MBCs (purple). Resting, intermediate, atypical, and activated MBCs are identified by expression of CD21 and CD27 (left panel). CD21 serves as a marker of proliferation activity (right panel). Representative contour plots are shown for donor 1, day 19 after the second SARS-CoV-2 vaccination (A and B) and donor 2, day 8 after the third vaccination (C and D).

STAR Protocols

Protocol



The MBC compartment can be further characterized based on antibody isotypes and activation status, as well as specificity towards SARS-CoV-2. Spike-specific cells directed against the S1 and S2 subunits and the RBD can be identified as shown in [Figure 1B](#). After exclusion of streptavidin-binding MBCs, antigen-specific cells are identified as double positive for the respective antigen probes (S1, S2, RBD). This way, MBCs specifically binding to the respective fluorophores can be excluded from the analysis. Furthermore, unswitched MBCs (IgM⁺) can be distinguished from class-switched MBCs of the isotypes IgG and IgA ([Figure 1C](#)). CD21 and CD27 can be used to assess the distribution of resting (CD21⁺CD27⁺), intermediate (CD21⁺CD27⁻), activated (CD21⁻CD27⁺) and atypical (CD21⁺CD27⁻) MBCs, and CD71 serves as an additional proliferation marker ([Figure 1D](#)). Activated/proliferating MBCs resemble plasma cell precursors⁵ and are expected to be induced in response to vaccination or infection.

The gating strategies shown in [Figures 1B–1D](#) can be conducted in different orders and combinations, depending on the objective of the analysis. The gating hierarchy shown in [Figure 1B](#) followed by [Figure 1C](#) can be used to analyze the relative contribution of each isotype to the total spike-specific B cell population. This may be useful for understanding differences in isotype distribution between infection and vaccination. Reversing the order, i.e., applying gates shown in [Figure 1C](#) before gates shown in [Figure 1B](#), can be more feasible to monitor the frequency of spike-specific B cells within each MBC isotype over time. The activation status of MBCs can differ between the spike-specific cell population and the total MBC compartment, as illustrated for the IgG isotype in the exemplary plots ([Figure 1D](#)). However, it might also be interesting to characterize the activation status of spike-specific cells at different time points (e.g., before and after booster vaccination or infection) or in different settings (e.g., vaccination versus infection).

Generally, antigen-specific MBCs are expected to be rare or non-existent in naïve individuals and to be induced upon vaccination or infection. They can persist in the human body for up to years or decades, with their frequency strongly depending on the time point after vaccination or infection, the type and schedule of vaccines administered, as well as the individual preconditions.^{2,6} In [Figure 2](#), we illustrate the frequencies of S1-specific MBCs in the IgG⁺ MBC population, as detected at different time points before and after SARS-CoV-2 vaccination in four healthy donors (see also [Table 4](#)). In all four individuals, S1-specific IgG⁺ MBCs are not detectable at baseline, but emerge following vaccination. The frequencies of S1-specific cells range between 0.22%–1.00% of IgG⁺ MBCs after two vaccinations (depending on donor and time point) and further increase to 1.12%–4.82% following a third vaccination. For donor 4, S1-specific cells are additionally characterized following a breakthrough infection experienced 15 weeks after the third vaccination, showing a frequency of 2.54% in the IgG⁺ MBC population.

The exemplary plots shown in [Figure 2](#) aim to illustrate possible outcomes of the protocol described above. However, they do not suffice to comprehensively describe MBC dynamics induced by SARS-CoV-2 vaccination and infection, which have been addressed in numerous studies by different research groups. For example, Dan et al.⁷ analyzed frequencies of IgM⁺, IgG⁺ and IgA⁺ MBCs for up to 8 months after SARS-CoV-2 infection. Goel et al.⁸ describe differences in the MBC population induced by mRNA vaccination in naïve and SARS-CoV-2 recovered individuals, providing frequencies and isotype distribution. A comprehensive analysis of MBCs induced by different SARS-CoV-2 vaccines has been conducted by Zhang et al.⁹ and the impact of booster vaccinations and breakthrough infections on the MBC compartment is addressed in a study by Buckner et al.¹⁰

LIMITATIONS

Peripheral blood is an important resource for the study of immune responses, as it can be obtained easily from study participants. However, the frequency of antigen-specific B cells in peripheral blood is very low,¹¹ leading to the amount of PBMCs being a limiting factor for this analysis. We recommend to use at least 5 million PBMCs for each sample, as lower numbers would reduce the sensitivity

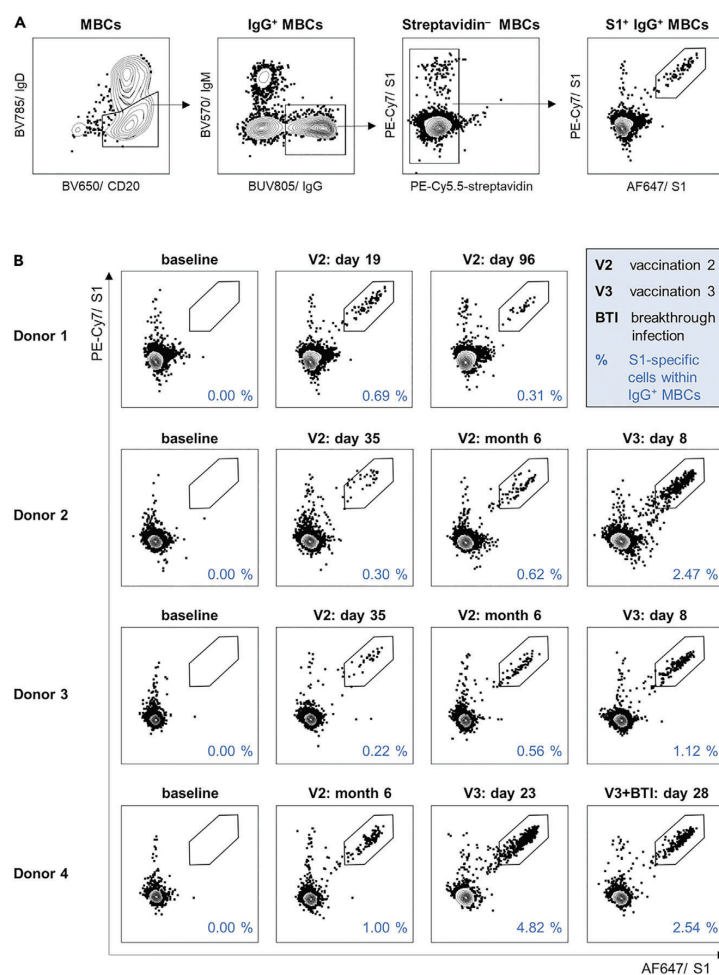


Figure 2. Frequencies of S1-specific IgG⁺ MBCs detected at different time points after vaccination

(A) Gating Strategy for identification of S1-specific IgG⁺ MBCs from the MBC population. Representative contour plots are shown for donor 1.

(B) Frequencies of S1-specific IgG⁺ MBCs. Exemplary plots are shown for donors 1–4 at baseline and at different time points after the second and third vaccination (V2, V3) as well as after breakthrough infection (BTI). Percentages indicate the frequency of S1-specific cells within the IgG⁺ MBC population.

of the assay. To gain further insights into the compartments of MBCs and especially long-lived plasma cells, an additional analysis of lymphoid tissue and bone marrow would be of interest, as only a small portion of antigen-experienced B cells is trafficking through peripheral blood.⁴

Despite performance of QC prior to each experiment, slight changes in the laser intensities might occur between measurements conducted on different days. If possible, samples and the related controls (e.g., baseline and later time points of the same study participant) should be measured the same day to reduce batch effects. Clearly separated negative and positive populations are not as sensitive to batch effects, but especially data from continuously expressed markers have to be interpreted carefully if measured on different days.


Table 4. Healthy donors: Baseline characteristics and SARS-CoV-2 vaccinations

| Baseline characteristics | | | SARS-CoV-2 vaccinations | | |
|--------------------------|--------|----------|-------------------------|------|------|
| Donor | Sex | Age | V1 | V2 | V3 |
| 1 | female | 43 years | ChAd | mRNA | N/A |
| 2 | female | 29 years | mRNA | mRNA | mRNA |
| 3 | female | 29 years | mRNA | mRNA | mRNA |
| 4 | male | 33 years | mRNA | mRNA | mRNA |

V1, V2, V3: Vaccination 1, 2, 3; ChAd: Vaxzevria (Astra Zeneca); mRNA: Comirnaty (Biontech/ Pfizer) or Spikevax (Moderna Biotech); N/A: not applicable.

TROUBLESHOOTING

Problem 1

This protocol requires 5 to 10 million PBMCs per staining. However, this amount might not always be available when working with clinical samples (steps 4–7/[expected outcomes](#)).

Potential solution

The staining can in principle also be performed on lower numbers of PBMCs, using the same concentration of antibodies and antigen probes. The identification of B cell populations (naïve B cells, ASCs, MBCs) as well as MBC subsets (isotypes, activation state) can be performed as described above. Using lower numbers of PBMCs mostly affects the ability to detect antigen-specific MBCs. Due to their low frequency in PBMCs, their detection may be difficult and less reproducible when working with low numbers of PBMCs. This has to be kept in mind, especially when analyzing samples with very low antigen-specific MBC counts expected (e.g., late follow-up time points after infection or vaccination). However, analysis of antigen-specific cells is possible with lower numbers of PBMCs, when analyzing samples with relatively high frequencies of MBCs expected (e.g., a few weeks after booster vaccination or breakthrough infection).

Problem 2

Low numbers of cells are detected during acquisition of samples at the Cytex Aurora, despite staining of 5–10 million PBMCs (step 31).

Potential solution

Low detectable cell numbers may be caused by the loss of cells during the staining procedure. During staining and washing steps, make sure to decant the supernatant directly after centrifugation of cells (steps 9–16). Otherwise, the cell pellet might dissolve and parts of it may be discarded with the supernatant. Cell loss during the washing steps may also be reduced by increasing the duration of the centrifugation steps. Furthermore, cells may stick to the wells of the V-bottom plate and can be lost upon transfer to the flow cytometry tube. Make sure to thoroughly resuspend the cells prior to transfer and collect residual cells from the wells with additional staining buffer (step 31d).

Problem 3

High frequencies of dead cells are detected during acquisition, resulting in a smaller population of living lymphocytes for further analysis (step 31).

Potential solution

High numbers of dead cells may result either from bad sample quality of frozen PBMCs, or from inappropriate handling of cells during the thawing and staining procedure. As freezing media containing DMSO are toxic to PBMCs upon thawing, make sure to work fast when thawing PBMCs and only thaw up to 4 vials at a time (step 5). When counting the PBMCs, make sure to check their viability prior to proceeding to the next step and keep the samples on ice during the whole staining procedure. If desired, the portion of dead cells can be reduced by resting of PBMCs for



16–24 h at 37°C, 5% CO₂ and a concentration of 4×10^6 PBMCs per mL in RPMI medium complemented with 10% FBS (before proceeding to step 7). However, this does not improve the absolute cell count of living cells.

Problem 4

No or very few antigen-specific B cells are detected in samples collected following vaccination or infection (step 31/[expected outcomes](#)).

Potential solution

The frequency of antigen-specific B cells might be very low (see [Figure 2](#) for examples), depending on the time point of blood drawing after infection or vaccination, as well as the kind of vaccine administered and the individual characteristics of the donor. Thus, if frequencies of IgG⁺ MBCs are undetectable or lower than expected, it may be difficult to conclude if the results are valid. It may therefore be useful to include a positive control into each measurement, i.e., a sample that is known to have a relatively high frequency of antigen-specific MBCs. For time points where antigen-specific MBCs are expected to be very rare, it might be more efficient to stain more than 10 million PBMCs, adjusting the volume of staining reagents, or to enrich B cells from PBMCs prior to the flow cytometric staining, e.g., via magnetic activated cell sorting (MACS).^{12,13}

Problem 5

We designed our antibody panel for acquisition on a 5 laser Cytex Aurora. However, this flow cytometer may not always be available ([materials and equipment/Table 3](#)).

Potential solution

The staining protocol can be adjusted for acquisition on different flow cytometers with less lasers available or different configurations of detection channels. To reduce the number of fluorophores, different markers can be left out and/or changed to other fluorophores, depending on the objective of the analysis (step 8). For example, the antigen-specific staining can be reduced to one antigen, resulting in three fluorophores less. For some studies, it might be sufficient to analyze MBCs of the IgG isotype and remove the antibodies for detection of IgM and IgA from the panel. If changing the fluorophores used for certain antibodies or antigen probes, make sure to use bright fluorophores for the detection of markers that are expressed at low levels or cell populations of low frequency, such as antigen-specific MBCs. Note that the antibody dilutions indicated in the [key resources table](#) refer to the staining mix using the whole antibody panel described in this protocol. If leaving out some antibodies, we recommend to stick with the volumes indicated in [Table 2](#), which will result in slightly increased final antibody concentrations due to reduced total volume of the staining mix.

RESOURCE AVAILABILITY

Lead contact

Further information and requests for resources and reagents should be directed to and will be fulfilled by the lead contact, Leonie M. Weskamm (m.weskamm@uke.de).

Materials availability

This study did not generate new unique reagents.

Data and code availability

This study did not generate or analyze datasets or code.

ACKNOWLEDGMENTS

This work was funded by the German Center for Infection Research (DZIF), grant numbers FKZ8009701709 and FKZ8009801921. We want to thank Anahita Fathi for support of the clinical management, Johannes Brandi for sharing his expertise on the Cytex Aurora and Leonie Mayer for supporting the review process, as well as Monika Friedrich, Cordula Grüttner, My Linh Ly, and

STAR Protocols

Protocol



Maren Sandkuhl for general technical support and isolation of PBMCs. We also want to thank all study participants for their contribution to this study.

AUTHOR CONTRIBUTIONS

Conceptualization, L.M.W., C.D.; methodology, L.M.W.; investigation, L.M.W.; writing – original draft, L.M.W.; writing – review & editing, L.M.W., C.D.; funding acquisition, C.D., M.M.A.; resources, M.M.A.; supervision, C.D., M.M.A.

DECLARATION OF INTERESTS

The authors declare no competing interests.

REFERENCES

- Weskamm, L.M., Fathi, A., Raadsen, M.P., Mykytyn, A.Z., Koch, T., Spohn, M., Friedrich, M., MVA-MERS-S Study Group, Haagmans, B.L., Becker, S., et al. (2022). Persistence of MERS-CoV-spike-specific B cells and antibodies after late third immunization with the MVA-MERS-S vaccine. *Cell Rep. Med.* **3**, 100685.
- Akkaya, M., Kwak, K., and Pierce, S.K. (2020). B cell memory: building two walls of protection against pathogens. *Nat. Rev. Immunol.* **20**, 229–238. <https://doi.org/10.1038/s41577-019-0244-2>.
- Blanchard-Rohner, G., Pulickal, A.S., Jol-van der Zijde, C.M., Snape, M.D., and Pollard, A.J. (2009). Appearance of peripheral blood plasma cells and memory B cells in a primary and secondary immune response in humans. *Blood* **114**, 4998–5002. <https://doi.org/10.1182/blood-2009-03-211052>.
- Palm, A.K.E., and Henry, C. (2019). Remembrance of things past: long-term B cell memory after infection and vaccination. *Front. Immunol.* **10**, 1787.
- Sanz, I., Wei, C., Jenks, S.A., Cashman, K.S., Tipton, C., Woodruff, M.C., Hom, J., and Lee, F.E.H. (2019). Challenges and opportunities for consistent classification of human B cell and plasma cell populations. *Front. Immunol.* **10**, 2458.
- Siegrist, C.-A. (2018). 2 - vaccine immunology. In Plotkin's Vaccines, Seventh Edition, S.A. Plotkin, W.A. Orenstein, P.A. Offit, and K.M. Edwards, eds. (Elsevier), pp. 16–34.e17. <https://doi.org/10.1016/B978-0-323-35761-6.00002-X>.
- Dan, J.M., Mateus, J., Kato, Y., Hastie, K.M., Yu, E.D., Faliti, C.E., Grifoni, A., Ramirez, S.I., Haupt, S., Frazier, A., et al. (2021). Immunological memory to SARS-CoV-2 assessed for up to 8 months after infection. *Science* **371**, eabf4063.
- Goel, R.R., Apostolidis, S.A., Painter, M.M., Mathew, D., Pattekar, A., Kuthuru, O., Gouma, S., Hicks, P., Meng, W., Rosenfeld, A.M., et al. (2021). Distinct antibody and memory B cell responses in SARS-CoV-2 naïve and recovered individuals following mRNA vaccination. *Sci. Immunol.* **6**, eabi6950. <https://doi.org/10.1126/sciimmunol.abi6950>.
- Zhang, Z., Mateus, J., Coelho, C.H., Dan, J.M., Moderbacher, C.R., Gálvez, R.I., Cortes, F.H., Grifoni, A., Tarke, A., Chang, J., et al. (2022). Humoral and cellular immune memory to four COVID-19 vaccines. Preprint at bioRxiv. <https://doi.org/10.1101/2022.03.18.484953>.
- Buckner, C.M., Kardava, L., El Merhebi, O., Narpala, S.R., Serebryanny, L., Lin, B.C., Wang, W., Zhang, X., Lopes de Assis, F., Kelly, S.E.M., et al. (2022). Interval between prior SARS-CoV-2 infection and booster vaccination impacts magnitude and quality of antibody and B cell responses. *Cell* **185**, 4333–4346.e14. <https://doi.org/10.1016/j.cell.2022.09.032>.
- Waltari, E., McGeever, A., Friedland, N., Kim, P.S., and McCutcheon, K.M. (2019). Functional enrichment and analysis of antigen-specific memory B cell antibody repertoires in PBMCs. *Front. Immunol.* **10**, 1452. <https://doi.org/10.3389/fimmu.2019.01452>.
- Moore, D.K., Motaung, B., du Plessis, N., Shabangu, A.N., and Loxton, A.G.; SU-IRG Consortium (2019). Isolation of B-cells using Miltenyi MACS bead isolation kits. *PLoS One* **14**, e0213832. <https://doi.org/10.1371/journal.pone.0213832>.
- Boonyaratanakornkit, J., and Taylor, J.J. (2019). Techniques to study antigen-specific B cell responses. *Front. Immunol.* **10**, 1694. <https://doi.org/10.3389/fimmu.2019.01694>.

2.3 Humoral and cellular immunogenicity of two MVA-based COVID-19 vaccine candidates compared to ChAd and mRNA platforms

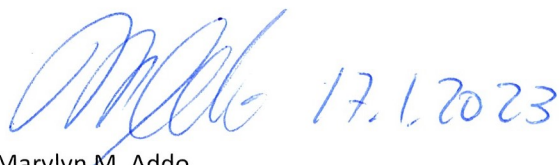
Leonie Mayer,* **Leonie M. Weskamm**,* Anahita Fathi, Maya Kono, Jasmin Heidepriem, Sibylle C. Mellinghoff, My Linh Ly, Monika Friedrich, Svenja Hardtke, Saskia Borregaard, Thomas Hesterkamp, Felix F. Loeffler, the MVA-SARS-2 Study Group, Asisa Volz, Gerd Sutter, Stephan Becker, Christine Dahlke,* Marylyn M. Addo*

*These authors contributed equally

Submitted to *Nature Communications* (16.12.2022)

This manuscript was jointly prepared by Leonie Mayer, responsible for the investigation of T cell responses, and Leonie Marie Weskamm, responsible for the investigation of antibodies and B cells. Leonie Marie Weskamm established the IgG ELISpot assay for analysis of SARS-CoV-2 spike-specific B cells and planned the experiments for analysis of antigen-specific B cells as well as antibody isotypes and subclasses. She was also involved in the execution of these experiments, conducted the data analysis of B cell and antibody assays and was involved in writing and editing of the manuscript draft. Visualization of study cohorts and experimental data in Figures 1 to 8 was jointly performed by Leonie Mayer and Leonie Marie Weskamm. Leonie Marie Weskamm was also involved in the isolation and cryopreservation of serum, plasma and PBMCs from human blood samples, as well as the coordination of sample collection and processing for the different study cohorts.

I hereby confirm the accuracy of these contributions



Prof. Dr. med. Marylyn M. Addo

1 **Humoral and cellular immunogenicity of two MVA-based COVID-19 vaccine candidates compared**
2 **to ChAdOx1 and mRNA platforms**

3

4 Leonie Mayer^{1,2,3,17}, Leonie M. Weskamm^{1,2,3,17}, Anahita Fathi^{1,2,3,4}, Maya Kono^{1,2,3}, Jasmin Heidepriem⁵,
5 Sibylle C. Mellinghoff^{6,7}, My Linh Ly^{1,2,3}, Monika Friedrich^{1,2,3}, Svenja Hardtke^{1,2,3}, Saskia Borregaard⁸,
6 Thomas Hesterkamp⁹, Felix F. Loeffler⁵, the MVA-SARS-2 Study Group¹⁰, Asisa Volz^{11,12}, Gerd Sutter^{13,14},
7 Stephan Becker^{15,16}, Christine Dahlke^{*1,2,3,17}, Marylyn M. Addo^{1,2,3,4,17}

8 ¹Institute for Infection Research and Vaccine Development (IIRVD), University Medical Centre
9 Hamburg-Eppendorf, Hamburg, Germany

10 ²Department for Clinical Immunology of Infectious Diseases, Bernhard Nocht Institute for Tropical
11 Medicine, Hamburg, Germany

12 ³German Centre for Infection Research, partner sites Hamburg-Lübeck-Borstel-Riems, Hamburg,
13 Germany

14 ⁴First Department of Medicine, Division of Infectious Diseases, University Medical Centre Hamburg-
15 Eppendorf, Hamburg, Germany

16 ⁵Max Planck Institute of Colloids and Interfaces, Department of Biomolecular Systems, Potsdam,
17 Germany

18 ⁶Faculty of Medicine and University Hospital of Cologne, Department I of Internal Medicine, Centre for
19 Integrated Oncology Aachen Bonn Cologne Düsseldorf (CIO ABCD), German CLL Group (GCLLSG),
20 University of Cologne, Cologne, Germany

21 ⁷German Centre for Infection Research, partner site Bonn-Cologne, Cologne, Germany

22 ⁸Clinical Trial Center North GmbH & Co. KG, Hamburg, Germany

23 ⁹German Centre for Infection Research, Translational Project Management Office, Brunswick, Germany

24 ¹⁰For the MVA-SARS-2 Study Group members see end of paper

25 ¹¹Institute of Virology, University of Veterinary Medicine Hannover, Foundation, Hanover, Germany

26 ¹²German Centre for Infection Research, partner site Hannover-Brunswick, Hanover, Germany

27 ¹³Division of Virology, Institute for Infectious Diseases and Zoonoses, Department of Veterinary
28 Sciences, LMU Munich, Munich, Germany

29 ¹⁴German Centre for Infection Research, partner site Munich, Munich, Germany

30 ¹⁵Institute for Virology, Philipps University Marburg, Marburg, Germany

31 ¹⁶German Centre for Infection Research, partner site Gießen-Marburg-Langen, Marburg, Germany

32 ¹⁷These authors contributed equally to this work

33 *Correspondence: c.dahlke@uke.de (C.D.)

34 Abstract

35 In response to the COVID-19 pandemic, multiple vaccines were developed using platforms such as
36 mRNA and viral vectors. Here, we report data from phase 1 clinical trials of two recombinant Modified
37 Vaccinia virus Ankara (rMVA)-based vaccine candidates, MVA-SARS-2-S and MVA-SARS-2-ST, encoding
38 different conformations of the SARS-CoV-2 spike protein. Humoral and cellular immunogenicity were
39 assessed in direct comparison to licensed mRNA- and ChAdOx1-based COVID-19 vaccines, revealing
40 distinct immune signatures. MVA-SARS-2-ST was more immunogenic than MVA-SARS-2-S, with
41 differential specificity towards the spike subunits S1 and S2. Both rMVA-based vaccines were less
42 immunogenic in naïve individuals compared to the licensed vaccines. In heterologous vaccination,
43 MVA-SARS-2-S enhanced the functionality and MVA-SARS-2-ST was able to boost the frequency of
44 antigen-specific T cells. Additionally, we observed distinct IgG subclass patterns after repeated mRNA
45 vaccination. These data underscore the impact of vaccine design on immunogenicity and the potential
46 of immune bridging to assess novel vaccine candidates.

47 Keywords

48 SARS-CoV-2, COVID-19, vaccine platforms, rMVA, antibodies, T cells

49 Introduction

50 The severe acute respiratory syndrome coronavirus 2 (SARS-CoV-2) causing coronavirus disease 2019
51 (COVID-19) has led to significant morbidity and mortality since its emergence in 2019 and subsequent
52 global spread. Vaccines against COVID-19 were rapidly available and their widespread use has
53 significantly reduced mortality and disease burden in the past two years ¹⁻⁴. The accelerated
54 development of COVID-19 vaccines was, in part, possible since the emergence of SARS-CoV and *Middle*
55 *East respiratory syndrome coronavirus (MERS-CoV)* had advanced research on *Betacoronaviruses* and
56 especially on the function of the characteristic spike (S) glycoprotein ^{5,6}. Due to its crucial role in virus
57 entry and exposed position on the virus surface, the S-protein is an important target of the host
58 immune response and thus a promising vaccine antigen ⁷. Furthermore, vaccine platforms such as
59 mRNA and viral vectors had been optimized prior to the pandemic and could quickly be adjusted to
60 encode the new antigen upon emergence of SARS-CoV-2 ⁸.

61 One promising vaccine platform against emerging viruses is the recombinant Modified Vaccinia virus
62 Ankara (rMVA): an attenuated poxviral vector that efficiently infects but cannot replicate in human
63 cells. MVA has been administered as a third-generation smallpox vaccine and rMVA as viral vaccine
64 vector against different pathogens, also to immunocompromised patients and infants, providing
65 extensive favorable safety data ^{9,10}. Using the rMVA platform, two vaccine candidates against COVID-19
66 were developed ^{11,12}, leveraging the prior experience with an rMVA-based vaccine candidate against
67 MERS (MVA-MERS-S), which encodes the native, full-length MERS-CoV S-protein and was shown to be
68 safe and immunogenic in a first-in-human phase 1 clinical trial ¹³⁻¹⁵.

69 The vaccine candidate MVA-SARS-2-S (MVA-S) was constructed to encode the native, full-length
70 SARS-CoV-2 S-protein, whereas the second vaccine, named MVA-SARS-2-ST (MVA-ST), encodes a
71 prefusion-stabilized version of the S-protein with an inactivated S1/S2 cleavage site. Both vaccine
72 candidates showed protective efficacy in mice and hamsters ^{11,12} and proceeded to evaluation in phase
73 1 clinical trials in October 2020 (MVA-S, ClinicalTrials.gov: NCT04569383) and July 2021 (MVA-ST,
74 ClinicalTrials.gov: NCT04895449), respectively. Both candidates were given to SARS-CoV-2 naïve

75 individuals in a two-dose schedule, 28 days apart, and MVA-ST was additionally tested as a one-dose
76 booster vaccination for mRNA-vaccinated individuals.

77 To evaluate the immunogenicity of the rMVA-based COVID-19 vaccine candidates, we performed a
78 side-by-side comparison to the first three COVID-19 vaccines licensed in the EU. BNT162b2 (Comirnaty)
79 and mRNA-1273 (Spikevax) are mRNA vaccines encoding a prefusion-stabilized SARS-CoV-2 S-protein
80 with the native S1/S2 cleavage site, formulated in lipid-nanoparticles that are given in a two-dose
81 scheme 21 and 28 days apart, respectively¹⁶⁻¹⁸. Both vaccines are here referred to as mRNA. ChAdOx1
82 nCov-19 (Vaxzevria), here referred to as ChAd, is a viral vector vaccine based on a replication-deficient
83 chimpanzee adenovirus, encoding the native, full-length SARS-CoV-2 spike protein. It is administered
84 in a two-dose schedule, most commonly 12 weeks apart^{19,20}. The remarkably high efficacies of the
85 mRNA and ChAd vaccines against symptomatic COVID-19 have been associated with high titers of S-
86 specific binding immunoglobulin G (IgG) and neutralizing antibodies^{21,22}. Nevertheless, these
87 antibodies wane over time and provide an incomplete picture of the adaptive immune response to
88 vaccination as additional parameters, such as memory B and T cells, contribute to long-term immune
89 memory²³⁻²⁶. Due to the lack of standardized assays, the immune response induced by different
90 vaccine platforms should be evaluated side-by-side, in order to identify distinct signatures that may
91 determine protection^{27,28}.

92 In this study, we assessed the immunogenicity of two rMVA-based vaccine candidates in SARS-CoV-2
93 naïve individuals and as a booster vaccination for mRNA-vaccinated individuals, in comparison to two
94 cohorts receiving the licensed mRNA and ChAd vaccines. For this purpose, peripheral blood samples
95 were collected before and at defined time points after vaccination, allowing for a comprehensive and
96 longitudinal comparison of the immune response in individuals receiving five different vaccination
97 regimens. We analyzed S1- and S2-specific antibody isotypes, IgG subclasses, potential IgG epitopes,
98 antigen-specific B cells, and the magnitude and cytokine profile of T cell responses. Our findings
99 highlight the distinct characteristics of the adaptive immune response induced by different S-antigen
100 conformations and vaccine platforms.

101 **Results**

102 To gain insight into the humoral and cellular immune response induced by different vaccine regimens,
103 we evaluated immunogenicity in three cohorts receiving the novel rMVA-based COVID-19 vaccine
104 candidates (MVA-S/mRNA, MVA-ST, mRNA/MVA-ST) in comparison to two control cohorts vaccinated
105 with the licensed ChAd and mRNA vaccines (mRNA, ChAd/mRNA). A detailed description of the
106 vaccination schedules is shown in Fig. 1a. Participant demographics and time intervals between
107 vaccinations of the five study cohorts are shown in Supplementary Tables 1 and 2. Peripheral blood
108 samples were collected longitudinally at T0 (baseline before vaccination), T1 (1-2 weeks), T2 (3-5
109 weeks), T3 (12 weeks), and T4 (17-29 weeks) post vaccination (Fig. 1b; Supplementary Table 3), with
110 weeks referring to time since last vaccination (V1-V4). A total of 452 blood samples were obtained
111 from 75 donors. To characterize the antigen-specific humoral and cellular immune response, we
112 longitudinally measured serum antibodies and performed various phenotypic B and T cell assays as
113 described in Fig. 1c.

114 ***Dynamics of antibody isotypes and subclasses induced by mRNA-, ChAd- and rMVA-based vaccines***

115 In a first step, plasma IgM, IgA and IgG antibodies against the S1 and S2 subunits of the S-protein were
116 measured using a bead-based multiplex enzyme-linked immunosorbent assay (ELISA) which quantifies

117 the relative antibody response based on the median fluorescence intensity (MFI) (Fig. 2a). In general,
118 IgM antibodies were induced at relatively low levels throughout all cohorts, with the strongest
119 induction observed after the first two immunizations with mRNA and MVA-ST vaccines. Compared to
120 IgM, IgA was induced more strongly, especially after repeated vaccination across the cohorts. IgG
121 followed similar kinetics as IgA, but was induced at higher overall magnitude. For all three isotypes,
122 S1-specific antibodies were undetectable at baseline (T0), whereas S2-specific antibodies were already
123 detectable at this time point. Upon vaccination, S1- and S2-specific responses followed similar overall
124 dynamics and remained detectable until the last measured time point. Below, we further describe the
125 S1-specific IgG response, as it shows the strongest induction throughout all cohorts.

126 In the mRNA control cohort, primary mRNA vaccination led to a rapid induction of S1-specific IgG levels
127 (median MFI = 6590; fold change = 1650.2), that were further increased by second mRNA vaccination
128 (median MFI = 19295). IgG levels then waned over a period of six months (median MFI = 5907) and
129 were re-boosted by a third mRNA vaccination to similar levels as seen after the second vaccination. At
130 six months after the third vaccination, IgG levels remained at higher levels (median MFI = 10961)
131 compared to the same time point after the second vaccination. In the ChAd/mRNA control cohort,
132 primary ChAd vaccination led to a rapid induction of S1-specific IgG levels, but at lower magnitude
133 (median MFI = 4373; fold change = 149.8) compared to primary mRNA vaccination. Second vaccination
134 with mRNA further increased the IgG levels in the ChAd/mRNA cohort (median MFI = 14558) to levels
135 comparable with the mRNA cohort. Third vaccination with mRNA also re-boosted the IgG levels in this
136 cohort.

137 In contrast, vaccination with two doses of the MVA-S vaccine candidate (V1 and V2) showed lower
138 levels of S1-specific IgG (median MFI = 19). However, S1-specific IgG was induced at higher levels after
139 the first mRNA vaccination (V3) in this MVA-S/mRNA cohort (median MFI = 10687) compared to the
140 first mRNA vaccination (V1) in the mRNA cohort (median MFI = 6590). Compared to the MVA-S
141 vaccine, two doses of MVA-ST induced a stronger S1-specific IgG response (median MFI = 2942).
142 Nevertheless, levels seen after two mRNA vaccinations (median MFI = 19295) were not reached. When
143 used as a third vaccination in previously mRNA vaccinated (mRNA/MVA-ST cohort), MVA-ST only
144 induced a slight increase of S1-specific IgG (fold change = 1.2) compared to a third mRNA vaccination
145 (fold change = 3.7).

146 Next, we longitudinally analyzed S1- (top panel) and S2- (bottom panel) specific IgG1-IgG4 responses
147 using the bead-based multiplex ELISA (Fig. 2b). Primary vaccination with mRNA, ChAd and MVA-ST
148 induced mainly IgG1 and IgG3, that were boosted by subsequent vaccinations. Overall, both IgG1 and
149 IgG3 followed similar kinetics as observed for total IgG (Fig. 2a). Notably, IgG2 and IgG4 subclasses
150 were only induced in the mRNA and ChAd/mRNA cohorts, where they were first detectable after the
151 second dose of mRNA vaccination, which corresponds to V2 in the mRNA cohort and to V3 in the
152 ChAd/mRNA cohort. These responses were further boosted after the third mRNA vaccination in the
153 mRNA cohort (Fig. 2b).

154 ***Detection of immunogenic B cell epitopes in the S1 and S2 subunits of the S-protein***

155 To further investigate the antigen specificity of vaccine-induced antibodies, we analyzed IgG and IgA
156 binding to S-specific peptides using microarrays. An exemplary heatmap is shown in Fig. 3a, depicting
157 antibody binding measured in arbitrary fluorescent units (AFU). Heatmaps of all cohorts are shown in
158 Supplementary Table 9. Vaccine-induced responses were defined by comparing AFU after vaccination
159 to baseline, and IgG binding to S-specific epitopes was detected in all cohorts after vaccination (Fig.

160 3b). Immunogenic regions in which vaccine recipients from several cohorts showed antibody binding
161 were identified in the S1 subunit (amino acids (AA) 537-635) and in the S2 subunit (AA 763-853, AA
162 1137-1159). One region in the S1/S2 junction (AA 651-707) was only identified in the mRNA cohort.
163 Interestingly, only in the cohorts that had received an MVA vaccination, epitopes were detected in the
164 cytoplasmic tail of the S2 subunit (AA 1245-1273). We did not detect a change in binding of IgA
165 antibodies to S-specific epitopes after vaccination compared to baseline (Supplementary Table 9).

166 ***Dynamics of cellular immune responses induced by mRNA-, ChAd- and rMVA-based vaccines***

167 We characterized the dynamics of the B and T cellular immune response using antigen-specific IgG and
168 interferon gamma (IFN- γ) enzyme-linked immunospot (ELISpot) assay. Representative ELISpot assay
169 wells are shown in Fig. 4d.

170 B cells specific for the S1 and S2 subunits were quantified as IgG spot-forming cells (SFC) per million
171 peripheral blood mononuclear cells (PBMCs) and total IgG-secreting B cells served as a positive control.
172 Overall, the S1- and S2-specific B cell dynamic resembled the S1- and S2-specific IgG antibody response
173 shown in Fig. 2a. In the mRNA cohort, S1- and S2-specific B cells were detected at low frequencies after
174 primary mRNA vaccination (S1: median = 44 SFC; S2: median = 19 SFC), that increased upon second
175 mRNA vaccination (S1: median = 371 SFC; S2 = 122) and were boosted by third vaccination (S1: median
176 = 1200 SFC; S2: median = 220 SFC) (Fig. 4a). S1- and S2-specific B cells persisted at T4 at higher
177 frequencies after the third (S1: median = 200 SFC; S2 = 125 SFC) compared to the second (S1: median
178 = 120 SFC; S2: median = 83 SFC) mRNA vaccination. The ChAd/mRNA cohort showed similar dynamics,
179 with low frequencies of S1- and S2-specific B cells after primary ChAd vaccination (S1: median = 15 SFC;
180 S2: median = 13 SFC) that increased upon second (S1: median = 316 SFC; S2: median = 191 SFC) and
181 third vaccination (S1: median = 556 SFC; S2: median = 175 SFC) with the mRNA vaccine. In the MVA-
182 S/mRNA cohort, a slight induction of S-specific B cells was observed after two MVA-S vaccinations (S1:
183 median = 10 SFC; S2: median = 25 SFC). Of note, S2-specific B cells expanded rapidly after the first
184 mRNA vaccination in this cohort (V3), reaching a median response of 102 SFC compared to 10 SFC in
185 the mRNA cohort without previous MVA-S vaccination (V1). A two-dose vaccination with MVA-ST
186 induced S1- and S2-specific B cells at detectable but low levels in vaccine-naïve participants (MVA-ST
187 cohort S1: median = 14 SFC; S2: median = 14 SFC). In comparison, using MVA-ST as a booster vaccine
188 did not further increase the frequency of S1-and S2-specific B cells in previously mRNA-vaccinated
189 participants (mRNA/MVA-ST cohort).

190 S-specific T cells were analyzed by IFN- γ ELISpot assay. PBMCs were stimulated with an overlapping
191 peptide (OLP) pool spanning the entire S-protein. Results were quantified as IFN- γ -secreting SFC per
192 million PBMCs. In the mRNA cohort, a rapid induction of S-specific T cells was observed after primary
193 vaccination that peaked at V1:T1 (median = 74 SFC) and was increased upon second vaccination (V2:T1:
194 median = 356 SFC) (Fig. 4b). T cells waned during the following six months but remained at higher levels
195 compared to post primary vaccination (V2:T4: median = 93 SFC). Third mRNA vaccination restored the
196 T cell response to levels seen after second vaccination (V3:T1: median = 341 SFC). Of note, S-specific T
197 cells persisted at 3-fold higher frequency after the third vaccination (V3:T4: median = 295 SFC)
198 compared to the second vaccination. In the ChAd/mRNA cohort, S-specific T cells were induced by
199 primary ChAd vaccination at V1:T1 but peaked at V1:T2 (median = 62 SFC). The dynamics upon
200 subsequent vaccinations in this cohort were comparable to the mRNA cohort (V2:T1: median = 306
201 SFC; V2:T4: median = 90 SFC; V3:T1: median = 300 SFC). In the MVA-S/mRNA cohort 67 % (8/12) of
202 study participants had a detectable T cell response (> 8 SFC and 3-fold above baseline) at least at one

203 time point after MVA-S vaccination, but the median peak response of 9 SFC at V1:T2 was low.
204 Interestingly, as also observed for S2-specific B cell responses (Fig. 4a), there was a more rapid
205 induction of S-specific T cells upon first mRNA vaccination in this cohort (fold change V3:T1 vs. V2:T4=
206 19.6) compared to the mRNA cohort (fold change V3:T1 vs. V2:T4 = 5.1). Two doses of the optimized
207 MVA-ST vaccine candidate induced T cell responses that were similar in magnitude as seen after a
208 single mRNA vaccination (MVA-ST V2:T2= 53 SFC; mRNA V1:T2 = 58 SFC). Used as a third vaccination,
209 MVA-ST boosted the T cell response (V3:T2 vs. V2:T4 fold change= 1.8) at levels comparable to third
210 mRNA vaccination (V3:T2 vs. V2:T4 fold change = 2.8).

211 To confirm the T cell dynamics described above, we additionally used a commercial T cell assay
212 measuring the S-specific IFN- γ response after whole blood stimulation at T0, T2 and T4 (Fig. 4c). Results
213 correlated with those of the IFN- γ ELISpot (Spearman $r = 0.7$; $p < 0.0001$), providing additional evidence
214 for the robustness of these assays (Fig. 4e).

215 ***Cytokine polyfunctionality of CD4⁺ and CD8⁺ T cells differs between vaccine regimens***

216 The polyfunctionality of S-specific memory T cells was assessed 3-5 weeks after V1 and V2 for the
217 mRNA and ChAd/mRNA cohorts, and after V3 and V4 for the MVA-S/mRNA cohort (Fig. 5a).
218 Intracellular cytokine staining was used to analyze production of IFN- γ , interleukin-2 (IL-2) and tumor
219 necrosis factor alpha (TNF- α) by CD4⁺ and CD8⁺ T cells (gating shown in Fig. 5b and Supplementary
220 Fig. 1).

221 Vaccination induced S-specific, cytokine-producing CD4⁺ memory T cells at median frequencies (mfr)
222 that were significantly above baseline in all cohorts for IFN- γ (mRNA: mfr = 0.71 %, $p = 0.0039$;
223 ChAd/mRNA: mfr = 0.06 %, $p = 0.0313$; MVA-S/mRNA: mfr = 0.08 %, $p = 0.0005$), IL-2 (mRNA: mfr =
224 0.05 %, $p = 0.0020$; ChAd/mRNA: mfr = 0.05 %, $p = 0.0156$; MVA-S/mRNA: mfr = 0.04 %, $p = 0.0049$)
225 and TNF- α (mRNA: mfr = 0.05 %, $p = 0.0195$; ChAd/mRNA: mfr = 0.02 %, $p = 0.0156$; MVA-S/mRNA: mfr
226 = 0.04 %, $p = 0.0098$) (Fig. 5c). The frequency of total cytokine-producing CD4⁺ T cells was highest in
227 the MVA-S/mRNA cohort, both after the first (mfr = 0.08 %) and second mRNA vaccination (mfr = 0.14
228 %) (Fig. 5d). The median frequency of polyfunctional CD4⁺ memory T cells expressing all three cytokines
229 was higher after the first vaccination in those who had received MVA-S previously (mRNA: mfr = 0.003
230 %; ChAd/mRNA: mfr = 0.007 %; MVA-S/mRNA: mfr = 0.013 %) and comparable between all cohorts
231 post second vaccination (mRNA: mfr = 0.017 %; ChAd/mRNA: mfr = 0.014 %; MVA-S/mRNA: mfr =
232 0.017 %).

233 The cytokine-producing CD8⁺ memory T cell response was less pronounced compared to the CD4⁺
234 response after vaccination. A significant induction of IFN- γ -producing CD8⁺ memory T cells was only
235 observed in the mRNA cohort (mfr = 0.05 %, $p = 0.0195$) and the MVA-S/mRNA cohort (mfr = 0.07 %,
236 $p = 0.0244$) (Fig. 5c). Interestingly, the participants of this cohort with IFN- γ -producing CD8⁺ memory T
237 cells above 0.2 % already had a measurable T cell response after MVA-S vaccination, as measured by
238 IFN- γ -ELISpot (Fig. 4b). The memory CD8⁺ T cell response was dominated by cells expressing a single
239 cytokine, with a low frequency of polyfunctional CD8⁺ cells in all three cohorts (Fig. 5d). Notably, a
240 higher median frequency of total cytokine-producing CD8⁺ memory T cells was observed already after
241 the first mRNA vaccination in the MVA-S/mRNA cohort (mfr = 0.1 %) compared to the mRNA cohort
242 (mfr = 0.02 %).

243 Additionally, we measured 13 cytokines in the supernatant of S-protein-stimulated whole blood using
244 a bead-based assay (Fig. 5e). We observed distinct cytokine signatures between the different cohorts,

245 with multiple cytokines showing a stronger induction in the two cohorts who had received two doses
246 of mRNA vaccine (mRNA and MVA-S/mRNA) compared to the ChAd/mRNA cohort. The MVA-S/mRNA
247 cohort showed the highest fold-induction of IL-6, MIP-1 α , IL-2 and IFN- γ , whereas the strongest
248 increase in MIP-1 β and IL-1RA was observed in the mRNA cohort.

249 ***Induction of differential IgG subclasses and cytokine profiles after repeated mRNA vaccination***

250 Comparing the humoral and cellular immune response across the different cohorts, we observed an
251 IgG subclass distribution changing over time upon repeated mRNA vaccination in the mRNA and
252 ChAd/mRNA cohorts (Fig. 6a). S1-specific IgG1 and IgG3 dynamics were comparable over time between
253 these two cohorts, with a strong induction after V1 and peaking at V2:T1 and V3:T1. In contrast, IgG2
254 and IgG4 induction was only observed after second mRNA vaccination, corresponding to V2 in the
255 mRNA cohort and V3 in the ChAd/mRNA cohort. IgG2 was induced slightly after second mRNA
256 vaccination in the mRNA cohort (V2:T1: median MFI = 10) and in the ChAd/mRNA cohort (V3:T1:
257 median MFI = 50). IgG2 levels were then boosted by third mRNA vaccination in the mRNA cohort
258 (V3:T1: median MFI = 5428). IgG4 levels increased starting after the second mRNA vaccination in the
259 mRNA cohort (V2:T4: median MFI = 75.5) and were boosted by third mRNA vaccination (V3:T1: median
260 MFI = 7204). A similar pattern of IgG4 induction starting after the second mRNA vaccination was seen
261 in the ChAd/mRNA cohort (V3:T1: median MFI = 337) (Fig. 6b). Overall, after completed three-dose
262 vaccination, IgG2 and IgG4 titers were higher in the mRNA cohort compared to the ChAd/mRNA cohort.

263 Interestingly, different signatures were also observed in the cytokines induced in the two cohorts.
264 While the pro-inflammatory IL-2 response was similar between the cohorts, anti-inflammatory IL-10
265 and IL-1RA were elevated in the thrice mRNA-vaccinated cohort. The Th2 associated IL-4 cytokine was
266 elevated at V2:T2 in the mRNA cohort (fold change = 10.3) and at V3:T2 in the ChAd/mRNA cohort
267 (fold change = 3.9) (Fig. 6c).

268 ***S-protein conformation influences antibody and T cell specificity towards S1 and S2 subunits***

269 To gain insight into the impact of the S-protein conformation and vaccine dose on the immune
270 response induced by MVA-S and MVA-ST, we analyzed the antigen specificity of the antibodies and T
271 cells. As depicted in Figure 7a, MVA-ST induced a significantly higher IgG response against the S1
272 subunit compared to MVA-S (MVA-ST: median MFI = 2942; MVA-S: median MFI = 18; $p < 0.0001$). In
273 contrast, S2-specific IgG levels were induced at similar levels (MVA-ST: median MFI = 1764; MVA-S:
274 median MFI = 2296). For both vaccines, the higher dose was more immunogenic than the low dose in
275 terms of S1 and S2-specific IgG titers (Fig. 7b). When using OLPs covering the whole S-protein, two
276 doses of MVA-ST but not MVA-S induced a detectable IFN- γ T cell response above baseline (MVA-S:
277 median MFI = 4; MVA-ST: median MFI = 68, $p = 0.0001$) Fig. 7c). No dose effect was seen, although T
278 cell responses were highly variable between participants (data not shown). We then quantified the T
279 cell response against the two spike subunits by stimulating with four OLP pools separately, where pools
280 M1-M2 mainly cover the S1 and M3-M4 the S2 subunit. One dose of MVA-S induced a T cell response
281 that was biased towards the S2 subunit, which was not enhanced by secondary vaccination. MVA-ST
282 in turn induced an S1-biased T cell response with highest magnitude after second vaccination (Fig. 7d).
283 Overall, the bias towards the S1 subunit after MVA-ST and towards the S2 subunit after MVA-S
284 vaccination is reflected both in the humoral and T cellular immune response.

285 ***Baseline dependency of the immune response induced by MVA-ST booster vaccination***

286 The MVA-ST candidate was tested as a third vaccination using three different dose groups in a cohort
287 of participants who had received two doses of mRNA vaccination six months prior to enrolling in the
288 study (Fig. 8a). Median IgG titers increased in all MVA-ST dose groups compared to the baseline levels
289 six months after second mRNA vaccination. However, the fold induction of IgG was lower in the
290 mRNA/MVA-ST cohort (low dose: 1.2; middle dose: 1.6; high dose: 1.3), compared to the mRNA cohort
291 (mRNA: 3.7) (Fig. 8b). The MVA-ST vaccine boosted the T cell response, most pronounced in the middle
292 dose group (median = 401 SFC; fold change = 1.4), to levels comparable to the mRNA cohort (median
293 = 341 SFC; fold change = 5.1) at time point V3:T1. Interestingly, while the S-specific T cell response
294 peaked at this early time point in the mRNA cohort, it further increased in the MVA-ST cohort until
295 time point V3:T2 (median = 570 SFC; fold change = 3.1) (Fig. 8c). High baseline levels of antibody titers
296 and T cells were observed before the third vaccination, which varied greatly between all participants
297 and dose groups. Notably, a significant increase of S1-specific antibodies ($p = 0.0003$) and S-specific T
298 cells ($p = 0.0001$) was seen in participants with lower baseline levels of these parameters, whereas
299 those with higher baselines did not show significant antibody or T cell induction (Fig. 8d-e).

300 Discussion

301 In this study, we report on the immunogenicity of two rMVA-based COVID-19 vaccine candidates as a
302 two-dose primary vaccination series in naïve individuals and as a third dose after mRNA vaccination.
303 By a direct comparison with licensed mRNA and ChAd vaccination schemes, we were able to show
304 distinct signatures of the S-specific adaptive immune response according to vaccine platform and
305 S-protein conformation. This approach provides an example for evaluation of novel vaccine candidates
306 in comparison to licensed vaccines.

307 Two primary doses of MVA-S (encoding the native S-protein) showed low humoral and cellular
308 immunogenicity in SARS-CoV-2 naïve individuals. However, after subsequent mRNA vaccination we
309 observed an earlier induction of S2-specific IgG-secreting B and IFN- γ -producing T cells as well as an
310 overall higher frequency of cytokine-secreting T cells compared to the mRNA control cohort. This may
311 indicate a priming effect of MVA-S, resulting in a recall-response of memory B and T cells upon mRNA
312 vaccination. With regard to the two different MVA candidates, MVA-ST (encoding a prefusion-
313 stabilized S-protein) was shown to be more immunogenic than MVA-S. While the humoral immune
314 response was less pronounced, the IFN- γ T cell response elicited by a two-dose MVA-ST vaccination
315 was comparable in magnitude to one dose ChAd or mRNA vaccine. Notably, Routhu et al. also tested
316 two rMVA-based COVID-19 vaccines encoding different conformations of the S-protein in pre-clinical
317 studies^{29,30}. Their optimized candidate encoding a similar prefusion-stabilized S-protein as MVA-ST, in
318 combination with the nucleocapsid antigen, led to higher neutralizing antibody titers in non-human
319 primates (NHP). It was subsequently tested in a phase 1 clinical trial, given in a two-dose schedule, 28
320 days apart²⁹⁻³¹. Since different assays were used, antibody titers and T cell frequencies cannot directly
321 be compared, but the overall dynamics of antibody and T cell responses observed by Routhu et al. are
322 in line with our observations for the MVA-ST cohort.

323 In our study, comparative analysis of the MVA-S and MVA-ST vaccines provided the opportunity to
324 directly investigate the impact of the different S-protein conformations on the vaccine-induced
325 immune response in humans. In fact, we observed differential specificity towards the S1 and S2
326 subunits of the S-protein for our two vaccine candidates. Both MVA-S and MVA-ST increased the S2-
327 specific IgG levels that were already present at baseline, possibly as a result of cross-reactive antibodies
328 from previous infections with common cold coronaviruses^{32,33}. In contrast, S1-specific IgG was elicited

329 at significantly higher levels by MVA-ST vaccination. In line with this, the antigen-specific T cell
330 response was biased towards the S2 and S1 subunit after MVA-S and MVA-ST vaccination, respectively.
331 A similar pattern was seen in preclinical studies, with lower S1-specific seroconversion in MVA-S
332 vaccinated, compared to MVA-ST-vaccinated hamsters. These results could be explained by the
333 differential cell surface expression of the native and prefusion-stabilized S-protein, as shown in *in vitro*
334 experiments¹². The S1 subunit contains the receptor-binding domain (RBD) and has been shown to be
335 the main target of SARS-CoV-2 neutralizing antibodies³⁴. However, antibodies targeting epitopes in
336 the more conserved S2 subunit are also induced at substantial levels after vaccination and could be
337 important for protection against SARS-CoV-2 variants and other human coronaviruses^{35,36}. We
338 detected linear B cell epitopes that were localized outside of the RBD, in the C-terminal part of the S1
339 subunit and along the S2 subunit, across all study cohorts. Of note, we identified an immunogenic
340 region in the S2 domain (AA 763-853) that contains the epitope specificity (AA 814-826) of a recently
341 described neutralizing antibody with pan-coronavirus reactivity³⁷. We also detected one immunogenic
342 region in the C-terminal transmembrane domain of S2 (AA 1245-1273) that was only detected in the
343 cohorts who had received at least one MVA vaccination. Two epitopes in the same region were also
344 described after MVA-MERS-S vaccination (AA 1225-1247, AA 1333-1353), suggesting that epitope
345 specificity of the B cell response may also be shaped by vaccine platform¹⁵. Whether the induced S2-
346 specific antibody response and identified immunogenic regions in this subunit may provide a basis for
347 pan-coronavirus vaccines needs to be further evaluated in future studies.

348 Apart from antigen specificity, insights into the functionality of vaccine-induced antibodies are
349 increasingly important in view of waning neutralizing titers and emerging viral variants^{21,22}. Non-
350 neutralizing antibody functions such as antibody-dependent cellular cytotoxicity (ADCC) and
351 phagocytosis (ADCP) are driven by differential IgG subclass binding to Fc-receptors on effector cells,
352 and have been suggested to be part of the protective immunity against many viral diseases³⁸⁻⁴⁰. We
353 observed induction of the pro-inflammatory and highly functional IgG1 and IgG3 subclasses in all
354 cohorts, irrespective of vaccination scheme, which is in line with results of licensed mRNA and ChAd
355 COVID-19 vaccines⁴¹⁻⁴³. In contrast, IgG2 and IgG4 – both possessing low functional potency and in
356 general not induced by protein-based vaccination – were only detectable after the second mRNA dose.
357 Subsequently, their levels continuously increased and reached a peak after third mRNA vaccination,
358 similarly observed by Irrgang et al.⁴⁴. The observed IL-4/IL-10 cytokine response early after second
359 mRNA vaccination, together with a continuous antigen exposure in the prolonged germinal center as
360 described after mRNA vaccination, may result in a continuous class switch recombination towards anti-
361 inflammatory IgG4^{45,46}. The clinical relevance of this phenomenon remains poorly understood and
362 requires further investigation.

363 Analyzing MVA-ST and mRNA vaccines as booster vaccines, we observed that the residual humoral and
364 cellular immune response from two previous mRNA vaccinations negatively affected the boosting
365 capacity of both platforms. This baseline-dependency was seen in the S1-specific IgG as well as the S-
366 specific T cell response. Comparing their peak responses, mRNA and MVA-ST vaccines induced similar
367 T cell frequencies despite higher baseline levels of MVA-ST compared to the mRNA cohort. The
368 phenomenon of baseline-dependency has been reported in observational studies of booster
369 vaccinations using licensed vaccines against several pathogens⁴⁷. Recent follow-up data of our
370 MVA-MERS-S trial shows that a third immunization 12 months after the primary vaccination series
371 enhances the magnitude and persistence of spike-specific antibodies and memory B cells, supporting

372 the potential of using rMVA-based vaccines as booster vaccinations and underscore the importance of
373 an optimized time interval between immunizations ^{14,15}.

374 Even though restricted to peripheral blood and small sample sizes within each cohort, the longitudinal
375 sampling of all study participants in combination with a comprehensive side-by-side analysis of
376 different vaccine regimens represents a strength of our manuscript, providing important insights into
377 the impact of platform, schedule and antigen conformation on vaccine-induced immune responses. In
378 this study, we show that the immunogenicity of rMVA-based COVID-19 vaccine candidates in humans
379 can be enhanced by conformational changes in the S-protein. While MVA-ST did not induce an immune
380 response at levels comparable to the licensed mRNA and ChAd vaccines, it shows potential for
381 enhancing T cell polyfunctionality, as has been shown for other rMVA-based vaccines ^{48,49}. A
382 polyfunctional T cell response has been associated with a less severe course of COVID-19 disease and
383 better survival in patients with B cell malignancies ⁵⁰. Thus, vaccine platforms that induce potent T cell
384 responses and show a high safety profile, such as MVA, may be important for future boosting strategies
385 in high risk groups and in the face of emerging variants ⁵¹. With this study, we propose a strategy to
386 use the immunogenicity of licensed vaccines as a benchmark for evaluating new vaccine candidates.
387 This approach may be applied to facilitate immune bridging to other vaccine platforms or pathogens.

388 **Methods**

389 *Experimental model and subject details*

390 Vaccines

391 MVA-SARS-2-S (MVA-S) is a vaccine candidate based on the rMVA vector, encoding the full-length
392 S-protein of SARS-CoV-2 ¹¹. MVA-SARS-2-ST (MVA-ST) is an optimized version of MVA-S that encodes
393 for a pre-fusion-stabilized S protein with an inactivated S1/S2 furin cleavage site, as described in Natrup
394 et al. ¹². BNT162b2 and mRNA-1273 (mRNA) are licensed vaccines consisting of nucleoside-modified
395 mRNA encoding the prefusion-stabilized S-protein, formulated in lipid-nanoparticles ^{1,4}. ChAdOx1
396 nCoV-19 (ChAd) is a licensed vaccine based on the modified chimpanzee adenovirus ChAdOx1 vector,
397 encoding the full-length S-protein and a tissue plasminogen activator leader sequence ¹⁹.

398 Study approval

399 The below described phase 1 clinical trials were reviewed and approved by the National Competent
400 Authority (Paul-Ehrlich-Institute) and the Ethics Committee of the Hamburg Medical Association
401 (reference numbers: 2020-10164-AMG-ff; 2021-100621-AMG-ff) conducted under the sponsorship of
402 the University Medical Center Hamburg-Eppendorf (Hamburg, Germany) in accordance with ICH-GCP
403 and the EU directives 2001/20/EC and 2001/83/EC and are registered at ClinicalTrials.gov.
404 (NCT04569383; NCT04895449). The clinical study with licensed vaccines was approved by the Ethics
405 Committee of the Hamburg Medical Association (reference number: 2020-10376-BO-ff).

406 Study design and blood sampling

407 NCT04569383 is a phase 1 clinical trial to evaluate the MVA-SARS-2-S vaccine candidate in 30
408 seronegative individuals, divided into two ascending dose groups. Participants received two single
409 injections 28 days apart of either low dose $\geq 1 \times 10^7$ IU (N=15) or high dose $\geq 1 \times 10^8$ IU (N=15). The
410 MVA-S/mRNA cohort is a subgroup of this trial (N=12), who received two doses of the BNT162b2
411 vaccine 21 days apart, at least six months after the last MVA-SARS-2-S vaccination.

412 NCT04895449 is a phase 1b clinical trial to evaluate the MVA-SARS-2-ST vaccine candidate in
413 seronegative individuals (Part A) and individuals who had previously received two doses of BNT162b2
414 vaccine (Part B). In Part A, participants received two single injections 28 days apart of either low dose
415 $\geq 1 \times 10^7$ IU (N=8) or middle dose $\geq 5 \times 10^7$ IU (N=8). In Part B, participants received a single injection
416 of low dose $\geq 1 \times 10^7$ IU (N=12), middle dose $\geq 5 \times 10^7$ IU (N=10), or high dose $\geq 1 \times 10^8$ IU (N=8)
417 MVA-SARS-2-ST, at least six months after their last BNT162b2 vaccination. Here, the MVA-ST cohort
418 refers to Part A, while the mRNA/MVA-ST refers to Part B of this study (Fig. 1A).

419 The mRNA and ChAd/mRNA study cohorts consist of participants who received two doses of mRNA
420 vaccine (21 or 28 days apart) or one dose ChAd plus one dose mRNA (84 days apart) respectively, and
421 a booster vaccination of mRNA after six months. The studies were conducted at the University Medical
422 Center Hamburg-Eppendorf.

423 A total of 452 peripheral blood samples were obtained from 75 donors. The blood sample collection
424 schedule is shown in Fig. 1A and the number of samples of each individual in Fig. 1B. Blood was
425 collected at T0 (baseline before vaccination), T1 (1-2 weeks), T2 (3-5 weeks), T3 (12 weeks), and T4
426 (17-29 weeks) post vaccination. Weeks refer to time since last vaccination. Exact time intervals
427 between vaccinations and blood collections are shown in Supplementary Tables 2 and 3.

428 **Method details**

429 PBMC and plasma isolation

430 Whole blood was collected in EDTA vacutainers. After centrifugation, plasma was removed and stored
431 at -80°C . PBMCs were isolated by density-gradient centrifugation using Ficoll-Histopaque (Sigma) or
432 SepMate™ (Stemcell), cryopreserved and stored in liquid nitrogen.

433 Bead-based multiplex ELISA

434 A bead-based multiplex ELISA was used to separately measure plasma antibody isotypes and IgG
435 subclasses directed against the S1 and S2 subunit of the SARS-CoV-2 S-protein. For the detection of
436 isotypes IgM, IgA and IgG, the MILLIPLEX® SARS-CoV-2 Antigen Panel 1 IgM/IgA/IgG kits (Merck KGaA)
437 were used according to the manufacturer's instructions with adjusted concentration of detection
438 antibodies. Briefly, magnetic beads coated with SARS-CoV-2 S1 and S2 antigens were added to a black,
439 clear-bottom 96 well plate for each isotype. Plasma samples were added at a final dilution of 1:600
440 and plates were incubated on a plate shaker at 650 rpm at room temperature (RT) for 2 hours. After
441 washing, 45 μl of PE-anti-human IgG, IgA or IgM conjugate were added per well and incubated on a
442 plate shaker at 650 rpm at RT for 1.5 hours. After another washing step, beads were resuspended in
443 150 μl sheath fluid per well and stored overnight at 4°C . Plates were analyzed the next day, using a
444 Bio-Plex™ 200 system. For detection of IgG subclasses, the MILLIPLEX® SARS-CoV-2 Antigen Panel 1 IgG
445 kit (Merck KGaA) was used as described above, but detection antibodies were substituted with PE-
446 conjugated antibodies specific to IgG1-4 (SouthernBiotech), added at a concentration of 0.65 $\mu\text{g}/\text{ml}$ in
447 80 μl per well. For each isotype and subclass, wells without plasma samples were measured as a control
448 for unspecific background signal and subtracted from measured sample values. MFI values below 2
449 were set to 2. Results are shown as mean of duplicate wells.

450 IgG ELISpot assay

451 SARS-CoV-2 S-specific B cells were analyzed using an IgG ELISpot. To activate antibody secretion of B
452 cells, PBMCs at a concentration of $2 \times 10^6/\text{ml}$ in R10 medium [RPMI 1640 (Sigma) supplemented with

453 10 % fetal bovine serum (FBS) and 1 % streptomycin/penicillin] containing 1 % HEPES (Thermo Fisher
454 Scientific), were stimulated with 0.5 µg/ml Resiquimod (R848, Mabtech) and 5 ng/ml interleukin-2
455 (IL-2, Mabtech) for 75±1 hours at 37 °C and 5% CO₂. PVDF-MultiScreen-IP plates (Millipore) were
456 treated with 35% ethanol and coated with anti-IgG capture antibody (15 µg/ml; Mabtech). After
457 blocking with R10 containing 1 % HEPES, pre-stimulated PBMCs were added to the wells at different
458 concentrations and incubated for 16 hours at 37 °C and 5 % CO₂. For the positive control (total IgG-
459 secreting B cells), 1x10⁴ PBMCs were added per well, whereas numbers between 1x10⁴ and 8x10⁵ cells
460 were used for the antigen-specific assay, depending on the time point post vaccination. Biotinylated
461 SARS-CoV-2 S-protein S1 or S2 subunit (S1: 0.1 µg/ml, S2: 0.2 µg/ml; SinoBiological) and anti-IgG
462 detection antibody (1 µg/ml; Mabtech) were added for detection of antigen-specific and total IgG-
463 secreting B cells, respectively. For development of spots, streptavidin-ALP and BCIP/NBT-plus substrate
464 solution (Mabtech) were used according to the manufacturer's protocol. Plates were analyzed using
465 an AID multisport reader. All samples were measured in duplicates and the mean was used for further
466 analysis. Results below the LLOD (2 SFC/10⁶ PBMCs) were set to 1 SFC/10⁶ PBMCs.

467 Peptide microarrays

468 To identify linear B cell epitopes in the spike protein, we screened the sera of study participants using
469 high-density peptide microarrays as described in ⁵². The sequence of the SARS-CoV-2 spike protein
470 (GenBank ID: MN908947.3) consisting of 1273 AA was mapped as a total of 634 overlapping 15-mer
471 peptides with a lateral shift of two AA on peptide microarrays obtained from PEPperPRINT GmbH
472 (Heidelberg, Germany). Serum samples were incubated on the arrays in 1:200 dilution, IgG antibody
473 interactions were then detected with fluorescently labeled secondary antibodies, and quantified in
474 arbitrary fluorescence units (AFU). Epitope binding was defined as positive if the mean AFU of three
475 successive peptides was higher than 400 and 2.5-fold above baseline before vaccination (if available).

476 IFN-γ ELISpot assay

477 SARS-CoV-2 S-specific T cells were analyzed using the Human IFN-γ ELISpotPLUS (ALP) kit (Mabtech).
478 After overnight resting in R10 containing 1 % HEPES, PBMCs were seeded at 1.25x10⁵ cells/well in
479 PVDF-MultiScreen-IP plates, pre-coated with anti-IFN-γ-mAb 1-D1K (Mabtech). Cells were then
480 stimulated with a peptide pool (15-mers overlapping by 11 amino acids; Supplementary Table 10)
481 spanning the SARS-CoV-2 spike protein sequence (GenBank ID: MN908947.3) (2.5µg/ml in 0.1 %
482 Dimethyl sulfoxide (DMSO); JPT Peptide Technologies) for 16 hours at 37°C and 5 % CO₂. Medium with
483 an equimolar concentration of DMSO was used as a negative control. Phytohaemagglutinin (PHA) (1
484 µg/ml; Sigma) and CMV/EBV/Influenza (CEF) peptide pool (2 µg/ml; JPT Peptide Technologies) were
485 used as positive control stimulations. Plates were then incubated with biotinylated anti-IFN-γ (1 µg/ml
486 in PBS-0.5 % FCS; clone mAb-7B6-1; Mabtech) for 2 hours, followed by Streptavidin-ALP (1:1000 in PBS-
487 0.5 % FCS; Mabtech) for 1 hour at room temperature. Plates were developed using substrate solution
488 (BCIP/NBT; Mabtech). Spots were counted using an AID ELISpot Reader System (AID GmbH). Results
489 are reported as spot-forming cells (SFC) per million PBMCs, calculated by subtracting the mean count
490 of triplicate negative control wells from the mean count of duplicate peptide-stimulated wells. Results
491 were normalized to the total reactive T cells of each participant using Phytohemagglutinin (PHA)
492 stimulation as a positive control. Results below the LLOD (8 SFC/10⁶ PBMCs) were set to 4 SFC/10⁶
493 PBMCs.

494 IFN-γ release assay (IGRA)

495 IFN- γ secretion by S-specific T cells was analyzed in whole blood using a commercial, standardized
496 Interferon Gamma Release Assay (IGRA) (ET 2606-3003, Euroimmun, Lübeck, Germany). After a 20- to
497 24-hour stimulation, IFN- γ was measured in the plasma using an IFN- γ ELISA (EQ 6841-9601,
498 Euroimmun, Lübeck, Germany) according to the manufacturer's instructions. IFN- γ secretion was
499 quantified using a 5PL sigmoidal standard curve and data are shown as background subtracted
500 concentrations using an unstimulated control for each sample. Samples outside the standard curve
501 were repeated in higher dilutions.

502 Cytokine multiplex

503 Cytokine concentrations were measured in the supernatant of the IGRA using a customized 13-Plex
504 human cytokine bead-based immunoassay (LEGENDplex Biolegend) according to the manufacturer's
505 instructions. Samples were measured in duplicate and background subtracted. Results are shown as
506 fold-change compared to baseline. Samples used for fold-change were measured on the same plate.

507 Intracellular cytokine staining (ICS) assay

508 After overnight resting, PBMCs were stimulated with spike peptides (2.5 ug/ml) for 7h at 37°C in the
509 presence of Golgi-Plug, Golgi-Stop, and anti-CD28/CD49 (#9035982; BD Biosciences) in 96-well
510 V-bottom plates (Sarstedt). For each sample, cell incubated with an equimolar amount of DMSO (0.1
511 %) and Phorbol-12-myristate-13-acetate (50 ng/ml) and ionomycin (0.5 ug/ml) served as negative and
512 positive controls, respectively. Cells were then washed and stained with an antibody mix of anti-CD3-
513 BUV395 (#564001; BD Biosciences), anti-CD4-AF700 (#300526; BioLegend), anti-CD19-BV510
514 (#302242; BioLegend), anti-CD14-BV510 (#301842; BioLegend), anti-CD8-APC-Cy7 (#344714;
515 BioLegend), anti-CCR7-AF647 (#353218; BioLegend), anti-CD45RO-FITC (#304242; BioLegend), and
516 Zombie Aqua™ Fixable Viability Kit (#423101; BioLegend) in FACS buffer [PBS supplemented with 2 %
517 FBS and 2 mM EDTA] for 15 minutes at 37°C. Subsequently, cells were fixed (eBioscience™), washed
518 and then stained with intracellular markers anti-IFN- γ -PE-Cy7 (#506518; BioLegend), anti-TNF- α -
519 PE/Dazzle™ 594 (#50296; BioLegend) and IL-2-PerCP-Cy5.5 (#500322, BioLegend), in PERM buffer
520 (eBioscience™) at RT for 15 minutes. Samples were stored in FACS buffer at 4°C and analyzed on the
521 BD Fortessa the following day. A representative gating strategy is shown in Supplementary Fig. 1.
522 Cytokine secreting memory T cells were identified by excluding CCR7⁺/CD45RO⁻ naïve T cells and then
523 gating the individual cytokines on CD4⁺ and CD8⁺ T cells separately. Results are shown as background
524 (DMSO) subtracted data (Fig 4). Multifunctional profiles were identified using Boolean gating. Results
525 of the Boolean gates were summed up for each sample based on the number of functions.

526 Statistical analysis

527 Statistical analysis was done using two-tailed Wilcoxon matched-pairs signed rank test and Mann-
528 Whitney-U test for paired and unpaired samples, respectively, at a significance level of 0.05.
529 Correlations were calculated using non-parametric Spearman's correlation. Statistical analysis was
530 performed using GraphPad Prism (v8.0.1). Analysis of flow cytometry data was done using FlowJo
531 (v.10.8.1). Figures were created with GraphPad Prism (v8.4.2), R (v4.2.0) and BioRender.com.

532 **References**

533 1. Polack, F. P. *et al.* Safety and Efficacy of the BNT162b2 mRNA Covid-19 Vaccine. *New England*
534 *Journal of Medicine* **383**, 2603–2615 (2020).

- 535 2. Voysey, M. *et al.* Safety and efficacy of the ChAdOx1 nCoV-19 vaccine (AZD1222) against SARS-
536 CoV-2: an interim analysis of four randomised controlled trials in Brazil, South Africa, and the UK.
537 *The Lancet* (2020) doi:10.1016/S0140-6736(20)32661-1.
- 538 3. Watson, O. J. *et al.* Global impact of the first year of COVID-19 vaccination: a mathematical
539 modelling study. *The Lancet Infectious Diseases* **22**, 1293–1302 (2022).
- 540 4. Baden, L. R. *et al.* Efficacy and Safety of the mRNA-1273 SARS-CoV-2 Vaccine. *New England Journal*
541 *of Medicine* **384**, 403–416 (2021).
- 542 5. Li, F. Structure, Function, and Evolution of Coronavirus Spike Proteins. *Annu Rev Virol* **3**, 237–261
543 (2016).
- 544 6. Song, F. *et al.* Middle East Respiratory Syndrome Coronavirus Spike Protein Delivered by Modified
545 Vaccinia Virus Ankara Efficiently Induces Virus-Neutralizing Antibodies. *J Virol* **87**, 11950–11954
546 (2013).
- 547 7. Du, L. *et al.* The spike protein of SARS-CoV--a target for vaccine and therapeutic development. *Nat*
548 *Rev Microbiol* **7**, 226–236 (2009).
- 549 8. van Riel, D. & de Wit, E. Next-generation vaccine platforms for COVID-19. *Nat. Mater.* **19**, 810–812
550 (2020).
- 551 9. Volz, A. & Sutter, G. Modified Vaccinia Virus Ankara: History, Value in Basic Research, and Current
552 Perspectives for Vaccine Development. *Adv Virus Res* **97**, 187–243 (2017).
- 553 10. Volkmann, A. *et al.* The Brighton Collaboration standardized template for collection of key
554 information for risk/benefit assessment of a Modified Vaccinia Ankara (MVA) vaccine platform.
555 *Vaccine* **39**, 3067–3080 (2021).
- 556 11. Tscherne, A. *et al.* Immunogenicity and efficacy of the COVID-19 candidate vector vaccine MVA-
557 SARS-2-S in preclinical vaccination. *Proc Natl Acad Sci U S A* **118**, e2026207118 (2021).
- 558 12. Natrup, C. M. zu *et al.* Stabilized recombinant SARS-CoV-2 spike antigen enhances vaccine
559 immunogenicity and protective capacity. *J Clin Invest* (2022) doi:10.1172/JCI159895.
- 560 13. Koch, T. *et al.* Safety and immunogenicity of a modified vaccinia virus Ankara vector vaccine
561 candidate for Middle East respiratory syndrome: an open-label, phase 1 trial. *The Lancet Infectious*
562 *Diseases* **20**, 827–838 (2020).
- 563 14. Weskamm, L. M. *et al.* Persistence of MERS-CoV-spike-specific B cells and antibodies after late
564 third immunization with the MVA-MERS-S vaccine. *Cell Reports Medicine* **3**, 100685 (2022).
- 565 15. Fathi, A. *et al.* Increased neutralization and IgG epitope identification after MVA-MERS-S booster
566 vaccination against Middle East respiratory syndrome. *Nat Commun* **13**, 4182 (2022).
- 567 16. Jackson, L. A. *et al.* An mRNA Vaccine against SARS-CoV-2 — Preliminary Report. *New England*
568 *Journal of Medicine* **383**, 1920–1931 (2020).
- 569 17. Vogel, A. B. *et al.* BNT162b vaccines protect rhesus macaques from SARS-CoV-2. *Nature* **592**, 283–
570 289 (2021).
- 571 18. Wrapp, D. *et al.* Cryo-EM structure of the 2019-nCoV spike in the prefusion conformation. *Science*
572 **367**, 1260–1263 (2020).
- 573 19. Folegatti, P. M. *et al.* Safety and immunogenicity of the ChAdOx1 nCoV-19 vaccine against SARS-
574 CoV-2: a preliminary report of a phase 1/2, single-blind, randomised controlled trial. *The Lancet*
575 **396**, 467–478 (2020).
- 576 20. Voysey, M. *et al.* Single-dose administration and the influence of the timing of the booster dose
577 on immunogenicity and efficacy of ChAdOx1 nCoV-19 (AZD1222) vaccine: a pooled analysis of four
578 randomised trials. *The Lancet* **397**, 881–891 (2021).
- 579 21. Gilbert, P. B. *et al.* Immune correlates analysis of the mRNA-1273 COVID-19 vaccine efficacy clinical
580 trial. *Science* **375**, 43–50 (2022).

- 581 22. Khoury, D. S. *et al.* Neutralizing antibody levels are highly predictive of immune protection from
582 symptomatic SARS-CoV-2 infection. *Nat Med* **27**, 1205–1211 (2021).
- 583 23. Siegrist, C.-A. Vaccine Immunology. in *Vaccines* (Elsevier, 2008).
- 584 24. Palm, A.-K. E. & Henry, C. Remembrance of Things Past: Long-Term B Cell Memory After Infection
585 and Vaccination. *Frontiers in Immunology* **10**, (2019).
- 586 25. Akkaya, M., Kwak, K. & Pierce, S. K. B cell memory: building two walls of protection against
587 pathogens. *Nat Rev Immunol* **20**, 229–238 (2020).
- 588 26. Bertoletti, A., Le Bert, N., Qui, M. & Tan, A. T. SARS-CoV-2-specific T cells in infection and
589 vaccination. *Cell Mol Immunol* (2021) doi:10.1038/s41423-021-00743-3.
- 590 27. Munro, A. P. S. *et al.* Safety and immunogenicity of seven COVID-19 vaccines as a third dose
591 (booster) following two doses of ChAdOx1 nCov-19 or BNT162b2 in the UK (COV-BOOST): a
592 blinded, multicentre, randomised, controlled, phase 2 trial. *The Lancet* **398**, 2258–2276 (2021).
- 593 28. Zhang, Z. *et al.* Humoral and cellular immune memory to four COVID-19 vaccines. *Cell* **185**, 2434-
594 2451.e17 (2022).
- 595 29. Routhu, N. K. *et al.* A modified vaccinia Ankara vector-based vaccine protects macaques from
596 SARS-CoV-2 infection, immune pathology, and dysfunction in the lungs. *Immunity* **54**, 542-556.e9
597 (2021).
- 598 30. Routhu, N. K. *et al.* A modified vaccinia Ankara vaccine expressing spike and nucleocapsid protects
599 rhesus macaques against SARS-CoV-2 Delta infection. *Science Immunology* **7**, eabo0226 (2022).
- 600 31. Chiuppesi, F. *et al.* Safety and immunogenicity of a synthetic multiantigen modified vaccinia virus
601 Ankara-based COVID-19 vaccine (COH04S1): an open-label and randomised, phase 1 trial. *The*
602 *Lancet Microbe* **3**, e252–e264 (2022).
- 603 32. Khan, S. *et al.* Analysis of Serologic Cross-Reactivity Between Common Human Coronaviruses and
604 SARS-CoV-2 Using Coronavirus Antigen Microarray. *bioRxiv* 2020.03.24.006544 (2020)
605 doi:10.1101/2020.03.24.006544.
- 606 33. Nguyen-Contant, P. *et al.* S Protein-Reactive IgG and Memory B Cell Production after Human SARS-
607 CoV-2 Infection Includes Broad Reactivity to the S2 Subunit. *mBio* **11**, e01991-20 (2020).
- 608 34. Sette, A. & Crotty, S. Adaptive immunity to SARS-CoV-2 and COVID-19. *Cell* (2021)
609 doi:10.1016/j.cell.2021.01.007.
- 610 35. Amanat, F. *et al.* SARS-CoV-2 mRNA vaccination induces functionally diverse antibodies to NTD,
611 RBD, and S2. *Cell* **184**, 3936-3948.e10 (2021).
- 612 36. Ng, K. W. *et al.* SARS-CoV-2 S2-targeted vaccination elicits broadly neutralizing antibodies. *Science*
613 *Translational Medicine* **14**, eabn3715 (2022).
- 614 37. Sun, X. *et al.* Neutralization mechanism of a human antibody with pan-coronavirus reactivity
615 including SARS-CoV-2. *Nat Microbiol* **7**, 1063–1074 (2022).
- 616 38. Vidarsson, G., Dekkers, G. & Rispen, T. IgG Subclasses and Allotypes: From Structure to Effector
617 Functions. *Frontiers in Immunology* **5**, (2014).
- 618 39. Lu, L. L., Suscovich, T. J., Fortune, S. M. & Alter, G. Beyond binding: antibody effector functions in
619 infectious diseases. *Nat Rev Immunol* **18**, 46–61 (2018).
- 620 40. Tay, M. Z., Wiehe, K. & Pollara, J. Antibody-Dependent Cellular Phagocytosis in Antiviral Immune
621 Responses. *Front Immunol* **10**, 332 (2019).
- 622 41. Farkash, I. *et al.* Anti-SARS-CoV-2 antibodies elicited by COVID-19 mRNA vaccine exhibit a unique
623 glycosylation pattern. *Cell Reports* **37**, (2021).
- 624 42. Tejedor Vaquero, S. *et al.* The mRNA-1273 Vaccine Induces Cross-Variant Antibody Responses to
625 SARS-CoV-2 With Distinct Profiles in Individuals With or Without Pre-Existing Immunity. *Frontiers*
626 *in Immunology* **12**, (2021).

- 627 43. Barrett, J. R. *et al.* Phase 1/2 trial of SARS-CoV-2 vaccine ChAdOx1 nCoV-19 with a booster dose
628 induces multifunctional antibody responses. *Nat Med* **27**, 279–288 (2021).
- 629 44. Class switch towards non-inflammatory IgG isotypes after repeated SARS-CoV-2 mRNA vaccination
630 | medRxiv. <https://www.medrxiv.org/content/10.1101/2022.07.05.22277189v1>.
- 631 45. Kim, W. *et al.* Germinal centre-driven maturation of B cell response to mRNA vaccination. *Nature*
632 **604**, 141–145 (2022).
- 633 46. Jeannin, P., Lecoanet, S., Delneste, Y., Gauchat, J. F. & Bonnefoy, J. Y. IgE versus IgG4 production
634 can be differentially regulated by IL-10. *J Immunol* **160**, 3555–3561 (1998).
- 635 47. Das, S. *et al.* Pre-existing antibody levels negatively correlate with antibody titers after a single
636 dose of BBV152 vaccination. *Nat Commun* **13**, 3451 (2022).
- 637 48. Ewer, K. J. *et al.* Protective CD8+ T-cell immunity to human malaria induced by chimpanzee
638 adenovirus-MVA immunisation. *Nat Commun* **4**, 2836 (2013).
- 639 49. Precopio, M. L. *et al.* Immunization with vaccinia virus induces polyfunctional and phenotypically
640 distinctive CD8+ T cell responses. *Journal of Experimental Medicine* **204**, 1405–1416 (2007).
- 641 50. Bange, E. M. *et al.* CD8+ T cells contribute to survival in patients with COVID-19 and hematologic
642 cancer. *Nat Med* **27**, 1280–1289 (2021).
- 643 51. Tarke, A. *et al.* Negligible impact of SARS-CoV-2 variants on CD4+ and CD8+ T cell reactivity in
644 COVID-19 exposed donors and vaccinees. *bioRxiv* 2021.02.27.433180 (2021)
645 doi:10.1101/2021.02.27.433180.
- 646 52. Heidepriem, J. *et al.* Longitudinal Development of Antibody Responses in COVID-19 Patients of
647 Different Severity with ELISA, Peptide, and Glycan Arrays: An Immunological Case Series.
648 *Pathogens* **10**, 438 (2021).

649 **Acknowledgements**

650 We thank all volunteers for their participation in these vaccine studies and their commitment and
651 dedication to research against emerging coronaviruses. We would also like to express our sincere
652 gratitude to all trial center members for their extraordinary work (Clinical Trial Center North GmbH &
653 Co. KG, Hamburg), especially Laura Kaltenberg. We also thank Thomas Brehm for providing additional
654 PBMC and plasma samples.

655 **Author Contributions**

656 Conceptualization, M.M.A., S.Be., G.S., A.F., C.D., S.C.M., A.V., S.Bo.; Methodology, L.M., L.M.W, C.D.,
657 J.H., F.F.L.; Investigation, L.M., L.M.W., M.K., M.L.L., J.H., MVA-SARS-2 Study Group; Formal analysis
658 and visualization, L.M., L.M.W.; Writing – original draft, L.M., L.M.W., C.D.; Writing – review and
659 editing, L.M., L.M.W., C.D., M.M.A., A.F., S.C.M., J.H., F.F.L., S.H., G.S., T.H., S.Bo., A.V.; Supervision,
660 C.D., M.M.A; Project administration, T.H., S.H., S.Bo.

661 **MVA-SARS-2 Study Group**

662 Amelie Alberti, Marie-Louise Dieck, Stefanie Gräfe, Cordula Grüttner, Jana Kochmann, Niclas Renevier,
663 Monika Rottstegge, Maren Sandkuhl, Claudia Schlesner, Yashin Simsek, Paulina Tarnow. All members
664 of the MVA-SARS-2 Study Group are affiliated with the Institute for Infection Research and Vaccine
665 Development (IIRVD) at the University Medical Center Hamburg-Eppendorf, the Department for
666 Clinical Immunology of Infectious Diseases at the Bernhard Nocht Institute for Tropical Medicine
667 (BNITM), and the German Centre for Infection Research (DZIF).

668 Declarations of Interest

669 The authors declare no competing interests.

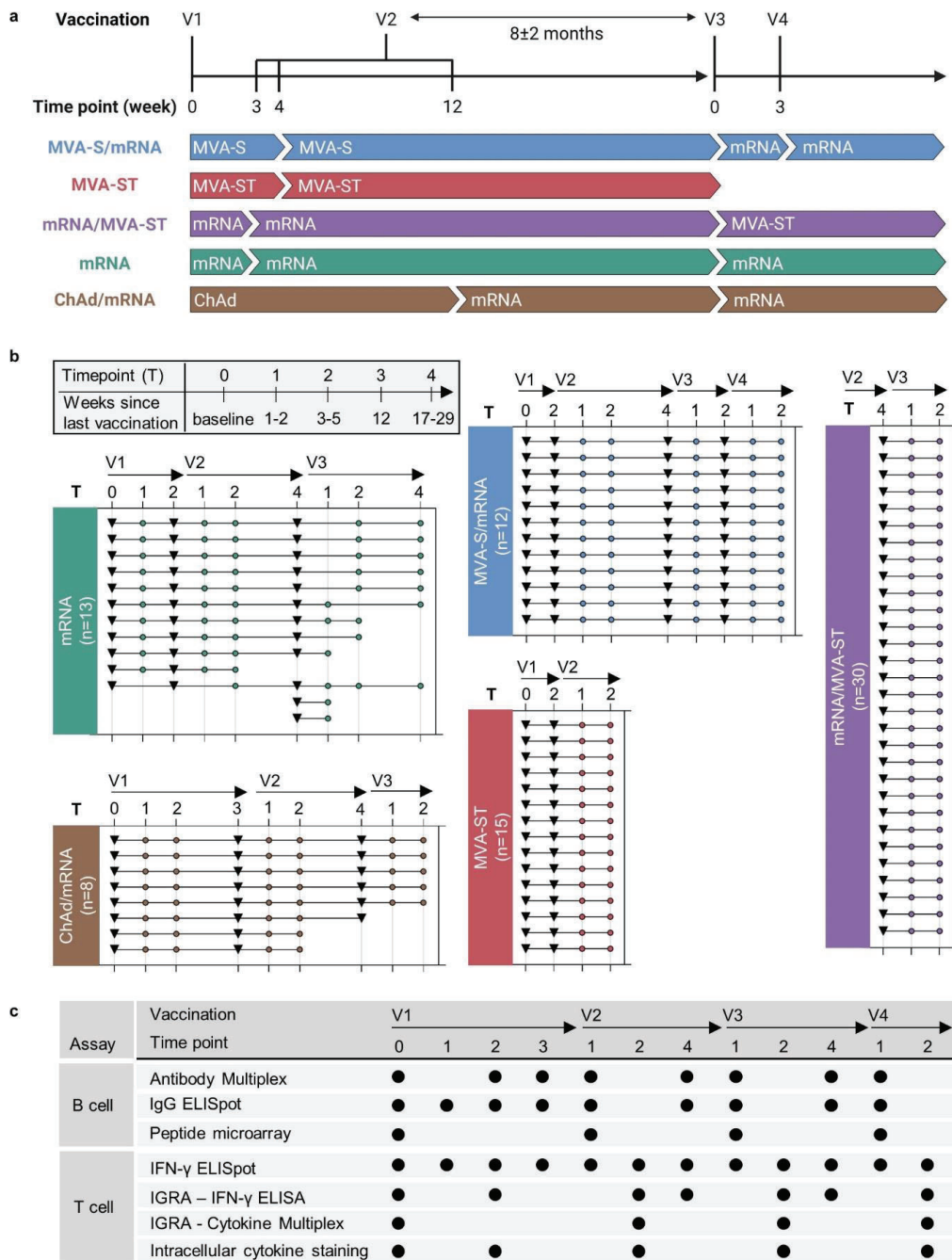
670 Funding

671 This work was funded by the German Center for Infection Research (DZIF), grant numbers
672 FKZ8009801924, FKZ8009701709, FKZ8009701702, FKZ80095CLSIM, and FKZ8009801921, the German
673 Federal Ministry of Education and Research (BMBF), grant number 13XP5050A, and the MPG-FhG
674 cooperation (Glyco3Display).

675 Figures

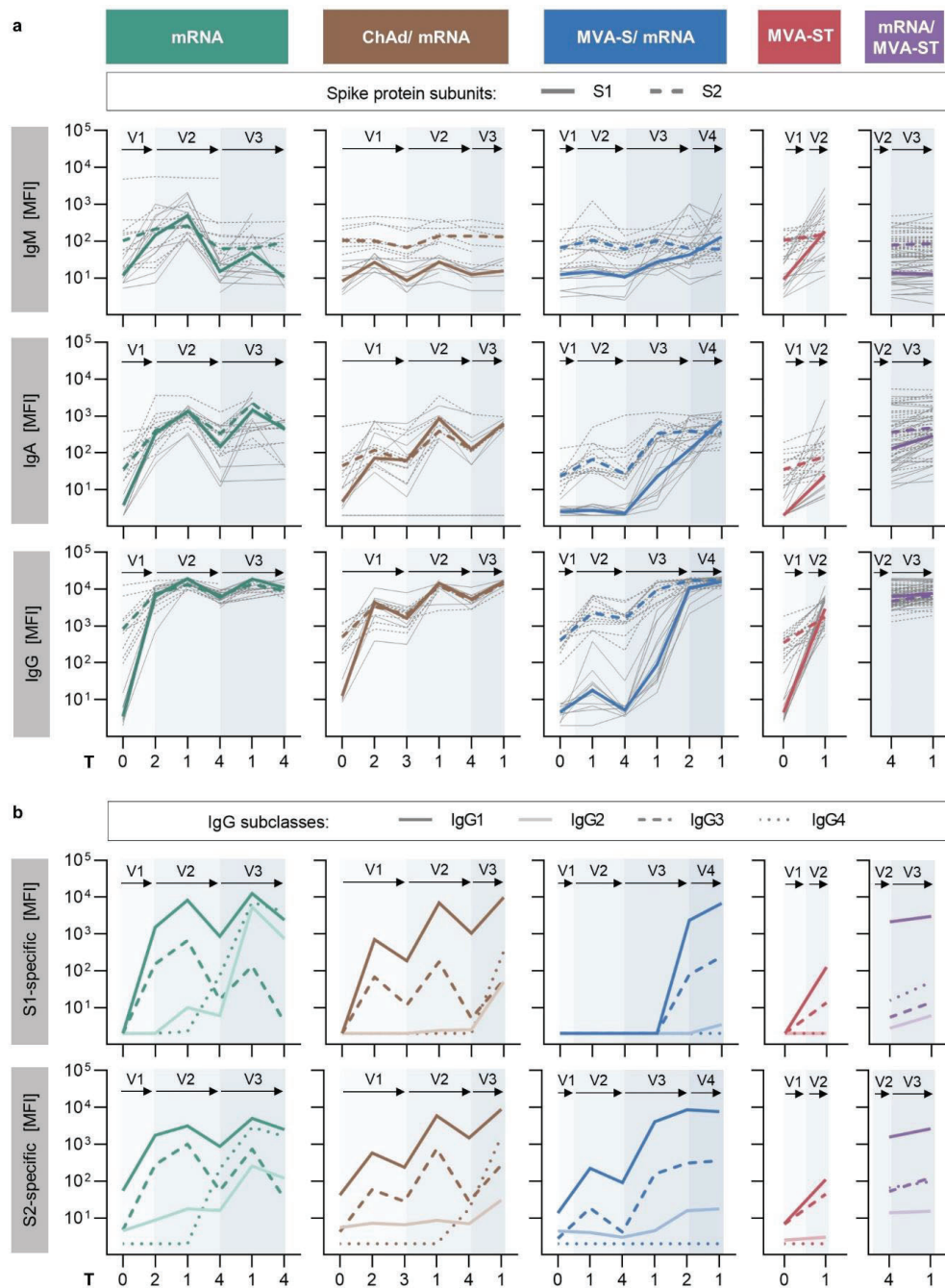
676

677



678 **Figure 1: Study design.** a Participants of five study cohorts received up to 4 vaccinations (V1 to V4) with different COVID-19 vaccines.
 679 Time intervals between vaccinations differed between the cohorts and are indicated in the upper panel. The vaccines administered
 680 in this study include the two rMVA-based vaccine candidates MVA-SARS-2-S (MVA-S) and MVA-SARS-2-ST (MVA-ST), as well as the
 681 licensed vaccines BNT162b2 and mRNA-1273 (together referred to as mRNA) and ChAdOx1 nCov-19 (ChAd). b Blood samples were
 682 collected at different time points after vaccination, labeled as T0 (baseline), T1 (1-2 weeks), T2 (3-5 weeks), T3 (12 weeks), and T4
 683 (17-29 weeks), referring to the time since last vaccination (V1-V4). Time points of longitudinal blood sampling are shown for each
 684 participant of the different cohorts, with vaccinations indicated by black triangles. c The humoral and cellular immune response was
 685 analyzed using different phenotypic assays. Dots represent a summary of the time points at which each of the assays was performed.
 686 See Supplementary Tables 4-8 for detailed number of samples and analyzed time points by assay and study cohort.
 687

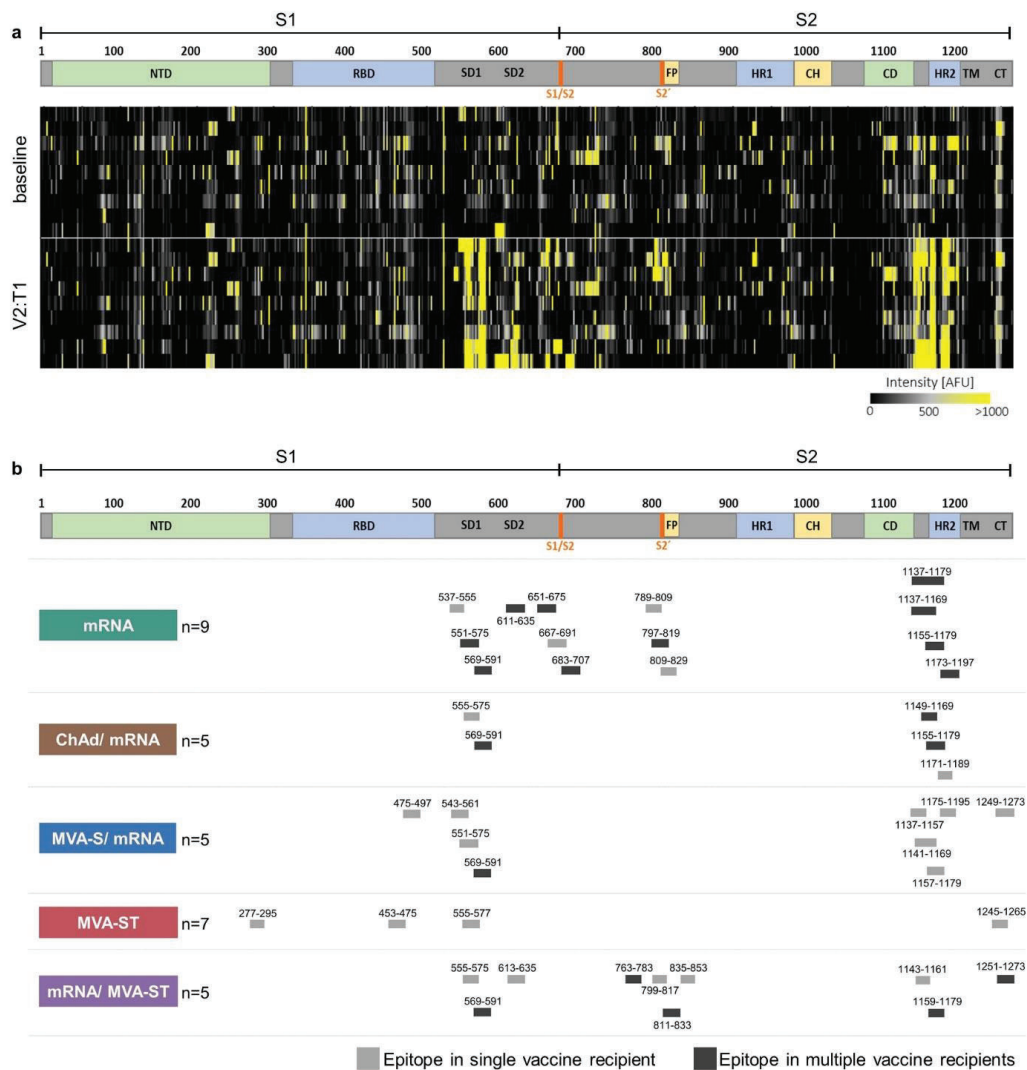
18



688

689 **Figure 2: Antibody isotype and IgG subclass response.** a S1- and S2- specific IgM, IgA, and IgG responses of the different study
 690 cohorts measured at baseline and longitudinally after each vaccination. Colored lines depict median MFI (measured by bead-based
 691 ELISA). Grey lines show dynamics of each study participant. b S1- (top) and S2- (bottom) specific IgG subclasses (measured by bead-
 692 based ELISA). Median MFI of IgG1-4 are shown as differently dotted lines. Vaccinations V1 to V4 are indicated by arrows and time
 693 points after vaccination are indicated as T0 (baseline), T1 (1-2 weeks), T2 (3-5 weeks), T3 (12 weeks), and T4 (17-29 weeks) (a, b).

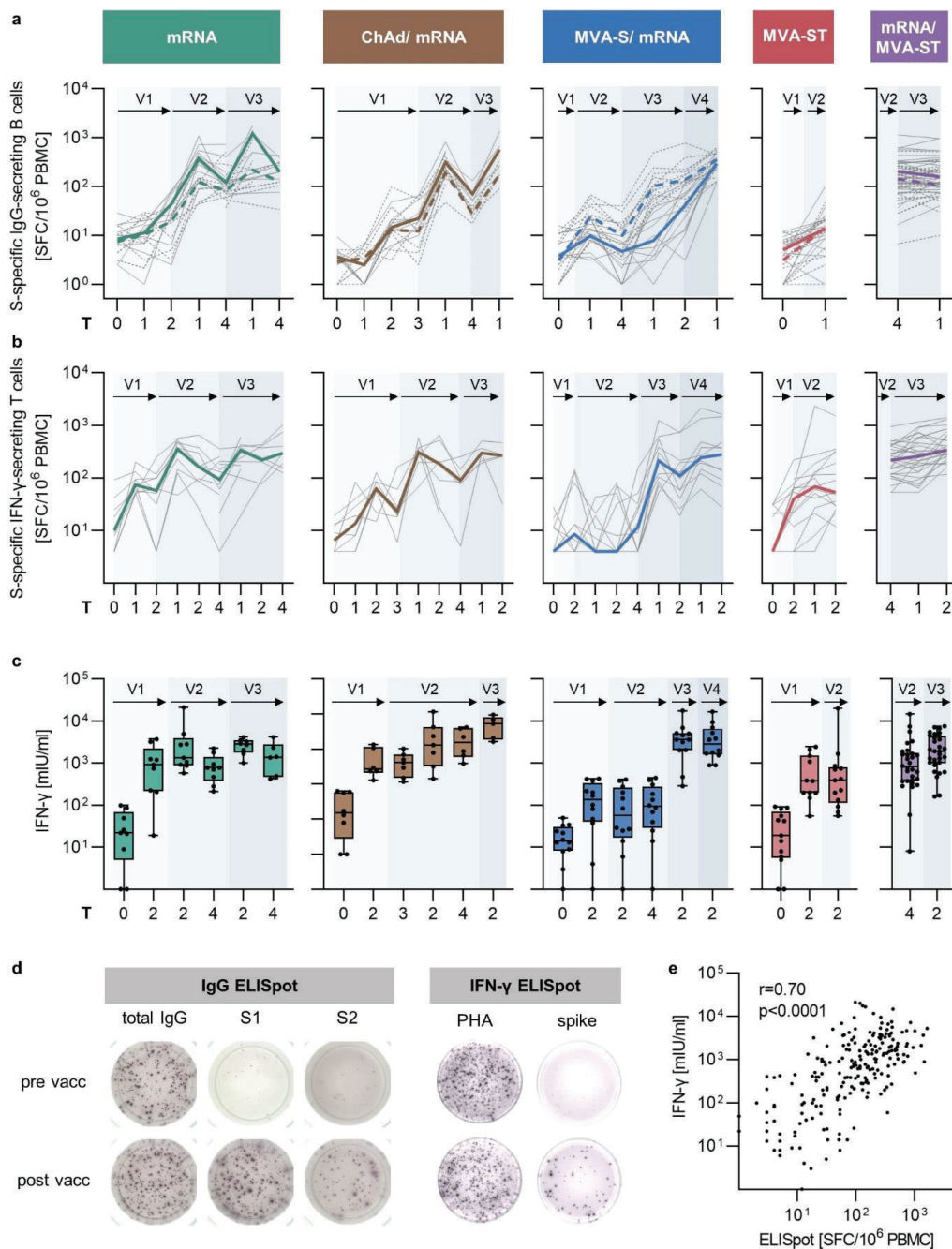
19



694

695 **Figure 3: S-specific IgG epitopes.** **a** Representative heatmap of B cell epitopes measured on peptide microarrays and identified by
 696 increased fluorescent intensity (as arbitrary fluorescence units, AFU) at baseline and seven days after second mRNA vaccination
 697 (V2:T1) in nine participants of the mRNA cohort, aligned to a schematic depiction of the S-protein. **b** Schematic representation of
 698 immunogenic B cell epitopes identified in the five study cohorts in one (grey) or multiple (black) individuals, aligned to a schematic
 699 depiction of the S-protein¹⁸. Positive epitope binding was defined as >400 mean AFU of three successive peptides (for all cohorts)
 700 and 2.5-fold above baseline (i.e. before vaccination, for all cohorts except MVA-ST/mRNA). Time points analyzed after vaccination:
 701 mRNA (V2:T1), ChAd/mRNA (V2:T1; V3:T1), MVA-S/mRNA (V2:T1; V4:T1), MVA-ST (V2:T1), mRNA/MVA-ST (V3:T0; V3:T1). (NTD: N-
 702 terminal domain, RBD: receptor-binding domain, SD1, SD2: subdomain 1 and 2, S1/S2: S1/S2 cleavage site, S2': S2' cleavage site, FP:
 703 fusion peptide, HR1: heptad repeat 1, CH: central helix, CD: connector domain, HR2: heptad repeat 2, TM: transmembrane domain,
 704 CT: cytoplasmic domain) (**a,b**).

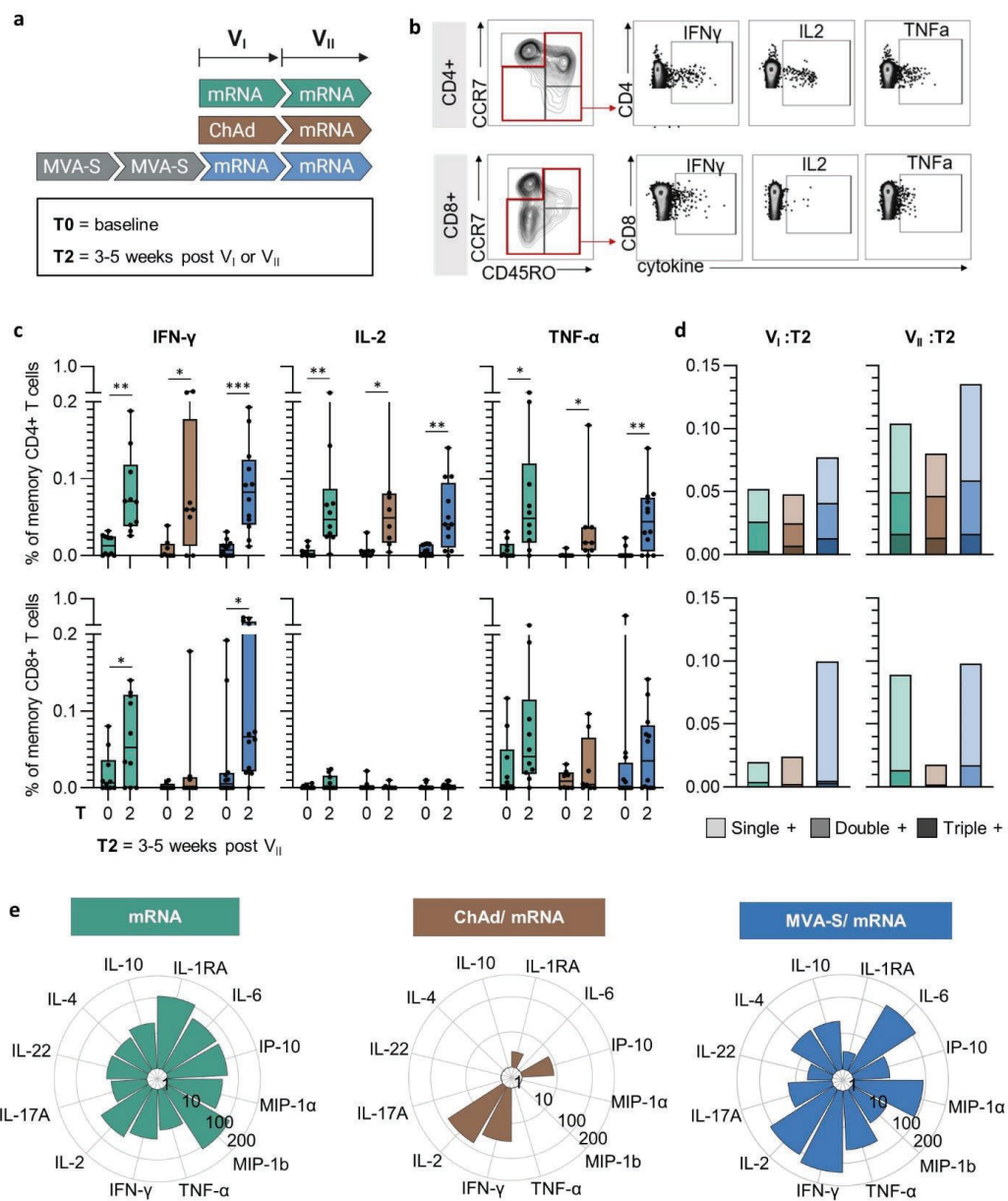
20



705

706 **Figure 4: S-specific B and T cell responses.** **a** Frequencies of IgG-secreting B cells shown as SFC/10⁶ PBMCs (mean of technical
707 duplicates) measured by IgG ELISpot. Colored lines depict median S1- and S2-specific responses for each cohort. Grey lines show the
708 dynamics of individual participants. **b** Frequencies of IFN- γ -producing T cells shown as SFC/10⁶ PBMCs (mean of technical triplicates)
709 measured by IFN- γ ELISpot. Colored lines depict median responses for each cohort. Grey lines show the dynamics of individual
710 participants. **c** IFN- γ secretion of S-specific T cells after whole-blood stimulation (measured by IGRA) shown as mIU/ml. Data are
711 represented as individual data points. Boxes indicate median \pm IQR; whiskers are min. to max. **d** Representative images of IgG ELISpot
712 total IgG (positive control) and S1/S2-specific wells taken before and after vaccination (left). Representative images of IFN- γ ELISpot
713 wells stimulated with PHA (positive control) or spike peptides (right). **e** Spearman correlation of IFN- γ T cell response as measured
714 by ELISpot (SFC/10⁶ PBMCs) and IGRA assay (mIU/ml). Vaccinations V1 to V4 are indicated by arrows and time points after vaccination
715 are indicated by T0 (baseline), T1 (1-2 weeks), T2 (3-5 weeks), T3 (12 weeks), and T4 (17-29 weeks) (**a**, **b**, **c**).

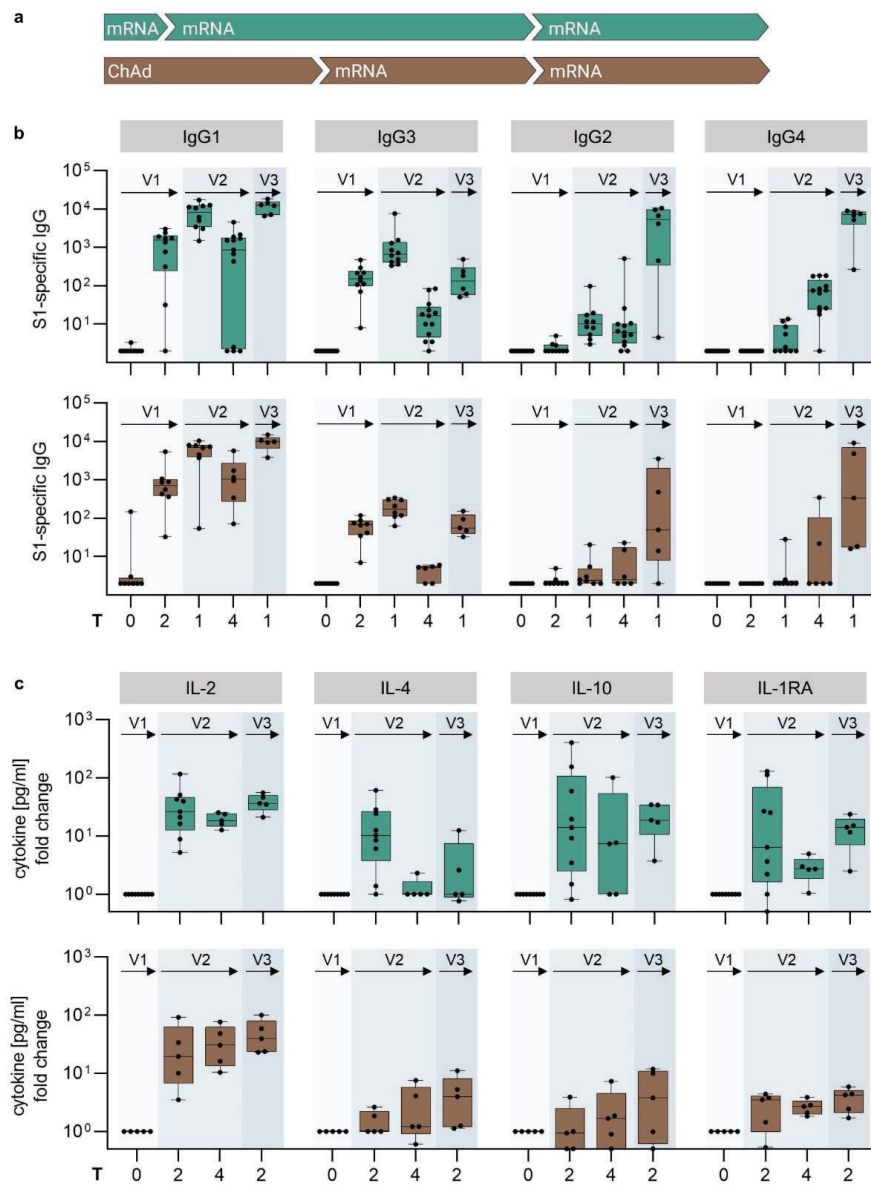
21



716

717 **Figure 5: Cytokine response of vaccine-induced CD4⁺ and CD8⁺ memory T cells.** **a** Overview showing the analyzed study cohorts:
 718 mRNA (green), ChAd/mRNA (brown), and MVA-S/mRNA (blue) at baseline (T0) and time points after vaccinations V_I and V_{II} (T2). **b**
 719 Representative gating strategy of cytokine-secreting CD4⁺ (top) and CD8⁺ (bottom) memory T cells after stimulation with peptides
 720 covering the S-protein. **c** Frequency of IFN- γ , IL-2, and TNF- α -positive T cells out of total CD4⁺ (top) and CD8⁺ (bottom) memory T
 721 cells at baseline and time point T2 post V_I and V_{II}. Data are represented as individual data points. Boxes indicate median \pm IQR;
 722 whiskers are min. to max. Significant p-values as calculated by Wilcoxon signed rank test are indicated as *p<0.5, **p<0.01,
 723 ***p<0.001. **d** Median frequencies of single positive (IFN- γ ⁺ or IL-2⁺ or TNF- α ⁺), double positive (IFN- γ ⁺ IL-2⁺ TNF- α ⁺ or IFN- γ ⁺ IL-2⁺
 724 TNF- α ⁺ or IFN- γ ⁺ IL-2⁺ TNF- α ⁺), and triple positive (IFN- γ ⁺ IL-2⁺ TNF- α ⁺) T cells out of total CD4⁺ (top) and CD8⁺ (bottom) memory T
 725 cells. Results were obtained by Boolean gating of the cytokine gates shown in panel **b**. **e** Circular bar plots of cytokine levels (pg/ml)
 726 measured in IGRA supernatant after S-specific whole-blood stimulation using a bead-based assay. Shown are the median fold
 727 changes of each cytokine at T2 post V_{II} compared to baseline. Axes depict fold change in log-scale.

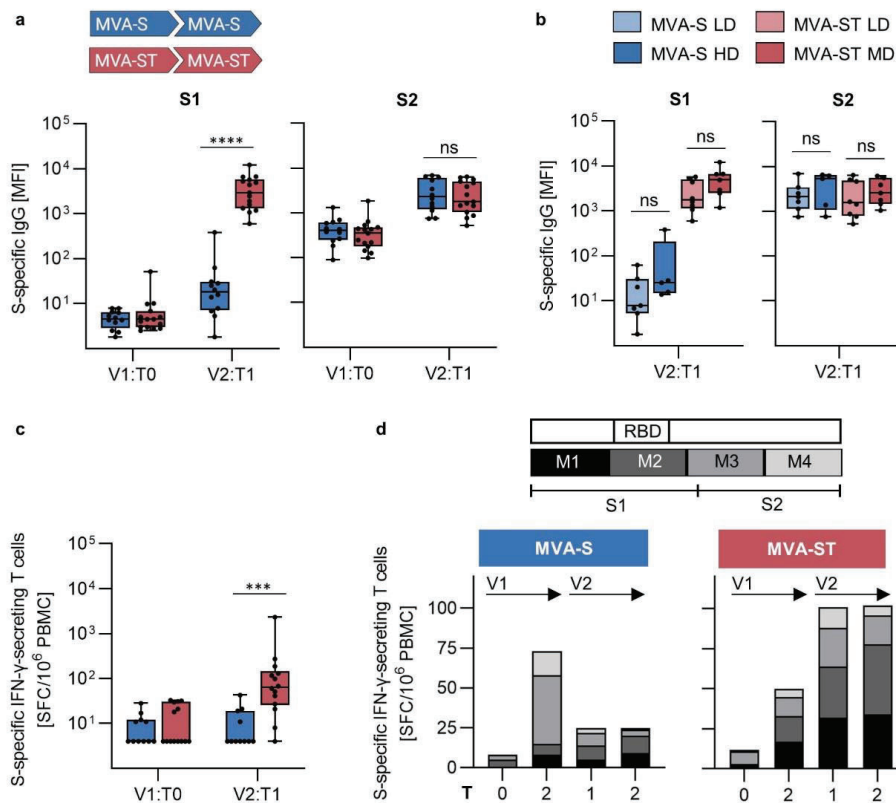
22



728

729 **Figure 6: IgG subclass and cytokine signature after repeated mRNA vaccination.** **a** Vaccination schedule of the mRNA (green) and
 730 ChAd/mRNA (brown) cohorts. **b** Longitudinal S1-specific IgG1-4 dynamics in the mRNA (top) and ChAd/mRNA (bottom) cohorts. **c**
 731 Cytokine levels (pg/ml) measured in IGRA supernatant after spike-specific whole-blood stimulation using a bead-based assay. Shown
 732 are fold changes of the mRNA (top) and ChAd/mRNA (bottom) cohorts at different time points compared to baseline. Boxes indicate
 733 median ± IQR; whiskers are min. to max. (**a, b**). Vaccinations V1 to V3 are indicated by arrows and time points after vaccination are
 734 indicated by T0 (baseline), T1 (1-2 weeks), T2 (3-5 weeks), T3 (12 weeks), and T4 (17-29 weeks) (**a, b**).

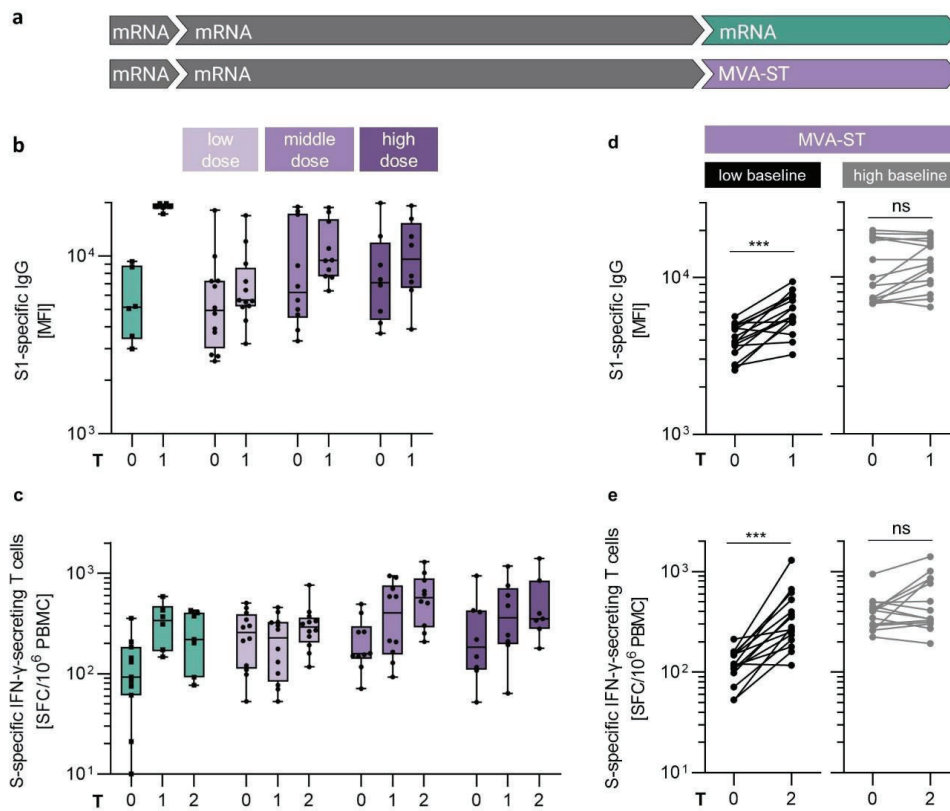
23



735

736 **Figure 7: S1- and S2-specific immunogenicity of MVA-S and MVA-ST.** **a** S1- (left) and S2- (right) specific IgG levels (MFI) at baseline
 737 and T1 (1-2 weeks) after second vaccination with the MVA-S (blue) and MVA-ST (red) vaccines. **b** S1- (left) and S2- (right) specific IgG
 738 levels (MFI) at T1 after second vaccination with the MVA-S (blue) and MVA-ST (red) vaccines, divided by dose group (LD: low dose,
 739 MD: middle dose, HD: high dose). **c** Spike-specific IFN- γ -secreting T cells measured by IFN- γ ELISpot (SFC/10⁶ PBMCs) at baseline and
 740 T1 after second vaccination with the MVA-S (blue) and MVA-ST (red) vaccines. Data are represented as individual data points. Boxes
 741 indicate median \pm IQR; whiskers are min. to max. (**a**, **b**, **c**). **d** T cell responses (SFC/10⁶ PBMCs) induced by stimulation with individual
 742 peptide pools M1-M4, resembling the S1 and S2 subunits of the S-protein (technical triplicates). For each time point data are shown
 743 as the sum of the median responses of pools M1-M4. P-values are indicated as calculated by Mann Whitney U test: ns = not
 744 significant, ***p<0.001, ****p<0.0001 (**a**, **b**, **c**). S1, S2: S-protein subunits, RBD: receptor binding domain.

24

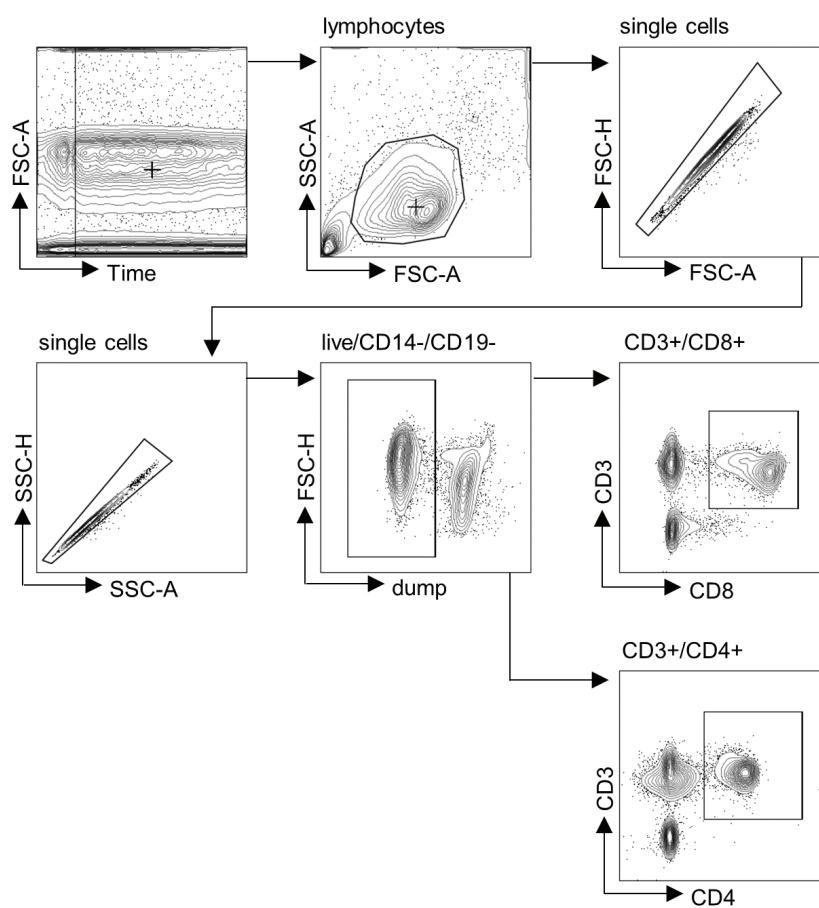


745

746 **Figure 8: Immunogenicity of mRNA or MVA-ST as third vaccinations.** a Vaccination scheme of the mRNA (green) and
 747 mRNA/MVA-ST cohort (purple; different shading indicates low, middle and high dose group). b S1-specific IgG levels (MFI) and c S-
 748 specific IFN- γ -secreting T cells measured by IFN- γ ELISpot (SFC/ 10^6 PBMCs) before and after third vaccination with mRNA or MVA-ST
 749 (divided by dose group). Data are represented as individual data points and median \pm IQR (b, c). d Individual dynamics of S1-specific
 750 IgG levels (MFI). e S-specific IFN- γ -secreting T cells induced by MVA-ST vaccination. Participants are divided into groups with low
 751 (left) and high (right) baseline levels. P-values are indicated as calculated by Wilcoxon signed rank test: ns = not significant,
 752 *** $p < 0.001$ (d, e). Time points are indicated as T0 (baseline prior to V3), T1 (1-2 weeks post V3), and T2 (3-5 weeks post V3) (b, c,
 753 d, e).

754

Supplementary Figure



Suppl. Fig. 1 | T cell gating strategy. Gating strategy for intracellular cytokine staining T cell assay. Contour plots show representative data from an individual of the ChAd/mRNA cohort at V2:T2.

Supplementary Tables

Table S1 | Baseline characteristics of study participants

| | mRNA n=13 | ChAd/mRNA n=8 | MVA-S/mRNA n=12 | MVA-ST n=15 | mRNA/MVA-ST n=30 |
|---|--------------|------------------|--------------------|----------------|---------------------|
| Sex | | | | | |
| Female | 8 (62%) | 7 (88%) | 4 (33%) | 10 (67%) | 18 (60%) |
| Male | 5 (38%) | 1 (12%) | 8 (67%) | 5 (33%) | 12 (40%) |
| Age | | | | | |
| mean, years | 33.2 (8.9) | 32.3 (5.9) | 37.8 (9.0) | 40.7 (11.3) | 31.9 (11.1) |
| range, years | 23-51 | 24 - 44 | 21 - 51 | 22 - 62 | 19 - 64 |
| BMI | | | | | |
| kg/m ² | 21.4 (2.4) | 21.7 (1.3) | 24.9 (3.4) | 24.1 (3.3) | 24.4 (3.1) |
| Data is shown in mean (SD), unless otherwise indicated. BMI=body-mass index. BMI of n=2 of the mRNA cohort missing. | | | | | |

Table S2 | Time interval between vaccinations

| | mRNA n=13 | ChAd/mRNA n=8 | MVA-S/mRNA n=12 | MVA-ST n=15 | mRNA/MVA-ST n=30 |
|--------------------------------------|---------------|------------------|--------------------|----------------|---------------------|
| Vaccination interval | | | | | |
| V1-V2 | 21 (21-40) | 84 (77-84) | 28 | 28 | |
| V2-V3 | 252 (196-291) | 183 (170-211) | 203 (185-211) | | 222 (186-364) |
| V3-V4 | | | 22 (21-28) | | |
| Data is shown as median days (range) | | | | | |

Table S3 | Blood collection time since last vaccination

| | mRNA n=13 | ChAd/mRNA n=8 | MVA-S/mRNA n=12 | MVA-ST n=15 | mRNA/MVA-ST n=30 |
|--------------------------------------|-----------------|------------------|--------------------|----------------|---------------------|
| V1 | | | | | |
| T1 | 7 | 7 (7-8) | - | - | - |
| T2 | 21 (20-23) | 28 (28-31) | 28 (28-29) | 28 | - |
| T3 | - | 80.5 (56-83) | - | - | - |
| V2 | | | | | |
| T1 | 7 (7-8) | 7 (7-10) | 14 (12-16) | 14 (14-17) | - |
| T2 | 35 (34-38) | 36.5 (29-42) | 29 (27-33) | 28 (28-35) | - |
| T4 | 164 (147-169) | 169 (168-171) | 203 (185-211) | - | 7 (7-14) |
| V3 | | | | | |
| T1 | 8.5 (7-15) | 7 (7-8) | 7 | - | 28 (25-34) |
| T2 | 28 (28-36) | 28 (27-32) | 21.5 (21-28) | | - |
| T4 | 124.5 (119-137) | - | - | - | - |
| V4 | | | | | |
| T1 | - | - | 7 (6-7) | - | - |
| T2 | - | - | 28 (28-33) | | - |
| Data is shown as median days (range) | | | | | |

Table S4 | Number of samples – mRNA cohort

| Assay | Timepoint | V1:T0 | V1:T1 | V1:T2 | V2:T1 | V2:T2 | V2:T4 | V3:T1 | V3:T2 | V3:T4 |
|--------|----------------------------------|-------|-------|-------|-------|-------|-------|-------|-------|-------|
| B cell | Antibody isotypes and subclasses | 10 | | 10 | 10 | | 13 | 6 | | 7 |
| | IgG ELISpot | 10 | 10 | 10 | 10 | | 13 | 5 | | 7 |
| | IgG epitope array | 9 | | | 9 | | | | | |
| T cell | IFN γ ELISpot | 10 | 10 | 10 | 10 | 10 | 13 | 6 | 7 | 7 |
| | IGRA - IFN γ ELISA | 9 | | 9 | | 9 | 9 | | 8 | 6 |
| | IGRA – Cytokine multiplex | 9 | | | | 9 | 5 | | 5 | |
| | Intracellular cytokine staining | 10 | | 10 | | 10 | | | | |

Table S5 | Number of samples – ChAd/mRNA cohort

| Assay | Timepoint | V1:T0 | V1:T1 | V1:T2 | V1:T3 | V2:T1 | V2:T2 | V2:T4 | V3:T1 | V3:T2 |
|--------|----------------------------------|-------|-------|-------|-------|-------|-------|-------|-------|-------|
| B cell | Antibody isotypes and subclasses | 8 | | 8 | 8 | 8 | 8 | 6 | 5 | |
| | IgG ELISpot | 8 | 8 | 8 | 8 | 8 | | 6 | 5 | |
| | IgG epitope array | 5 | | | | 5 | | | 5 | |
| T cell | IFN γ ELISpot | 8 | 8 | 8 | 8 | 8 | 8 | 6 | 5 | 5 |
| | IGRA - IFN γ ELISA | 8 | | 6 | 7 | | 7 | 6 | | 5 |
| | IGRA – Cytokine multiplex | 5 | | | | | 5 | 5 | | 5 |
| | Intracellular cytokine staining | 8 | | 8 | | | 8 | | | |

Table S6 | Number of samples – MVA-S/mRNA cohort

| Assay | Timepoint | V1:T0 | V1:T2 | V2:T1 | V2:T2 | V2:T4 | V3:T1 | V3:T2 | V4:T1 | V4:T2 |
|--------|----------------------------------|-------|-------|-------|-------|-------|----------------|----------------|-------|-------|
| B cell | Antibody isotypes and subclasses | 12 | | 12 | | 12 | 12 | 12 | 12 | |
| | S1-specific IgG ELISpot | 12 | | 12 | | 12 | S1: 12, S2: 11 | S1: 12, S2: 11 | 12 | |
| | Epitope array | 5 | | 5 | | | | | 5 | |
| T cell | IFN γ ELISpot | 12 | 10 | 11 | 12 | 12 | 12 | 12 | 12 | 12 |
| | IGRA - IFN γ ELISA | 12 | 12 | | 12 | 12 | | 12 | | 12 |
| | IGRA – Cytokine multiplex | 12 | | | | | | | | 12 |
| | Intracellular cytokine staining | 12 | | | | | | 12 | | 12 |

Table S7 | Number of samples – MVA-ST

| Assay | Timepoint | V1:T0 | V1:T2 | V2:T1 | V2:T2 |
|--------|----------------------------------|-------------------|-------|-------|-------|
| B cell | Antibody isotypes and subclasses | 15 | | 15 | |
| | IgG ELISpot | S1: 15, S2: 14 | | 15 | |
| | IgG epitope array | 7 | | 7 | |
| T cell | IFN γ ELISpot | 14 | 15 | 15 | 15 |
| | IGRA - IFN γ ELISA | 13 | 11 | | 13 |
| | IGRA – Cytokine multiplex | | | | |
| | Intracellular cytokine staining | | | | |

Table S8 | Number of samples – mRNA/MVA-ST

| Assay | Timepoint | V2:T4 | V3:T1 | V3:T2 |
|--------|----------------------------------|-------|-------|-------|
| B cell | Antibody isotypes and subclasses | 30 | 30 | |
| | IgG ELISpot | 29 | 29 | |
| | IgG epitope array | | | |
| T cell | IFN γ ELISpot | 30 | 30 | 29 |
| | IGRA - IFN γ ELISA | 30 | | 30 |
| | IGRA – Cytokine multiplex | | | |
| | Intracellular cytokine staining | | | |

2.4 Stabilized recombinant SARS-CoV-2 spike antigen enhances vaccine immunogenicity and protective capacity


Christian Meyer zu Natrup,* Alina Tscherne,* Christine Dahlke, Malgorzata Ciurkiewicz, Dai-Lun Shin, Anahita Fathi, Cornelius Rohde, Georgia Kalodimou, Sandro Halwe, Leonard Limpinsel, Jan H. Schwarz, Martha Klug, Meral Esen, Nicole Schneiderhan-Marra, Alex Dulovic, Alexandra Kupke, Katrin Brosinski, Sabrina Clever, Lisa-Marie Schünemann, Georg Beythien, Federico Armando, Leonie Mayer, **Marie L. Weskamm**, Sylvia Jany, Astrid Freudenstein, Tamara Tuchel, Wolfgang Baumgärtner, Peter Kremsner, Rolf Fendel, Marylyn M. Addo, Stephan Becker, Gerd Sutter, and Asisa Volz

*These authors contributed equally

Published in *The Journal of Clinical Investigation*, DOI: 10.1172/JCI159895

Leonie Marie Weskamm was involved in the processing of the serum samples provided for the analysis of human antibody responses. She was also involved in the coordination of the laboratory work and optimization of protocols used for the processing of human blood samples in the phase 1 clinical trials of the MVA-SARS-2-S and MVA-SARS-2-ST vaccine candidates.

I hereby confirm the accuracy of these contributions

 17.1.2023
Prof. Dr. med. Marylyn M. Addo

Stabilized recombinant SARS-CoV-2 spike antigen enhances vaccine immunogenicity and protective capacity

Christian Meyer zu Natrup,¹ Alina Tscherne,^{2,3} Christine Dahlke,^{4,5} Malgorzata Ciurkiewicz,⁶ Dai-Lun Shin,¹ Anahita Fathi,^{4,5,7} Cornelius Rohde,^{8,9} Georgia Kalodimou,^{2,3} Sandro Halwe,⁹ Leonard Limpinsel,² Jan H. Schwarz,² Martha Klug,^{10,11} Meral Esen,^{10,11} Nicole Schneiderhan-Marra,¹² Alex Dulovic,¹² Alexandra Kupke,^{8,9} Katrin Brosinski,² Sabrina Clever,¹ Lisa-Marie Schünemann,¹ Georg Beythien,⁶ Federico Armando,⁶ Leonie Mayer,^{4,5,7} Marie L. Weskamm,^{4,5,7} Sylvia Jany,² Astrid Freudenstein,² Tamara Tuchel,¹ Wolfgang Baumgärtner,⁶ Peter Kremsner,^{10,11,13} Rolf Fendel,^{10,11} Marylyn M. Addo,^{5,10} Stephan Becker,^{8,9} Gerd Sutter,^{2,3} and Asisa Volz^{1,14}

¹Institute of Virology, University of Veterinary Medicine Hannover, Foundation, Hannover, Germany. ²Division of Virology, Department of Veterinary Sciences, LMU Munich, Munich, Germany. ³German Center for Infection Research, partner site Munich, and ⁴partner site Hamburg-Lübeck-Borstel-Riems. ⁵University Medical Center Hamburg-Eppendorf, Institute for Infection Research and Vaccine Development (IIRVD), Hamburg, Germany. ⁶Department of Pathology, University of Veterinary Medicine Hannover, Foundation, Hannover, Germany. ⁷University Medical Center Hamburg-Eppendorf, Division of Infectious Diseases, Hamburg, Germany. ⁸German Center for Infection Research, partner site Gießen-Marburg-Langen. ⁹Institute of Virology, Philipps University Marburg, Marburg, Germany. ¹⁰German Center for Infection Research, partner site Tübingen. ¹¹Institute of Tropical Medicine, University of Tübingen, Tübingen, Germany. ¹²NMI Natural and Medical Sciences Institute at the University of Tübingen, Reutlingen, Germany. ¹³Centre de Recherches Médicales de Lambarene, Gabon. ¹⁴German Center for Infection Research, partner site Hanover-Braunschweig.

The SARS-CoV-2 spike (S) glycoprotein is synthesized as a large precursor protein and must be activated by proteolytic cleavage into S1 and S2. A recombinant modified vaccinia virus Ankara (MVA) expressing native, full-length S protein (MVA-SARS-2-S) is currently under investigation as a candidate vaccine in phase I clinical studies. Initial results from immunogenicity monitoring revealed induction of S-specific antibodies binding to S2, but low-level antibody responses to the S1 domain. Follow-up investigations of native S antigen synthesis in MVA-SARS-2-S-infected cells revealed limited levels of S1 protein on the cell surface. In contrast, we found superior S1 cell surface presentation upon infection with a recombinant MVA expressing a stabilized version of SARS-CoV-2 S protein with an inactivated S1/S2 cleavage site and K986P and V987P mutations (MVA-SARS-2-ST). When comparing immunogenicity of MVA vector vaccines, mice vaccinated with MVA-SARS-2-ST mounted substantial levels of broadly reactive anti-S antibodies that effectively neutralized different SARS-CoV-2 variants. Importantly, intramuscular MVA-SARS-2-ST immunization of hamsters and mice resulted in potent immune responses upon challenge infection and protected from disease and severe lung pathology. Our results suggest that MVA-SARS-2-ST represents an improved clinical candidate vaccine and that the presence of plasma membrane-bound S1 is highly beneficial to induce protective antibody levels.

Introduction

All COVID-19 vaccines licensed to date include the complete SARS-CoV-2 spike (S) protein as key antigen to elicit protective immune responses. Trimers of this large viral surface protein form the distinctive spikes of the coronavirus (1). Monomeric S is a glycosylated transmembrane protein consisting of a large N-terminal ectodomain and a short C-terminal endodomain. The full-length SARS-CoV-2 S protein is cleaved by a furin-like protease into 2 almost equally sized polypeptides called S1 (N-terminus of S) and S2 (membrane-anchored C-terminus of S). S1 harbors the receptor

binding domain (RBD), which interacts with the cellular receptor molecule angiotensin-converting enzyme 2 (ACE2) and serves, together with other parts of S1, as an important target for antibodies that can interfere with host cell receptor binding capable of neutralizing SARS-CoV-2 infection. S2 mediates fusion between the virus and cell membrane, and is also an important target for antibodies that can interfere with virus entry.

S-specific virus-neutralizing antibodies are a major component of the vaccine-induced immune response protecting against SARS-CoV-2 infection (2). COVID-19 vaccines with reported efficacy deliver as an antigen either native S polypeptides (3–5) or modified versions of the full-length S protein (6–9). The modified S antigens contain 2 proline amino acid substitutions in the S2 protein between the fusion peptide and the first hinge region sequence to arrest the S protein in the prefusion conformation (1). Two S vaccine antigens harbor additional mutations to prevent S1/S2 cleavage by furin-like proteases (6, 8). While all of the different candidate vaccines based on S antigens elicit protective

Authorship note: CMZN and AT contributed equally to this work

Conflict of interest: The authors have declared that no conflict of interest exists.

Copyright: © 2022, Meyer zu Natrup et al. This is an open access article published under the terms of the Creative Commons Attribution 4.0 International License.

Submitted: March 3, 2022; **Accepted:** October 21, 2022; **Published:** December 15, 2022.

Reference information: *J Clin Invest.* 2022;132(24):e159895.

<https://doi.org/10.1172/JCI159895>.

immunity in humans, they seem to induce distinct levels of vaccine efficacy and S-specific antibody responses (10). Structural features of the various S antigens might account for these differences in vaccine immunogenicity and/or vaccine efficacy and warrant further investigation. Moreover, recent studies demonstrated that the persistence of immune responses induced by approved COVID-19 vaccines and/or infection is limited. While all approved vaccine candidates provide a high level of protection against severe disease and death, protection against SARS-CoV-2 infection and/or transmission declines due to the waning of S-specific antibodies and the emergence of variants. To address this limitation, improved vaccination strategies that could be used as booster vaccines are urgently needed.

Modified vaccinia virus Ankara (MVA), a replication-deficient orthopoxvirus vaccine strain, has long served as an advanced vaccine technology platform for developing viral vector vaccines against emerging infectious disease (10–14).

Recent work addressed the preclinical development of MVA vector vaccines against COVID-19, including our candidate vaccine MVA-SARS-2-S (MVA-S) (15). Immunizations with MVA-S in animal models demonstrated the safety, immunogenicity, and protective efficacy of this vector vaccine delivering the native full-length SARS-CoV-2 S antigen. Further, MVA-S entered phase Ia clinical evaluation to assess the clinical safety and tolerability of 2 administrations and 2 ascending dose levels in healthy adults (ClinicalTrials.gov NCT04569383).

One objective of this study was to more closely examine the S-specific antibody responses following MVA-S immunization. Preliminary data from this immunogenicity monitoring suggested that most of the vaccine-induced native S-antigen-specific antibodies bound to the S2 but not the S1 antigen domain. This interesting observation prompted us to construct a vaccine vector delivering a modified stabilized version of the SARS-CoV-2 S antigen, with an inactivated S1/S2 cleavage site, called MVA-SARS-2-ST (for stabilized S antigen, MVA-ST) to compare with the original MVA-S in preclinical studies.

Here, we show that MVA-ST produces a full-length SARS-CoV-2 S protein that is not processed into S1 and S2 protein subunits, but anchored to the membrane of MVA-ST-infected cells. We found enhanced levels of cell-surface S1 antigen upon infection with MVA-ST compared with MVA-S. Moreover, when comparatively tested as a vaccine in animal models, MVA-ST not only elicited substantially higher levels of S1-binding and SARS-CoV-2-neutralizing antibodies, but also robustly protected vaccinated mice and hamsters against SARS-CoV-2 respiratory infection and lung pathology. Currently, MVA-ST is being investigated in a phase Ib clinical trial as an optimized MVA vector candidate vaccine against COVID-19.

Results

Antibody response against different S protein domains in human volunteers vaccinated with MVA-S. The MVA-based candidate vaccine MVA-S, encoding an unmodified, full-length SARS-CoV-2 S protein, is being tested in a phase Ia clinical study. This involved a prime-boost intramuscular vaccination schedule comparing low dose (1×10^7 infectious units [IU]) versus high dose (1×10^8 IU). The full prime-boost vaccination regimen was administered to

30 participants at an interval of 28 days. We collected blood from these individuals at several time points, including before vaccination (day 0), after the first vaccination (day 28), and at 2 time points after the second vaccination (days 42 and 84).

To characterize the antigen binding capacities of the SARS-CoV-2-specific antibodies, we performed a high-throughput, automated bead-based multiplex assay called Multi-CoV-Ab (16, 17), where 4 different SARS-CoV-2-specific antigens (trimeric full-length S protein [S trimer], receptor-binding domain [RBD], and S1 and S2) are expressed and immobilized on LUMINEX MAGPLEX beads. Seroconversion was estimated by a comparison relative to a calibrator sample. To examine MVA-S-induced seroconversion, we used the trimer antigen assay (Figure 1A). All individuals vaccinated with the low dose mounted low levels of trimer-binding antibodies that peaked on day 42, with a mean titer expressed as a median fluorescence intensity (MFI) of 787.7. Thirty-three percent ($n = 5/15$) of the individuals reached antibody titers relevant for seroconversion. In the high-dose vaccination group, we detected marginally increased trimer-specific antibody responses with a mean titer of 1274 MFI peaking 2 weeks after the second vaccine dose, and 33.3% ($n = 5/15$) of the individuals seroconverted (Figure 1A).

When evaluating serum reactivity against the RBD of the SARS-CoV-2 S protein we found markedly lower quantities of antigen-binding antibodies (Figure 1B). Only 26.7% ($n = 4/15$) of the vaccinees receiving the high-dose immunization produced an anti-RBD response (with a peak mean titer of 232.9 MFI on day 42), and of these, only 2 individuals reached elevated RBD-specific antibody levels compared with the calibrator. In the sera from low-dose vaccinees, we did not detect any RBD-specific antibodies.

Analyzing the IgG response directed against the S1 and S2 subdomains of the SARS-CoV-2 spike protein (Figure 1, C and D) revealed marginal levels of S1-specific antibodies in a few individuals only, irrespective of the dosage used for vaccination (Figure 1C). In contrast, we measured substantial quantities of S2-binding antibodies in sera from all vaccinees, irrespective of the dosage used for vaccination (Figure 1D). Again, seroconversion was estimated by comparison relative to a calibrator sample. To avoid any false positive results due to extensive background fluorescence associated with the S2 subdomain, we defined the cutoff values as $2 \times$ (day 0 MFI). The S2-specific antibody response peaked on day 84 in the low-dose group, with a mean titer of 4206.5 MFI. In the high-dose group, half of the vaccinees exhibited a peak on day 42 (mean titer of 3271.2 MFI), whereas the rest developed steadily increasing levels of SARS-CoV-2 S2-binding antibodies until day 84 (mean titer of 2928.9 MFI). Altogether, these results indicated that vaccination with the candidate vaccine MVA-S expressing a full-length unmodified S protein predominantly induces an S2-specific antibody response in humans.

Generation and characterization of the modified candidate vaccine MVA-ST. To investigate the possible impact of fusogenic activity and proteolytic cleavage of the native full-length S protein delivered by MVA-S, we generated a matching MVA vector vaccine producing a modified version of the SARS-CoV-2 S antigen, MVA-ST. To obtain an S antigen stabilized in a prefusion conformation we introduced 5 amino acid (aa) exchanges within the 1273-aa S polypeptide, inactivating the S1/S2 furin cleavage site and creating 2 new proline residues (K986P, V987P) between the first heptad repeat (HR1)

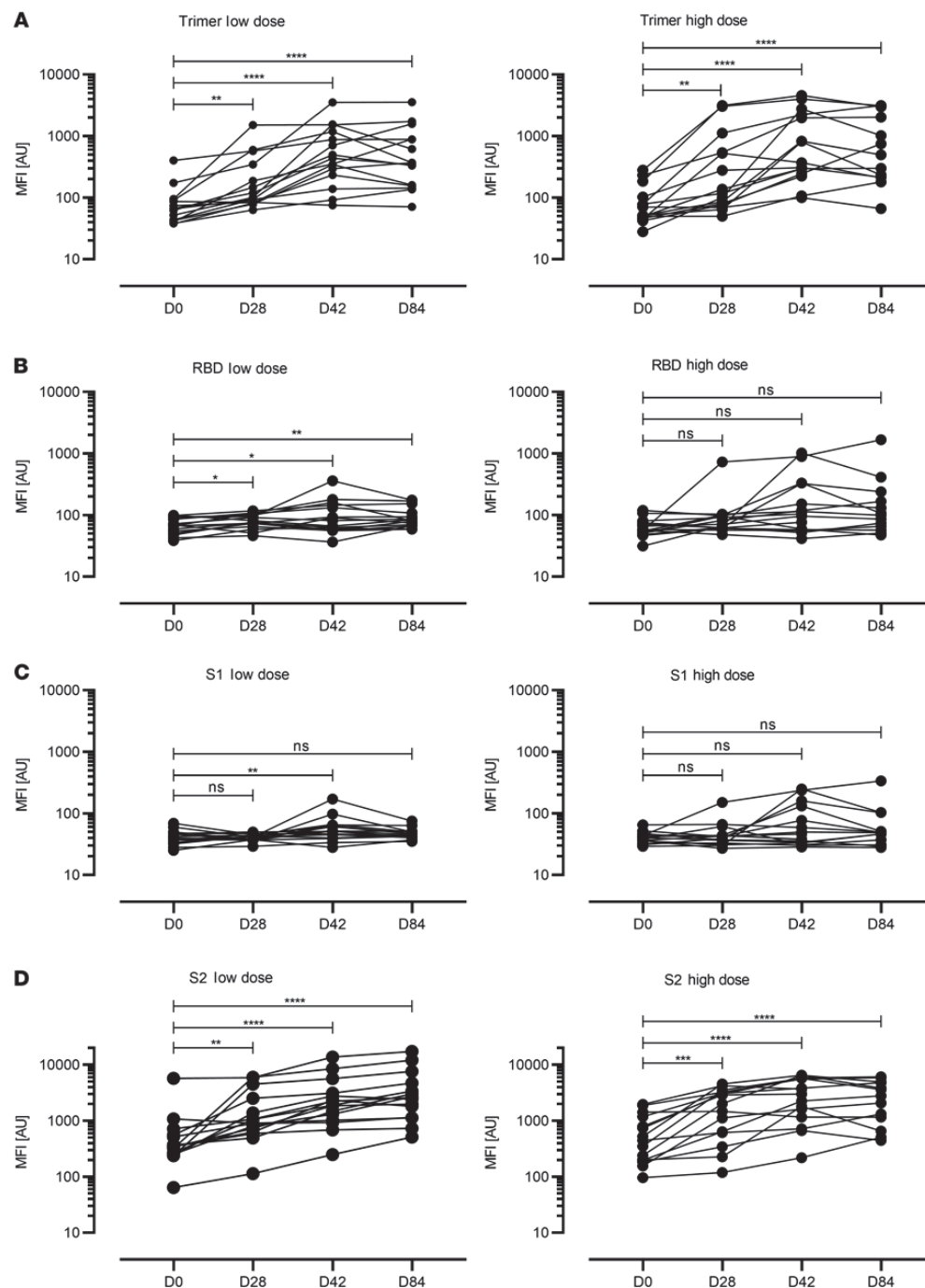


Figure 1. SARS-CoV-2-specific antibody responses in human volunteers vaccinated with MVA-S. Scatterplots represent data from individual participants. Humoral immunity against the SARS-CoV-2 spike protein domains were characterized using a multiplex bead array. Antibody reactivity was measured against (A) the full spike protein expressed as a trimeric antigen (S), (B) the receptor binding domain of the spike protein (RBD), (C) the S1 domain (S1), and (D) the S2 domain (S2). Antibody levels were quantified at baseline (BL), before vaccine boost (D28), 2 weeks after vaccine boost (D42), and 8 weeks after vaccine boost (D84) in the low- (left panels) and high-dose (right panels) groups. Seroconversion was estimated by comparison to a calibrator sample. Cutoff values: trimer = 1085 MFI, RBD = 640 MFI, S2 = 2 × BL MFI. * $P < 0.05$, ** $P < 0.01$, *** $P < 0.001$, **** $P < 0.0001$ by 1-way ANOVA with Dunnett's multiple comparisons test of log-transformed data.

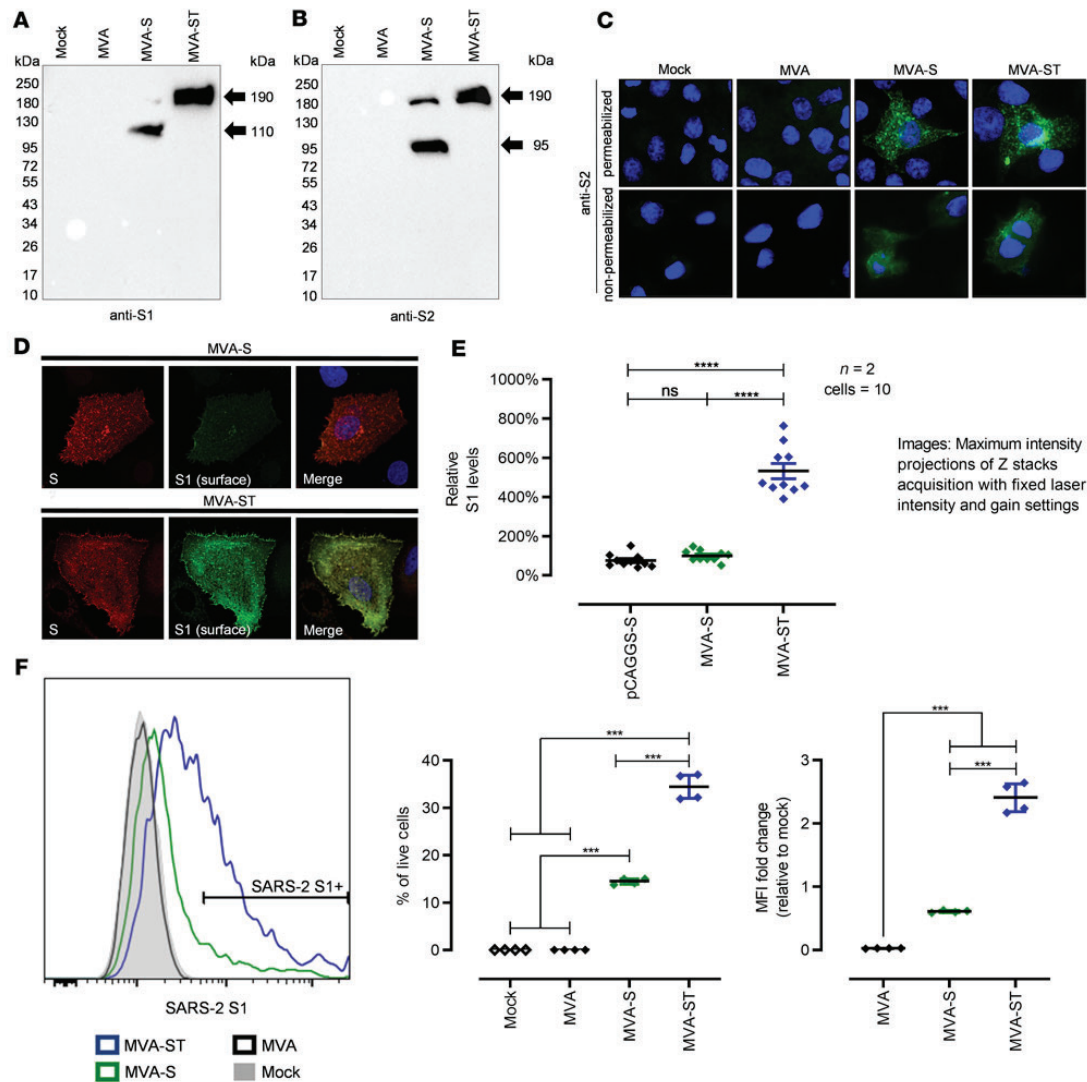


Figure 2. Synthesis and processing of spike glycoprotein (S) in MVA-S- and MVA-ST-infected cells. (A and B) Western blot analysis of S in lysates of MVA-S- and MVA-ST-infected cells. Noninfected (mock) or MVA-infected cells served as controls. DF-1 and Vero cells were infected with an MOI of 10 and collected 24 hours after infection. Polypeptides were resolved by SDS-PAGE and analyzed with a monoclonal antibody against (A) SARS-CoV-2 S1 or (B) SARS-CoV-2 S2. (C) Immunofluorescent staining of S in MVA-, MVA-S-, and MVA-ST-infected Vero cells (MOI = 0.5). Cells were permeabilized or non-permeabilized and probed with mouse monoclonal antibodies against SARS-CoV-2 S protein (S2 domain, green). Cell nuclei were counterstained with DAPI (blue). (D and E) Immunofluorescent single-cell staining of surface S levels. Huh-7 cells were infected with MVA-S, MVA-ST, or transfected with plasmids encoding unmodified S (pCAGGS-S). (D) At 18 hours after infection, cell-surface S was labeled with anti-S1 monoclonal antibody and total S was labeled with anti-S2 antibody after fixation and permeabilization. Nuclei were counterstained with DAPI. Original magnification, $\times 100$ (C) and $\times 630$ (D). (E) For quantification, fluorescence intensity of surface S was measured and set in relation to that of total S. In total, 10 cells from 2 independent experiments were analyzed for each setup. (F) Flow cytometric analysis of surface S1 expression by MVA-S- or MVA-ST-infected A549 cells. Graphs show the percentage of S1⁺ cells ($n = 4$) and the fold change in S1 median fluorescence intensity (MFI) relative to the mock control ($n = 4$). *** $P < 0.001$, **** $P < 0.0001$ by 1-way ANOVA with Tukey's multiple comparisons test.

and the central helix of the S2 protein (Supplemental Figure 1, A-C; supplemental material available online with this article; <https://doi.org/10.1172/JCI159895DS1>). The recombinant MVA-ST was clonally isolated in plaque purifications in DF-1 cell cultures and

PCR analyses of the viral genome confirmed the genetic integrity and genetic stability of the vector virus (Supplemental Figure 1, D-G). The suitability of MVA-ST for production at industrial scale under conditions of biosafety level 1 was indicated by data from

growth testing in DF-1 producer cells and in cell lines of human origin (Supplemental Figure 2).

Synthesis of the stabilized ST antigen in MVA-ST-infected cell cultures was demonstrated by Western blot analysis, which confirmed the absence of proteolytic cleavage. A single protein band with a molecular mass of approximately 190 kDa was detected in cells infected with MVA-ST using either S1- or S2-specific monoclonal antibodies (Figure 2, A and B). In contrast, lysates from cells infected with the original recombinant MVA-S contained additional protein bands that migrated at molecular masses corresponding to the sizes of the S1 and S2 cleavage products.

Next, we used immunofluorescent staining with S2-specific primary antibodies to assess cell surface expression and trafficking of the different S proteins in Vero cells infected with MVA-ST compared to cells infected with MVA-S (Figure 2C). Similar to our findings with MVA-S, we observed a reticular pattern with juxtanuclear accumulation of the stabilized S protein in permeabilized and MVA-ST-infected cells. Immunostaining without cell permeabilization specifically revealed abundant S2 protein on the cell surface of either MVA-S- or MVA-ST-infected cells.

To comparatively analyze and quantify predicted cellular localization of the S1 and S2 subunits by confocal microscopy, we infected Huh-7 cells with either MVA-S or MVA-ST (Figure 2, D and E). Infected cells were fixed 18 hours after infection and S located at the cell surface was labeled prior to fixation using an anti-S1 human-derived monoclonal antibody (18). Subsequently, cells were fixed, permeabilized, and total S was labeled using an anti-S2 antibody from mouse and secondary Alexa Fluor 488- and 594-conjugated antibodies (18). As anticipated, we saw a similar staining pattern for both recombinant viruses using S2-specific antibodies, indicating comparable amounts of S2 protein on the cell surface of both MVA-S- and MVA-ST-infected cells.

In MVA-ST-infected cells, the S1-specific immunostaining also revealed ample amounts of S1 protein on the cell surface. Surprisingly, and in contrast, we observed significantly lower levels of S1-specific cell surface staining in MVA-S-infected cells (Figure 2, D and E). Likewise, analyzing infected cells for S1 cell surface expression using immunostaining and FACS analysis detected significantly lower levels of S1 cell surface expression in cells infected with MVA-S (14.4%), in contrast to S1-specific staining in 34.5% of viable human A549 cells infected with MVA-ST. This was also confirmed when analyzing the fold change in S1 MFI relative to mock infection in the live cell compartment (0.61-fold change for MVA-S, 2.40-fold change for MVA-ST; Figure 2F).

MVA-ST-induced S-specific immune responses in BALB/c mice. To comparatively assess vaccine safety and immunogenicity, we vaccinated BALB/c mice intramuscularly with 1×10^8 PFU of MVA-S or MVA-ST using a 21-day interval prime-boost schedule (Supplemental Figure 3).

The induction of S-binding antibodies was analyzed by ELISA using different SARS-CoV-2 S polypeptides as target antigens (full-length S, RBD, S1, or S2) (Figure 3, A–D). Initially, we confirmed seroconversion by ELISA using wells coated with purified trimeric S protein. Seroconversion was detected in 100% of vaccinated mice after prime-boost vaccination, with a mean titer of 1:1125 for MVA-S and 1:1200 for MVA-ST (Figure 3A). All MVA-ST-immunized mice already mounted antibodies binding to RBD on day 18, with a mean

titer of 1:1500 (Figure 3B). Only 16.7% ($n = 1/6$) of MVA-S-vaccinated animals produced measurable amounts of RBD-specific antibodies, with a titer of 1:300. Boost vaccination on day 21 resulted in lower levels of RBD-specific antibodies following MVA-S vaccination (mean titer of 1:1850) than the significantly increased levels induced by MVA-ST vaccination (mean titer of 1:30,375).

In S1 ELISAs, no or only low-level responses were detected in sera of vaccinated mice after prime immunization (Figure 3C). We found that 37.5% ($n = 3/8$) of mice vaccinated with MVA-ST mounted S1-binding antibodies with a mean titer of 1:100. However, substantial levels of S1-binding antibodies developed after the boost vaccination with MVA-ST, with a mean titer of 1:6075; in contrast, mice that received MVA-S developed a significantly lower titer of 1:337. Marginal levels of antibodies binding to S2 protein were measured after a single vaccination with MVA-S or MVA-ST (Figure 3D). Boost vaccination significantly increased the amounts of S2-binding antibodies for both candidate vaccines, with a mean titer of 1:728 for MVA-ST-vaccinated and 1:1350 for MVA-S-vaccinated animals.

In addition, we analyzed antibody binding capacity against the Beta variant of SARS-CoV-2 using ELISA plates coated with synthetic Beta SARS-CoV-2 S protein (Figure 3E). A single MVA-S vaccination did not result in obvious levels of binding antibodies, whereas mice vaccinated with MVA-ST mounted detectable levels of binding antibodies, with a mean titer of 1:143. After boost vaccination, MVA-S-vaccinated mice did show activation of antibodies specific for the Beta variant S protein, with a mean titer of 1:116. However, MVA-ST booster immunization significantly increased these antibody levels, with a mean titer of 1:3825.

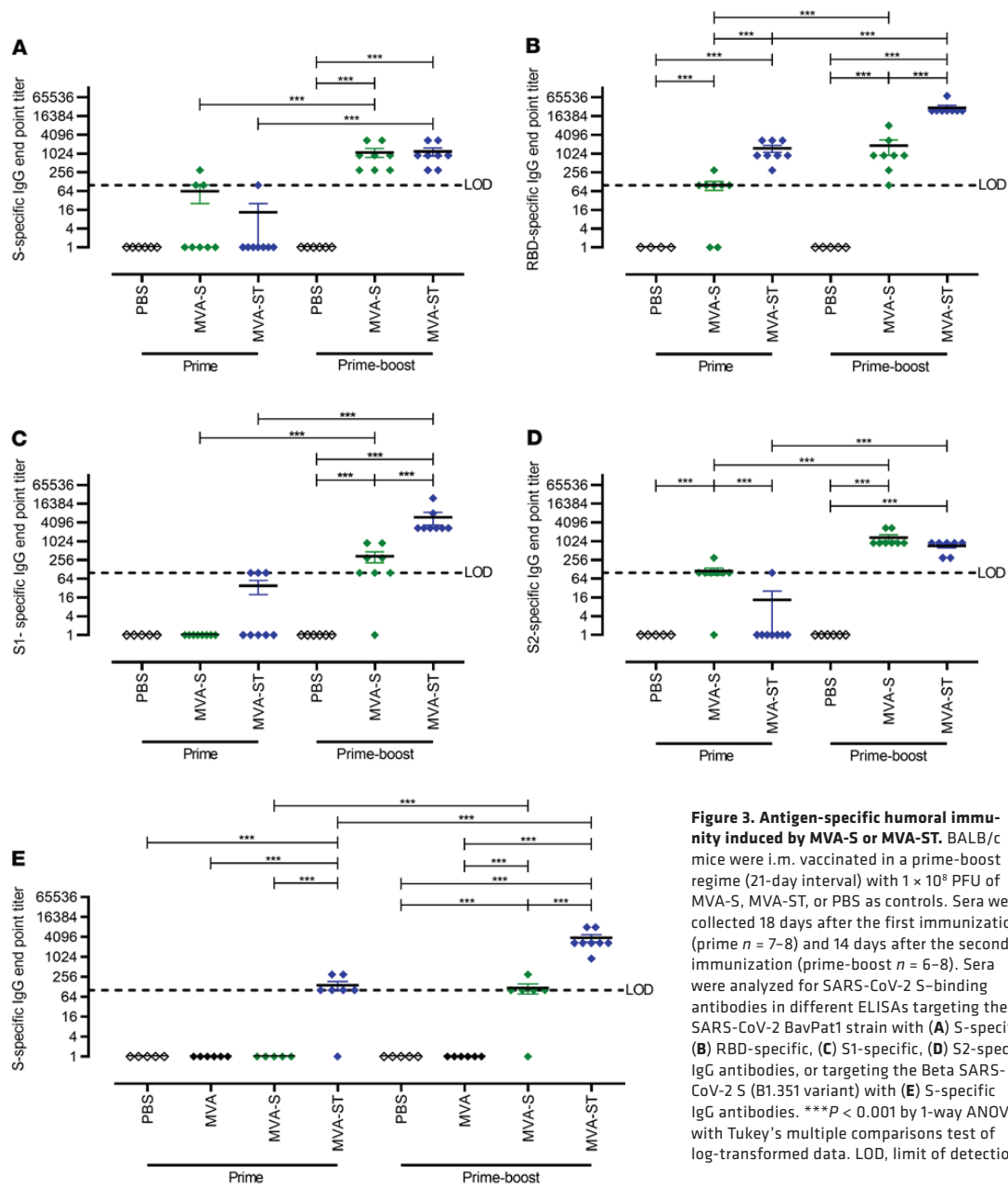
To evaluate neutralizing antibodies, we performed the 50% plaque reduction neutralization test (PRNT₅₀) as well as the virus neutralization titer (VNT₁₀₀) assay (Figure 4). Immunization with MVA-S induced low levels of neutralizing antibodies against the SARS-CoV-2 isolate Germany/BavPat1/2020 (henceforth called SARS-CoV-2 BavPat1), reaching a mean titer of 1:3437 in the more sensitive PRNT₅₀ and a mean titer of 1:81 in the more demanding VNT₁₀₀ assay (Figure 4, A and B). In comparison, MVA-ST prime-boost vaccination resulted in significantly better SARS-CoV-2 BavPat1 neutralization, with mean titers of 1:6400 in PRNT₅₀ and 1:848 in the VNT₁₀₀ assay (Figure 4, A and B).

Our candidate vaccines are based on the S protein sequence of the SARS-CoV-2 isolate Wuhan HU-1 from 2020 (15). Thus, we used the mouse sera generated above to evaluate the capacity of the antibody responses to neutralize infections with SARS-CoV-2 variants Alpha (B.1.1.7), Beta (B.1.351), and Zeta (P.2) using the VNT₁₀₀ assay (Figure 4C). Similar to previous findings using this assay, MVA-S vaccination resulted in low levels of detectable neutralizing antibodies against the original SARS-CoV-2 BavPat1 (geometric mean titer 31). In accordance with these results, only a few mice mounted neutralizing responses against the SARS-CoV-2 variants Alpha (2/6, mean titer of 1:46), Beta (1/6, mean titer of 1:8), and Zeta (1/6, mean titer 1:31). In sharp contrast, MVA-ST vaccination elicited robust levels of circulating antibodies that neutralized the original SARS-CoV-2 BavPat1 (6/6, mean titer of 1:1874) and the variant viruses Alpha (6/6, mean titer of 1:1761), Beta (6/6, mean titer of 1:1002), and Zeta (6/6, mean titer of 1:824).

To characterize the neutralizing capacities against the more recent SARS-CoV-2 variants Delta (B.1.617.2) and the highly

RESEARCH ARTICLE

The Journal of Clinical Investigation



contagious Omicron (B.1.1.529), we again performed prime-boost vaccination in BALB/c mice as above (Figure 4, D and E). Control mice that had been either mock or nonrecombinant MVA vaccinated did not mount any neutralizing antibodies against Delta or Omicron. MVA-S-vaccinated mice mounted low levels of Delta-neutralizing antibodies, with a mean titer of 1:90. In contrast, MVA-ST vaccination resulted in robust activation of Delta-neutralizing antibodies, with a mean titer of 1:275. When analyzing neutralization against Omicron, MVA-S-vaccinated

mice showed low titers resulting in a mean titer of 1:8, compared with MVA-ST-vaccinated mice, with a mean of 1:184. To ensure comparability with the BALB/c vaccination experiments above, PRNT₅₀ against the BavPat1 isolate was performed (Supplemental Figure 4). Altogether, these results indicate that immunization with MVA-ST induces a superior anti-SARS-CoV-2-S humoral response resulting in the generation of cross-neutralizing anti-SARS-CoV-2 S antibodies against all the variants tested so far: Alpha, Beta, Zeta, Delta, and Omicron.

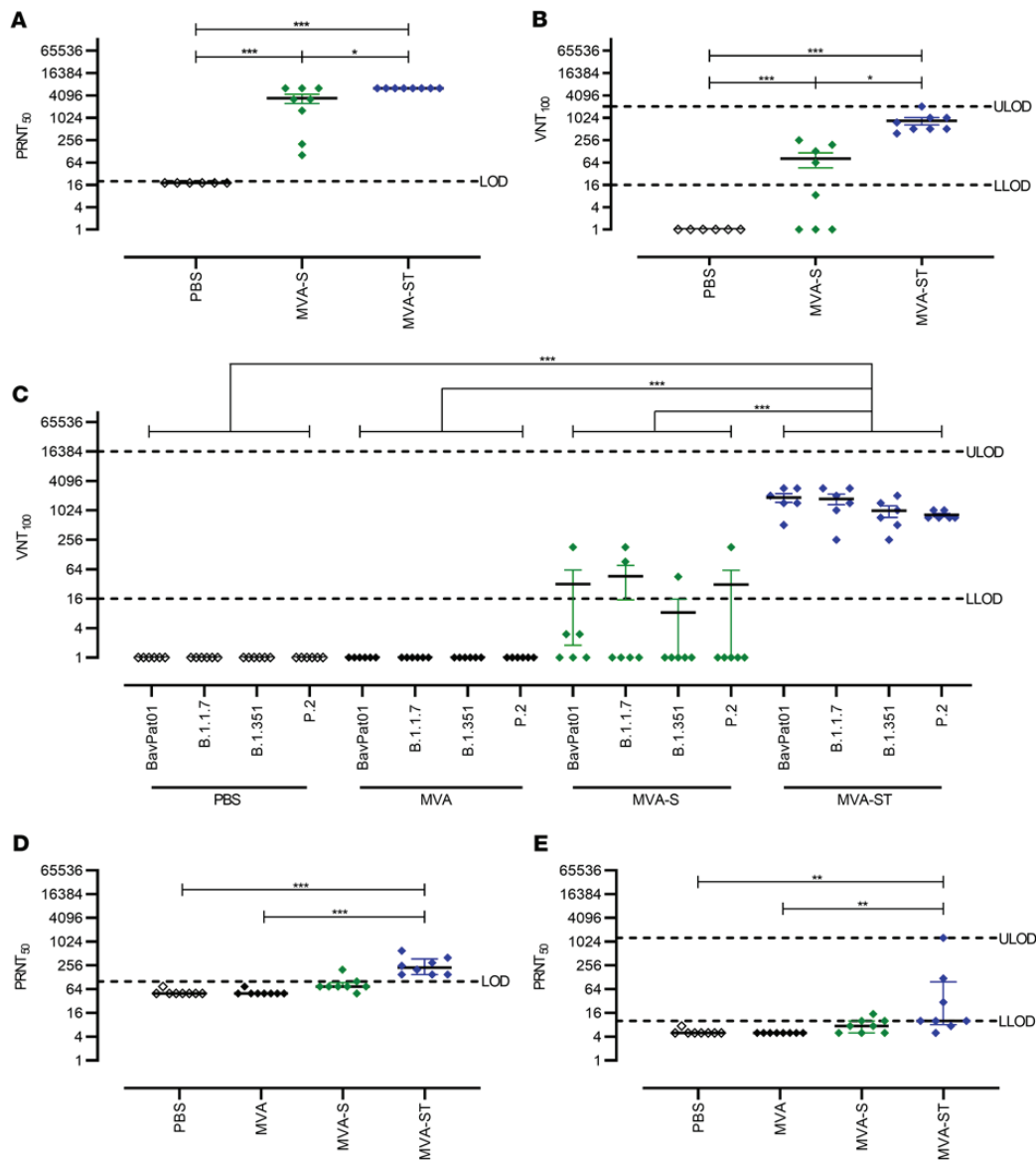


Figure 4. Virus-neutralizing antibody responses to SARS-CoV-2 BavPat1, Alpha, Beta, Zeta, Delta, and Omicron variants in vaccinated BALB/c mice. SARS-CoV-2 neutralization titers measured by the plaque reduction assay ($PRNT_{50}$) and virus neutralization test (VNT_{100}) from BALB/c mice vaccinated with PBS, MVA, MVA-S, or MVA-ST. (A) $PRNT_{50}$ and (B) VNT_{100} assays using SARS-CoV-2 BavPat1. (C) VNT_{100} against SARS-CoV-2 BavPat1, Alpha, Beta, and Zeta variants. $PRNT_{50}$ assay using SARS-CoV-2 (D) Delta and (E) Omicron variants. * $P < 0.05$, ** $P < 0.01$, *** $P < 0.001$ by 1-way ANOVA with Tukey's multiple comparisons test of log-transformed data (A–C) and Kruskal-Wallis test with Dunn's multiple comparisons test (D and E). LOD, limit of detection; ULOD and LLOD, upper and lower LOD.

To characterize the activation of SARS-CoV-2-specific cellular immunity following prime-boost vaccination in BALB/c mice, we monitored S1 epitope-specific $CD8^+$ T cells using IFN- γ ELISPOT assays and FACS analysis (Figure 5). Boost vaccinations with MVA-S activated substantial numbers of $S_{268-276}$ epitope-specific $CD8^+$ T cells, with a mean number of 1571 IFN- γ^+ spot-forming cells (SFC) in

1×10^6 splenocytes (Figure 5A). Comparable results were obtained for boost vaccinations with MVA-ST (mean of 1349 IFN- γ^+ SFC; Figure 5A). In agreement with these data, FACS analysis of T cells stimulated in vitro with peptide $S_{268-276}$ and stained for intracellular IFN- γ showed robust frequencies of IFN- γ^+ $CD8^+$ T cells in splenocytes from mice immunized with MVA-S (mean of 1.51%) or MVA-ST (mean

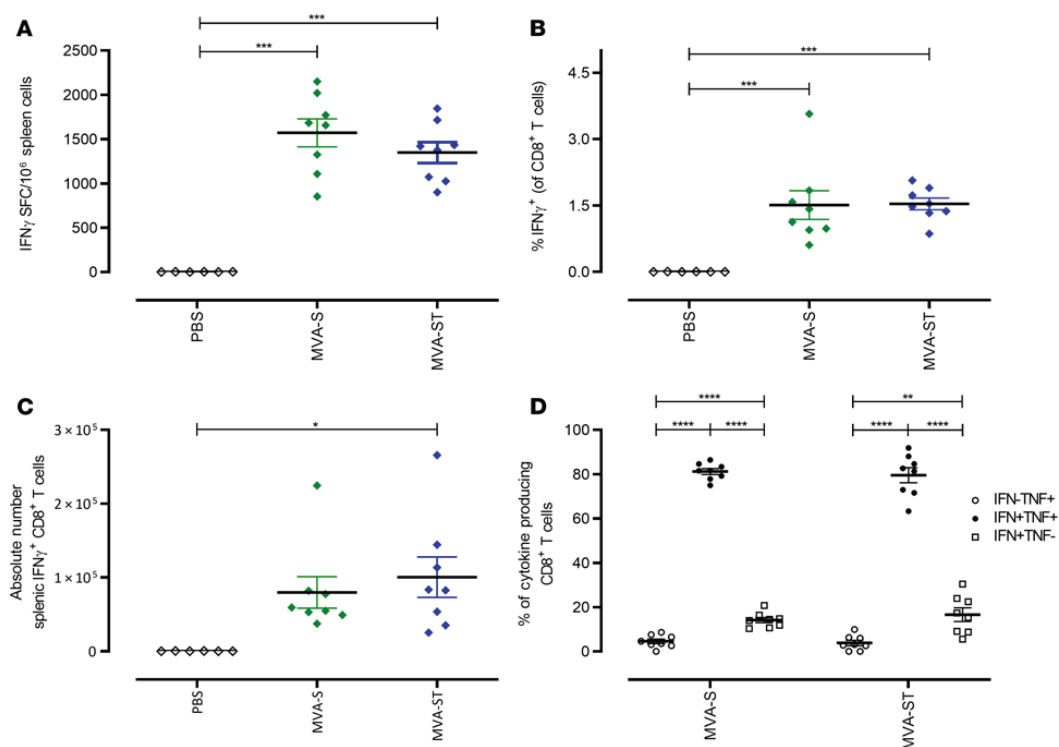


Figure 5. Activation of S-specific CD8⁺ T cells after prime-boost immunization with MVA-S or MVA-ST. Groups of BALB/c mice ($n = 4-8$) were immunized i.m. twice with 1×10^8 PFU MVA-S, MVA-ST, or PBS as negative controls. (A–D) Splenocytes were collected and prepared on day 14 after boost immunization and stimulated with the H2-Kd-restricted peptide S₂₆₈₋₂₇₆ (S1; GYLQPRFL) and tested using ELISPOT assays and ICS FACS analyses. (A) IFN- γ SFC measured by ELISPOT assays. (B and C) IFN- γ -producing CD8⁺ T cells measured by FACS analysis. (D) IFN- γ - and TNF- α -producing CD8⁺ T cells measured by FACS analysis. * $P < 0.05$, ** $P < 0.01$, *** $P < 0.001$, **** $P < 0.0001$ by 1-way ANOVA with Tukey's multiple comparisons test.

of 1.53%) compared with mock-vaccinated control mice (mean of 0.01%) (Figure 5, B and C). Substantial numbers of the activated IFN- γ ⁺CD8⁺ T cells also coexpressed TNF- α (81% for MVA-S and 79% for MVA-ST; Figure 5D). Of note, mice immunized with MVA-S or MVA-ST mounted similar levels of SARS-CoV-2-S-specific CD8⁺ T cells and MVA-specific CD8⁺ T cells (Supplemental Figure 5).

Protective capacity of MVA-S and MVA-ST upon SARS-CoV-2 respiratory challenge in Syrian hamsters. To further investigate the impact of prime-boost immunization against SARS-CoV-2-induced disease, we used Syrian hamsters as a well-established preclinical model for efficacy testing (Figures 6 and 7). Two cohorts of hamsters were vaccinated within a 21-day interval twice intramuscularly with 1×10^8 PFU candidate vaccine in each case, comparing MVA and MVA-S and then MVA and MVA-ST. Safety and immunogenicity were analyzed as established before (Supplemental Figure 6). SARS-CoV-2-binding antibodies were analyzed by different ELISAs specific for trimeric S protein or S1 subunit antigen. Immunizations with nonrecombinant vector elicited no detectable S-specific antibodies in control hamsters (MVA; Figure 6A). However, antibodies specific for trimeric S proteins could be detected in all hamsters vaccinated with MVA-S (mean titer 1:700) or MVA-ST (mean titer 1:728) already after single vaccination. Boost vacci-

nations further increased the levels, resulting in comparable titers of 1:2250 for MVA-S and 1:1157 for MVA-ST vaccination.

Underlining the mouse model results, we observed a different pattern for vaccine-induced S1-binding antibodies. Only 37.5% ($n = 3/8$) of MVA-S-vaccinated hamsters mounted S1-binding antibodies after the first immunization (mean titer of 1:38), while boost vaccinations elicited low-level seroconversion in 87.5% ($n = 7/8$) of MVA-S-vaccinated animals (mean titer of 1:112). In sharp contrast, prime MVA-ST vaccination induced high levels of S1-binding antibodies (100% seroconversion, mean titer of 1:2442), and boost vaccination on day 21 further increased these levels to a mean titer of 1:4242 (Figure 6B).

Similarly, after prime immunization we measured low levels of SARS-CoV-2 BavPat1-neutralizing antibodies in sera from 87.5% ($n = 7/8$) of MVA-S-vaccinated hamsters (mean titer of 1:65; Figure 6C), whereas all hamsters immunized with MVA-ST mounted readily detectable neutralizing antibodies (100% seroconversion), with an average titer of 1:321 PRNT₅₀ at 3 weeks after priming (Figure 6C).

Compared with SARS-CoV-2 BavPat1, reduced neutralizing activity against Delta and Omicron were measured. MVA-S vaccination resulted in marginal antibody titers neutralizing Delta (mean titer of 1:71; Figure 6D). No detectable titers against Omicron were

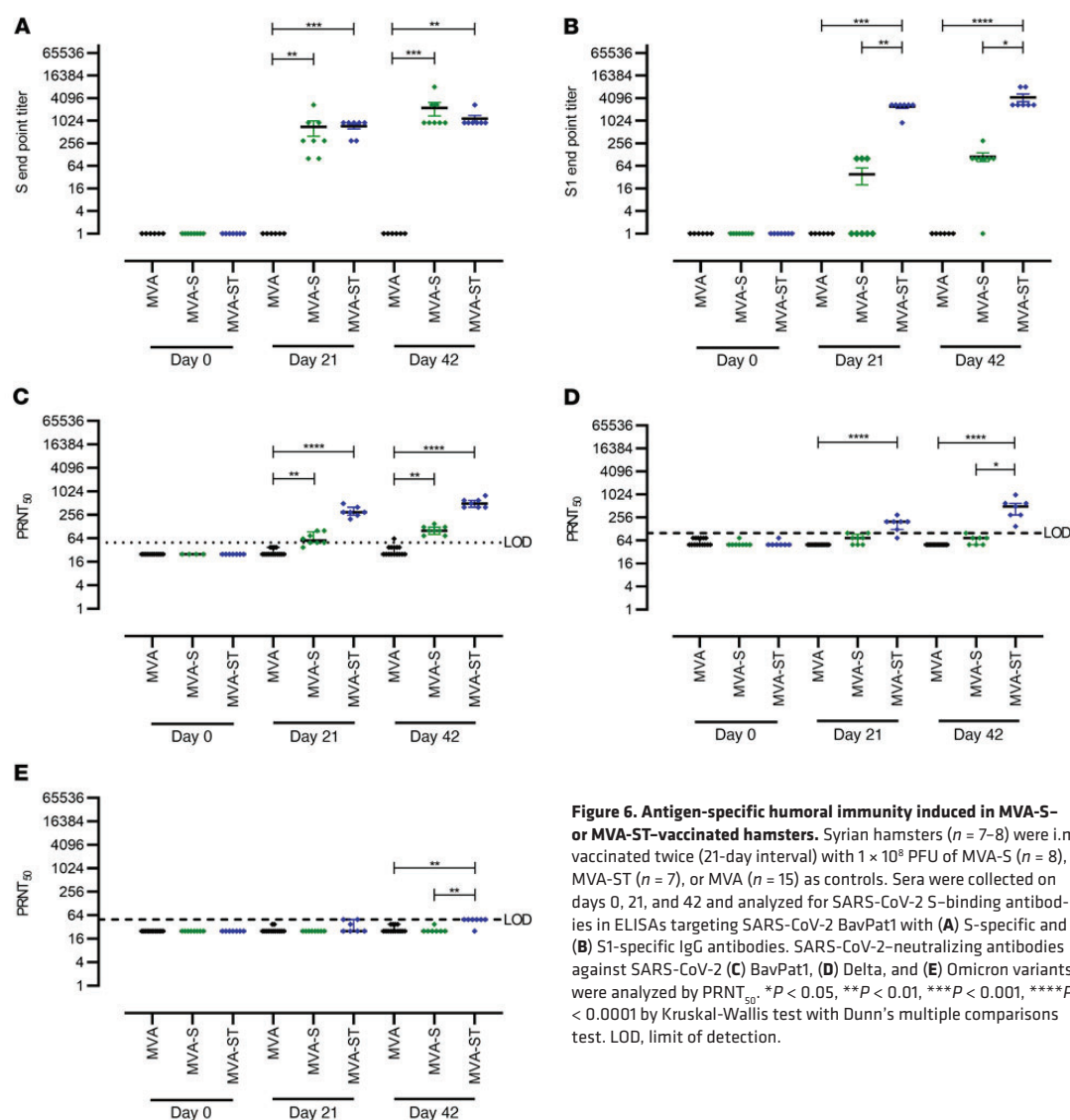


Figure 6. Antigen-specific humoral immunity induced in MVA-S- or MVA-ST-vaccinated hamsters. Syrian hamsters ($n = 7-8$) were i.m. vaccinated twice (21-day interval) with 1×10^8 PFU of MVA-S ($n = 8$), MVA-ST ($n = 7$), or MVA ($n = 15$) as controls. Sera were collected on days 0, 21, and 42 and analyzed for SARS-CoV-2 S-binding antibodies in ELISAs targeting SARS-CoV-2 BavPat1 with (A) S-specific and (B) S1-specific IgG antibodies. SARS-CoV-2-neutralizing antibodies against SARS-CoV-2 (C) BavPat1, (D) Delta, and (E) Omicron variants were analyzed by PRNT₅₀. * $P < 0.05$, ** $P < 0.01$, *** $P < 0.001$, **** $P < 0.0001$ by Kruskal-Wallis test with Dunn's multiple comparisons test. LOD, limit of detection.

measured after prime MVA-S vaccination (Figure 6E). Hamsters that had been vaccinated with MVA-ST mounted a mean titer of 1:185.7 against Delta (Figure 6D) and a titer below the detection limit against Omicron (mean titer of 1:33.9; Figure 6E). After the boost vaccination, sera from all MVA-S-vaccinated hamsters (100% seroconversion) revealed low neutralizing activity, with minor titers of approximately 1:100 PRNT₅₀ against SARS-CoV-2 BavPat1 (Figure 6C). One out of 7 animals had confirmed seroconversion against Delta, exhibiting a mean titer of 1:67 after boost vaccination (Figure 6D). In MVA-S-vaccinated animals, no seroconversion was detected against Omicron (Figure 6E). In contrast, in all sera from hamsters vaccinated with MVA-ST we detected increased amounts of SARS-CoV-2-neutralizing antibodies against SARS-CoV-2 BavPat1 after the boost immunization, with a mean titer of 1:529 PRNT₅₀

(Figure 6C). For Delta, a mean titer of 1:500 was measured in these vaccinated animals (100% seroconversion; Figure 6D), whereas no obvious titers of Omicron-neutralizing antibodies were detected in MVA-ST-vaccinated animals (mean titer of 1:46; Figure 6E).

Four weeks after the boost immunization, the animals were intranasally infected with 1×10^4 50% tissue culture infectious dose (TCID₅₀) SARS-CoV-2 BavPat1 (Figure 7). Starting on day 3, MVA-vaccinated control hamsters demonstrated reduced body weights, and at 6 days after infection all animals had lost approximately 10% of their initial body weight. No body weight loss could be detected for hamsters immunized with MVA-S or MVA-ST (Figure 7A). Control animals also showed characteristic clinical symptoms associated with SARS-CoV-2 respiratory tract infection, including labored breathing, reduced activity, and scruffy fur.

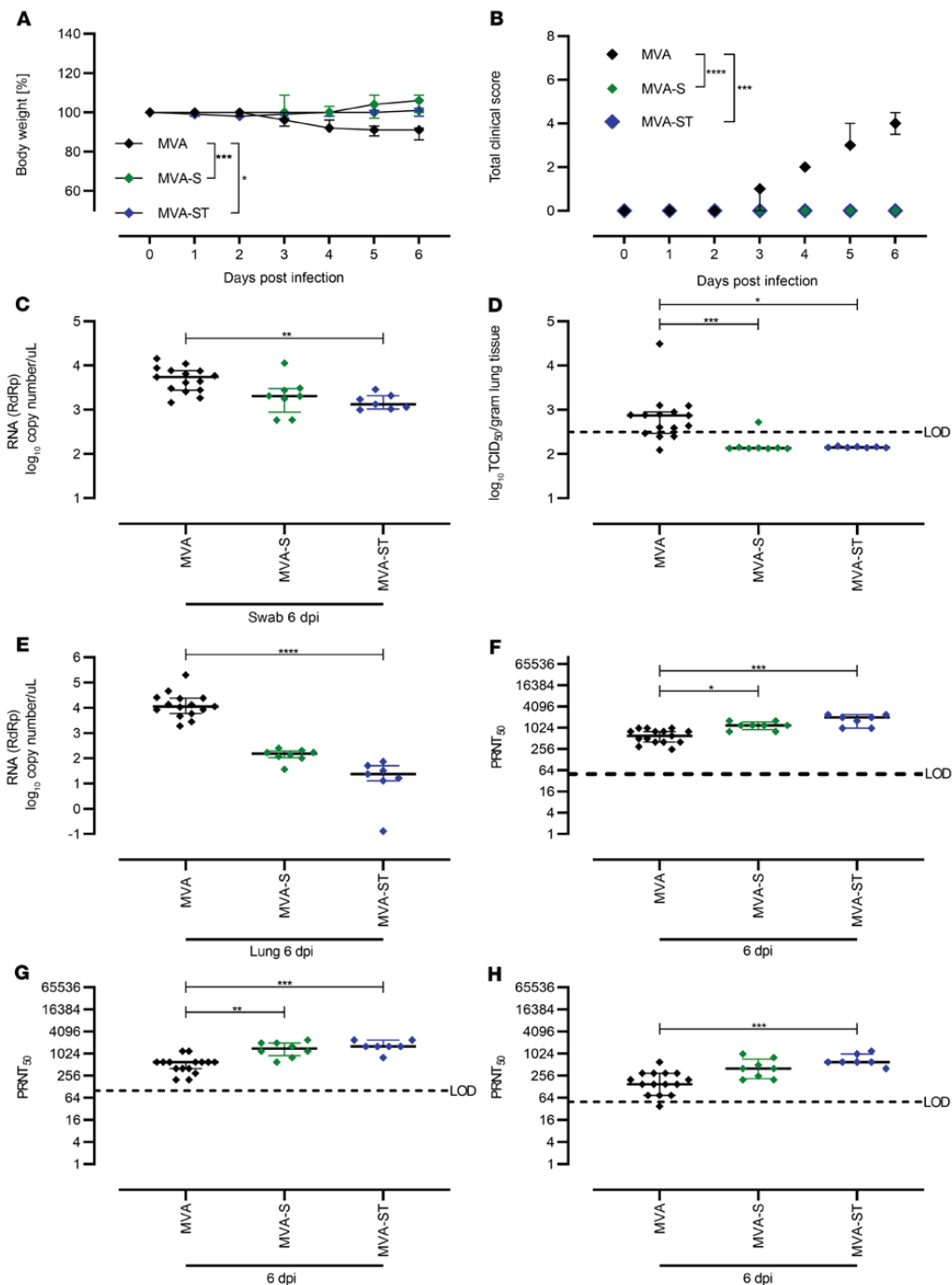


Figure 7. Protective capacity of MVA-S or MVA-ST immunization against SARS-CoV-2 BavPat1 infection in Syrian hamsters. Syrian hamsters vaccinated with MVA ($n = 15$) control, MVA-S ($n = 8$), or MVA-ST ($n = 7$) were i.n. challenged with 1×10^4 TCID₅₀ SARS-CoV-2 BavPat1. **(A)** Body weight was monitored daily and **(B)** spontaneous behavior and general condition were evaluated by clinical scores. **(C)** Oropharyngeal swabs on day 6 after challenge infection were analyzed for SARS-CoV-2 gRNA copies. **(D)** and **(E)** Lungs were harvested and analyzed for **(D)** infectious SARS-CoV-2 by TCID₅₀/gram lung tissue, and **(E)** SARS-CoV-2 gRNA copies. Sera were prepared on day 6 after challenge and analyzed for SARS-CoV-2 **(F)** BavPat1, **(G)** Delta, and **(H)** Omicron variant-neutralizing antibodies by PRNT₅₀. * $P < 0.05$, ** $P < 0.01$, *** $P < 0.001$, **** $P < 0.0001$ by Kruskal-Wallis test with Dunn's multiple comparisons test **(C-H)** of AUC **(A)** and **(B)**. LOD, limit of detection.

No MVA-S- or MVA-ST-vaccinated animals showed any signs of clinical disease (Figure 7B).

To evaluate viral loads and pathological changes in lung tissues, we euthanized all animals at 6 days after infection. Blood and swab samples were taken at necropsy, and lungs were harvested for further analysis. Substantial amounts of viral RNA were detected in oropharyngeal swabs of control animals (mean of 7.7×10^3 RNA copy numbers/ μ L; Figure 7C). Swab samples from hamsters vaccinated with MVA-S contained marginally reduced levels of viral RNA (on average 3×10^3 RNA copy numbers/ μ L), whereas swabs from animals vaccinated with MVA-ST contained significantly reduced levels of SARS-CoV-2 RNA (mean of 1.6×10^3 RNA copy numbers/ μ L; Figure 7C).

Correspondingly, lung tissues from control hamsters harbored infectious SARS-CoV-2 (mean of 2.9×10^3 TCID₅₀/gram lung tissue; Figure 7D), whereas no infectious SARS-CoV-2 was detected in the lungs of vaccinated hamsters (with the exception of tissue from 1 MVA-S-vaccinated animal containing 5.6×10^2 TCID₅₀/gram lung tissue). These data were confirmed by real-time RT-PCR analysis of viral RNA loads. In lung tissues from both MVA-S- and MVA-ST-immunized animals, we found lower levels of SARS-CoV-2 RNA compared with control hamsters ($<3 \times 10^1$ genome equivalents/ng total RNA; Figure 7E).

Only after SARS-CoV-2 BavPat1 infection did we detect SARS-CoV-2-binding antibodies in control (MVA) hamsters, with a mean titer of 1:16,883 for S-specific antibodies and 1:5600 for S1-binding antibodies (Supplemental Figure 7, A and B). Thus, although all the control hamsters became moribund, we observed detectable titers of SARS-CoV-2 BavPat1-neutralizing antibodies that averaged to 1:632 PRNT₅₀ after challenge infection (Figure 7F). Against Delta, an average mean titer of 1:1013 was measured in control MVA-vaccinated hamsters (Figure 7G). Lower titers reaching a mean of 1:204 were present against Omicron detected by PRNT₅₀ (Figure 7H). In line with data from viral load and clinical disease outcome, we detected markedly higher levels of SARS-CoV-2 S-specific antibodies in sera from immunized hamsters. After challenge, we measured substantial levels of S-binding antibodies, with a mean titer of 1:38,185 or 1:50,194 after MVA-S or MVA-ST immunization (Supplemental Figure 7B). S1-binding antibodies in MVA-S-vaccinated hamsters reached a mean titer of 1:23,528; MVA-ST-vaccinated hamsters had a higher mean titer of 1:72,900 (Supplemental Figure 7A). MVA-S vaccination resulted in SARS-CoV-2 BavPat1-neutralizing activities with an average PRNT₅₀ titer of 1:1200, compared with the MVA-ST mean titer of 1:1771 (Figure 7F). In MVA-S-vaccinated hamsters, a mean titer of 1:1475 against Delta and 1:468 against Omicron were detected (Figure 7, G and H). After MVA-ST vaccination, hamsters mounted mean titers of 1:1714 against Delta and 1:714 against Omicron (Figure 7, G and H).

To evaluate lung pathology in vaccinated and infected animals, we performed histological analysis of hematoxylin and eosin-stained lung sections (Figure 8). Control hamsters (MVA) had large areas of lung consolidation. Alveolar lesions were characterized by the accumulation of neutrophils and mononuclear cells that expanded alveolar septae and filled alveolar lumina (Figure 8, A and E). Inflammation was associated with necrosis of alveolar epithelia, fibrin exudation, and a prominent pneumocyte type II hyperplasia. A mixed inflammatory infiltrate, epithelial degeneration, and hyperplasia were found in bronchi and bronchioli. In addition, animals showed

marked vascular lesions, characterized by endothelial hypertrophy, endothelialitis, mural and perivascular infiltrates, loss of vascular wall integrity, and perivascular edema.

MVA-S-vaccinated hamsters also revealed areas of inflammation and consolidation, although the overall extent of alveolar, bronchial/bronchiolar, and vascular lesions was less than in control animals (Figure 8C). Lungs of MVA-ST-vaccinated hamsters showed negligible or markedly reduced lung pathology (Figure 8G). Almost all the animals in this group demonstrated only mild to moderate inflammatory lesions confined to the airways and some vessels, while alveolar lesions were absent or minimal, affecting less than 1% of the lung lobes. Only 1 animal showed higher lesion scores in the alveolar and vascular compartment, affecting below 25% of the entire lobe.

Semiquantitative scoring of alveolar, airway, and vascular lesions showed a significant reduction in all parameters in animals vaccinated with recombinant MVA vaccines compared with the control group (Figure 8I). Importantly, MVA-ST-vaccinated hamsters showed substantially lower inflammation scores than MVA-S-vaccinated animals. Using immunohistochemistry, SARS-CoV-2 nucleoprotein was detected in the lungs of all control hamsters, but in none of the MVA-S- or MVA-ST-immunized animals (Figure 8, J and K).

MVA-S or MVA-ST vaccination provides protection from lethal SARS-CoV-2 disease outcomes in K18-hACE2 mice. To evaluate immunogenicity and protective efficacy in a lethal animal model, we used K18-hACE2 mice. K18-hACE2 mice are highly susceptible to intranasal SARS-CoV-2 infection characterized by high viral loads in the lungs, severe interstitial pneumonia, and death by day 6 or 8 after inoculation. Mice were vaccinated with MVA, MVA-S, or MVA-ST using an intramuscular prime-boost schedule as above.

As expected, we did not detect SARS-CoV-2 BavPat1-neutralizing antibodies in control mice vaccinated with MVA. Single vaccination with MVA-S or MVA-ST resulted in obvious titers of neutralizing antibodies against SARS-CoV-2 BavPat1, with a mean titer of 1:880 for MVA-S and 1:2880 for MVA-ST. Boost vaccination on day 21 further increased SARS-CoV-2 BavPat1-neutralizing antibodies to a mean titer of 1:660 or 1:3840 in MVA-S- or MVA-ST-vaccinated mice (Figure 9A). However, neutralizing activities against SARS-CoV-2 Delta and Omicron were lower compared with SARS-CoV-2 BavPat1 following MVA-S and MVA-ST vaccination (Figure 9, B and C).

Mice immunized with MVA-S mounted sufficient levels of Delta-neutralizing antibodies after prime or boost application (Figure 9B; mean of 1:208 or 1:575). MVA-ST vaccination resulted in a mean titer of 1:675 after prime and 1:1400 after boost (Figure 9B). For Omicron, no detectable titers of neutralizing antibodies were present in mice after single vaccination with either candidate vaccine. MVA-S boost vaccination again did not result in obvious titers of Omicron-neutralizing antibodies (Figure 9C). Marginal titers of Omicron-neutralizing antibodies were present in sera of mice after boost vaccination with MVA-ST (Figure 9C; mean titer of 1:75).

At 4 weeks after boost vaccinations, mice were intranasally challenged with a lethal dose of 3.6×10^4 TCID₅₀ SARS-CoV-2 BavPat1. Control mice significantly lost weight and showed clinical signs of disease starting on day 3, and all succumbed to infection by day 6, whereas MVA-S- and MVA-ST-vaccinated mice showed no weight loss or clinical disease (Figure 9, D-F). At 4 days after infection, substantial levels of viral RNA shedding were observed from the upper respiratory tract of control vaccinated mice (mean

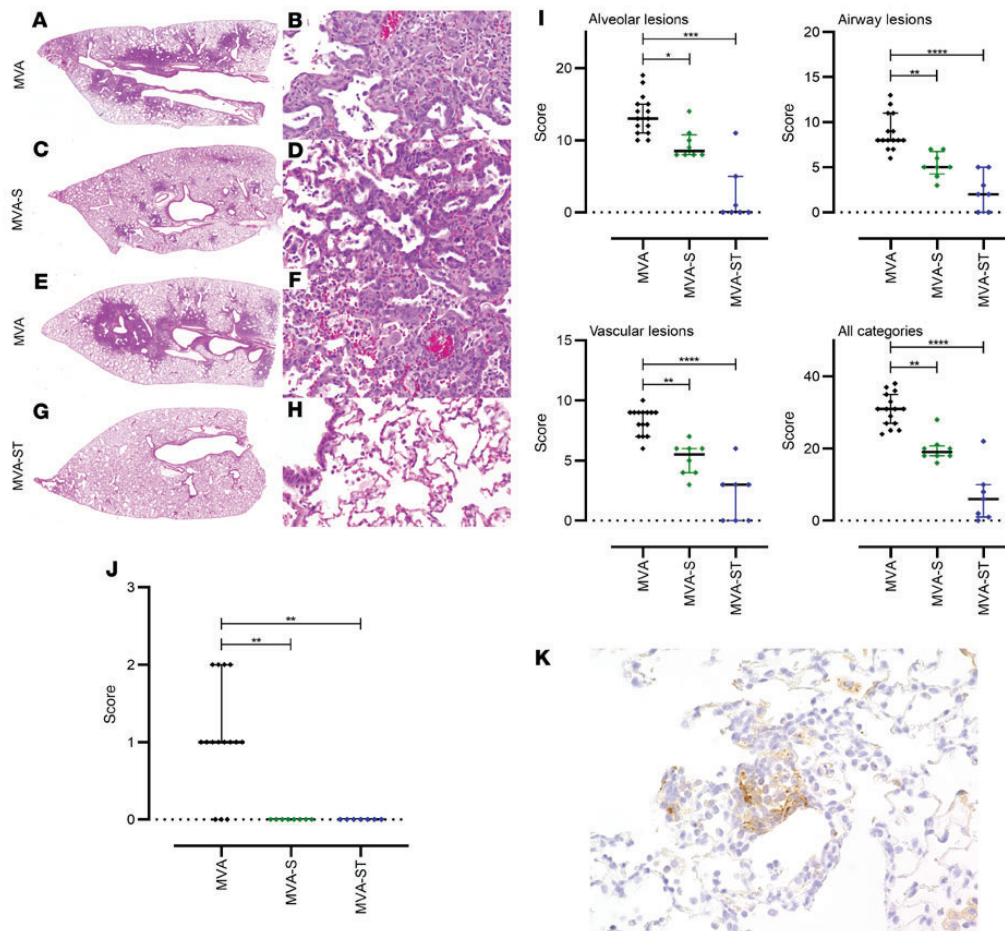


Figure 8. Histopathological lesions in the lungs of SARS-CoV-2 BavPat1-challenged hamsters vaccinated with MVA, MVA-S, or MVA-ST. (A, C, E, and G) Representative overview images of hematoxylin and eosin-stained lung sections and (B, D, F, and H) associated ×100 magnifications. (A and E) Images from MVA control-vaccinated animals show extensive areas of alveolar consolidation (arrowheads). Higher magnification (B and F) reveals markedly thickened alveolar septae, inflammatory infiltrates, and prominent pneumocyte type II hyperplasia with many atypical, large cells (arrowheads) and mitotic figures (arrow). (C and D) MVA-S-vaccinated animals show less lung pathology with multifocal, small foci of alveolar consolidation, which are qualitatively similar to the lesions in controls. (G and H) Most MVA-ST-vaccinated animals show no alveolar lesions. (I) Quantification of histopathological lesions. Vaccination with recombinant MVAs significantly reduces lung lesions compared with control groups. (J and K) Immunohistochemistry for SARS-CoV-2 nucleoprotein in the lungs of hamsters vaccinated with MVA (control), MVA-S, or MVA-ST, challenged with SARS-CoV-2 BavPat1. (J) Semiquantitative scoring of viral antigen amount. No viral antigen was detected in MVA-S- or MVA-ST-vaccinated animals. (K) SARS-CoV-2 antigen (brown signal) is predominantly found in pneumocytes lining alveoli (×100 magnification). Dotted lines mark the zero value. * $P < 0.05$, ** $P < 0.01$, *** $P < 0.001$, **** $P < 0.0001$ by Kruskal-Wallis test with Dunn's multiple comparisons test.

of 6.6×10^3 genome equivalents/ μL). In MVA-S-vaccinated mice, we found low but detectable levels of SARS-CoV-2 RNA shedding in oropharyngeal swabs (mean of 27 genome equivalents/ μL). MVA-ST-vaccinated mice did not produce detectable viral RNA levels in oropharyngeal swabs (Figure 9G).

When monitoring viral loads in the lung and brain homogenates of mice at time of death (day 6 after infection [MVA-vaccinated mice] or 8 days after challenge [MVA-S/MVA-ST-vaccinated animals]), we failed to detect SARS-CoV-2 BavPat1 in the lungs and brains of MVA-S- or MVA-ST-vaccinated mice, but found large amounts of

infectious virus in the organs from control MVA-vaccinated mice (Figure 9H). These data were confirmed by real-time RT-PCR analysis of viral RNA loads. In the control MVA-vaccinated mice, we detected substantial levels of viral RNA, with a mean of 1.19×10^7 or 1.14×10^8 genome equivalents/ng total RNA in lungs or brains. Both MVA-S- and MVA-ST-immunized animals exhibited lower levels of SARS-CoV-2 RNA than control mice in the lungs (a mean of 3.7×10^2 genome equivalents/ng total RNA for MVA-S and 1.31 for MVA-ST; Figure 7I) and in the brains (a mean of 9.73 genome equivalents/ng total RNA for MVA-S and 1.58 for MVA-ST).

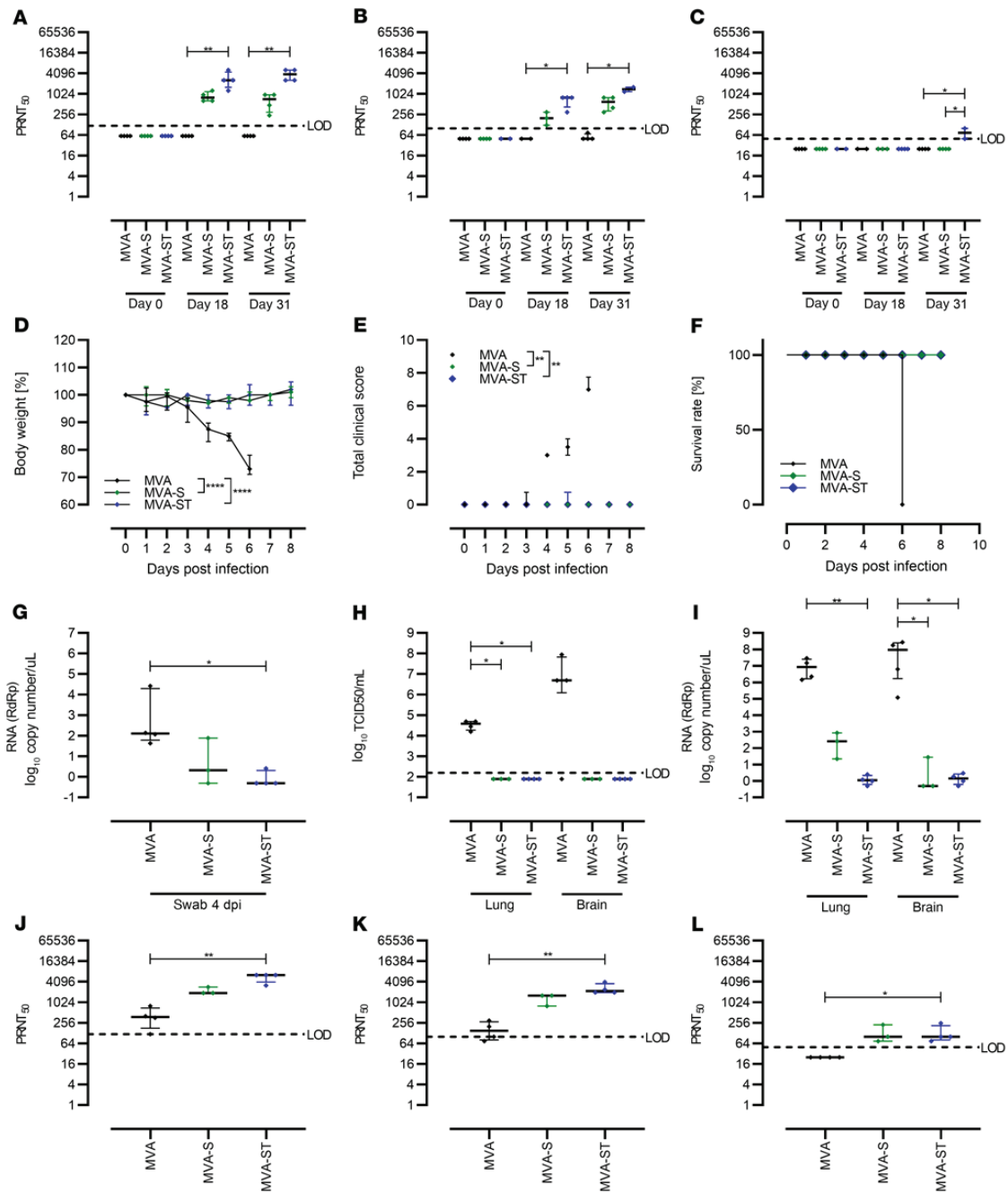


Figure 9. Protective capacity of MVA-S or MVA-ST immunization against SARS-CoV-2 in K18-hACE2 mice. K18-hACE2 mice were i.m. immunized twice with 1×10^8 PFU MVA-S ($n = 4$), MVA-ST ($n = 4$), or MVA ($n = 4$) as a control in a 21-day interval. Sera were collected on days 0, 18, and 31 and analyzed for SARS-CoV-2-neutralizing antibodies against (A) BavPat1, (B) Delta, and (C) Omicron variants by PRNT₅₀. After SARS-CoV-2 BavPat1 challenge infection, (D) body weight was monitored daily, (E) spontaneous behavior and general condition were evaluated in clinical scores, and (F) survival rate was determined retrospectively. (G) Oropharyngeal swabs from 4 days after infection were analyzed for SARS-CoV-2 gRNA copies. RdRp, RNA-dependent RNA polymerase. At the end of the experiment (day 6 for MVA-, day 8 for MVA-S/MVA-ST-vaccinated mice), lungs and brains were harvested and analyzed for (H) amounts of infectious SARS-CoV-2 by TCID₅₀/mL and (I) viral RNA by qRT-PCR. Sera were analyzed for (J) BavPat1, (K) Delta, and (L) Omicron variant-neutralizing antibodies by PRNT₅₀. * $P < 0.05$, ** $P < 0.01$, **** $P < 0.0001$ by Kruskal-Wallis test with Dunn's multiple comparisons test (A-C and G-L) of AUC (E) and 1-way ANOVA with Tukey's multiple comparisons test of AUC (D). LOD, limit of detection.

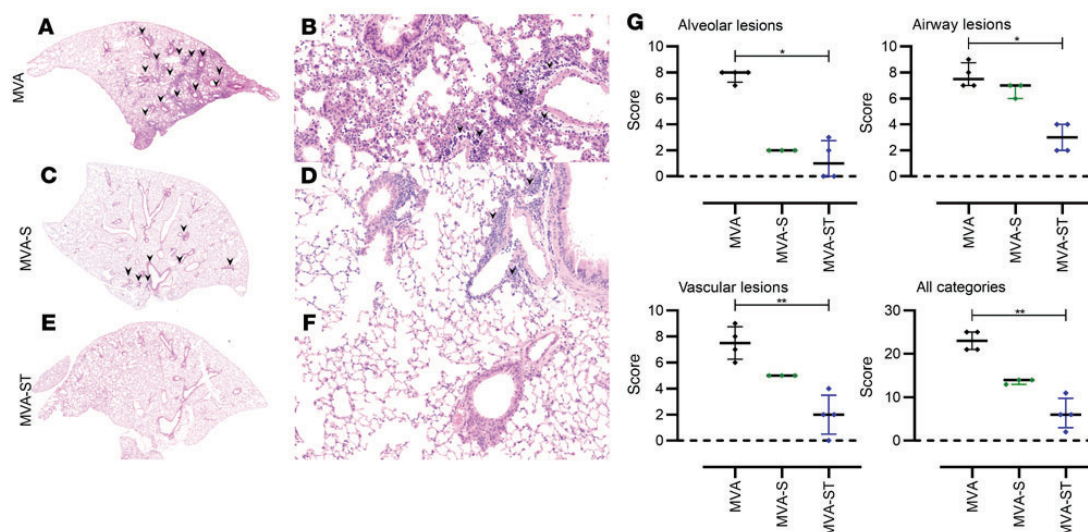


Figure 10. Histopathological lesions in the lungs of K18-hACE2 mice vaccinated with MVA, MVA-S, or MVA-ST, challenged with SARS-CoV-2 BavPat1. (A, C, and E) Representative overview images of hematoxylin and eosin–stained lung sections and (B, D, and F) associated $\times 100$ magnifications. (A) MVA control–vaccinated animals show multifocal areas of immune cell infiltration (arrowheads). (B) Higher magnification reveals markedly thickened alveolar septae, inflammatory infiltrates, and a prominent perivascular immune cell infiltration (arrowheads) as well as multifocal perivascular edema. (C and D) MVA-S–vaccinated animals show less lung pathology with multifocal, small foci of thickened alveolar septae and mild to moderate perivascular infiltrates. (E and F) Most MVA-ST–vaccinated animals show no alveolar and fewer vascular lesions. (G) Quantification of histopathological lesions. Vaccination with recombinant MVAs reduces lung lesions compared with the control MVA group. Dotted lines mark the zero value. * $P < 0.05$, ** $P < 0.01$ by Kruskal–Wallis test with Dunn’s multiple comparisons test.

Neutralizing antibodies against ancestral SARS-CoV-2 BavPat1, SARS-CoV-2 Delta, and Omicron were analyzed at the end of the experiment. Marginal titers of BavPat1- and Delta-neutralizing antibodies were present in sera of control MVA-vaccinated mice after SARS-CoV-2 BavPat1 challenge infection (mean of 1:420 for BavPat1, mean of 1:168.75 for Delta; Figure 9, J and K). No titers of Omicron-neutralizing antibodies were found in MVA-vaccinated animals (Figure 9L). However, robust titers of neutralizing antibodies were present in sera of MVA-S- and MVA-ST-vaccinated mice after SARS-CoV-2 BavPat1 challenge infection (Figure 9, J–L). Against BavPat1, MVA-S vaccination resulted in a mean titer of 1:2240; MVA-ST vaccination resulted in an even higher mean titer of 1:5600.

Against Delta, MVA-S vaccination resulted in a mean titer of 1:1333. Confirming previous results, antibody levels in MVA-ST-vaccinated mice were markedly higher, with a mean titer of 1:2400. However, against Omicron, a lower mean titer of 1:133 was measured for both candidate vaccines (Figure 9L).

Consistent with data from viral load in the lungs, control MVA-vaccinated animals showed pronounced lung pathology, which was associated with moderate to severe perivascular edema and inflammation with lymphocytes, macrophages, and small numbers of neutrophils surrounding small and intermediate vessels. Considerable inflammatory changes were also found in the alveolar and peribronchiolar compartments, characterized by moderate to marked interstitial and luminal immune cell infiltrates, with multifocal areas of completely obscured alveolar architecture. In animals vaccinated with MVA-S, despite the absence of severe and widespread inflammation in the alveolar compartment, substantial

perivascular and peribronchiolar inflammation was also present in the lungs. Interestingly, MVA-ST-vaccinated mice showed only very mild signs of pulmonary lesions after SARS-CoV-2 BavPat1 challenge infection (Figure 10). Our data so far showed that robust protective vaccination by a prime-boost application of 1×10^8 PFU MVA candidate vaccines is associated with substantial titers of neutralizing antibodies in K18-hACE2 mice.

Discussion

Here, we report that vaccination with a prefusion, stabilized SARS-CoV-2 S protein (ST) expressed by recombinant MVA (MVA-ST) elicits a better humoral immune response and provides protection upon SARS-CoV-2 BavPat1 challenge infection compared with the original recombinant MVA vaccine delivering the nonmodified SARS-CoV-2 S antigen (MVA-S).

Although several approved vaccines against SARS-CoV-2 are currently available, COVID-19 vaccine development still remains an important goal due to unsolved questions such as longevity and duration of immunity, virus transmission after asymptomatic infection, and arising virus variants of concern (VOCs). Thus, the development of innovative vaccination modalities that also confer robust and more broadly effective protection are urgently required. In general, there are several strategies to further improve vaccine candidates. A promising approach includes the presentation of a selected antigen. This may be of importance when processable fusion proteins are used as immunogens in vaccine development, since their metastability or processing also affects the kinetics of immune responses.

Based on our positive experience using a nonmodified S protein for generating an MVA-based candidate vaccine against MERS-CoV (11), we initially decided to use the same strategy to develop a COVID-19 candidate vaccine. Our MVA-S candidate vaccine expressing the authentic 2019 Wuhan Hu-1 S protein was confirmed to be immunogenic and protective in preclinical evaluation when tested in a mouse model for COVID-19 (15). Comparable results have been reported from the Oxford-AstraZeneca ChAdOx1 nCoV-19 vaccine, which also expresses a nonstabilized S protein and was confirmed to be immunogenic and protective in different preclinical animal models (19–21). Of note, the Oxford-AstraZeneca ChAdOx1 nCoV-19 was approved as a COVID-19 vaccine for application in humans and more than 2 billion doses of the vaccine have already been administered (22, 23).

In this current study, we report on the evaluation of the COVID-19 candidate vector vaccine MVA-S in a phase Ia clinical trial in humans. Here, we again confirmed advantageous safety and tolerability (data not shown). However, preliminary results revealed a pattern of antibody responses in individuals vaccinated with high or low doses of MVA-S, indicating a low S1-specific antibody response irrespective of vaccine dosage, while these individuals mounted substantial titers of S2-binding antibodies. Overall, levels of S-specific antibodies were shown to be below the levels of a comparable study evaluating an MVA-based candidate vaccine against MERS-CoV (11).

A recent study indicated that the efficiency of furin-mediated cleavage in the S1/S2 polybasic cleavage site in SARS-CoV-2 is enhanced compared with MERS-CoV (24). From these preliminary *in vitro* results, we hypothesize that a lower furin-mediated cleavage in MERS-CoV S protein expressed by MVA results in S protein that is still maintained in a prefusion state, still allowing S1-specific immune response activation. Since our recent data suggested proper folding and authentic presentation of the trimeric S protein expressed by the MVA vector (15), we hypothesized that processing involving furin-mediated cleavage of the S protein into its membrane-associated S2 subunit and the distal S1 subunit also occurs. Proteolytic cleavage can be followed by shedding of S1, leaving the S2 subunit anchored within the membrane (25). Our results again confirmed the authentic processing of the nonmodified S protein, with prominent S2 expression on the cell surface and obvious S1 shedding.

In previous studies, betacoronavirus S1 shedding had already been observed to inadvertently influence the activation of S-specific antibodies (6, 26, 27). This has also been confirmed for the activation of SARS-CoV-2-neutralizing antibodies after vaccination with the Oxford-AstraZeneca ChAdOx1 nCoV-19 vaccine. The authors discuss that the shedding of cleaved S1 may contribute to a higher proportion of non-neutralizing relative to neutralizing antibodies (28). This is in line with data from a recent study where Barros-Martins and colleagues evaluated the impact of heterologous versus homologous ChAdOx1nCoV-19/BNT162b2 vaccination in humans. Here, individuals who received a homologous BNT162b2 vaccination in a prime-boost schedule showed stronger antibody responses than those receiving homologous ChAdOx1nCoV-19 immunizations (29). Since BNT162b2 is based on a stabilized S protein, we hypothesized that S protein presentation influences immunogenicity, and that S1 dissociation from S2 influences the quantity and quality of MVA-S-activated immune responses. In another study, Dangi and colleagues confirmed that humans vaccinated

with a modified S protein exhibited a cross-protective immune response against heterologous coronaviruses (30).

Several approaches have been used to stabilize various class I fusion proteins in their precleaved conformation through structure-based design. For betacoronaviruses it has been suggested that presentation of the S protein in pre- or postfusion conformation has a substantial impact on the ratio of immune responses. In previous studies, 2 proline substitutions at the apex of the central helix and HR1 have been identified that could effectively stabilize MERS-CoV, SARS-CoV, and human coronavirus HKU1 S proteins in the precleaved conformation (27, 31, 32). Such stabilized S proteins were confirmed to be more immunogenic than wild-type S proteins (33, 34).

To evaluate the impact of structural processing of the labile S protein using our vector platform technology, we generated an MVA candidate vaccine expressing precleavage-stabilized S (MVA-ST). Modifications of full-length SARS-CoV-2 S protein expressed by MVA have already been used in other studies (26, 30, 35). As expected, when tested *in vivo* in mice and hamsters, we observed an improved antibody response after MVA-ST vaccination compared with the original MVA-S candidate vaccine. In line with previous results (36), the general activation of neutralizing antibodies against the Omicron variant was markedly reduced compared with ancestral BavPat1 and Delta variant. Of note, MVA-ST vaccination still induced marginally improved levels of Omicron-neutralizing antibodies compared with MVA-S.

The pattern of antibody responses in MVA-ST-immunized mice clearly exhibited advantageous activation of RBD-, S1-, and S2-binding antibodies. RBD is located in the S1 subunit known as the S protein ectodomain, and both are involved in binding to the specific cellular receptor. Thus both RBD-binding antibodies and those binding S1 elsewhere contribute to efficiently blocking SARS-CoV-2 receptor binding. Moreover, since the fusion peptide region is located within the S2 subunit, S2-binding antibodies are important for inhibiting fusion of the viral and host membranes, which enables release of the viral genome into host cells.

Since coronaviruses can readily generate antibody-escape mutations in the RBD and S1 subunit, activation of antibodies covering the entire S protein is considered desirable to ameliorate vaccine-induced immunity in such events. Indeed, the effectiveness of broadly reactive antibodies has already been confirmed for COVID-19 where REGN-COV2, an antibody cocktail mixture containing 2 neutralizing antibodies targeting the RBD of the SARS-CoV-2 S protein, efficiently reduced viral load in COVID-19 patients (37). Thus, the activation of antibodies targeting different epitopes within the S protein could also be effective against different SARS-CoV-2 VOCs. This was confirmed by our findings that, compared with MVA-S vaccination, superior activation of neutralizing antibodies specific for the S protein of Alpha, Beta, and Gamma variants and against the more recent SARS-CoV-2 variants Delta and Omicron, was achieved in mice and hamsters vaccinated with MVA-ST. The Omicron-characteristic immune evasion is based on a high number of amino acid substitutions present in the RBD. Yet, there is a fraction of broadly reactive antibodies that bind to sites inside and outside the RBD and potentially neutralize Omicron (38).

Based on previous studies from other betacoronaviruses, and also from influenza viruses, we hypothesize that this broadly neutralizing capacity may be explained by abundant presentation of

RESEARCH ARTICLE

The Journal of Clinical Investigation

the prefusion S2 conformation. S2 has been confirmed to be more highly conserved than S1, and represents a promising antigen to contribute to the induction of broadly protective immunity against current and newly arising coronaviruses (27, 39, 40). In our study, we confirmed more prominent presentation of S2 as a precleavage-stabilized cell-surface protein. This S2 prefusion conformation, in contrast to the postfusion S2 structure, might also contribute to more effectively activating host immune responses (41, 42) and against VOCs harboring high numbers of mutations in S1. We also confirmed the characteristic pattern of S-specific humoral immunity when we comprehensively tested our COVID-19 candidate vaccines in K18-hACE2 mice and the Syrian hamster model. Interestingly, despite these obvious differences in activation of humoral immune responses, the activation of an S1-specific cellular immune response appeared to be comparable following MVA-S and MVA-ST vaccination in mice. In our case, the S1 subunit including the presumed immunodominant SARS-CoV-2 S H2-Kd epitope S₂₆₉₋₂₇₈ is required to induce S1 epitope-specific CD8⁺ T cells (15).

However, since both of the S proteins are initially processed via the *trans*-Golgi network, direct MHC-I presentation should also be efficient in activating CD8⁺ T cell responses specific for S1 epitopes. This is further confirmed by results from Western blot analysis, which detected sufficient and comparable production of S1 antigen in the cell lysates of both MVA-S candidate vaccines. From these data we hypothesize that S1 is properly processed by direct antigen presentation, resulting in sufficient activation of S1-specific CD8⁺ T cells. Here it will be of interest to further characterize levels of S1- and S2-epitope-specific T cells in more detail, especially concerning their role in protective efficacy. A robust activation of S1-epitope-specific T cells should also contribute to a protective immune response against SARS-CoV-2 variants including Omicron that has been confirmed to efficiently evade recognition by many RBD-specific antibodies. Indeed, Omicron-specific CD8⁺ and CD4⁺ T cell responses are well conserved, suggesting negligible immune escape at the level of cellular immunity (43).

Thus, we hypothesize that robust MVA-ST-mediated protection against SARS-CoV-2 variants, including Omicron, will rely on the activation of broadly reactive antibodies targeting conserved antigenic sites within the S protein and the induction of cellular immunity.

Intriguingly, when we evaluated protective efficacy against intranasal SARS-CoV-2 BavPat1 infection, the clinical outcome of both MVA-S- and MVA-ST-vaccinated animals appeared similar, since neither group showed any weight loss or morbidity. Since the primary goal of current SARS-CoV-2 vaccine development and approved vaccines is to prevent symptomatic COVID-19 (2), our results from the infection models indicate that both MVA COVID candidate vaccines are suitable for achieving this. Reduced morbidity is matched by reduced viral loads in the upper and lower respiratory tract of vaccinated animals, although MVA-ST appeared to increase the rate of reduction. One can surmise that significantly reducing SARS-CoV-2 viral load in the lungs results in moderating the severity of the disease. Of note, compared with the MVA-S-vaccinated hamsters, those vaccinated with MVA-ST also showed significantly reduced viral shedding on day 6. This might also be the result of the broader reactive antibody response combined with a robust activation of neutralizing antibodies, leading to rapid virus control in the upper and lower respiratory tract.

Of particular interest, when we characterized the vaccination effect in the hamsters in more detail, postmortem at 6 days after infection, we found that MVA-ST-vaccinated animals seemed more robustly protected from lung pathology, particularly in the alveolar compartment. Diffuse alveolar damage resulting from SARS-CoV-2 BavPat1 infection represents a clinically relevant pathomorphological lesion associated with impaired gas exchange, potentially resulting in acute respiratory distress syndrome. Here, in most of the MVA-ST-vaccinated animals alveolar lesions were completely absent or minimal. In the MVA-S-vaccinated group, the extent of alveolar inflammation and damage was also reduced compared with controls, correlating with the lack of clinical symptoms. However, mild to moderate lesions involving up to 25% to 50% of the lung lobe were still present in all these animals, suggesting incomplete protection of these tissues.

The absence of substantial alveolar pathology and inflammation without any SARS-CoV-2 N antigen expression in the lungs of MVA-ST-vaccinated hamsters favors the idea that the risk of developing long COVID is also reduced. However, this needs to be confirmed in future studies. Since the K18-hACE2 mouse model recapitulates the outcome of severe COVID-19 in humans, efficacy testing of SARS-CoV-2 candidate vaccines in the K18hACE2 SARS-CoV-2 infection model is of substantial value (32, 42). We confirmed the severe and lethal disease outcome in this model for mice that had been vaccinated with nonrecombinant MVA. Despite the absence of death, disease, and even viral load in the lungs of MVA-S-vaccinated mice, substantial pulmonary pathology, including vasculitis and bronchitis, were observed. Of note, vasculitis has been also described as one of the complications of COVID-19 in humans (43).

In contrast, such pathological outcomes were not detected at all in mice vaccinated with MVA-ST. However, since the severity of disease in this model is also mediated by neurological involvement, both the candidate vaccines appeared to readily protect against the lethal outcome of disease presumably through rapidly inhibiting initial replication in the respiratory tract (44). Despite this robust protection achieved in these mice, the observed differences in the outcome of pathology in this model further support the advantage of the modified S protein.

Vice versa, our data also indicate that authentic S processing during viral infection plays an important role in terms of SARS-CoV-2 pathogenesis as an immune evasion strategy. This hypothesis is supported by our results that MVA-S immunogenicity is markedly lower than that of the MVA-ST candidate vaccine. Importantly, we confirmed that a precleavage-stabilized S protein activates a beneficial antibody response. These data suggest that a deeper understanding of the SARS-CoV-2 replication cycle and its potential immune evasion strategies is not only important for better understanding the viral pathogenesis, but also for developing new vaccination strategies.

Taken together, the results show that the availability of a vaccine that not only prevents the obvious development of clinical disease after SARS-CoV-2 infection, but also avoids excessive alveolar damage, inflammation, and subsequent remodeling is highly desirable.

Here, we confirmed the improved efficacy of MVA-ST in pre-clinical models. These findings merit clinical studies using the MVA-ST candidate vaccine to further characterize the immune responses in humans, not only in homologous immunization cohorts but also

in heterologous schedules using mRNA or adenoviral vectors as primary vaccinations. It will also be of particular interest to evaluate how long protective immune responses are maintained and whether broader protection can be achieved. These studies are important due to the still ongoing pandemic and the fact that we still lack data on the impact of vaccine-induced immune-response durability on protection against SARS-CoV-2 infection.

Methods

Study design and participants

A phase I clinical trial was conducted to address safety and immunogenicity of the vaccine candidate MVA-S in healthy adults (ClinicalTrials.gov NCT04569383). The study was conducted in Hamburg (Germany) at the University Medical Center Hamburg-Eppendorf (UKE). Study participants were divided into 2 dose groups that received either 1×10^7 IU (low dose) or 1×10^8 IU (high dose) on days 0 and 28 (11).

Bead-based serological multiplex assay

Serum samples were obtained by venipuncture from vaccinated individuals. Bead-based serological multiplex assay was performed using the MultiCoV-Ab assay validated previously (16, 17). MagPlex Microspheres (Luminex) conjugated to different parts of the S protein based on SARS-CoV-2 Wuhan-Hu-1 reference strain (GenBank accession no. MN908947.3) were used: purified trimeric S protein, S1 domain, RBD (all produced in-house), and S2 domain (Sino Biological). Serum samples were incubated at a dilution of 1:400 for 2 hours at room temperature. Subsequently, the beads were washed using 100 μ L of washing buffer (PBS supplemented with 0.05% [v/v] Tween 20) per well with the aid of a LifeSep magnetic separator unit (Dexter Magnetic Technologies). After 3 washing steps, bound antibodies were detected using PE-coupled secondary anti-human IgG antibodies (Dianova, 109-116-098, lot 148837; 3 μ g/mL), incubated for 45 minutes at room temperature. Samples were measured using the Bio-Plex 200 System (Bio-Rad Laboratories), controlled by BioPlex manager software, version 5.0.0.531. Cutoff samples with a known MFI value were generated as previously established (44) and included on each plate as quality control.

Immunofluorescent staining and confocal microscopy

To quantify the cellular localization of S1 and S2, Huh-7 cells were infected with MVA-S or -ST (MOI 0.5) or transfected with plasmids encoding non-stabilized S protein. Eighteen hours after transfection/infection, S located at the cell surface was labeled at 4°C prior to fixation using a human-derived anti-S1 monoclonal antibody (generated and provided by F. Klein, Institute of Virology, University Hospital of Cologne, Germany; ref. 18). Subsequently, cells were fixed with 4% paraformaldehyde, permeabilized with 0.1% Triton X-100, and total S was labeled using anti-S2 antibody from mouse (GeneTex, GTX632604, clone 1A9; 1:100). Polyclonal goat anti-mouse-Alexa Fluor 594 (catalog A-11005) and goat anti-human-Alexa Fluor 488 (catalog A-48276) secondary antibodies (Thermo Fisher Scientific; 1:200) were used to visualize S-specific staining by fluorescence. Nuclei were stained with 1 μ g/mL DAPI (Sigma-Aldrich, D9542) and cells were analyzed using the Leica SP2 confocal microscope (Leica) with $\times 63$ objective. All quantification of immunofluorescence-related data was performed with ImageJ/Fiji v.1.51 (45). To quantify surface S, optical sections of Huh-7 cells (500 nm/slice) were acquired in order to project the entire cell. Pixel intensities were measured in S1 (surface

and in S2 (total S) channels. The ratio between S1 and S2 values was calculated to yield the relative surface expression. Prior to each analysis, cell borders were determined using standard selection tools.

SARS-CoV-2 S1 surface staining for flow cytometry

A549 cells were infected with 1 MOI MVA-S/-ST and MVA and incubated for 16 hours at 37°C, and cells were harvested and plated onto 96-well U-bottom plates at 2×10^5 cells/well. Cells were incubated with purified anti-mouse CD16/CD32 (Fc block; BioLegend, clone 93; 1:500) for 15 minutes on ice. Cells were incubated with anti-S1 human monoclonal antibody (see above) for 30 minutes on ice and then with goat anti-human IgG (H+L)-Alexa Fluor 488 (Thermo Fisher Scientific, A-48276; 1:3000) for 30 minutes on ice. Cells were then stained with fixable dead cell viability dye Zombie Aqua (BioLegend, 423101; 1:1000). After staining, cells were fixed using Fixation Buffer (BioLegend) according to the manufacturer's protocol. Data were acquired using the MACSQuant VYB Flow Analyzer (Miltenyi Biotec) and analyzed using FlowJo (FlowJo LLC, BD Life Sciences).

PRNT₅₀

Serum samples were used to analyze neutralization capacity against SARS-CoV-2 (isolate Germany/BavPat1/2020; isolate hCoV-19/USA/PHC658/2021, lineage B.1.617.2 Delta variant; isolate hCoV-19/USA/MD-HP20874/2021, lineage B.1.1.529, Omicron variant) received from BEI Resources, NIAID, NIH, as previously described with some modifications (46). Heat-inactivated serum samples were serially diluted 2-fold in duplicate in 50 μ L DMEM. Then, 50 μ L of virus suspension (600 TCID₅₀) was added to each well and incubated at 37°C for 1 hour before placing the mixtures on Vero E6 cells (ATCC, CRL-1586), seeded in 96-well plates. After incubation for 45 minutes, 100 μ L of a 1:1 mixture of prewarmed DMEM and Avicel RC-591 (Dupont, Nutrition & Biosciences) was added and plates were incubated for 24 hours. After incubation, cells were fixed with 4% formaldehyde/PBS and stained with a polyclonal rabbit antibody against SARS-CoV-2 nucleoprotein (Sino Biological, 40588-T62; 1:2000) and a secondary HRP-labeled goat anti-rabbit IgG (Agilent Dako, PO44801-2; 1:1000). The signal was developed using a precipitate-forming TMB substrate (True Blue, KPL SeraCare, 5510-0030) and the number of infected cells per well was counted by using an ImmunoSpot reader (CTL Europe GmbH). The reciprocal of the highest serum dilution allowing reduction of greater than 50% plaque formation was calculated as the serum neutralization titer (PRNT₅₀) using the BioSpot Software Suite (CTL Europe GmbH).

SARS-CoV-2 VNT₁₀₀

The neutralizing activity of mouse serum antibodies was investigated based on a previously published protocol (47). Briefly, samples were serially diluted in 96-well plates starting from a 1:16 serum dilution. Samples were incubated for 1 hour at 37°C together with 100 PFU of SARS-CoV-2. Cytopathic effects on Vero cells were analyzed 4 days (BavPat1, Alpha, Gamma) or 6 days (Zeta) after infection. Neutralization was defined as absence of the cytopathic effects compared with virus controls. For each test, a positive control (human monoclonal antibody; refs. 18, 48) was used in quadruplicate as an interassay neutralization standard.

Challenge-infection experiments in Syrian hamsters and K18-hACE2 mice

For SARS-CoV-2 challenge infection, animals were kept in individually ventilated cages (IVCs, Tecniplast) in approved BSL-3 facilities.

RESEARCH ARTICLE

The Journal of Clinical Investigation

All animal and laboratory work with infectious SARS-CoV-2 was performed in a BSL-3e laboratory and facilities at the Research Center for Emerging Infections and Zoonoses (RIZ), University of Veterinary Medicine, Hanover, Germany.

All animals were infected under anesthesia via the intranasal route with 1×10^4 (hamsters) or 3.6×10^4 (mice) TCID₅₀ of SARS-CoV-2 (isolate Germany/BavPat1/2020, NR-52370) received from BEI Resources, NIAID, NIH. After challenge infection, hamsters and mice were monitored at least twice daily for well being, health constitution, and clinical signs using a clinical score sheet (Supplemental Table 2). Body weights were checked daily.

Viruses

SARS-CoV-2 (isolate Germany/BavPat1/2020, NR-52370; isolate hCoV-19/USA/PHC658/2021, lineage B.1.617.2 Delta variant, NR-55611; isolate hCoV-19/USA/MD-HP20874/2021, lineage B.1.1.529, Omicron variant, NR-56461) received from BEI Resources, NIAID, NIH, were propagated in Vero cells in DMEM (Sigma-Aldrich) supplemented with 2% FBS, 1% penicillin-streptomycin, and 1% L-glutamine at 37°C. All infection experiments with SARS-CoV-2 were performed in BSL-3 laboratories at the RIZ, University of Veterinary Medicine Hannover, Germany or the Institute of Virology, Philipps University Marburg, Germany.

Measurement of viral burden

Lung tissue samples of immunized and challenged hamsters or mice excised from the right lung lobes, and brain tissue excised from the right brain of mice were homogenized in 1 mL DMEM containing antibiotics (penicillin and streptomycin, Gibco). Tissue was homogenized using the TissueLyser-II (Qiagen), and aliquots were stored at -80°C. Viral titers were determined on Vero cells as median TCID₅₀ units. Briefly, Vero cells were seeded in 96-well plates and serial 10-fold dilutions of homogenized lung samples in DMEM containing 5% FBS. After incubation for 96 hours at 37°C, cytopathic effects in Vero cells were evaluated and calculated as TCID₅₀ unit per gram or mL using the Reed-Muench method. For samples without cytopathic effect, data points were set to half of the detection limit for statistical analysis purposes.

Statistics

Data were prepared using GraphPad Prism 9.0.0 and R 4.2.1 (<https://cran.r-project.org/>) and expressed as mean \pm standard error of the mean (SEM) or median \pm interquartile range. Data were analyzed by 1-way ANOVA and Kruskal-Wallis test to compare 3 or more groups. A *P* value of less than 0.05 was used as the threshold for statistical significance.

Study approval

Human specimens. The study design was reviewed and approved by the Competent National Authority (Paul-Ehrlich-Institut [PEI], Langen, Germany) and the Ethics Committee of the Hamburg Medical Association. The study was performed in accordance with the Declaration of

Helsinki in its version of Fortaleza 2013 and ICH-GCP. All participants voluntarily enrolled in the study by signing an informed consent form after receiving detailed information about the clinical study.

Hamster and mouse studies. All animal experiments including SARS-CoV-2 infection under BSL-3 conditions were handled in compliance with the European and national regulations for animal experimentation (European Directive 2010/63/EU; Animal Welfare Acts in Germany) and Animal Welfare Act, approved by the Regierung von Oberbayern (Munich, Germany) and the Niedersächsisches Landesamt für Verbraucherschutz und Lebensmittelsicherheit (LAVES, Lower Saxony, Germany).

Author contributions

AV and GS conceptualized the study and revised the manuscript. AT constructed and characterized the vaccines, and performed experiments for safety and immunogenicity in BALB/c mice together with JHS, LL, GK, KB, SJ, and A Freudenstein. CMZN established in vivo SARS-CoV-2 infection models, performed in vitro and in vivo experiments to characterize safety, immunogenicity, and efficacy together with DLS, TT, SC, LMS, and AV. CR, SH, AK, and SB characterized S protein expression and VNT₁₀₀ CD, A Fathi, MLW, LM, and MMA provided human sera from the phase I trial. RF, MK, ME, NSM, AD, and PK analyzed human sera. MC, FA, GB, and WB provided pathological investigations. CMZN and AT performed experiments, acquired data, interpreted data, and revised the manuscript. CMZN, AT, AV, and GS wrote the manuscript together with all coauthors.

Acknowledgments

We thank Monika Berg, Saskia Oppermann, Darren Markillie, Matthias Herberg, Bernd Vollbrecht, and Sandra Pfeifer for expert help in animal studies. We thank Patrizia Bonert, Ursula Klostermeier, Johannes Döring, and Axel Groß for expert help in mouse studies. We thank the phase I clinical study participants for their dedication and willingness to contribute to this research study in the middle of a pandemic. We thank the Hamburg clinical trial and laboratory teams for conducting the first-in-human clinical study and specimen processing. This work was supported by the German Center for Infection Research (DZIF: projects TTU 01.921 to GS, MMA, and SB; TTU 01.712 to GS), the Federal Ministry of Education and Research (BMBF 01KI20702 to GS, MMA, and SB; ZOO-VAC 01KI1718 to AV; RAPID 01KI1723G to AV and WB), Ministry of Science and Culture of Lower Saxony, Germany (14 - 76103-184 CORONA-15/20 to AV and WB), and the DFG (German Research Foundation 398066876/GRK 2485/1 to AV, GS, and WB).

Address correspondence to: Asisa Volz, Institute of Virology, University of Veterinary Medicine Hannover, Buenteweg 17, 30559 Hanover, Germany. Phone: 49.511.953.8857; Email: Asisa.Volz@tiho-hannover.de.

1. Wrapp D, et al. Cryo-EM structure of the 2019-nCoV spike in the prefusion conformation. *Science*. 2020;367(6483):1260-1263.

2. Corbett KS, et al. Immune correlates of protection by mRNA-1273 vaccine against SARS-CoV-2 in nonhuman primates. *Science*. 2021;373(6561):eabj0299.

3. Folegatti PM, et al. Safety and immunogenicity of the ChAdOx1 nCoV-19 vaccine against SARS-CoV-2: a preliminary report of a phase 1/2, single-blind, randomised controlled trial. *Lancet*. 2020;396(10249):467-478.

4. Logunov DY, et al. Safety and immunogenicity of an rAd26 and rAd5 vector-based heterologous

prime-boost COVID-19 vaccine in two formulations: two open, non-randomised phase 1/2 studies from Russia. *Lancet*. 2020;396(10255):887-897.

5. Zhu FC, et al. Safety, tolerability, and immunogenicity of a recombinant adenovirus type-5 vectored COVID-19 vaccine: a dose-escalation, open-label, non-randomised, first-in-human

The Journal of Clinical Investigation

RESEARCH ARTICLE

- trial. *Lancet*. 2020;395(10240):1845–1854.
6. Bos R, et al. Ad26 vector-based COVID-19 vaccine encoding a prefusion-stabilized SARS-CoV-2 spike immunogen induces potent humoral and cellular immune responses. *NPJ Vaccines*. 2020;5(1):91.
 7. Jackson LA, et al. An mRNA vaccine against SARS-CoV-2 - preliminary report. *N Engl J Med*. 2020;383(20):1920–1931.
 8. Keech C, et al. Phase 1-2 trial of a SARS-CoV-2 recombinant spike protein nanoparticle vaccine. *N Engl J Med*. 2021;384(16):1576–1577.
 9. Skowronski DM, De Serres G. Safety and efficacy of the BNT162b2 mRNA Covid-19 vaccine. *N Engl J Med*. 2021;384(16):1576–1577.
 10. Sadarangani M, et al. Immunological mechanisms of vaccine-induced protection against COVID-19 in humans. *Nat Rev Immunol*. 2021;21(8):475–484.
 11. Koch T, et al. Safety and immunogenicity of a modified vaccinia virus Ankara vector vaccine candidate for Middle East respiratory syndrome: an open-label, phase 1 trial. *Lancet Infect Dis*. 2020;20(7):827–838.
 12. Krejtz JHCM, et al. Safety and immunogenicity of a modified-vaccinia-virus-Ankara-based influenza A H5N1 vaccine: a randomised, double-blind phase 1/2a clinical trial. *Lancet Infect Dis*. 2014;14(12):1196–1207.
 13. Volz A, et al. Protective efficacy of recombinant modified vaccinia virus ankara delivering Middle East respiratory syndrome coronavirus spike glycoprotein. *J Virol*. 2015;89(16):8651–8656.
 14. Volz A, Sutter G. Modified vaccinia virus ankara: history, value in basic research, and current perspectives for vaccine development. *Adv Virus Res*. 2017;97:187–243.
 15. Tscherny A, et al. Immunogenicity and efficacy of the COVID-19 candidate vector vaccine MVA-SARS-2-S in preclinical vaccination. *Proc Natl Acad Sci U S A*. 2021;118(28):e2026207118.
 16. Becker M, et al. Immune response to SARS-CoV-2 variants of concern in vaccinated individuals. *Nat Commun*. 2021;12(1):3109.
 17. Becker M, et al. Exploring beyond clinical routine SARS-CoV-2 serology using MultiCoV-Ab to evaluate endemic coronavirus cross-reactivity. *Nat Commun*. 2021;12(1):1152.
 18. Kreer C, et al. Longitudinal isolation of potent near-germline SARS-CoV-2-neutralizing antibodies from COVID-19 patients. *Cell*. 2020;182(4):843–854.
 19. van Doremalen N, et al. Intranasal ChAdOx1 nCoV-19/AZD1222 vaccination reduces viral shedding after SARS-CoV-2 D614G challenge in preclinical models. *Sci Transl Med*. 2021;13(607):eab0755.
 20. Fischer RJ, et al. ChAdOx1 nCoV-19 (AZD1222) protects Syrian hamsters against SARS-CoV-2 B.1.351 and B.1.1.7. *Nat Commun*. 2021;12(1):5868.
 21. van Doremalen N, et al. ChAdOx1 nCoV-19 vaccine prevents SARS-CoV-2 pneumonia in rhesus macaques. *Nature*. 2020;586(7830):578–582.
 22. European commission. Public Health - Union Register of medicinal products. <https://ec.europa.eu/health/documents/community-register/html/h1529.htm>. Updated October 7, 2022. Accessed October 10, 2022.
 23. AstraZeneca. Zwei Milliarden Dosen des AstraZeneca-Impfstoffs gegen COVID-19 in weniger als zwölf Monaten weltweit zur Verfügung gestellt. <https://www.astrazeneca.de/medien/press-releases/2021/zwei-milliarden-dosen-des-astrazeneca-impfstoffs-gegen-covid-19-zur-verfuegung-gestellt.html>. Updated November 23, 2021. Accessed February 7, 2022.
 24. Örd M, et al. The sequence at Spike S1/S2 site enables cleavage by furin and phospho-regulation in SARS-CoV2 but not in SARS-CoV1 or MERS-CoV. *Sci Rep*. 2020;10(1):16944.
 25. Brun J, et al. Assessing antigen structural integrity through glycosylation analysis of the SARS-CoV-2 viral spike. *ACS Cent Sci*. 2021;7(4):586–593.
 26. Liu R, et al. One or two injections of MVA-vectored vaccine shields hACE2 transgenic mice from SARS-CoV-2 upper and lower respiratory tract infection. *Proc Natl Acad Sci U S A*. 2021;118(12):e2026785118.
 27. Pallesen J, et al. Immunogenicity and structures of a rationally designed prefusion MERS-CoV spike antigen. *Proc Natl Acad Sci U S A*. 2017;114(35):E7348–E7357.
 28. Watanabe Y, et al. Native-like SARS-CoV-2 spike glycoprotein expressed by ChAdOx1 nCoV-19/AZD1222 vaccine. *ACS Cent Sci*. 2021;7(4):594–602.
 29. Barros-Martins J, et al. Immune responses against SARS-CoV-2 variants after heterologous and homologous ChAdOx1 nCoV-19/BNT162b2 vaccination. *Nat Med*. 2021;27(9):1525–1529.
 30. Dangi T, et al. Cross-protective immunity following coronavirus vaccination and coronavirus infection. *J Clin Invest*. 2021;131(24):e151969.
 31. Kirchdoerfer RN, et al. Pre-fusion structure of a human coronavirus spike protein. *Nature*. 2016;531(7592):118–121.
 32. Walls AC, et al. Cryo-electron microscopy structure of a coronavirus spike glycoprotein trimer. *Nature*. 2016;531(7592):114–117.
 33. Graham BS, Corbett KS. Prototype pathogen approach for pandemic preparedness: world on fire. *J Clin Invest*. 2020;130(7):3348–3349.
 34. Graham BS, Sullivan NJ. Emerging viral diseases from a vaccinology perspective: preparing for the next pandemic. *Nat Immunol*. 2018;19(1):20–28.
 35. Routhu NK, et al. A modified vaccinia Ankara vector-based vaccine protects macaques from SARS-CoV-2 infection, immune pathology, and dysfunction in the lungs. *Immunity*. 2021;54(3):542–556.
 36. Cheng SMS, et al. Neutralizing antibodies against the SARS-CoV-2 Omicron variant BA.1 following homologous and heterologous CoronaVac or BNT162b2 vaccination. *Nat Med*. 2022;28(3):486–489.
 37. Weinreich DM, et al. REGN-COV2, a neutralizing antibody cocktail, in outpatients with Covid-19. *N Engl J Med*. 2020;384(3):238–251.
 38. Cameroni E, et al. Broadly neutralizing antibodies overcome SARS-CoV-2 Omicron antigenic shift. *Nature*. 2022;602(7898):664–670.
 39. Ekiert DC, et al. Antibody recognition of a highly conserved influenza virus epitope. *Science*. 2009;324(5924):246–251.
 40. Yassine HM, et al. Hemagglutinin-stem nanoparticles generate heterosubtypic influenza protection. *Nat Med*. 2015;21(9):1065–1070.
 41. Cai Y, et al. Distinct conformational states of SARS-CoV-2 spike protein. *Science*. 2020;369(6511):1586–1592.
 42. McLellan JS, et al. Structure-based design of a fusion glycoprotein vaccine for respiratory syncytial virus. *Science*. 2013;342(6158):592–598.
 43. GeurtsvanKessel CH, et al. Divergent SARS-CoV-2 Omicron-reactive T and B cell responses in COVID-19 vaccine recipients. *Sci Immunol*. 2022;7(69):eab02202.
 44. Planatscher H, et al. Systematic reference sample generation for multiplexed serological assays. *Sci Rep*. 2013;3(1):3259.
 45. Schindelin J, et al. Fiji: an open-source platform for biological-image analysis. *Nat Methods*. 2012;9(7):676–682.
 46. Okba NMA, et al. Severe acute respiratory syndrome coronavirus 2-specific antibody responses in Coronavirus disease patients. *Emerg Infect Dis*. 2020;26(7):1478–1488.
 47. Halwe S, et al. Intranasal administration of a monoclonal neutralizing antibody protects mice against SARS-CoV-2 infection. *Viruses*. 2021;13(8):1498.
 48. Vanshylla K, et al. Kinetics and correlates of the neutralizing antibody response to SARS-CoV-2 infection in humans. *Cell Host Microbe*. 2021;29(6):917–929.

2.5 SARS-CoV-2 specific cellular response following COVID-19 vaccination in patients with chronic lymphocytic leukemia

Sibylle C. Mellinghoff, Sandra Robrecht, Leonie Mayer, **Leonie M. Weskamm**, Christine Dahlke, Henning Gruell, Kanika Vanshylla, Hans A. Schlösser, Martin Thelen, Anna-Maria Fink, Kirsten Fischer, Florian Klein, Marylyn M. Addo, Barbara Eichhorst, Michael Hallek & Petra Langerbeins

Published in *Leukemia*, DOI: 10.1038/s41375-021-01500-1

Leonie Marie Weskamm established the protocol for investigation of SARS-CoV-2 spike-specific B cells by IgG ELISpot and conducted the related experiments and data analysis. She was also involved in the reviewing of manuscript and figures, and in the coordination and laboratory work to establish the healthy control cohort, including isolation and cryopreservation of PBMCs, plasma and serum from human blood samples.

I hereby confirm the accuracy of these contributions

 17.1.2023
Prof. Dr. med. Marylyn M. Addo

LETTER OPEN



CHRONIC LYMPHOCYTIC LEUKEMIA

SARS-CoV-2 specific cellular response following COVID-19 vaccination in patients with chronic lymphocytic leukemia

Sibylle C. Mellingshoff^{1,2,3}✉, Sandra Robrecht¹, Leonie Mayer^{1,3,4,5}, Leonie M. Weskamm^{1,3,4,5}, Christine Dahlke^{1,3,4,5}, Henning Gruell⁶, Kanika Vanshylla⁶, Hans A. Schlösser⁷, Martin Thelen⁷, Anna-Maria Fink¹, Kirsten Fischer¹, Florian Klein⁶, Marylyn M. Addo^{1,3,4,5}, Barbara Eichhorst¹, Michael Hallek¹ and Petra Langerbeins¹

© The Author(s) 2021

Leukemia (2022) 36:562–565; <https://doi.org/10.1038/s41375-021-01500-1>

Chatzikonstantinou et al. [1] conducted a large follow-up analysis of COVID-19 in patients with chronic lymphocytic leukemia (CLL) and confirmed a high mortality rate, especially in patients with older age, comorbidity and previous CLL-treatment. The results emphasize the importance of prevention and mitigation of COVID-19 by vaccination, especially in patients with hematological malignancies. The COVID-19 vaccine-induced immunity is mediated by the interaction of both, humoral and cellular components [2, 3]. While several studies have confirmed low humoral immunogenicity in CLL patients [4–7], very few describe cellular responses to determine immunogenicity and report reduced T cell response [8]. In this prospective cohort study, we hence investigated cellular immunogenicity and the interplay with humoral immunogenicity following COVID-19 vaccination in SLL/CLL patients as compared with healthy controls (HC).

Blood samples of CLL registry (NCT02863692) patients were centrally evaluated after full COVID-19 vaccination. In total, 21/23 patients were included in the analyses (samples missing in 2/23). Vaccinated healthcare workers served as HC cohort ($n = 12$). Both studies were approved by the local ethics committee.

Patient and disease characteristics and vaccination schedules are summarized in Table 1 and Supplemental Table 1. Patient blood samples were collected at a median of 47 (range 19–94 days) and HC at a median of 35 (range 32–38) days after the second vaccination.

SARS-CoV-2 receptor-binding domain (RBD) specific IgG antibodies, determined using Alinity ci SARS-CoV-2 IgG II Quant assay (Abbott), were detectable in 8/21 (38.1%) patients with SLL/CLL and 100% of HC ($p = 0.001$; Fig. 1A, B). Neutralizing activity, determined by using heat-inactivated serum in a lentiviral-based pseudovirus neutralization assay against Wu-01 strain of SARS-CoV-2, was observed in serum samples from all HC (GeoMean ID_{50} 409) (Fig. 1C). No neutralizing activity ($ID_{50} < 10$) was detectable in the majority of CLL patients (14/21, 67%, 0), including all seronegative individuals.

However, CLL patients with detectable activity (7/21, 30%) had a response that was comparable to HC (ID_{50} 523, $p = 0.9$).

Peripheral blood mononuclear cells (PBMCs) were used for SARS-CoV-2 spike-specific T cells (Human IFN γ ELISpot^{PLUS} [ALP] kit [Mabtech]) and B cells (IgG ELISpot) analyses. Results are reported as spot-forming cells (SFC) per million PBMCs. T cell responses to SARS-CoV-2 peptide pool ([15-mers overlapping by 11 amino acids] spanning the entire spike protein) were considered positive if higher than twice the median response of pre-pandemic HC (48 SFC/10⁶). The median number of SARS-CoV-2 specific T cells was 21.3 SFC (interquartile range [IQR] 0.0–145.0) for CLL patients as compared with 177.3 SFC [IQR 138.0–403.3] in HC ($p = 0.008$; Fig. 1D). While 8/21 (38.1%) CLL patients had a SARS-CoV-2 spike-specific T cell response measurable above cut-off, 90% of HC mounted a response ($p = 0.009$).

SARS-CoV-2 S1/2-specific antibody-secreting cells (ASC) were analyzed in 14/21 (66.7%) SLL/CLL patients. The cut-off value for positive responses were defined as the mean plus two standard deviations of the responses observed in pre-pandemic HC (62 SFC/10⁶). Overall, 1/14 SLL/CLL patients (7.1%) had detectable S-specific ASC (138 SFC) as compared with 100% in HC (median 193 SFC, range 89–464 SFC). The SARS-CoV-2 specific IgG titer of the ASC responding patient was with 11 360 BAU/ml the highest within the group of CLL patients. Looking at total IgG-secreting B cells, 13 patients without S-specific ASC did neither show any IgG-secreting B cells. Spots were too faint to be counted or detected at numbers below the cut-off.

In a descriptive analysis (Table 1 and Supplemental Table 2 and 3), potential variables to be associated with humoral and T cell responses were investigated. While 3/21 (14.3%) of patients had both a humoral and a T cellular response, eight patients (38.1%) were double negative and a discordant response, defined by detection of either T cellular or humoral immune response to vaccination was found in most patients (10/21, 47.6%).

¹Faculty of Medicine and University Hospital of Cologne, Department I of Internal Medicine, Centre for Integrated Oncology Aachen Bonn Cologne Düsseldorf (CIO ABCD), German CLL Group (GCLLSG), University of Cologne, Cologne, Germany. ²German Centre for Infection Research (DZIF), partner site Bonn-Cologne, Cologne, Germany. ³Department of Clinical Immunology of Infectious Diseases, Bernhard Nocht Institute for Tropical Medicine, Hamburg, Germany. ⁴Division of Infectious Diseases, First Department of Medicine, University Medical Centre Hamburg-Eppendorf, Hamburg, Germany. ⁵German Centre for Infection Research (DZIF), Partner Site Hamburg-Lübeck-Borstel-Riems, Hamburg, Germany. ⁶Institute of Virology, Faculty of Medicine and University Hospital Cologne, University of Cologne, Cologne, Germany. ⁷Centre for Molecular Medicine Cologne, University of Cologne, Faculty of Medicine and University Hospital Cologne, Cologne, Germany. ✉email: sibylle.mellingshoff@uk-koeln.de

Received: 8 November 2021 Revised: 2 December 2021 Accepted: 10 December 2021
Published online: 22 December 2021

Table 1. Patients baseline characteristics and disease characteristics in the overall cohort and by subgroups.

| Parameters N (%) | Patients with CLL (N = 23) | | | | |
|---|----------------------------|--|---|---|---|
| | Overall cohort | Humoral response negative T cell response negative | Humoral response negative, T cell response positive | Humoral response positive, T cell response negative | Humoral response positive, T cell response positive |
| Overall COVID-19 vaccine immune response | | 8 (38.1) ^a | 5 (23.8) ^a | 5 (23.8) ^a | 3 (14.3) ^a |
| Age, median (range) (years) | 70 (46–79) | 70.5 (48–79) | 71.0 (53–79) | 74.0 (62–77) | 59.0 (49–62) |
| Age group (years) | | | | | |
| >65 | 13 (56.5) | 6 (75.0) | 3 (60.0) | 4 (80.0) | 0 (0.0) |
| >70 | 11 (47.8) | 4 (50.0) | 3 (60.0) | 4 (80.0) | 0 (0.0) |
| Male sex | 20 (87) | 6 (75.0) | 4 (80.0) | 5 (100.0) | 3 (100.0) |
| Disease / treatment status | | | | | |
| Treatment-naïve | 1 (4.3) | 0 (0.0) | 0 (0.0) | 1 (20.0) | 0 (0.0) |
| Previously treated | 22 (95.7) | 8 (100.0) | 5 (100.0) | 4 (80.0) | 3 (100.0) |
| Treatment prior vaccination | 22 (95.7) | | | | |
| Line of treatment, median (range) | 2 (1–8) | 2 (1–8) | 3 (2–5) | 2 (1–5) | 2 (1–2) |
| 1 st line | 6 (27.3) | 2 (25.0) | 0 (0.0) | 2 (50.0) | 1 (33.3) |
| >1 st line | 16 (72.7) | 6 (75.0) | 5 (100.0) | 2 (40.0) | 2 (66.7) |
| Treatment < 12 months prior vaccination | 9 (40.9) | 3 (37.5) | 4 (80.0) | 1 (25.0) | 0 (0.0) |
| without anti CD20 ^b | 2 (9.1) | 0 (0.0) | 1 (20.0) | 1 (20.0) | 0 (0.0) |
| with anti CD20 ^c | 7 (31.8) | 3 (37.5) | 3 (60.0) | 0 (0.0) | 0 (0.0) |
| Type according to hierarchical model^d | 21 (91.3) | | | | |
| del(17p) | 4 (19.0) | 3 (37.5) | 1 (20.0) | 0 (0.0) | 0 (0.0) |
| del(11q) | 5 (23.8) | 1 (12.5) | 1 (20.0) | 1 (33.3) | 2 (66.7) |
| Trisomy 12 | 4 (19.0) | 1 (12.5) | 0 (0.0) | 0 (0.0) | 1 (33.3) |
| No abnormalities | 1 (4.8) | 0 (0.0) | 0 (0.0) | 1 (33.3) | 0 (0.0) |
| del(13q) [single] | 7 (33.3) | 3 (37.5) | 3 (60.0) | 1 (33.3) | 0 (0.0) |
| IGHV mutational status | 18 (78.3) | | | | |
| Unmutated | 13 (72.2) | 6 (75.0) | 2 (66.7) | 2 (66.7) | 2 (100.0) |
| Mutated | 5 (27.8) | 2 (25.0) | 1 (33.3) | 1 (33.3) | 0 (0.0) |
| TP53 mutational status | 19 (82.6) | | | | |
| Mutated | 2 (10.5) | 5 (71.4) | 4 (100.0) | 3 (100.0) | 3 (100.0) |
| Unmutated | 17 (89.5) | 2 (28.6) | 0 (0.0) | 0 (0.0) | 0 (0.0) |

^aHumoral and T cell response measured in 21/23 patients.^bAcalabrutinib, Ibrutinib.^cObinutuzumab, Obinutuzumab/Venetoclax, Acalabrutinib/Obinutuzumab, Acalabrutinib/Obinutuzumab/Venetoclax.^dCytogenetic subgroups were determined according to the hierarchical model of Döhner et al. [11].

In conclusion, humoral and cellular immunogenicity following COVID-19 vaccination was significantly impaired in patients with SLL/CLL as described previously. SARS-CoV-2 specific antibodies and T cells were detectable in 38.1% each. In the majority of seroconverted patients, SARS-CoV-2 neutralizing serum activity of diverse magnitude was detectable indicating functionality of antibodies if at all mounted. While less than 15% of patients had both a humoral and cellular response, most patients showed a discordant response with only either detectable humoral or cellular response. Clinical features of the two subgroups differed with regard to previous treatment lines, which seem to affect the humoral more than the T cell axis. CLL-targeted treatments as well the underlying diseases itself affect B cells and self-evidently impact the humoral response. Our findings encourage immunization of

patients even at advanced disease stages or heavily pre-treated as a subgroup that may respond with the T cellular axis.

Two patients showed a particular strong T cell response: One had been vaccinated thrice and the other had received a heterologous boosting (Fig. 1D). Data from more patients will need to prove if a booster vaccination is more likely to induce T cell response. Our data emphasize the importance of assessing the T cell response in patients with a limited serologic response. The best vaccination regime to promote those key players remains to be investigated. While heterologous immunization appears to elicit stronger T cell responses than homologous immunization [9], the chronological order for immunocompromised patients is unclear and needs further study.

A limitation of this study is the small sample size and the younger age of the control group (as compared with the SLL/CLL

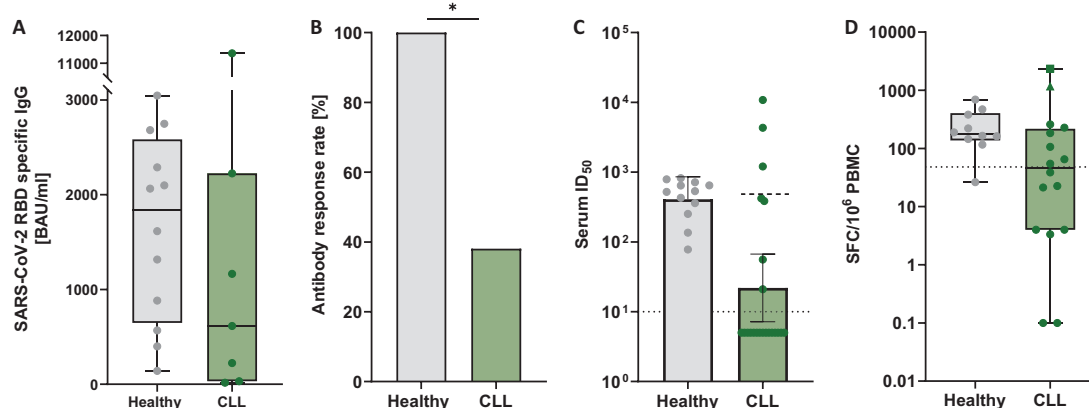


Fig. 1 Humoral and T cell immune responses after COVID-19 vaccination. **A** SARS-CoV-2 RBD specific IgG in CLL patients (median 889.9 BAU/ml, IQR 80.2–2127.4, for responders) and healthy controls (median 1839.8 BAU/ml, IQR 647.0–2583.4) measured by ELISA. **B** Antibody response rate in CLL patients and healthy volunteers. $*p = 0.001$. **C** Serum neutralizing activity (50% inhibitory serum dilution) determined in a pseudovirus neutralizing assay against the Wu-01 pseudovirus strain. Bars indicating geometric mean ID₅₀ with 95% confidence intervals. A dashed line indicates limit of detection [10]. Samples with no detectable neutralization (ID₅₀ < 10) were plotted with an arbitrary ID₅₀ of 5 for graphical representation. Dashed line in the CLL group shows geometric mean ID₅₀ for individuals with a detectable neutralizing response. **D** Interferon-γ T cell ELISpot response in CLL patients and HC. Shown values are mean spots in peptide-stimulated wells minus background in negative control wells. Error bars represent median ± interquartile range. The dotted line indicates the positive threshold of 48 SFC/10⁶ PBMC. Samples were acquired 35 days after the second vaccination in HC and at a median of 47 days after second vaccination in CLL patients. Two patients had much higher correlated of T cell immunity after vaccination: One was vaccinated thrice and one was the only patient of the entire cohort that had received heterologous prime-boost immunization with BNT162b and ChAdOx1. BNT BNT162b, ChAd ChAdOx1, HC Healthy Control.

patients), as older individuals respond with lower antibody levels to vaccination. However, in the rather small fraction of SLL/CLL patients who responded to vaccination, similar titers of neutralizing antibodies were detectable in HC. Further, we only included one treatment-naïve patient and therefore cannot fully conclude the impact of CLL-directed treatment as compared with untreated CLL on cellular immunity. Previous trials reported inferior serologic immunogenicity in treatment-naïve patients as compared with patients previously treated [4, 5, 10]. Future studies should provide more data comparing those two subgroups of CLL patients and further focus on cellular immunity.

In conclusion, we demonstrate inferior T cell response to COVID-19 vaccines in SLL/CLL patients as compared with HC, supporting the importance of a third vaccine dose for those. The prime-boost regime, in particular the choice of best vaccine combination, is yet to determine. Our observation of discordant immune responses in the majority of patients indicates that the humoral response may not be reliable as the sole surrogate marker of protection in the patients with CLL and further B cell depleting malignancies, at least if negative.

REFERENCES

- Chatzikonstantinou T, Kapetanakis A, Scarfò L, Karakatsoulis G, Allsup D, Cabrero AA, et al. COVID-19 severity and mortality in patients with CLL: An update of the international ERIC and Campus CLL study. *Leukemia*. 2021;35:3444–54.
- Koch T, Mellinghoff SC, Shamsrizi P, Addo MM, Dahlke C. Correlates of vaccine-induced protection against SARS-CoV-2. *Vaccines*. 2021;9:238.
- Braun J, Loyal L, Frensch M, Wendisch D, Georg P, Kurth F, et al. SARS-CoV-2-reactive T cells in healthy donors and patients with COVID-19. *Nature*. 2020;587:270–4.
- Benjamini O, Rokach L, Itchaki G, Braester A, Shvidel L, Goldschmidt N, et al. Safety and efficacy of BNT162b mRNA Covid19 Vaccine in patients with chronic lymphocytic leukemia. *Haematologica*. 2021. <https://doi.org/10.3324/haematol.2021.279196>. Epub ahead of print.
- Herishanu Y, Avivi I, Aharon A, Shefer G, Levi S, Bronstein Y, et al. Efficacy of the BNT162b2 mRNA COVID-19 vaccine in patients with chronic lymphocytic leukemia. *Blood*. 2021;137:3165–73.
- Tadmor T, Benjamini O, Braester A, Rahav G, Rokach L. Antibody persistence 100 days following the second dose of BNT162b mRNA Covid19 vaccine in patients with chronic lymphocytic leukemia. *Leukemia*. 2021;35:2727–30.

- Parry H, McIlroy G, Bruton R, Ali M, Stephens C, Damery S, et al. Antibody responses after first and second Covid-19 vaccination in patients with chronic lymphocytic leukaemia. *Blood. Cancer J*. 2021;11:136.
- Ehmsen S, Asmussen A, Jeppesen SS, Nilsson AC, Østerlev S, Vestergaard H, et al. Antibody and T cell immune responses following mRNA COVID-19 vaccination in patients with cancer. *Cancer Cell*. 2021;39:1034–6.
- Pozzetto B, Legros V, Djebali S, Barateau V, Guibert N, Villard M, et al. Immunogenicity and efficacy of heterologous ChAdOx1-BNT162b2 vaccination. *Nature*. 2021. <https://doi.org/10.1038/s41586-021-04120-y>. Epub ahead of print.
- da Cunha-Bang C, Kirkby NS, Friis-Hansen L, Niemann CU. Serological response following vaccination with BNT162b2 mRNA in patients with chronic lymphocytic leukemia. *Leuk Lymphoma*. 2021;1–3. <https://doi.org/10.1080/10428194.2021.1973673>. Epub ahead of print.
- Döhner H, Stilgenbauer S, Benner A, Leupolt E, Kröber A, Bullinger L, et al. Genomic aberrations and survival in chronic lymphocytic leukemia. *N Engl J Med*. 2000;343:1910–6.

ACKNOWLEDGEMENTS

We thank the working groups of PD Hans-Anton Schlößer, Florian Klein, and Marylyn M. Addo for all logistical and technical support. Especially, we thank Larisa Idrizovic and Tatjana Lammertz for their continuous support.

AUTHOR CONTRIBUTIONS

SCM and PL implemented the research and design of the study. They were responsible for data assessment, coordination, and conduction of the study and authored the paper. SR performed the statistical analyses and co-authored the paper. LMW and LM performed the T and B cell vaccine response laboratory analyses and co-authored the paper. HG and KV the humoral vaccine response laboratory analyses and co-authored the manuscript. HAS and MT performed blood sample processing and co-authored the paper. CD, MMA, FK, AMF, KF, BE, and MH supervised the conduct of the study, gave advice for study design and laboratory analyses, and co-authored the paper.

FUNDING

Open Access funding enabled and organized by Projekt DEAL.

S.C. Mellinghoff et al.

565

COMPETING INTERESTS

SCM reports grants from DZIF (Clinical Leave Stipend). AMF reports research funding from Celgene/Bristol Myers Squibb (Inst), AstraZeneca (Inst), and travel Expenses by AbbVie. KF reports other from Roche, other from AbbVie. BE reports grants and personal fees from Janssen-Cilag, grants and personal fees from Roche, personal fees from Novartis, grants and personal fees from AbbVie, personal fees from Celgene, personal fees from ArQule, personal fees from AstraZeneca, personal fees from Oxford Biomedica (UK), grants and personal fees from Gilead, grants from BeiGene, outside the submitted work. MH reports other from AbbVie, other from F. Hoffman-LaRoche, other from Gilead, other from Janssen-Cilag, other from Mundipharma, during the conduct of the study. PL reports grants and personal fees from Janssen-Cilag, personal fees from Abbvie, other from F. Hoffman-LaRoche, personal fees from AstraZeneca. The remaining authors declare no competing financial interests for this study.

ADDITIONAL INFORMATION

Supplementary information The online version contains supplementary material available at <https://doi.org/10.1038/s41375-021-01500-1>.

Correspondence and requests for materials should be addressed to Sibylle C. Mellinghoff.

Reprints and permission information is available at <http://www.nature.com/reprints>

Publisher's note Springer Nature remains neutral with regard to jurisdictional claims in published maps and institutional affiliations.



Open Access This article is licensed under a Creative Commons Attribution 4.0 International License, which permits use, sharing, adaptation, distribution and reproduction in any medium or format, as long as you give appropriate credit to the original author(s) and the source, provide a link to the Creative Commons license, and indicate if changes were made. The images or other third party material in this article are included in the article's Creative Commons license, unless indicated otherwise in a credit line to the material. If material is not included in the article's Creative Commons license and your intended use is not permitted by statutory regulation or exceeds the permitted use, you will need to obtain permission directly from the copyright holder. To view a copy of this license, visit <http://creativecommons.org/licenses/by/4.0/>.

© The Author(s) 2021

2.6 SARS-CoV-2-specific cellular response following third COVID-19 vaccination in patients with chronic lymphocytic leukemia

Sibylle C. Mellinghoff,* Leonie Mayer,* Sandra Robrecht, **Leonie M. Weskamm**, Christine Dahlke, Henning Gruell, Maïke Schlotz, Kanika Vanshylla, Hans A. Schlößer, Martin Thelen, AnnaMaria Fink, Kirsten Fischer, Florian Klein, Marylyn M. Addo, Barbara Eichhorst, Michael Hallek and Petra Langerbeins

*These authors contributed equally

Published in *Haematologica*, DOI: 10.3324/haematol.2022.280982

Leonie Marie Weskamm was involved in study design and reviewing of the manuscript and figures. She was also involved in the coordination and laboratory work to establish the healthy control cohort, including isolation and cryopreservation of PBMCs, plasma and serum from human blood samples.

I hereby confirm the accuracy of these contributions

 17.1.2023

Prof. Dr. med. Marylyn M. Addo

LETTER TO THE EDITOR

SARS-CoV-2-specific cellular response following third COVID-19 vaccination in patients with chronic lymphocytic leukemia

With great interest we read the study published by Blixt *et al.* showing that compared to healthy controls (HC), half as many of chronic lymphocytic leukemia (CLL) patients developed a T-cell response after two COVID-19 vaccine doses.¹ Effects of a third vaccine dose on T cells in CLL patients is yet unknown, while approximately 20% fail achieving a humoral immune response.² In this prospective cohort study we investigated the interplay of humoral and cellular response and report follow-up data of CLL patients 31 days (range, 19–94 days) after third vaccination (V3).³

Blood samples of CLL registry (clinicaltrials.gov. Identifier: NCT02863692) patients were evaluated after three COVID-19 vaccinations. Six of the initially 21 patients³ were included in the analyses, three with homologous and three with heterologous vaccination schedule (mean interval between vaccination 2 [V2] and V3 163 days; minimum 117 days and maximum 189 apart). Four vaccinated health care workers served as HC (mean interval between V2 and V3 266 days; range, 254–291 days). Both studies were approved by the local ethics committee. Patient and disease characteristics as well as vaccination schedules are summarized in Table 1.

SARS-CoV-2 spike receptor binding domain (RBD)-specific immunoglobulin G (IgG) antibodies, determined using the Alinity ci SARS-CoV-2 IgG II Quant assay (Abbott), were detectable in four of six (66.7%) CLL patients after compared to two of six (33.3%) before booster vaccination (Figure 1A), cut-off ≥ 7.1 BAU/mL. In the one individual with detectable RBD-specific IgG after V2, V3 resulted in increased levels. In another individual, the V3 raised the IgG titer to similar levels as seen shortly after V2 (Figure 1B and C). Detectable neutralizing serum activity, determined by a lentivirus-based pseudovirus neutralization assay against the Wu01 strain of SARS-CoV-2 was limited to the two individuals with the highest levels of RBD-binding IgG (Figure 1D).

Peripheral blood mononuclear cells (PBMC) were used for SARS-CoV-2 spike-specific T-cell analyses (Human IFN γ ELISpot^{PLUS} [ALP] kit [Mabtech]). Results are reported as spot-forming cells (SFC) per million PBMC. A SARS-CoV-2 peptide pool (15-mers overlapping by 11 amino acids which stimulate responses mediated by both CD4 + and CD8 + T cells) spanning the entire spike protein was used for measuring T-cell responses. The median number of SARS-CoV-2 spike-specific T cells in the CLL cohort after V2

BNT162b was 31 SFC (interquartile range [IQR], 4.0–96.0) (Figure 2A). The response after V2 in the here described subgroup was significantly lower (1.7 SFC; IQR, 0.0–3.8 but increased to 8 SFC; IQR, 5.7–21.3) after booster vaccination. Overall, four of six (66.7%) showed a detectable increase of T-cell activity and two a decrease (Figure 2B). In comparison, T-cell responses in HC remained above the cut-off in 100% (4/4), but did not increase further.

Of the included patients, all received either B-cell-depleting (anti-CD20 monoclonal antibodies) or -directed (bruton tyrosine kinase inhibitors) treatment within 6 months prior to V3. Despite B-cell-affecting treatment, the majority (4/6) showed an increase of serum IgG (Figure 1C). Patients under B-cell-depleting treatment (2/6) mounted low levels of IgG antibodies after boost that did not result in detectable neutralizing serum activity (Table 1). Patients without detectable T cells prior to boost that received a heterologous booster immunization showed an increase in T-cell response. In contrast, homologous booster led to an increase in only one of three patients and did not show an effect on the remaining two patients (Figure 2B). A discordant immune response with T cell, but lacking humoral response was seen in two of six patients, indicating that cellular protection may be generated, probably in patients with lesser extent of CLL-associated T-cell exhaustion, whereas treatment-associated B-cell impairment may not be overcome.

In conclusion, we report an increase of vaccine-induced cellular and humoral immune responses in CLL patients by a V3 COVID-19 vaccination.

Recent data showed a significant increased humoral response after COVID-19 vaccination, but less pronounced enhancement of the cellular response in healthy individuals, likely to be dependent on the specific booster vaccine.^{4–6} Our data from the HC cohort – all vaccinated with a homologous BNT162b2 dose – confirm these findings and show a stable, but not relevantly increased T-cell response. As already shown for rheumatologic and solid organ transplant patients, this may not generally be the case for immunocompromised patients.^{7,8}

We here report an increase of the humoral response in CLL patients after COVID-19 V3 despite B-cell-depleting treatment, as reported elsewhere,⁹ and in addition, an increase of the cellular response in four of six patients.

Our data show that V3 enhances IgG response in CLL patients, also in those that lacked detectable IgG after V2.

LETTER TO THE EDITOR

Table 1. Patient characteristics and outcomes versus healthy controls.

| Patient | Sex | Age in years | Vaccine (Prime) | Vaccine (Boost) | Days of sampling after booster | After V2 | | | After V3 | | | B-cell-depleting therapy | B-cell-directed therapy | State of disease |
|---------|-----|--------------|-----------------|-----------------|--------------------------------|----------|----------------------------|----------|----------|----------------------------|----------|--------------------------|-------------------------|------------------|
| | | | | | | IgG** | Serum ID ₅₀ *** | T cells* | IgG** | Serum ID ₅₀ *** | T cells* | | | |
| 1 | M | 78 | BNT/BNT | BNT | 13 | 33 | <10 | 4 | 42,9 | 44 | 25 | No | Yes | PR |
| 2 | M | 78 | BNT/BNT | AZD | 31 | neg. | <10 | 0 | neg. | <10 | 9 | No | Yes | PR |
| 3 | M | 76 | BNT/BNT | BNT | 28 | 2,225 | 1,206 | 3 | 10,999 | 19,214 | 0 | No | Yes | PR |
| 4 | M | 71 | BNT/BNT | AD | 63 | neg. | <10 | 0 | 8,3 | <10 | 7 | Yes | Yes | CR |
| 5 | F | 73 | BNT/BNT | AD | 36 | neg. | <10 | 0 | 11,8 | <10 | 81 | Yes | No | CR |
| 6 | M | 71 | BNT/BNT | BNT | 31 | neg. | <10 | 23 | neg. | <10 | 5 | No | Yes | PD |

| Healthy control | Sex | Age in years | Vaccine (Prime) | Vaccine (Boost) | Days of sampling after booster | After V2 | | After V3 | |
|-----------------|-----|--------------|-----------------|-----------------|--------------------------------|----------|-------|----------|-------|
| | | | | | | T cells* | IgG** | T cells* | IgG** |
| 1 | F | 25 | BNT/BNT | BNT | 28 | 165.3 | 202.7 | 404 | 428 |
| 2 | M | 30 | BNT/BNT | BNT | 28 | 381.3 | 428 | 428 | 77.3 |
| 3 | F | 38 | BNT/BNT | BNT | 37 | 692 | 116 | 116 | 116 |
| 4 | F | 49 | BNT/BNT | BNT | 27 | 116 | 116 | 116 | 116 |

*S-specific T cells (spot-forming cells/10⁶ peripheral blood mononuclear cells); **RBD-specific IgG (BAU/mL); ***neutralization activity (serum ID₅₀ Wu01 Pseudovirus), V2: second vaccination; V3: third vaccination; IgG: immunoglobulin G; F: female; M: male; ID₅₀: infective dose; AD: Ad26.COV2, AZ: AZD1222, BNT: BNT162b2; CR: complete remission; PD: progressive disease; PR: partial remission; neg: negative.

LETTER TO THE EDITOR

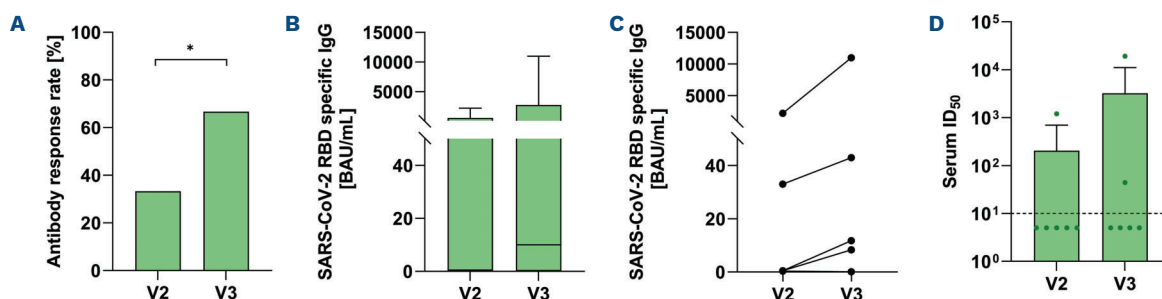


Figure 1. Humoral immune responses after COVID-19 vaccination (A) Antibody response rate in chronic lymphocytic leukemia (CLL) patients after second (V2) and after third (V3) vaccination. (B) SARS-CoV-2 spike receptor binding domain (RBD)-specific immunoglobulin G (IgG) in CLL patients after V2 and V3 (median 10.05 BAU/mL, range 0.1-10,998.6) measured by chemiluminescent microparticle immunoassay. (C) Individual course of IgG anti-bodies in CLL patients after V2 and V3. (D) Serum neutralizing activity (50% inhibitory serum dilution) determined in a pseudovirus neutralizing assay against the Wu-01 pseudovirus strain. Bars indicating geometric mean ID₅₀ with 95% confidence intervals. Dashed line indicates limit of detection (LOD, 10). Samples with no detectable neutralization (ID₅₀ <10) were plotted with an ID₅₀ of 5 (1/2 LOD) for graphical representation.

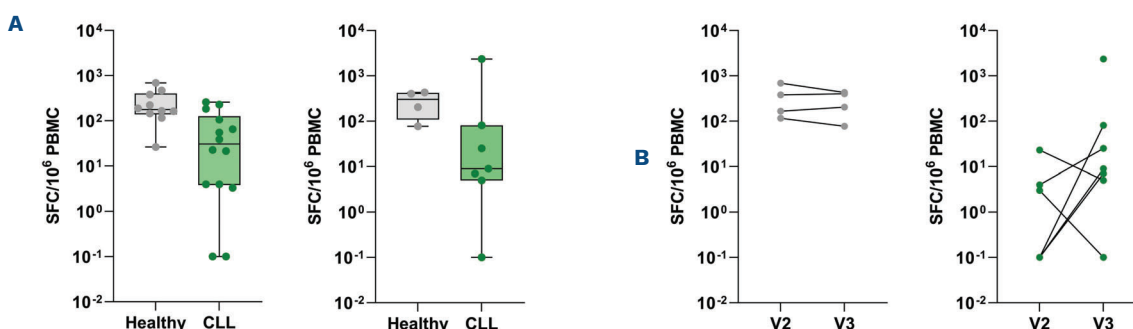


Figure 2. T-cell immune responses after COVID-19 vaccination. (A) Interferon- γ T-cell ELISpot response in chronic lymphocytic leukemia (CLL) patients and healthy controls (HC). Shown values are mean spots of duplicate wells, where background in negative control wells is subtracted from peptide-stimulated wells. The line displays the median response after second (V2) (left) and third (V3) vaccination (right). The limit of detection is 8 spot-forming cells/10⁶ peripheral blood mononuclear cells. Samples were acquired 28 days after V3 in HC and at a median of 47 and 31 days (V2 and V3, respectively) in CLL patients. (B) Individual course of Interferon- γ T cell ELISpot response in HC (left) and CLL patients (right) after V2 and V3.

We found that anti-SARS CoV-2 antibodies were higher in patients who received three doses of BNT162b2 compared to two doses of BNT162b2 and a vector vaccine as booster, but that the latter vaccine combination was able to mount a serologic response in two of three previously negative patients. Yet, neutralizing serum activity was only partly detectable. In order to elicit a neutralizing serum response, a fourth dose might be beneficial by further increasing IgG levels.^{10,11}

We can confirm previous data from immunocompromised patients with rheumatological disease,⁷ solid organ transplantation⁹ and solid malignancies¹² within our CLL cohort revealing that T-cell responses are enhanced following V3. Further indepth analyses may provide insights into their (poly-)functionality, proliferation capacity, or epigenetic profile change after (booster) vaccination despite the low

response-altitude and whether the response is biased towards CD4+ or CD8+ T cells.

Interestingly, all patients who received a heterologous boost (vector vaccine) showed an increased T cell response compared to our previous analysis, while only one of three after homologous boost. This supports recently published data from randomized controlled as well as observational studies suggesting a benefit of a heterologous boost for eliciting stronger T-cell responses compared to homologous immunization.^{4,13} If this offers additional protection for patients with low or absent neutralizing antibodies is yet unclear, particularly considering the low response levels with respect to quantity. Considering recent data on SARS-CoV-2-specific T cells from patients with agammaglobulinaemia^{14,15} showing protection from severe disease and even in patients infected with variants

LETTER TO THE EDITOR

of concern,¹⁶ we hypothesize a potential benefit of increased T-cell immunity. The impact of a fourth vaccine dose on altitude and functionality of T cells should be subject of forthcoming studies.

A limitation of this study is the small sample size. In addition, our small cohort consists of mostly male and comparably old patients. Male sex and advanced age known as relevant factors for an impaired immune response which likely affect our results, but also reflect the CLL patient population well.

In conclusion, we demonstrate an inferior T-cell response to COVID-19 vaccines in CLL patients as compared to HC, but possibly higher capacity in those patients to boost such response by V3 COVID-19. While the ideal primeboost regime is yet to determine, our data encourage to evaluate heterologous immunization by clinical trials in CLL patients.

Authors

Sibylle C. Mellingshoff,^{1,2,3*} Leonie Mayer,^{3,4,5*} Sandra Robrecht,¹ Leonie M. Weskamm,^{3,4,5} Christine Dahlke,^{3,4,5} Henning Gruell,⁶ Maïke Schlotz,⁵ Kanika Vanshylla,⁶ Hans A. Schlöber,⁷ Martin Thelen,⁷ AnnaMaria Fink,¹ Kirsten Fischer,¹ Florian Klein,^{2,6,7} Marylyn M. Addo,^{3,4,5} Barbara Eichhorst,¹ Michael Hallek¹ and Petra Langerbeins¹

¹Faculty of Medicine and University Hospital of Cologne, Department I of Internal Medicine, Center for Integrated Oncology Aachen Bonn Cologne Düsseldorf (CIO ABCD), University of Cologne, Cologne; ²German Center for Infection Research (DZIF), partner site Bonn-Cologne, Cologne; ³Department of Clinical Immunology of Infectious Diseases, Bernhard Nocht Institute for Tropical Medicine, Hamburg; ⁴Division of Infectious Diseases, First Department of Medicine, University Medical Center Hamburg-Eppendorf, Hamburg; ⁵German Center for Infection Research (DZIF), Partner Site Hamburg-Lübeck-Borstel-Riems, Hamburg; ⁶Institute of Virology, Faculty of Medicine and University Hospital Cologne, University of Cologne, Cologne and ⁷Center for Molecular Medicine Cologne, University of Cologne, Faculty of Medicine and University Hospital Cologne, Cologne, Germany

*SCM and LM contributed equally as co-first authors.

Correspondence:

S.C. MELLINGHOFF - sibylle.mellingshoff@uk-koeln.de

References

1. Blixt L, Wullmann D, Aleman S, et al. T cell immune responses following vaccination with mRNA BNT162b2 against SARS-CoV-2 in patients with chronic lymphocytic leukemia: results from a prospective open-label clinical trial. *Haematologica*. 2022;107(4):1000-1003.
2. Herishanu Y, Rahav G, Levi S, et al. Efficacy of a third BNT162b2 mRNA COVID-19 vaccine dose in patients with CLL who failed standard 2-dose vaccination. *Blood*. 2022;139(5):678-685.

<https://doi.org/10.3324/haematol.2022.280982>

Received: March 14, 2022.

Accepted: June 14, 2022.

Prepublished: June 23, 2022.

©2022 Ferrata Storti Foundation

Published under a CC BY-NC license 

Disclosures

SCM reports grants from DZIF (Clinical Leave Stipend). AMF reports research funding from Celgene/Bristol Myers Squibb (Inst), AstraZeneca (Inst), and travel expenses from AbbVie. KF reports other support from Roche and AbbVie. BE reports grants and personal fees from Janssen-Cilag, AbbVie, Roche and Gilead, personal fees from Novartis, Celgene, ArQule, AstraZeneca and Oxford Biomedica (UK), as well as grants from BeiGene, outside the submitted work. MH reports other support from AbbVie, F. Hoffman-LaRoche, Gilead, Janssen-Cilag and Mundipharma, during the conduct of the study. PL reports grants and personal fees from Janssen-Cilag, personal fees from AbbVie and AstraZeneca, and other support from F. Hoffman-LaRoche. SR reports honoraria from AstraZeneca. All other authors have no conflicts of interest to disclose.

Contributions

SCM and PL implemented the research and design of the study. They were responsible for data assessment, coordination and conduct of the study and authored the manuscript. LM performed the T-cell vaccine response laboratory analyses and co-authored the manuscript. HG and KV performed the humoral vaccine response laboratory analyses and co-authored the manuscript. HAS, MS and MT performed blood sample processing and co-authored the manuscript. LMW, SR, CD, MMA, FK, AMF, KF, BE and MH supervised the conduct of the study, gave advice for study design and laboratory analyses and co-authored the manuscript.

Acknowledgments

We thank the working groups of PD Dr. Hans-Anton Schlöber, Prof. Dr. Florian Klein and Prof. Dr. Marylyn M. Addo for all logistical and technical support. Especially, we thank Larisa Idrizovic, and Tatjana Lammertz for their continuous support.

Data-sharing statement

Data may be available upon request to the corresponding author.

LETTER TO THE EDITOR

3. Mellinghoff SC, Robrecht S, Mayer L, et al. SARS-CoV-2 specific cellular response following COVID-19 vaccination in patients with chronic lymphocytic leukemia. *Leukemia*. 2022;36(2):562-565.
4. Munro APS, Janani L, Cornelius V, et al. Safety and immunogenicity of seven COVID-19 vaccines as a third dose (booster) following two doses of ChAdOx1 nCov-19 or BNT162b2 in the UK (COV-BOOST): a blinded, multicentre, randomised, controlled, phase 2 trial. *Lancet*. 2021;398(10318):2258-2276.
5. Liu X, Shaw RH, Stuart ASV, et al. Safety and immunogenicity of heterologous versus homologous prime-boost schedules with an adenoviral vectored and mRNA COVID-19 vaccine (Com-COV): a single-blind, randomised, non-inferiority trial. *Lancet*. 2021;398(10303):856-869.
6. Flaxman A, Marchevsky NG, Jenkin D, et al. Reactogenicity and immunogenicity after a late second dose or a third dose of ChAdOx1 nCov-19 in the UK: a substudy of two randomised controlled trials (COV001 and COV002). *Lancet*. 2021;398(10304):981-990.
7. Bonelli M, Mrak D, Tobudic S, et al. Additional heterologous versus homologous booster vaccination in immunosuppressed patients without SARS-CoV-2 antibody seroconversion after primary mRNA vaccination: a randomised controlled trial. *Ann Rheum Dis*. 2022;81(5):687-694.
8. Schrezenmeier E, Rincon-Arevalo H, Stefanski A-L, et al. B and T cell responses after a third dose of SARS-CoV-2 vaccine in kidney transplant recipients. *J Am Soc Nephrol*. 2021;32(12):3027-3033.
9. Marlet J, Gatault P, Maakaroun Z, et al. Antibody responses after a third dose of COVID-19 vaccine in kidney transplant recipients and patients treated for chronic lymphocytic leukemia. *Vaccines (Basel)*. 2021;9(10):1055.
10. Krammer F. A correlate of protection for SARS-CoV-2 vaccines is urgently needed. *Nat Med*. 2021;27(7):1147-1148.
11. Earle KA, Ambrosino DM, Fiore-Gartland A, et al. Evidence for antibody as a protective correlate for COVID-19 vaccines. *Vaccine*. 2021;39(32):4423-4428.
12. Fendler A, Au L, Shepherd STC, et al. Functional antibody and T cell immunity following SARS-CoV-2 infection, including by variants of concern, in patients with cancer: the CAPTURE study. *Nat Cancer*. 2021;2(12):1321-1337.
13. Pozzetto B, Legros V, Djebali S, et al. Immunogenicity and efficacy of heterologous Cha-dOx1/BNT162b2 vaccination. *Nature*. 2021;600(7890):701-706.
14. Soresina A, Moratto D, Chiarini M, et al. Two X-linked agammaglobulinemia patients develop pneumonia as COVID-19 manifestation but recover. *Pediatr Allergy Immunol*. 2020;31(5):565-569.
15. Breathnach AS, Duncan CJA, Bouzidi KE, et al. Prior COVID-19 protects against reinfection, even in the absence of detectable antibodies. *J Infect*. 2021;83(2):237-279.
16. Keeton R, Tincho MB, Ngomti A, et al. T cell responses to SARS-CoV-2 spike cross-recognize Omicron. *Nature*. 2022;603(7901):488-492.

3 Unpublished Data

Based on the study cohort described in the manuscript “*Persistence of MERS-CoV-spike-specific B cells and antibodies after late third immunization with the MVA-MERS-S vaccine*”, additional analyses were conducted aiming at the investigation of non-neutralizing antibody functions, which have been suggested to play an important role in the protection from viral diseases (Tay et al., 2019, Lu et al., 2018). Briefly, study participants received two vaccinations (V1, V2) with the MVA-MERS-S vaccine candidate 28 days apart, and a late third vaccination (V3) was administered approximately one year after prime. The Fc-mediated antibody functions ADCP and ADNKA (antibody-dependent NK cell activation, used as a surrogate for ADCC (Morrison et al., 2017, Alter et al., 2004)) were analyzed using purified IgG from plasma samples obtained at different time points before (D0), as well as 28 days (D28) and twelve months (M12) after vaccination. The assay procedures and preliminary results of these analyses are reported below.

3.1 ADCP capacity induced by MVA-MERS-S vaccination

The ADCP capacity of MERS-CoV spike-specific IgG antibodies was assessed using the monocytic THP-1 cell line and fluorescent beads in combination with a flowcytometric readout. The assay was developed by Paulina Tarnow, based on protocols described by different research groups (Ackerman et al., 2011, Jennewein et al., 2022, Vono et al., 2021). Briefly, yellow-green fluorescent beads (NeutrAvidin-labeled FluoSpheres, Invitrogen) were coupled with previously biotinylated MERS-CoV spike S1 protein (Sino Biological) and subsequently incubated with purified IgG from vaccinee plasma samples, leading to immobilization of S1-specific antibodies on the bead surface. THP-1 cells were then incubated with the antibody-coated beads for 16 hours, followed by staining with the LIVE/DEAD Fixable Violet Dead Cell Stain Kit (Life Technologies). The flowcytometric readout was performed using the LSRFortessa (BD Biosciences) and subsequent data analysis was conducted using the FlowJo software (FlowJo, LLC). After exclusion of doublets and dead cells, the phagocytosis of beads by THP-1 cells was assessed via the emission of the yellow-green fluorescent beads in the fluorescein isothiocyanate (FITC) channel (Figure 9A). The antibodies' ADCP capacity was quantified as a phagocytic score, calculated based on the percentage of FITC-positive cells (reflecting the percentage of cells that internalized beads) and the mean fluorescence intensity (MFI) of FITC-positive cells (reflecting the number of internalized beads per cell) (Figure 9B).

A longitudinal analysis of S1-specific antibodies induced by MVA-MERS-S vaccination revealed a slight increase in the ADCP capacity after the first two vaccinations (V2D28), with a median foldchange of 1.2 compared to baseline (V1D0) (Figure 9C). In the following nine to fifteen months, the ADCP capacity of S1-specific antibodies decreased to baseline levels. After the late third vaccination, it increased again, resulting in significantly higher levels compared to the second vaccination (median foldchange V3D28 vs V1D0: 1.7). The ADCP capacity decreased again in the following months. However, as opposed to the course after the second vaccination, it remained elevated twelve months after the third vaccination (V3M12), with higher levels compared to the peak response observed after the second vaccination (V2D28).

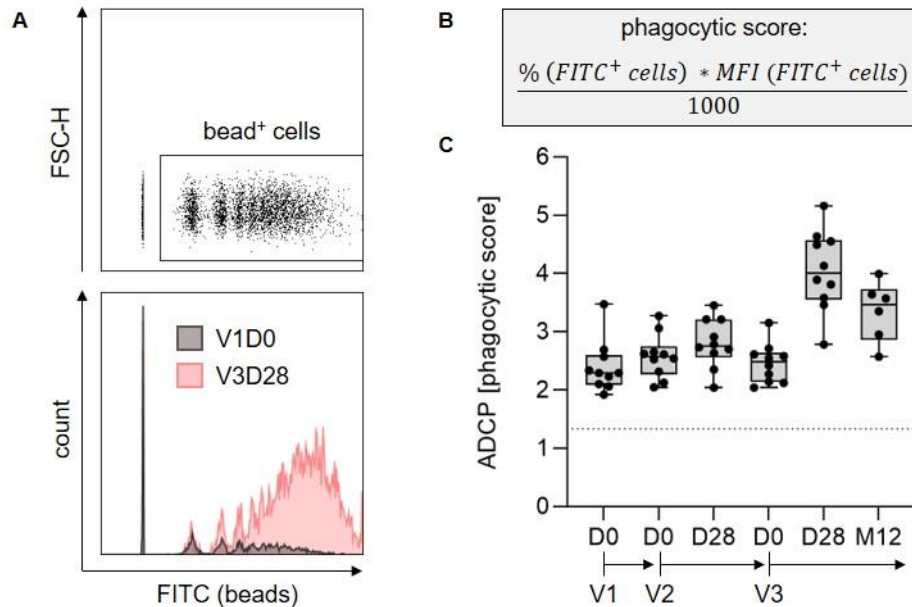


Figure 9: Antibody-dependent cellular phagocytosis (ADCP) capacity of MERS-CoV spike S1-specific antibodies induced by MVA-MERS-S vaccination. A) Flowcytometric readout. After exclusion of doublets and dead cells, THP-1 cells with internalized beads were identified based on their FITC signal (upper panel). Exemplary histograms of the FITC signal are shown for THP-1 cells assayed with beads coated with purified IgG samples collected at baseline (V1D0) and 28 days after the third vaccination (V3D28), respectively (lower panel). **B)** Formula for calculation of the phagocytic score, based on the percentage and mean fluorescence intensity (MFI) of FITC-positive THP-1 cells. **C)** Longitudinal ADCP capacity of S1-specific antibodies, displayed as phagocytic scores for individual study participants. Boxplots indicate median, interquartile range and min to max range. The dotted line indicates the phagocytic score measured for the PBS control. Measurements were performed in triplicates. V1, V2, V3: vaccination 1, 2, 3; D0, D28: day 0, 28; M12: month 12.

3.2 ADNKA capacity induced by MVA-MERS-S vaccination

The antibodies' ADNKA capacity was assessed using NK cells from healthy donors in combination with a flowcytometric readout, as previously reported in several studies (Damelang et al., 2021, Zohar et al., 2020, Bradley et al., 2017). Briefly, protein binding plates were coated with the MERS-CoV spike S1 protein (Sino Biological) and subsequently incubated with purified IgG from vaccinee plasma samples, leading to immobilization of S1-specific antibodies. NK cells were freshly isolated from a healthy donor using the RosetteSep Human NK Cell Enrichment Cocktail (STEMCELL Technologies) and incubated with immobilized S1-specific antibodies for five hours, in the presence of Monensin (Biolegend), Brefeldin A (BD Biosciences), and PE-conjugated anti-CD107 α antibody (Biolegend). Subsequently, the cells were stained with the Zombie NIR™ Fixable Viability Kit (Biolegend) and BV785-conjugated anti-CD56 antibody (Biolegend), followed by intracellular staining of interferon γ (IFN- γ) and macrophage inflammatory protein 1 β (MIP-1 β) with PE-Cy7-conjugated anti-IFN- γ antibody (Biolegend) and BV421-conjugated anti-MIP-1 β antibody (BD Biosciences). NK cell activation was measured using a flowcytometric readout with the spectral flow cytometer Cytek Aurora (Cytek Biosciences) and subsequent data analysis was performed using the FlowJo software (FlowJo, LLC). After exclusion of doublets and dead cells, NK cells were identified based on their expression of CD56, and ADNKA was assessed by their expression of CD107 α , IFN- γ and MIP-1 β (Figure 10A-C).

The longitudinal analysis of MERS-CoV S1-specific antibodies for their ADNKA capacity revealed the same overall dynamics as observed for ADCP, with a slight increase of all three NK cell activation markers (CD107 α , IFN- γ , MIP-1 β) after the first two vaccinations and a stronger increase following the late third vaccination (Figure 10D-F). After the second vaccination, CD107 α , IFN- γ and MIP-1 β showed increases of 1.6-, 1.5- and 1.5-fold, respectively (median foldchanges V2D28 vs V1D0), whereas the late booster vaccination induced significantly higher increases of 8.1-, 13.0- and 10.7-fold, respectively (median foldchanges V3D28 compared to V1D0). Twelve months after the third vaccination (V3M12), the expression of all three markers remained above the levels measured at V2D28.

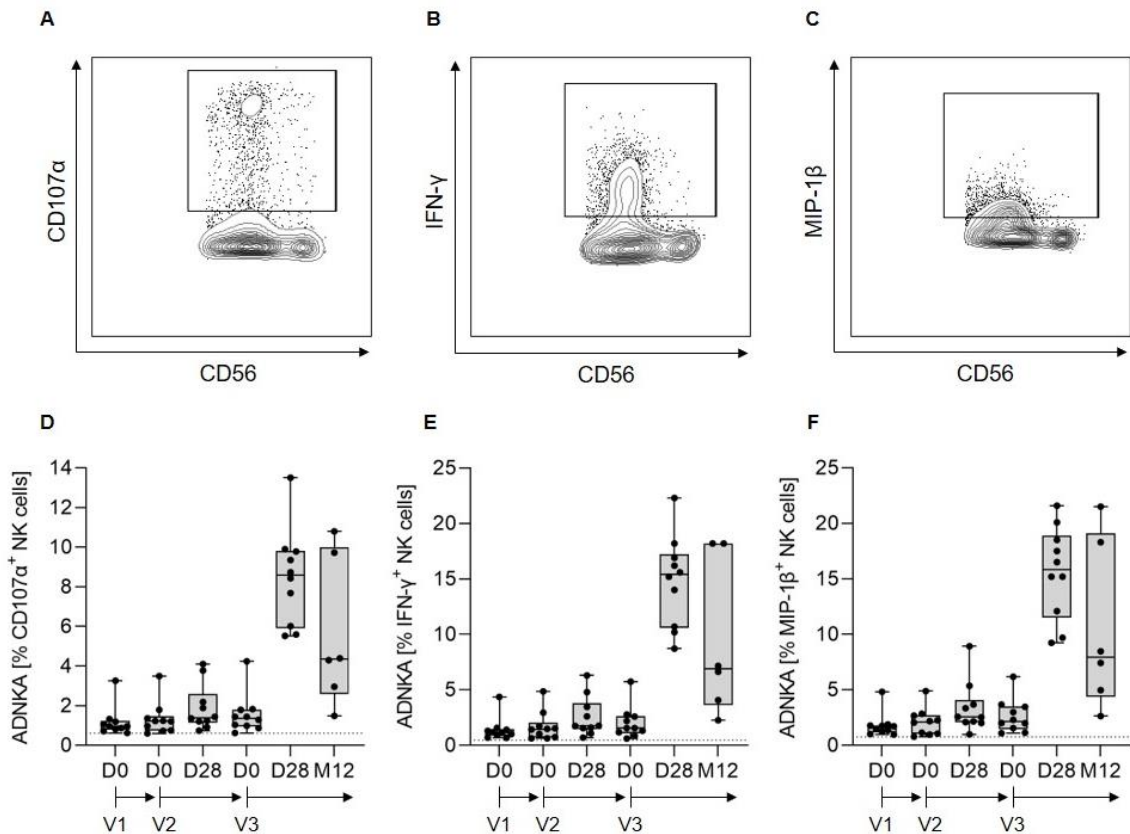


Figure 10: Antibody-dependent NK cell activation (ADNKA) capacity of MERS-CoV spike S1-specific antibodies induced by MVA-MERS-S vaccination. A-C) After exclusion of doublets and dead cells, and identification of NK cells based on their expression of CD56, ADNKA was assessed by expression of CD107 α , IFN- γ and MIP-1 β . Representative contour plots are shown for NK cells assayed with purified IgG from one study participant, collected 28 days after the third vaccination (V3D28). **D-F)** Longitudinal ADNKA capacity of S1-specific antibodies, displayed as expression of CD107 α , IFN- γ and MIP-1 β , induced by purified IgG antibodies from individual study participants. Boxplots indicate median, interquartile range and min to max range. The dotted lines indicate ADNKA induced by PBS control. V1, V2, V3: vaccination 1, 2, 3; D0, D28: day 0, 28; M12: month 12.

4 Discussion

4.1 Background and study design

The major focus of this thesis was the characterization of humoral and B cell responses elicited by the rMVA-based MERS and COVID-19 vaccine candidates tested at the UKE, namely MVA-MERS-S, MVA-SARS-2-S and MVA-SARS-2-ST (Figure 11). Additionally, the immunogenicity of MVA-SARS-2-S and MVA-SARS-2-ST was directly compared to observational cohorts of healthy individuals receiving different combinations of licensed COVID-19 vaccines based on the mRNA and ChAd vaccine platforms, to gain insights into the influence of platform technology and vaccination regimen on vaccine-induced immune mechanisms. As part of the work, a comprehensive repertoire of techniques was established, aiming at a detailed investigation of vaccine-induced humoral immune responses. Besides the magnitude of antigen-specific antibody and B cell responses, the analysis included antibody subclasses and non-neutralizing functionality as well as frequencies and phenotype of antigen-specific B cells.

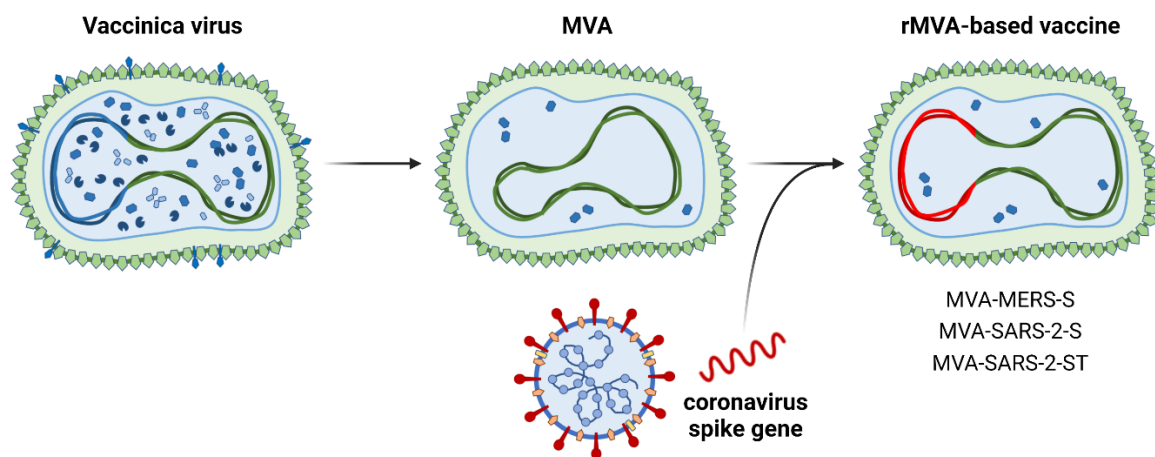


Figure 11: MVA as a platform for vaccines against emerging viruses. The Modified Vaccinia virus Ankara (MVA) was generated by serial tissue culture passage of the *Vaccinia virus* strain Ankara, leading to the loss of 15 % of the *Vaccinia virus* genome and the ability to replicate in mammalian cells. MVA was originally developed as a third-generation smallpox vaccine. Engineered to recombinantly express antigens of other pathogens, it can serve as a viral vector platform for vaccine development. The three recombinant MVA (rMVA)-based vaccine candidates MVA-MERS-S, MVA-SARS-2-S and MVA-SARS-2-ST, are encoding for the MERS-CoV and SARS-CoV-2 spike proteins, respectively, and were tested in early phase clinical trials at the University Medical Center Hamburg-Eppendorf.

4.1.1 rMVA as a vaccine platform

rMVA, the recombinant Modified Vaccinia virus Ankara, represents a promising viral vector platform for vaccine development against emerging pathogens. MVA is a highly attenuated orthopoxvirus strain that efficiently infects but does not replicate in human cells. Historically, it was developed by serial tissue culture passage of the *Vaccinia virus* strain Ankara in chicken embryo fibroblasts (CEF), leading to the loss of 15 % of the *Vaccinia virus* genome and the ability to replicate in mammalian cells (Ura et al., 2014, Volz and Sutter, 2017). Originally developed as a third-generation smallpox vaccine, MVA was administered to over 120,000 individuals including immunocompromised patients and infants, revealing high efficacy, as well as an extraordinary safety profile and considerably smaller skin lesions compared to conventional smallpox vaccination (Yoshikawa, 2021, Stickl et al., 1974, Sutter and Staib,

2003, Walsh et al., 2013, Overton et al., 2015). In the EU, MVA has been licensed against smallpox since 2013 (Imvanex, Bavarian Nordic) and has recently been rolled out as a vaccine against mpox (also known as monkeypox) during the 2022 mpox PHEIC (EMA, 2013, EMA, 2022). In the US, the same vaccine was licensed against smallpox and mpox in 2019, under the name Jynneos (FDA, 2019b). Engineered to recombinantly express antigens of different pathogens, rMVA is serving as a viral vector vaccine platform that has been evaluated in multiple clinical studies, revealing an acceptable safety profile and strong immunogenicity, as reviewed by Volz and Sutter (2017) and Orlova et al. (2022). Clinical trials were conducted for rMVA-based vaccines against different infectious diseases, including those caused by HIV-1 (Gómez et al., 2011, García et al., 2011, Bakari et al., 2011), *Hepatitis B virus* (Cavenaugh et al., 2011), *Influenza A virus* (Berthoud et al., 2011), *Plasmodium falciparum* (Sheehy et al., 2012, Bejon et al., 2007), *Mycobacterium tuberculosis* (Tameris et al., 2013), MERS-CoV (Koch et al., 2020, Fathi et al., 2022, Weskamm et al., 2022b), and SARS-CoV-2 (Chiuppesi et al., 2022)(Mayer and Weskamm, submitted to *Nature Communications*), as well as several hemorrhagic fever viruses (Yoshikawa, 2021). The first rMVA-based vaccine to be approved for medical use in humans was the MVA-BN-Filo vaccine against EVD, which is administered as the second immunization in a heterologous prime-boost vaccination regimen with Ad26.ZEBOV (Anywaine et al., 2019, Mutua et al., 2019, EMA, 2020b). Besides extensive favorable safety data reported from different study cohorts (Volz and Sutter, 2017, Volkmann et al., 2021, Gilbert, 2013), rMVA has been shown to strongly activate innate immune responses mediated by TLRs and the inflammasome, resulting in an adjuvant effect for the induction of adaptive immune responses (Price et al., 2013, Zhu et al., 2007). In comparison to other viral vectors, rMVA has a higher capacity for insertion of foreign genes (up to 25 kb), providing a benefit for the development of multivalent vaccines encoding several antigens (Mastrangelo et al., 2000, Smith and Moss, 1983, Chiuppesi et al., 2020, Henning et al., 2021, Lauer Katharina et al., 2017, Bockstal et al., 2022). Pre-existing immunity against MVA, resulting from smallpox or more recently mpox vaccination or infection, may influence the immunogenicity of MVA-based vaccines (Cooney et al., 1991, Altenburg et al., 2018). However, several studies have described an effective induction of insert-specific immune responses by rMVA-based vaccines, despite pre-existing anti-vector immunity (Walsh et al., 2012, Altenburg et al., 2018, Gudmundsdotter et al., 2009) and in the context of homologous prime-boost vaccination regimens (La Rosa et al., 2017, Kreijtz et al., 2014, Fathi et al., 2022).

4.1.2 The MVA-MERS-S vaccine candidate

MVA-MERS-S, an rMVA-based vaccine candidate against MERS, was developed to encode the full-length MERS-CoV spike protein (Song et al., 2013) and showed promising results in pre-clinical studies, inducing neutralizing antibodies in both mice and dromedary camels (Langenmayer et al., 2018, Volz et al., 2015, Song et al., 2013, Haagmans et al., 2016). A phase 1a clinical trial was conducted between 2017 and 2019 at the UKE, investigating MVA-MERS-S vaccination at two different dose levels in 23 healthy adults. A homologous vaccination schedule with two doses, administered 28 days apart, revealed a benign safety profile and was shown to induce humoral and cellular immunity against the MERS-CoV spike protein; however, antibody levels waned within one year after the second vaccination in most of the study participants (Koch et al., 2020). In follow-up to the phase 1a study, the impact of a late booster vaccination was investigated in a subgroup of ten participants in a proof-of-concept study. A third vaccination with MVA-MERS-S was administered approximately one year after prime and induced a substantial increase in the titers of binding and neutralizing antibodies, (Fathi et al., 2022). The study participants were followed up for another two years after the late third immunization,

providing the opportunity to obtain insight into long-term persistence of vaccine-induced immune responses. Based on this cohort, we conducted a comprehensive analysis of spike-specific antibodies and B cells using different techniques. The results of our analyses support the potential of a late booster immunization with MVA-MERS-S to improve the quality and longevity of vaccine-induced immunity and elucidate differences in the immunological mechanisms of prime and booster vaccination (Weskamm et al., 2022b).

4.1.3 The MVA-SARS-2-S and MVA-SARS-2-ST vaccine candidates

Based on our previous experience with the MVA-MERS-S vaccine, we developed a vaccine candidate against COVID-19, MVA-SARS-2-S, encoding the full-length native SARS-CoV-2 spike protein. Pre-clinical studies in mice and hamsters showed an induction of spike-specific antibodies and T cells, protecting the animals from SARS-CoV-2 infection and disease (Tscherne et al., 2021). The MVA-SARS-2-S vaccine candidate proceeded to early phase clinical evaluation in October 2020, where it was administered to 30 healthy adults at two different dose levels, in the same two-dose vaccination schedule as MVA-MERS-S, 28 days apart. Despite the promising results of the pre-clinical studies, the MVA-SARS-2-S vaccine showed only low immunogenicity in humans, underlining the fact that pre-clinical models provide only limited prediction of immunogenicity and vaccine efficacy in humans. To enhance immunogenicity, an optimized vaccine candidate was developed: MVA-SARS-2-ST, encoding a pre-fusion stabilized version of the spike protein with an inactivated S1/2 cleavage site, showed increased immunogenicity in mice and hamster models compared to MVA-SARS-2-S (Meyer Zu Natrup et al., 2022). The phase 1 clinical trial of the MVA-SARS-2-ST vaccine was initiated in July 2021, using the same vaccination schedule as the previous study and investigating two different dose levels in 15 SARS-CoV-2 naïve study participants. In October 2021, a second arm was included into the study, testing MVA-SARS-2-ST as a booster vaccine at three different dose levels. In this arm of the study, one dose of MVA-ST was administered to 30 individuals who had received two doses of an mRNA vaccine at least six months before.

Evaluating the immunogenicity and efficacy of new COVID-19 vaccine candidates in SARS-CoV-2 naïve individuals has become increasingly difficult, due to the high prevalence of SARS-CoV-2 immunity in the human population and ethical issues of placebo-controlled efficacy studies. Therefore, new approaches have to be implemented to evaluate new vaccine candidates, based on immune parameters that can be used as CoPs (Krammer, 2021, Jin et al., 2021, Goldblatt et al., 2022a). In our study (Mayer and Weskamm, submitted to *Nature Communications*), we established two control cohorts of individuals receiving different schedules of licensed mRNA- and ChAd-based COVID-19 vaccines, and performed a side-by-side comparison to the rMVA-based vaccine candidates, using the same techniques and protocols. In our manuscript we report on humoral and T cell responses elicited by the rMVA-based vaccine candidates in comparison to the control cohorts. Our findings highlight the differences observed between vaccination platforms and regimens, including a differing magnitude of humoral and cellular immune responses, as well as differential induction of IgG subclasses and cytokines.

4.2 The spike protein as a vaccine antigen for emerging HCoVs

The majority of SARS, MERS and COVID-19 vaccines that have been evaluated in pre-clinical and clinical trials are based on the spike protein (Du et al., 2009, Zhang et al., 2020, Zhang et al., 2022c, Choi and

Kim, 2022, Alagheband Bahrami et al., 2022). Located on the virus surface, the spike protein is responsible for the characteristic coronavirus shape and has been shown to be immunogenic in natural infection (Fehr and Perlman, 2015, Du et al., 2009, Pallesen et al., 2017, Chen et al., 2022a). It consists of two subunits, S1 and S2, that play different roles in virus entry. Binding to the host cell receptors DPP4 (MERS-CoV) and ACE2 (SARS-CoV-2) is mediated via the receptor binding domain (RBD) contained in the S1 subunit. This is followed by protease cleavage at the junction between the two subunits and subsequent fusion between virus and host cell membranes, mediated by the highly conserved S2 subunit (Borrega et al., 2021, Zhu et al., 2020, Ou et al., 2020, Lu et al., 2014, Li, 2016, Rabaan et al., 2020, Kirchdoerfer et al., 2016). Due to its exposed position on the virus surface and its critical role for virus entry into the host cell, antibodies directed against the spike protein may prevent infection by neutralizing the virus, making the spike protein an important target for therapeutic antibodies and vaccine development (Liu et al., 2020, Sharma et al., 2021, de Wit et al., 2016, Li, 2016, Kumavath et al., 2021, Du et al., 2009, Strohl et al., 2022).

In our studies, we used assays distinguishing between immune responses specific to the two subunits, S1 and S2, and observed differential immunogenicity for three rMVA-based vaccine candidates based on different spike proteins. MVA-MERS-S, designed to encode the full-length native MERS-CoV spike protein, was shown to be immunogenic and induced immune responses against both the S1 and S2 spike subunit (Fathi et al., 2022, Weskamm et al., 2022b). By contrast, the MVA-SARS-2-S candidate encoding the native spike protein of SARS-CoV-2 showed only limited immunogenicity in humans, with immune responses predominantly directed against the S2 subunit (Meyer Zu Natrup et al., 2022)(Mayer and Weskamm, submitted to *Nature Communications*). An optimized vaccine candidate, MVA-SARS-2-ST, was designed to encode a pre-fusion stabilized SARS-CoV-2 spike protein with an inactivated S1/2 furin cleavage site. In comparison to MVA-SARS-2-S, it was shown to be more immunogenic in both pre-clinical models and human studies, with enhanced humoral and T cellular immunogenicity observed especially against the spike S1 subunit containing the RBD (Meyer Zu Natrup et al., 2022)(Mayer and Weskamm, submitted to *Nature Communications*). Similar observations were described by Routhu et al. (2021, 2022) who tested different rMVA-based COVID-19 vaccines in pre-clinical models, revealing the strongest immunogenicity for a vaccine candidate encoding a spike protein similar to MVA-SARS-2-ST, with a pre-fusion stabilized conformation and an inactivated furin cleavage site. In both optimized vaccines, proline substitution of the two amino acids K986 and V987 contributed to the enhanced stability of the SARS-CoV-2 spike protein (Routhu et al., 2022, Meyer Zu Natrup et al., 2022). The same amino acid substitutions are also used in other COVID-19 vaccines, including the mRNA-based vaccines BNT162b2 (Walsh et al., 2020) and mRNA-1273 (Jackson et al., 2020), as well as the viral vector vaccine Ad26.COVS.2 (Bos et al., 2020) (Figure 12). Stabilizing modifications of the spike protein had also been described as measures to enhance immunogenicity of SARS-CoV and MERS-CoV spike proteins, prior to the emergence of SARS-CoV-2 (Pallesen et al., 2017, Kirchdoerfer et al., 2018). However, the spike protein of SARS-CoV-2 has been shown to contain additional cleavage sites that are suggested to be the cause of the high infectivity and may also explain the reduced stability of the SARS-CoV-2 spike protein, compared to other coronaviruses (Berger and Schaffitzel, 2020, Hatmal et al., 2020). This may have contributed to the differential immunogenicity of our two rMVA-based vaccine candidates encoding non-modified spike proteins of MERS-CoV and SARS-CoV-2, respectively.

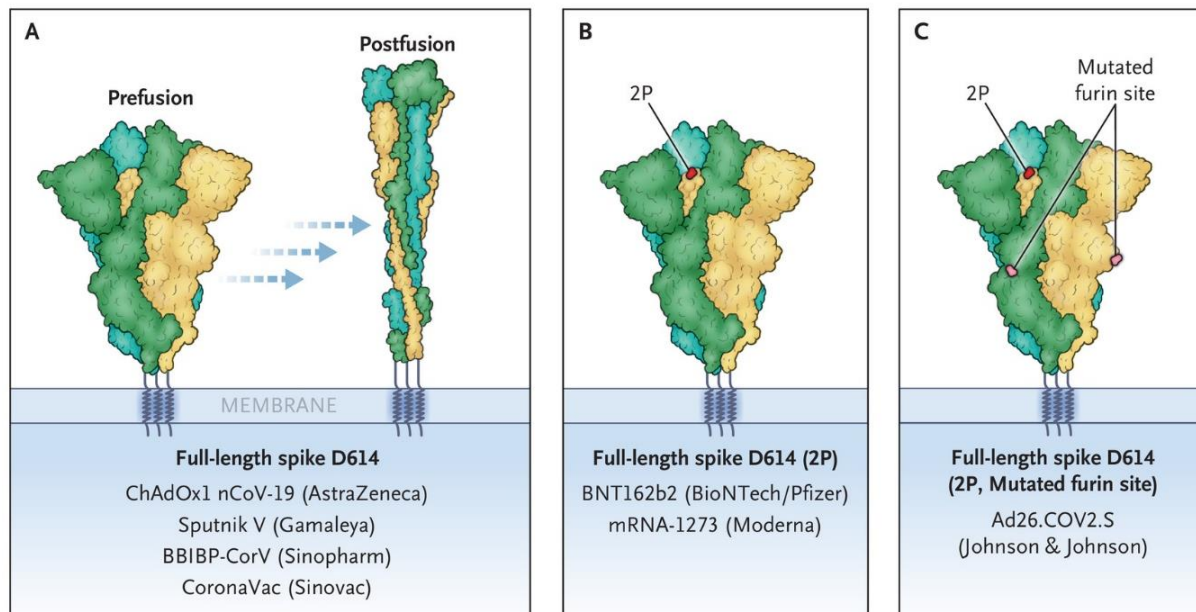


Figure 12: SARS-CoV-2 spike protein conformations used in licensed COVID-19 vaccines. Licensed COVID-19 vaccines are based on different conformations of the SARS-CoV-2 spike protein. While ChAdOx1 nCoV-19 (AstraZeneca, also referred to as ChAdOx1-S), Sputnik V (Gamaleya), BBIBP-CorV (Sinopharm) and CoronaVac (Sinovac) are based on the full-length native spike protein (**A**), different modifications are used in the BNT162b2 (BioNTech/Pfizer), mRNA-1273 (Moderna) and Ad26.COVS2.S (Janssen-Cilag GmbH, Johnson & Johnson) vaccines to stabilize the spike protein in a pre-fusion conformation (**B and C**). The spike protein mutant shown in panel B contains the stabilizing mutations K986P and V987P (2P), whereas the mutant shown in panel C additionally contains the mutations R682S and R685G in the S1/2 furin cleavage site. The rMVA-based COVID-19 vaccines tested at the University Medical Center Hamburg-Eppendorf are based on the native spike protein (MVA-SARS-2-S), as indicated in panel A, and on a pre-fusion stabilized spike protein with an inactivated S1/2 furin cleavage site, as shown in panel C (MVA-SARS-2-ST). Figure adjusted from Koenig and Schmidt (2021).

In addition to the spike protein conformation, another factor may contribute to differential immune responses towards the two subunits of the spike protein: pre-existing immunity against the spike protein resulting from previous infections with endemic HCoVs, namely HCoV-OC43, HCoV-229E, HCoV-HKU1, and HCoV-NL63, which circulate in the human population and account for 10 to 30 % of common colds (Liu et al., 2021a, Heikkinen and Järvinen, 2003). Cross-reacting antibodies have been observed for the S2 subunit, which is very conserved among HCoVs, whereas the RBD-containing S1 subunit differs between coronavirus species and demonstrates very low cross-reactivity between endemic and epidemic HCoVs (Khan et al., 2020, Okba et al., 2020). In a study by Nguyen-Contant et al. (2020), cross-reactive IgG antibodies against the S2 subunit of SARS-CoV-2 were detected in 86 % of unexposed individuals, whereas IgG antibodies specific for the SARS-CoV-2 RBD were not observed. Further, IgG-secreting memory B cells induced after SARS-CoV-2 infection were described to include a broad reactivity towards the SARS-CoV-2 S2 subunit but also cross-reactivity towards the S2 subunits of other human betacoronaviruses, especially HCoV-OC43 (Nguyen-Contant et al., 2020). In line with this, we detected higher baseline levels of SARS-CoV-2 S2- compared to S1-specific antibodies in naïve individuals of all our cohorts receiving COVID-19 vaccinations. Additionally, our analysis revealed differential dynamics for S1- and S2-specific immune responses upon vaccination with MVA-MERS-S. Both IgG1 and B cell responses against the MERS-CoV S2 subunit were already observed after the first vaccination in some of the study participants, whereas an immune response specific for the S1 subunit first appeared after the second vaccination. Nevertheless, S1-specific responses were potently induced

following the second and third vaccination with MVA-MERS-S, leading to S1-specific B cells and IgG1 antibodies that exceeded those specific for S2 in magnitude and persistence.

Overall, we observed robust immune responses against both spike protein subunits following two-dose vaccination with MVA-MERS-S and MVA-SARS-2-ST, as well as vaccination with licensed mRNA and ChAd vaccines. Neutralizing antibodies directed against the S1 subunit and especially the RBD have been suggested to be critical for protection against virus infection as they can prevent binding to the host cell receptor, and the RBD has been shown to be the main target of SARS-CoV-2 neutralizing antibodies induced by SARS-CoV-2 infection (Sette and Crotty, 2021, Errico et al., 2022, Piccoli et al., 2020, Steffen et al., 2020, Yuan et al., 2021, Ju et al., 2020). However, many of the mutations that occurred in SARS-CoV-2 variants have been shown to be located in the RBD and result in decreased neutralization capacity of RBD-directed antibodies elicited by vaccination or infection with the wild-type virus (Salleh et al., 2021, Weisblum et al., 2020, Liu et al., 2021b, Strohl et al., 2022, Focosi and Maggi, 2021, Starr et al., 2020, Planas et al., 2021). In contrast, antibodies targeting the more conserved S2 subunit could be important to provide protection against SARS-CoV-2 variants and other HCoV strains (Ng et al., 2022, Amanat et al., 2021). In the cohorts that received two mRNA vaccinations as a primary vaccination series, we identified an immunogenic region in the S2 domain close to the S1/S2 junction that contains an epitope (amino acids 814-826) which was recently described to be targeted by a neutralizing antibody with pan-coronavirus reactivity (Sun et al., 2022). Several studies have reported broadly neutralizing antibodies targeting epitopes of the S2 subunit, that were isolated from humans vaccinated or infected with MERS-CoV and SARS-CoV-2, underlining the functionality of S2-specific antibodies (Zhou et al., 2022, Wang et al., 2021). A study by Ng et al. (2022) suggested the utilization of an S2-targeted vaccine to achieve pan-SARS-CoV-2 immunity, showing promising results in mice with neutralization of diverse alpha- and betacoronaviruses. S2-targeting vaccines have also been suggested to achieve broad-spectrum activity against different isolates of MERS-CoV (Tai et al., 2022). Similar approaches targeting more conserved epitopes of viral antigens have been discussed in the context of a universal influenza virus vaccine (Nachbagauer et al., 2021). Antibodies with broadly neutralizing capacity against influenza viruses have been shown to target conserved epitopes in the stem region of the influenza virus hemagglutinin protein, rather than the more variable head domain (Corti et al., 2010, Ekiert et al., 2009). Based on these findings, a vaccine was developed containing only the hemagglutinin stem region and has been shown to confer broad protection in an animal model (Steel et al., 2010, Khan et al., 2020).

4.3 Influence of platform and dosing on vaccine immunogenicity

Vaccine-induced immune responses can be shaped by several parameters, including the nature of the vaccine antigen, as described above, but also the vaccine platform/technology, the dose, the immunization schedule and the route of administration (Zimmermann and Curtis, 2019, Pollard and Bijker, 2021). The factors influencing an immune response are often multilayered and the major determinants can differ between specific vaccines. For example, the nature of a vaccine and the use of specific platforms or adjuvants can directly influence the induction of innate immune responses and have thus also a strong impact on adaptive immune parameters. Generally, non-live vaccines (e.g. protein-based and inactivated virus vaccines) require adjuvants to trigger an efficient activation of the innate immune system, whereas vector-based and live vaccines have been shown to potently activate innate immune cells e.g. via PRRs, as they mimic a natural infection (Pollard and Bijker, 2021). The aim

of this section is to compare the immunogenicity of our rMVA-based vaccines to other MERS vaccine candidates and licensed vaccines against COVID-19, all of which are based on the spike protein but use different vaccine technologies. This section focusses on the primary vaccination series in naïve individuals, whereas the immune response to booster vaccinations will be discussed in the subsequent section.

4.3.1 MERS vaccine candidates

Currently, no licensed vaccines are available to prevent MERS-CoV infection and/or disease, and besides MVA-MERS-S, safety and immunogenicity data from clinical trials have only been reported for two other MERS vaccine candidates: ChAdOx1 MERS, based on a ChAd vector (Bosaeed et al., 2022, Folegatti et al., 2020a), and the DNA vaccine GLS-5300 (Modjarrad et al., 2019). Additional clinical trials are currently underway at the Gamaleya Research Institute (Moscow, Russia), investigating a heterologous prime-boost schedule with the BVRS-GamVac-Combi vaccine, based on Ad.26 and Ad.5 vectors as well as a single immunization with the BVRS-GamVac vaccine (ClinicalTrials.gov Identifiers: NCT04128059, NCT04130594). For these vaccine candidates, clinical data have not been published yet, but pre-clinical results are reported by Ozharovskaia et al. (2019) and Dolzhikova et al. (2020).

For MVA-MERS-S, a primary vaccination schedule with two doses administered 28 days apart revealed a benign safety profile and was shown to induce humoral and cellular immunity against the MERS-CoV spike protein. Seroconversion of S1-specific IgG was demonstrated in 75 % (n=9/12) of the low-dose cohort and 100 % (n=11/11) of the high-dose cohort (Koch et al., 2020). Comparable results were shown for a single immunization with ChAdOx1 MERS, which induced seroconversion in 83 % (low dose, n=5/6), 89 % (intermediate dose, n=8/9) and 100 % (high dose, n=9/9) of the study participants, respectively, as shown in two different studies conducted in the UK and in Saudi Arabia (Folegatti et al., 2020a, Bosaeed et al., 2022). The DNA vaccine GLS-5300 was administered using a three-dose-schedule during 12 weeks and induced seroconversion in 94 % (n=59/63) of the study participants, with no significant differences observed between the three tested dose groups (Modjarrad et al., 2019). A direct comparison of antibody titers between the studies is difficult due to the lack of standardized assays. However, all three MERS vaccine candidates were shown to be safe and immunogenic and induced the same overall dynamics of antibody responses peaking two to four weeks after vaccination and waning during the following 6-12 months, staying above baseline in some of the study participants (Koch et al., 2020, Folegatti et al., 2020a, Modjarrad et al., 2019, Bosaeed et al., 2022). In follow-up to the study reported by Koch et al. (2020), we investigated the impact of a late third MVA-MERS-S vaccination administered approximately one year after prime, and analyzed antibody and B cell responses in more detail (Weskamm et al., 2022b), which will be discussed in the following sections.

4.3.2 COVID-19 vaccine candidates and licensed vaccines

In response to the COVID-19 pandemic, numerous vaccine candidates have been developed and 242 of them were evaluated in clinical studies, based on multiple technologies such as mRNA, DNA, replicating and non-replicating viral vectors, protein subunit, inactivated viruses, and virus-like particles (COVID-19 vaccine tracker). The broad repertoire of vaccine technologies and immunization regimens used in COVID-19 vaccination provides a unique opportunity to study the impact of the different factors influencing vaccine-induced immunogenicity in the human population. In our study,

we investigated the immunogenicity of two rMVA-based COVID-19 vaccines tested at the UKE in direct comparison to two cohorts receiving licensed mRNA (BNT162b2 or mRNA-1273) and ChAd vaccines (ChAdOx1-S) (Mayer and Weskamm, submitted to *Nature Communications*).

Administered in a two-dose vaccination schedule, 28 days apart, MVA-SARS-2-ST, encoding a stabilized version of the SARS-CoV-2 spike protein, showed enhanced immunogenicity compared to the MVA-SARS-2-S vaccine based on a non-modified spike protein. S1-binding IgG antibodies were detected in 100 % of the study participants receiving two doses of MVA-SARS-2-ST (n=15/15), as well as in the control cohorts receiving either two doses of an mRNA vaccine, 21 days apart (n=10/10), or a combination of a ChAd and an mRNA vaccination, 12 weeks apart (n=8/8). However, side-by-side comparison between the cohorts revealed differences in the immunogenicity of the specific vaccination regimens: S1-specific IgG antibody levels measured after the second vaccination were 6.6-fold higher in the mRNA/mRNA cohort and 4-fold higher in the ChAd/mRNA cohort, compared to MVA-SARS-2-ST vaccinees. Besides the differing magnitude of antibody responses, a unique distribution of IgG subclasses was induced following repeated mRNA vaccination, which will be discussed below. Interestingly, immunogenicity of an rMVA-based vaccine candidate encoding a stabilized version of the SARS-CoV-2 spike protein and administered with the same schedule as MVA-SARS-2-ST was also assessed by Chiuppesi et al. (2022), showing spike-specific seroconversion of 100 % (n=37/37) of the study participants and similar antibody dynamics as observed in our study. Due to the lack of standardized assays, antibody titers cannot be directly compared at this point in time. However, CEPI has started to establish a global network of laboratories to standardize assays and centralize the evaluation of COVID-19 vaccine candidates (CEPI, 2020).

In addition to the influence of the different vaccine platforms, we observed an impact of the vaccine dose on the immunogenicity of both MVA-SARS-2-S and MVA-SARS-2-ST, with a trend towards higher spike-specific antibody responses elicited by the higher dose of each vaccine following twofold immunization. A dose dependency for MVA immunizations was also described by Wilck et al. (2010), who observed stronger binding and neutralizing antibody responses against MVA for the higher vaccine dose administered. Generally, higher vaccine doses are thought to favor the induction of plasma cells and may elicit higher primary antibody responses, whereas lower doses have been shown to preferentially drive the induction of B cell memory. A suggested mechanism for this effect is that lower doses increase the B cell competition for FDC-associated antigens in the GC reaction, resulting in reduced primary antibody responses, but in higher affinity antibodies and stronger secondary responses (Siegrist, 2018, Ahman et al., 1999).

4.4 Booster strategies and MBC recall responses

Especially for replication-deficient viral vectors and other non-live vaccines, a single immunization is often not sufficient to provide protection, and repeated vaccination can enhance immunogenicity. Secondary immune responses generally induce antibodies of higher affinity, and enhance the induction of LLPCs and MBCs, the two B cell subsets responsible for conferring long-term protection (Akkaya et al., 2020, Sallusto et al., 2010). Among other factors, one key determinant of the immune response to booster vaccinations is the immunization schedule. Closely spaced primary vaccine doses (referred to as “prime-boost” in this section) administered with a time interval of a few weeks can be beneficial in an outbreak situation or before travel. However, optimal MBC recall responses and induction of

persisting immune responses require longer intervals of at least three to four months (Siegrist, 2018, Sallusto et al., 2010, Maslow, 2017), with growing evidence for prolonged intervals increasing immunogenicity, as will be discussed below. In addition to the spacing of the primary vaccine doses, late booster vaccinations (referred to as “late booster” in this section) have been shown to enhance the persistence of vaccine-induced immunity, and are commonly used for many licensed vaccines, including vaccines against hepatitis A and B, rabies, tetanus, diphtheria, pertussis and poliomyelitis (STIKO, 2022b). The underlying mechanisms resulting in enhanced immunogenicity after prolonged intervals between vaccinations are not fully understood, but likely include two factors: Firstly, the processes of affinity maturation and isotype switching that are initiated within the GC reaction can continue for several months, and longer intervals may increase the affinity and thus neutralization capacity as well as Fc functionality of antibodies induced by a secondary response (MacLennan, 1994, Sallusto et al., 2010, Siegrist, 2018, Moriyama et al., 2021). Secondly, residual antibody titers from previous immunizations that are present at the time point of booster vaccination may provide negative stimuli to B cells via Fc receptors or form immune complexes with the newly administered vaccine antigen, reducing the amount of antigen available for BCR binding and B cell activation. In the context of viral vector vaccines, residual antibodies against the vector may play an additional role. They may neutralize the vaccine virus prior to entry into the host cell and transcription of the vaccine antigen, hampering booster responses (Siegrist, 2018, Pollard and Bijker, 2021). Therefore, besides increasing the interval between immunizations, heterologous prime-boost schedules are a widely-used strategy to overcome anti-vector immunity (Travieso et al., 2022, Ura et al., 2014).

4.4.1 Homologous versus heterologous prime-boost vaccination

Clinical studies have investigated heterologous prime-boost schedules using different viral vectors, as well as combinations of viral vector with DNA or mRNA vaccines, showing that the combination but also the specific order of vaccine platforms can influence vaccine-induced immunogenicity (Shaw et al., 2022, Ewer et al., 2016a, Venkatraman et al., 2019, Vuola et al., 2005, Deming and Lyke, 2021, Bockstal et al., 2022). The potency of the rMVA vector as a booster vaccine has been demonstrated by several studies investigating heterologous vaccination regimens with ChAd- (Ewer et al., 2016a, Venkatraman et al., 2019) and Ad26-based vaccines (Anywaine et al., 2019) against EVD, as well as with DNA- and fowlpox virus 9 (FP9)-based vaccines against malaria (Vuola et al., 2005). In the latter study, different combinations and orders of the three vaccines were tested, including homologous vaccinations with rMVA. Priming with DNA or FP9 vaccines, followed by rMVA booster vaccination were shown to be most immunogenic (Vuola et al., 2005).

Comparing homologous (ChAd-ChAd) versus heterologous (ChAd-mRNA) prime-boost vaccination against COVID-19, with both regimens administered 8-12 weeks apart, two studies by Schmidt et al. (2021a) and Barros-Martins et al. (2021) reported that the ChAd-mRNA regimen induced higher titers of IgG, IgA and neutralizing antibodies compared to ChAd-ChAd. Between heterologous ChAd-mRNA vaccination 8-12 weeks apart and homologous mRNA-mRNA vaccination 3 weeks apart, binding antibody titers, Wuhan neutralization and frequency of spike-specific CD4⁺ T cells were comparable, whereas neutralizing titers against the Alpha, Beta and Gamma variants, as well as CD8⁺ cytotoxic T cells were increased in the heterologous vaccination regimen (Schmidt et al., 2021a, Barros-Martins et al., 2021). In contrast, the same vaccination regimens revealed different results in our study, with mRNA-mRNA vaccination inducing slightly higher antibody titers compared to a heterologous ChAd-

mRNA schedule. Lv et al. (2022) compared different studies on homologous and heterologous COVID-19 vaccination, concluding that most studies obtained similar results to Schmidt et al. (2021a) and Barros-Martins et al. (2021). The Com-CoV vaccine trial by Shaw et al. (2022) compared the immunogenicity of different prime-boost regimens (mRNA-mRNA, mRNA-ChAd, ChAd-mRNA, ChAd-ChAd), all of them investigated at two different intervals of 4 and 12 weeks. This study reports the stronger antibody responses for the longer interval within each vaccination regimen, and the highest neutralizing antibody titers against the Wuhan, Beta and Delta strains after homologous mRNA vaccination within both interval groups, suggesting that the finding by Barros-Martins et al. (2021) might also be a consequence of the different intervals used for homologous mRNA-mRNA and heterologous ChAd-mRNA vaccination, rather than only the combination of vaccines.

4.4.2 The impact of the time interval between prime-boost vaccination

Besides the above-mentioned study by Shaw et al. (2022), several studies have reported enhanced immunogenicity as a consequence of a prolonged interval between the first and second dose of different COVID-19 vaccines. Immune responses to a second dose of the ChAdOx1-S vaccine were stronger when the interval between the doses was extended from 28 days to 84 days (Voysey et al., 2021, Voysey and Pollard, 2021), and further increased for intervals up to 45 weeks (Flaxman et al., 2021). Delaying the second dose of the BNT162b2 vaccine from 3-6 to 8-16 weeks resulted in enhanced humoral immune responses and improved virus neutralization in a study by Hall et al. (2022). For an rMVA-based COVID-19 vaccine, peak neutralizing antibody titers were shown to increase when the interval between the two doses was prolonged from 28 to 56 days (Chiuppesi et al., 2020). The beneficial effect of a prolonged interval on homologous and heterologous prime-boost regimens with (r)MVA had already been described prior to the COVID-19 pandemic: Palgen et al. (2020) described improved innate and humoral responses in cynomolgus macaques when increasing the time interval between two MVA immunizations from two weeks to two months, and in the clinical studies of the now licensed Ad26.ZEBOV/MVA-BN-Filo vaccine regimen against EVD, an interval of eight weeks elicited higher binding and neutralizing antibodies compared to a four week interval, independent of the order in which the Ad26- and MVA-based vaccines were administered (Anywaine et al., 2019).

4.4.3 The potential of a late booster vaccination

Late booster vaccinations are used for several licensed vaccines (STIKO, 2022b) and their potential has been described in several studies investigating viral vector vaccines. In the RV144 HIV vaccine trial combining vector- and protein-based vaccines, late booster immunizations were administered 12, 15, or 18 months after prime, respectively, with the latter leading to the highest IgG titers associated with increased neutralizing capacity (Pitisuttithum et al., 2020). The same effect was observed for the rMVA-based MVA-H5-sfMR vaccine against H5N1, which elicited the highest antibody responses with increased neutralizing and ADCC activity when the late booster was administered one year after prime immunization (Kreijtz et al., 2014, de Vries et al., 2018).

For MVA-MERS-S, we investigated the impact of a late third homologous vaccination approximately one year after prime, further underlining the findings of the above-mentioned studies. Compared to the second dose, the late third vaccination induced antibody and B cell responses that were strongly increased in magnitude, functionality, and persistence (Weskamm et al., 2022b). Briefly, the titers of spike-specific binding IgG increased 2.7-fold and we observed significant increases in neutralizing and

non-neutralizing antibody functionality, which will be further discussed below. The antibodies induced by the third vaccination, especially S1-specific IgG1, persisted at robust levels for two years, throughout the whole study period, whereas they had waned within a year after the second vaccination. Spike-specific IgG-secreting B cells were also induced at significantly higher numbers after the third compared to the second vaccination, with median fold-changes of 24.9 and 2.8 for S1- and S2-specific cells, respectively, as measured by IgG ELISpot. A flowcytometric analysis of MBCs confirmed the results obtained by ELISpot and provided additional insights into MBC isotypes and activation status. As described for vaccination against several pathogens (Ciabattini et al., 2021, Odendahl et al., 2005, Moldoveanu et al., 1995, Li et al., 2012), IgG⁺ MBCs were induced at higher levels compared to the IgA and IgM isotypes; the frequency of IgM⁺ MBCs did not increase in response to vaccination, whereas IgA⁺ MBCs showed a significant induction following the third vaccination, but at lower numbers compared to IgG. Notably, the population of IgG⁺ spike-specific MBCs did not only increase in frequency, but was also enriched for CD27⁺/CD21⁻ activated MBCs, resembling plasma cell precursors (Sanz et al., 2019). The strong and rapid increase of antibodies as well as MBCs after the third vaccination provide evidence for a recall response of MBCs induced by the second vaccination, even though these were only detected at very low frequencies prior to the late booster vaccination. Additionally, the persisting antibody titers after the third vaccination suggest an induction of not only MBCs, but also LLPCs, the second B cell subset contributing to immune memory (Siegrist, 2018, Akkaya et al., 2020). The high frequency of spike-specific B cells induced by the third vaccination decreased within the following year, but stayed above baseline in most study participants. Indeed, frequencies of antigen-specific B cells in peripheral blood have been described to be very low, as most of the MBCs and LLPCs reside in SLOs and the bone marrow, respectively (Palm and Henry, 2019, Waltari et al., 2019). Even though peripheral blood may not be the optimal tissue to study the induction of memory cells, it is an important resource to gain insights into human immune responses, as it can be obtained easily from study participants. The potential and limitations of a flowcytometric characterization of MBCs from peripheral blood are further discussed by Weskamm et al. (Weskamm et al., 2022a).

Surprisingly, we made a different observation for MVA-SARS-2-ST. When administered as a late booster vaccination approximately eight months after primary vaccination with two doses of an mRNA vaccine, MVA-SARS-2-ST increased antibody titers and T cell responses only in some of the study participants. Notably, all study participants had high remaining antibody titers against the SARS-CoV-2 spike protein at the time point of MVA-SARS-2-ST booster vaccination, and we observed an overall stronger antibody and T cell induction in those participants with lower baseline immunity prior to the late booster. This finding indicates that the low immunogenicity of MVA-SARS-2-ST as a late booster vaccine may, in part, be the consequence of negative regulation by persisting antibodies, as explained above. Overall, these findings suggest that waning antibodies against both the rMVA vector and the vaccine antigen might be key for the strong boosting effect observed for the MVA-MERS-S vaccine (Siegrist, 2018, Pollard and Bijker, 2021).

As opposed to MVA-SARS-2-ST, a late booster vaccination with a COVID-19 mRNA vaccine substantially increased the antibody titers in the control cohort independent of the high baseline immunity prior to the third vaccination, indicating that additional factors may impact the booster immune response. A potential explanation may be higher antigen levels induced by mRNA compared to MVA-SARS-2-ST vaccination, sufficient to overcome the negative regulation by residual antibodies. However, a negative correlation with pre-existing antibody titers has also been described for mRNA booster vaccinations in

a study by Dangi et al. (2022). Notably, vaccine-induced antibodies persisted at higher levels after the third, compared to the second mRNA vaccination, as was already observed for the MVA-MERS-S vaccine. More precisely, S1-specific IgG antibody titers were elevated 1.7-fold after the third compared to the second mRNA vaccination, looking at a time point four to six months post vaccination. These findings are in line with a study by Canetti et al. (2022), showing that a third vaccination with BNT162b2 increased the six-months-persistence of IgG binding and neutralizing antibodies compared to a second vaccination.

4.5 Route of vaccine administration

For the currently licensed vaccines, the most commonly used administration route is the intramuscular (IM) immunization, along with the subcutaneous (SC) route, due to their easy access and safety (Rosenbaum et al., 2020). However, muscle and subcutaneous tissue accommodate low numbers of immune cells and may thus not be the optimal site for immunization (Wiendl et al., 2005, Nguyen and Soulika, 2019). In contrast, skin tissue or more precisely dermis and epidermis, contain a broad repertoire of antigen-presenting cells which may improve the magnitude and duration of antigen-specific immune responses, making intradermal (ID) vaccination a promising alternative to IM and SC immunization (Nguyen and Soulika, 2019, Quaresma Juarez Antonio, 2019, Combadière et al., 2010). The advantages of skin-targeting vaccine administration have been described by several studies and include a potent induction of CD8⁺ cytotoxic T cells, as well as a dose-sparing of up to ten times compared to IM and SC administration, without reducing immunogenicity (Roosbeh et al., 2005, Belshe et al., 2007, Combadière et al., 2010, Belyakov et al., 2004). However, clinical application of ID immunization is still limited, due to difficulties in performing ID vaccination with existing techniques and equipment (Combadière et al., 2010, Laurent et al., 2007). The effect of the administration route has also been investigated for MVA, revealing a dose sparing effect for ID immunization which resulted in similar antibody titers as those elicited by IM or SC routes, but at a 10-fold lower dose (Wilck et al., 2010).

In the context of respiratory viruses, another administration route may gain significance: Mucosal immunization has the potential to elicit enhanced protective immune responses at the predominant site of pathogen entry, which in principle holds the potential to provide improved sterile immunity from infection, rather than predominantly protecting against disease symptoms once an infection has already been established (Lavelle and Ward, 2022, Wang et al., 2015, Sallusto et al., 2010, Russell et al., 2020). Adaptive immune responses induced at mucosal sites are characterized by special features such as secretory IgA (sIgA) and resident memory T (T_{RM}) cells. sIgA are potent antibodies that can neutralize pathogens in the mucosa using different pathways (Corthésy, 2013, Strugnell and Wijburg, 2010). T_{RM} cells have been shown to possess a stronger protective capacity than circulating T cells, with CD8⁺ T_{RM} cells being crucial for direct protection against influenza virus infection and CD4⁺ T_{RM} cells required for efficient formation of B cells and CD8⁺ T_{RM} cells (Son et al., 2021, Swarnalekha et al., 2021, Slütter et al., 2013). Despite the advantages of mucosal vaccines highlighted by several studies, immunization through the mucosal route remains limited to a few live vaccines, due to unique biopharmaceutical and technological hurdles that still have to be overcome (Wang et al., 2015, Siegrist, 2018). Currently in use are nine mucosal vaccines, most of them based on live-attenuated viruses or bacteria. They include one intranasally administered vaccine against influenza A and B viruses and eight

orally administered vaccines against poliovirus, rotavirus, *Vibrio cholerae* and *Salmonella typhimurium* (Lavelle and Ward, 2022).

The potential of mucosal and especially intranasal vaccines has also been discussed in the context of the COVID-19 pandemic, as the so far licensed vaccines have shown high systemic immunogenicity protecting from severe disease, but provide only limited protection against acquisition of infection (Alu et al., 2022, Förster et al., 2020, Gram et al., 2022). Several intranasal COVID-19 vaccines have reached evaluation in clinical studies, most of them based on viral vectors, and promising results have been reported by pre-clinical studies assessing intranasal administration of MVA-based vaccines (Alu et al., 2022, Bošnjak et al., 2021, Americo et al., 2022). However, a first-in-human study of an intranasal administration of the ChAdOx1-S vaccine revealed insufficient immunogenicity (Madhavan et al., 2022), underlining the difficulty to develop potent intranasal vaccines for the use in humans. Bošnjak et al. (2021) investigated the MVA-SARS-2-ST candidate administered as an IM prime followed by an intranasal booster immunization in mice and Syrian hamsters and reported a strong induction of systemic and lung tissue-resident spike-specific CD8⁺ T cells, as well as highly neutralizing IgG and IgA antibodies in both serum and bronchoalveolar lavage. A clinical study investigating MVA-SARS-2-ST as an inhalative booster vaccine for previously IM vaccinated individuals is currently underway (ClinicalTrials.gov Identifier: NCT05226390).

4.6 Impact of host factors on vaccine immunogenicity

In addition to vaccine and administration factors, vaccine-induced immunogenicity is strongly influenced by the individual characteristics of the host, including intrinsic host factors such as age, sex, genetics, and comorbidities, but also perinatal, environmental and behavioral factors, as extensively reviewed by Zimmermann and Curtis (2019). One intrinsic host factor increasingly recognized as an important determinant of vaccine-induced immunogenicity is the biological sex. Generally, females have been described to develop higher antibody titers but also experience more adverse events in response to vaccination compared to males. Underlying mechanisms may include hormonal, genetic, microbiotic, and environmental/ behavioral differences (Flanagan et al., 2017, Fehervari, 2019, Noho-Konteh et al., 2014, Fathi et al., 2020, Fischinger et al., 2019). Overall, this enhanced activation of the immune system in females may reflect better protection from infectious diseases but also a higher incidence of autoimmune diseases (Kronzer et al., 2021, Angum et al., 2020). Vaccine-induced immunity is also influenced by age, with the strongest differences observed in neonates and elderly people. Neonates have a lower capacity of antibody and T cell generation, and maternally derived antibodies may interfere with vaccine responsiveness (Zimmermann and Curtis, 2019, Siegrist, 2007, Voysey et al., 2017). Within the first two years of life, age has been shown to strongly influence the immune response to several vaccines, including those against poliomyelitis, diphtheria-tetanus-pertussis, hepatitis B and measles (Halsey and Galazka, 1985, di, 1950, Bialek et al., 2008, Nic Lochlainn et al., 2015). Generally, neonatal immune responses are characterized by inefficient interaction between antigen-presenting and T cells, leading to Th2 polarization and the induction of MBCs, rather than plasma cells secreting antibodies (Siegrist, 2001, Siegrist and Aspinall, 2009, Levy, 2007). Lower vaccine responsiveness and more rapid waning of antibodies has also been described for elderly people. This is explained by the process of immunosenescence, the age-associated decline in immune function. Mechanisms responsible for diminished B cell responses in elderly may include a decreasing generation of new B cells from precursors in the bone marrow, contributing to a shift from mostly

naive B cells in young people to mostly memory cells in elderly people. Reduced B cell proliferation and retention of immune complexes by FDCs may result in less efficient germinal center responses and interactions between B and T cells (Siegrist and Aspinall, 2009, Boraschi and Italiani, 2014). Additionally, aging is associated with a decline in CD8⁺ cytotoxic T cell responses, likely resulting from a shift towards the anti-inflammatory IL-10 (McElhane et al., 2012).

Besides neonates and elderly people, another vulnerable group are patients with immunodeficiencies such as hematologic malignancies, that may result in disease-induced dysfunction of the innate and adaptive immune system, or treatment-related immunodeficiencies (Piechotta et al., 2022, Hamblin and Hamblin, 2008). Depending on the type of disease or treatment, the impairment of the immune system may affect humoral or T cellular immunity, or both (Pollard and Bijker, 2021, R  thrich et al., 2022, Ravandi and O'Brien, 2006). As the early phase clinical trials conducted for our MVA-based vaccine candidates were based on relatively small groups of healthy adults aged between 18 and 59 years, we were not able to assess the influences of sex, age, or comorbidities in these trials. However, as part of an observational study, we were able to collect samples from a cohort of CLL patients, most of them receiving immunomodulatory therapy, vaccinated with licensed mRNA and/or ChAd COVID-19 vaccines. Comparing them to a control group of healthy adults receiving the same vaccination regimen, we observed that most CLL patients had either an impaired antibody or T cell response, or both, with only 14.3 % of the patients (n=3/21) showing both SARS-CoV-2 spike-specific antibodies and T cells compared to 100 % (n=10/10) in the healthy control group (Mellinghoff et al., 2022b). A follow-up study investigating the impact of a third COVID-19 vaccination in a subgroup of CLL patients receiving either B cell-directed or B cell-depleting treatment, revealed superior T cell responses in patients receiving a heterologous (ChAd), compared to a homologous (mRNA) booster vaccination (Mellinghoff et al., 2022a). These findings underline the potential of vaccination regimens including viral vector vaccines to improve T cell immunity, which has been previously described by several studies (Pozzetto et al., 2021, Coughlan et al., 2018, Ura et al., 2022, Ramezanzpour et al., 2016, Gilbert, 2012). A potent induction of T cell responses may be of special significance for immunocompromised patients and especially those receiving B cell-depleting therapies, as it may compensate for diminished humoral immunity (Schmidt et al., 2021b, R  thrich et al., 2022, Bahrs and Harrison, 2022, Bonelli et al., 2021).

Besides the difficulty to induce potent immune responses, vaccination of immunocompromised patients is challenging due to safety concerns. Generally, the use of live vaccines in immunocompromised patients is associated with the risk of vaccine-associated diseases, whereas the use of inactivated vaccines is considered to be safe but may result in insufficient immune responses (Ljungman, 2012). Due to the beneficial safety profile and a potent induction of T cell responses, replication-deficient viral vectors like the rMVA platform are promising platforms for vaccination of vulnerable groups, such as infants, elderly people and immunocompromised patients (Sasso et al., 2020). Safety and immunogenicity in infants and elderly have for instance been reported for rMVA-based vaccines against influenza, RSV, tuberculosis and malaria (Scriba et al., 2010, Tameris et al., 2013, Antrobus et al., 2012, Afolabi et al., 2016, Jordan et al., 2021). The MVA85A vaccine against tuberculosis was additionally tested in HIV-infected individuals, revealing to be safe and immunogenic (Minassian et al., 2011, Ndiaye et al., 2015).

4.7 Systems vaccinology and systems serology

Clinical studies are used to address vaccine efficacy, but provide only little insight into the mechanisms of human immune responses, which have been mostly addressed relying on experiments in animal models such as mice. However, animal studies are not always predictable of the human immune system, and new approaches are required to improve the insights that can be obtained from human studies (Pulendran et al., 2010, Pulendran et al., 2013). During the last decades, systems vaccinology approaches have emerged, using computational methods to gain more comprehensive insights into the mechanisms involved in vaccine-induced immunity and, for example, identify early transcriptional signatures that correlate with and predict subsequent adaptive immune responses (Querec et al., 2009, Pulendran et al., 2010, Nakaya et al., 2011, Pulendran et al., 2013, Nakaya et al., 2015). Systems serology approaches specifically aim at a detailed characterization of antibody structure and functionality, to gain a better understanding of the specific antibody features conferring protection against infection or disease (Ackerman et al., 2017, Arnold and Chung, 2018, Barrett et al., 2021).

In addition to the analysis of binding IgG and neutralizing antibodies, we here implemented systems serology approaches to analyze antibody isotypes and subclasses, as well as the non-neutralizing antibody functions ADCP and ADNKA, a surrogate for ADCC.

4.7.1 Antibody isotypes and subclasses

Throughout all cohorts analyzed in our study, vaccine-induced antibodies predominantly belonged to the IgG isotype, with IgA antibodies showing the same dynamics at lower levels, and IgM antibodies showing only a slight induction after primary vaccination. This is in line with data from other studies and represents the typical isotype pattern observed after IM vaccination (Moldoveanu et al., 1995, Sano et al., 2022, Tarkowski et al., 2021). Interestingly, IgG subclass profiling revealed distinct signatures for the different vaccination regimens. All three rMVA-based vaccines induced mainly IgG1 antibodies as well as a quantitative minor fraction of the IgG3 subclass, whereas IgG2 and IgG4 were undetectable. The same subclass distribution was induced by primary vaccination with mRNA and ChAd COVID-19 vaccines, which is in line with other studies analyzing antibody responses to BNT162b2 and ChAdOx1-S vaccination (Barrett et al., 2021, Fraley et al., 2021) but also vaccination with the inactivated CoronaVac vaccine (Sinovac Biotech) (Chen et al., 2022b). IgG1 and IgG3 are the two subclasses that are typically induced by protein antigens and are known to be pro-inflammatory and possess a high Fc functionality (Vidarsson et al., 2014, Schroeder and Cavacini, 2013).

However, we observed a different subclass distribution after repeated mRNA vaccination, with an atypical induction of IgG2 and IgG4 subclasses that reached similar levels to IgG1. Similar findings were recently described by Irrgang et al. (2022) and Buhre et al. (2023). IgG2 is typically induced by polysaccharide antigens and has a low capacity to induce Fc-mediated effector functions, due to its low affinity to Fc γ receptors (Vidarsson et al., 2014, Gunn and Alter, 2016). IgG4 is associated with repeated or long-term exposure to the same antigen and a Th2-biased immune response, and has been described to have an anti-inflammatory or tolerance-inducing activity (Vidarsson et al., 2014, Maslinska et al., 2022, Aalberse et al., 2009). Whether the atypical induction of IgG2 and IgG4 after repeated mRNA vaccination has an impact on the overall antibody functionality and, as a consequence, on antibody-mediated protection, needs to be further investigated in future studies. Also, it remains unclear whether the unique subclass distribution is a general feature of mRNA vaccines, or a

consequence of the vaccination schedule in combination with the induction of very high overall antibody titers and continuous antigen exposure in long-lasting GC reactions (Turner et al., 2021, Kim et al., 2022). In the context of chronic viral infections, sustained high levels of soluble antigens have been observed to induce tolerance or exhaustion of both B and T cells (Barber et al., 2006, Virgin et al., 2009, Wherry et al., 2007). Several studies have suggested that vaccine platform, adjuvants and vaccination regimen may impact subclass distribution and Fc-effector profiles of vaccine-induced antibodies (Gunn and Alter, 2016, Chung et al., 2015, Fischinger et al., 2021, Irrgang et al., 2022, Xu et al., 2022, Buhre et al., 2023). However, comprehensive data on this topic are still missing.

4.7.2 Antibody functionality

Longitudinal analysis of antibodies induced by MVA-MERS-S revealed a strong increase in both neutralizing and non-neutralizing antibody functions after the late booster vaccination. Comparing the responses observed 28 days after the third to those after the second vaccination, the neutralization capacity showed an 8-fold median increase (Weskamm et al., 2022b). A preliminary analysis of S1-specific non-neutralizing antibody functionality revealed median foldchanges of 5.4, 7.8 and 5.9 for the expression of CD107 α , IFN- γ and MIP-1 β , resembling ADNKA capacity, and a foldchange of 1.4 for the ADCP capacity comparing the third to the second vaccination (section 3, Unpublished Data). These findings suggest an enhanced functionality of both Fab and Fc antibody regions, which may be the result of continuative maturation processes induced in the GC reaction, as discussed above. Similar findings were reported by de Vries et al. (2018), who detected increased neutralizing and ADCC activity in response to an rMVA-based vaccine against H5N1 when the boost was administered one year after prime immunization. Barrett et al. (2021) report on enhanced neutralizing antibody titers and Fc-mediated antibody functionality including ADCP, ADNKA, and complement activation, after a second vaccination with ChAdOx1-S. In their study, a trend towards a stronger increase of Fc-mediated antibody functionality was observed when the interval between the doses was prolonged from 28 to 56 days. Linking innate and adaptive immune mechanisms, Fc-mediated antibody functions combine the antiviral activity of innate effector cells with the specificity of humoral immune responses, providing potent mechanisms to fight virus infections. ADCC mediates clearance of virus-infected cells by inducing NK cell degranulation, whereas ADCP results in the clearance of extracellular immune complexes and virus-infected cells, and stimulates adaptive immune responses by enhancing antigen presentation (Tay et al., 2019, Vivier et al., 2011, Nimmerjahn and Ravetch, 2008, Pincetic et al., 2014).

In addition to ADCP mediated by monocytes and ADCC, non-neutralizing antibody functions include ADCP mediated by neutrophils (sometimes also referred to as ADNP), and antibody-dependent complement deposition (ADCD). These were not addressed in this thesis, but could provide additional insights in future studies. In addition to the isotype and subclass of antibodies, glycan modifications of the Fc fragment have been shown to strongly influence the antibodies' functionality and to be impacted by the vaccine platform (Gunn and Alter, 2016, Mahan et al., 2016, Davies et al., 2001, Lu et al., 2018). A protocol to analyze Fc glycan modifications of MERS-CoV spike-specific antibodies is currently being developed, but needs to be further optimized. Future studies comparing vaccine platforms, antigens and regimens may provide important insights into mechanistic links between antibody structural and functional properties and reveal potential opportunities to drive vaccine-induced immunity via functional optimization of the humoral immune response (Bournazos and Ravetch, 2017, Kasturi et al., 2011).

4.8 CoPs against MERS and COVID-19

CoPs can substantially contribute to assess vaccine-mediated protection, but their identification remains challenging. Different approaches can support the finding of a CoPs, for example adoptive transfer and preclinical studies, vaccine efficacy trials analyzing immune responses in protected and unprotected subjects, and observations made in human challenge studies (Callegaro and Tibaldi, 2019, Nguipdop-Djomo et al., 2013, Qin et al., 2007, Koch et al., 2021, Plotkin, 2010). None of these approaches are feasible for MERS-CoV so far, however, some conclusions about CoPs against human coronaviruses can be drawn from human challenge studies conducted with HCoV-229E and SARS-CoV-2 (Killingley et al., 2022, Edwards and Neuzil, 2022, Barrow et al., 1990, Huang et al., 2020), as well as from the data collected on SARS-CoV-2 vaccination and infection during the COVID-19 pandemic.

Human challenge studies with the endemic HCoV-229E indicate that serum as well as mucosal antibody responses may serve as CoPs against coronavirus infection and disease, including serum IgG, IgA and neutralizing titers, as well as mucosal IgA (Barrow et al., 1990, Huang et al., 2020). Another study by Callow (1985) reported that the duration of viral shedding was specifically reduced by the induction of mucosal IgA. However, these studies reported that reinfections with the same virus may occur within one or two years, indicating that sterilizing immunity may be difficult to achieve for coronaviruses, as is also observed for SARS-CoV-2 (Huang et al., 2020, Flacco et al., 2022, Cohen and Burbelo, 2021).

In the context of SARS-CoV-2 infection and disease, CoPs have been extensively reviewed by several authors (Koch et al., 2021, Krammer, 2021, Goldblatt et al., 2022a). Multiple studies have described neutralizing as well as binding antibodies to correlate with protection from SARS-CoV-2 infection and/or disease (Earle et al., 2021, Lustig et al., 2021, Goldblatt et al., 2022b, Gilbert et al., 2022, Feng et al., 2021). For instance, Khoury et al. (2021) describe neutralizing antibody levels to be highly predictive of protection from symptomatic infection and suggest for them to be used to guide COVID-19 vaccine strategies. However, non-neutralizing antibody functions such as ADCC, ADCP and ADCD have been shown to contribute to protection against many viral diseases (Lu et al., 2018, Chung et al., 2015) and may also play a role in the protection against SARS-CoV-2, as discussed by Goldblatt et al. (2022a) and Zhang et al. (2022a). As described for HCoV-229E, mucosal IgA has also been suggested to be important for protection against SARS-CoV-2, and especially to provide protection against acquisition of infection, rather than disease (Chan et al., 2022, Hennings et al., 2022, Goldblatt et al., 2022a).

On the cellular level, T cells and MBCs may additionally contribute to protection against SARS-CoV-2, and especially newly emerging virus variants. T cells have been shown to play an important role in controlling viral loads by recognition and elimination of infected cells, as reviewed by Sette and Crotty (2021). Compared to neutralizing antibodies, they are suggested to be less affected by the mutations of virus variants and may therefore be especially important upon breakthrough infections with SARS-CoV-2 variants (Liu et al., 2022, Lu and Yamasaki, 2022). Antigen-specific MBCs are important to provide rapid antibody responses if a pathogen escapes circulating antibodies and T cells, and may also be of special significance for protection against virus variants, as they possess a broader repertoire of BCRs compared to LLPCs maintaining plasma antibody levels, and are activated more quickly than naïve B cells (Goldblatt et al., 2022a, Purtha et al., 2011, White, 2021, Tong et al., 2021, Paschold et al., 2022).

4.9 Conclusions and future perspectives

Taken together, the findings of this thesis provide comprehensive insights into the immunogenicity of the novel rMVA-based vaccine candidates MVA-MERS-S, MVA-SARS-2-S and MVA-SARS-2-ST, as well as the impact of spike protein conformation, vaccine platforms and immunization regimens on vaccine-induced B cell and antibody responses. Even though limited to small study cohorts, a strength of these studies is the frequent and prospective longitudinal sampling of PBMCs and plasma from each individual starting at baseline prior to vaccination, as well as the comprehensive analysis of various parameters of vaccine-induced adaptive immunity.

4.9.1 Techniques to study antigen-specific B cells and antibodies

As part of this thesis, a repertoire of techniques was established to study antigen-specific antibody and B cell responses against the MERS-CoV and SARS-CoV-2 spike protein subunits S1 and S2. These techniques can be easily adjusted to other antigens, allowing for a rapid assay development to investigate immune responses against different virus variants or other pathogens. For the analysis of antibodies, we here implemented assays to analyze antibody isotypes, subclasses and the non-neutralizing antibody functions ADNKA and monocyte-mediated ADCP. An additional analysis of ADCP mediated by neutrophils and ADCD, as well as Fc glycan modifications could provide further information on the antibody compartment. Combined with an integrative data analysis, this would likely reveal links between structural and functional antibody features, allowing for a better understanding of the mechanisms responsible for antibody-mediated protection and contributing to a more specific definition of immune correlates for protection.

Regarding antigen-specific B cells, additional insights into the BCR repertoire and the state of B cell maturation upon booster vaccination could be obtained using single cell sequencing. However, as for the ELISpot and flowcytometric analyses, the low frequency of antigen-specific B cells in peripheral blood is a limiting factor here, as discussed above. Peripheral blood is an important compartment to gain first insights into vaccine-induced immune responses in humans, as it can be obtained easily from study participants. As the majority of antigen-experienced B cells resides in the SLOs (MBCs) and the bone marrow (LLPCs) (Palm and Henry, 2019, Waltari et al., 2019), an additional analysis of these tissues could provide more detailed insights into vaccine-induced B cell immunity. However, given the more invasive procedures, obtaining these kinds of samples requires careful consideration.

Additionally, mucosal immunity may contribute to enhanced protection from respiratory viruses such as MERS-CoV and SARS-CoV-2 (Goldblatt et al., 2022a, Mettelman et al., 2022), but cannot be assessed based on peripheral blood. Therefore, sampling of nasopharyngeal swabs and saliva could be included in future trials to assess the vaccines' capacity to induce mucosal immunity and provide a more comprehensive picture of vaccine-induced immunity.

4.9.2 The MVA-MERS-S vaccine candidate

For the MVA-MERS-S vaccine candidate, we were able to show safety and immunogenicity in a phase 1a clinical trial, highlighting the potential of a late booster vaccination to improve long-term persistence of vaccine-induced immunity. A two-center, randomized, placebo-controlled, and double-blinded phase 1b trial (ClinicalTrials.gov Identifier: NCT04119440) is currently conducted at the UKE and the Erasmus Medical Center Rotterdam, investigating the safety and immunogenicity of three

vaccinations with MVA-MERS-S in a bigger cohort ($n = 135$). The study includes two different dose levels of the vaccine, as well as two different intervals for the primary vaccination series; the second vaccination is given either at day 28 or day 56, whereas all study participants receive a late booster vaccination approximately eight months after prime. Due to the bigger size of the study cohort, this trial provides the opportunity for a more comprehensive analysis of the factors influencing vaccine-induced adaptive immunity, such as innate immune responses, the biological sex, the vaccine dose, as well as the interval between the first two vaccinations.

Currently, no licensed vaccines or specific therapeutic options are available to prevent or treat MERS-CoV infection and/or disease. However, effective countermeasures are critical to prevent or respond to an outbreak situation (Yong et al., 2019). Administered to people who are frequently exposed to camels in the Middle East, a MERS vaccine could be used to prevent virus transmission in the first place, or to protect people from severe disease. Another target group for prophylactic vaccination could be healthcare workers in endemic areas or people travelling to the Middle East, including the large number of pilgrims traveling to Mecca for the Hajj (Folegatti et al., 2020a, Baharoon and Memish, 2019, Abdirizak et al., 2019, Azhar et al., 2022). The induction of MBCs and persistence of neutralizing antibodies following a third vaccination with MVA-MERS-S suggest this vaccine to be a suitable candidate for prophylactic vaccination prior to an outbreak scenario. However, a vaccine inducing potent immunogenicity already after a single dose, such as ChAdOx1 MERS, may be beneficial in an outbreak situation (Bosaeed et al., 2022, Folegatti et al., 2020a, Maslow, 2017). Aside from the primary vaccination series consisting of one or two vaccinations of ChAdOx1 MERS and MVA-MERS-S, respectively, both vaccines revealed to be immunogenic and induced similar antibody dynamics. Whether these vaccine-induced immune responses are protective against MERS-CoV infection and/or disease, needs to be investigated in future studies. As efficacy studies are not feasible in the absence of a pathogen circulating in the study population, precisely defined CoPs could facilitate immune bridging and thus the further vaccine development against MERS (Maslow, 2017, Plotkin, 2010).

4.9.3 COVID-19 vaccines

Our findings regarding the rMVA-based COVID-19 vaccine candidates MVA-SARS-2-S and MVA-SARS-2-ST revealed lower humoral immunogenicity of both candidates compared to licensed mRNA- and ChAd-based COVID-19 vaccines. However, our analysis highlights the potential of immune bridging to assess novel vaccine candidates, and we obtained important insights into the influence of antigen conformation, vaccine platform and regimen on vaccine-induced immunogenicity. Comparative studies of different COVID-19 vaccine candidates and regimens have been reported by several research groups (Munro et al., 2021, Molino et al., 2022, Fiolet et al., 2022, Shaw et al., 2022, Barbeau et al., 2022, Zhang et al., 2022b), highlighting the impact of specific platforms and intervals on primary and secondary responses of humoral and T cell immunity.

Our analysis revealed differential immunogenicity towards the S1 and S2 spike protein subunit for the two rMVA-based vaccines encoding for different conformations of the SARS-CoV-2 spike protein. Additionally, a baseline dependency was observed for antibody and T cell responses induced by a late booster vaccination with MVA-SARS-2-ST, with a higher magnitude of immune responses in individuals with lower spike-specific baseline immunity. These findings are in line with the results from other vaccine studies (Sasaki et al., 2008, Das et al., 2022, Dangi et al., 2022) and could provide implications for booster strategies with COVID-19 vaccines. Comparing different vaccine platforms and vaccination

regimens, we observed a differential distribution of IgG subclasses after repeated mRNA vaccination, with an atypical induction of the IgG2 and IgG4 subclasses, in line with recent studies by Irrgang et al. (2022) and (Buhre et al., 2023). Generally, IgG2 and IgG4 are known to be less functional compared to IgG1 and IgG3, and IgG4 has been described to possess anti-inflammatory functionality. Future studies should address the neutralizing and non-neutralizing functionality of SARS-CoV-2 spike-specific antibodies, to investigate whether the distinct profile of IgG subclasses induced by mRNA vaccination has an impact on antibody-mediated functionality and protection.

4.9.4 The rMVA vaccine platform

We observed differential immunogenicity for three rMVA-based vaccines against MERS and COVID-19, highlighting the complexity of vaccine-induced immune responses which are influenced by multiple factors including the vaccine platform but also the antigen. Generally, the advantages of rMVA-based vaccines include a beneficial safety profile, as well as a potent induction of humoral and T cell responses without the use of adjuvants (Volz and Sutter, 2017, Travieso et al., 2022, Price et al., 2013, Zhu et al., 2007, Volkmann et al., 2021, Gilbert, 2013). These properties make rMVA a promising vaccine platform for patients suffering from immunodeficiencies or receiving B cell depleting therapies due to hematologic malignancies. In addition, rMVA has a higher insertion capacity for foreign genes compared to other viral vectors, enabling the development of multivalent vaccines encoding several antigens (Mastrangelo et al., 2000, Smith and Moss, 1983, Chiuppesi et al., 2020, Henning et al., 2021, Lauer Katharina et al., 2017). Multivalent vaccines may be of interest to induce immune responses against several virus variants or pathogen strains at the same time and have been investigated e.g. in the context of influenza and coronaviruses (Arevalo et al., 2022, Dolgin, 2022, Prabakaran et al., 2014, Tai et al., 2022). Indeed, one of the two licensed vaccines against EVD contains an rMVA vector with a multivalent insert encoding for four filovirus antigens (Bockstal et al., 2022, EMA, 2020b).

Even though conventional production platforms based on primary CEF cultures are well established, a draw-back of the rMVA technology is that large-scale manufacturing remains challenging compared to vaccines based on other viral vectors such as adenoviruses, which can be easily produced at high titers in cell culture (Gränicher et al., 2021, Rauch et al., 2018, Ramezanpour et al., 2016). Primary CEF cultures have a limited lifespan and the supply with primary cell cultures can be challenging for large scale manufacturing. Alternative rMVA production systems based on cell lines such as DF-1 (derived from CEF) or the duck cell lines AGE1.CR and AGE1.CR.pIX are currently exploited as an approach to optimize the yield and cost-effectiveness for large-scale production of rMVA-based vaccines (Garber et al., 2009, Vázquez-Ramírez et al., 2019). The doses administered in the rMVA clinical trials reported here are in the same range as those of the licensed non-recombinant MVA vaccine against smallpox and mpox (Imvanex) (STIKO, 2022a). A dose dependency of vaccine-induced immune responses has been described for both MVA (Wilck et al., 2010) and rMVA (Zaeck et al., 2022), and a similar trend was observed for both MVA-SARS-2-S and MVA-SARS-2-ST in our studies, indicating that higher doses of rMVA-based vaccines may induce more potent immune responses. For several vaccines including MVA, intradermal vaccination has been shown to mediate a dose sparing effect compared to IM vaccination, due to a more efficient activation of antigen-presenting cells (Nguyen and Soulika, 2019, Quaresma Juarez Antonio, 2019, Combadière et al., 2010, Wilck et al., 2010). Intradermal administration of rMVA-based vaccines may therefore be addressed in future studies to overcome potential limiting effects of the vaccine dose on rMVA-induced immune responses.

5 References

- AALBERSE, R. C., STAPEL, S. O., SCHUURMAN, J. & RISPENS, T. 2009. Immunoglobulin G4: an odd antibody. *Clin Exp Allergy*, 39, 469-77.
- ABBAS, L., PILLAI 2017. *Cellular and Molecular Immunology*.
- ABDIRIZAK, F., LEWIS, R. & CHOWELL, G. 2019. Evaluating the potential impact of targeted vaccination strategies against severe acute respiratory syndrome coronavirus (SARS-CoV) and Middle East respiratory syndrome coronavirus (MERS-CoV) outbreaks in the healthcare setting. *Theoretical Biology and Medical Modelling*, 16, 16.
- ABEL, A. M., YANG, C., THAKAR, M. S. & MALARKANNAN, S. 2018. Natural Killer Cells: Development, Maturation, and Clinical Utilization.
- ACKERMAN, M. E., BAROUCH, D. H. & ALTER, G. 2017. Systems serology for evaluation of HIV vaccine trials. *Immunol Rev*, 275, 262-270.
- ACKERMAN, M. E., MOLDT, B., WYATT, R. T., DUGAST, A. S., MCANDREW, E., TSOUKAS, S., JOST, S., BERGER, C. T., SCIARANGHELLA, G., LIU, Q., IRVINE, D. J., BURTON, D. R. & ALTER, G. 2011. A robust, high-throughput assay to determine the phagocytic activity of clinical antibody samples. *J Immunol Methods*, 366, 8-19.
- ACUNA-SOTO, R., STAHL, D. W., CLEVELAND, M. K. & THERRELL, M. D. 2002. Megadrought and megadeath in 16th century Mexico. *Emerg Infect Dis*, 8, 360-2.
- AFOLABI, M. O., TIONO, A. B., ADETIFA, U. J., YARO, J. B., DRAMMEH, A., NÉBIÉ, I., BLISS, C., HODGSON, S. H., ANAGNOSTOU, N. A., SANOU, G. S., JAGNE, Y. J., OUEDRAOGO, O., TAMARA, C., OUEDRAOGO, N., OUEDRAOGO, M., NJIE-JOBE, J., DIARRA, A., DUNCAN, C. J., CORTESE, R., NICOSIA, A., ROBERTS, R., VIEBIG, N. K., LEROY, O., LAWRIE, A. M., FLANAGAN, K. L., KAMPMAN, B., BEJON, P., IMOUKHUEDE, E. B., EWER, K. J., HILL, A. V., BOJANG, K. & SIRIMA, S. B. 2016. Safety and Immunogenicity of ChAd63 and MVA ME-TRAP in West African Children and Infants. *Mol Ther*, 24, 1470-7.
- AFROUGH, B., DOWALL, S. & HEWSON, R. A.-O. 2019. Emerging viruses and current strategies for vaccine intervention. *Clin Exp Immunol*.
- AHMAN, H., KÄYHTY H FAU - VUORELA, A., VUORELA A FAU - LEROY, O., LEROY O FAU - ESKOLA, J. & ESKOLA, J. 1999. Dose dependency of antibody response in infants and children to pneumococcal polysaccharides conjugated to tetanus toxoid. *Vaccine*.
- AKIRA, S., UEMATSU, S. & TAKEUCHI, O. 2006. Pathogen recognition and innate immunity. *Cell*, 124, 783-801.
- AKKAYA, M., KWAK, K. & PIERCE, S. K. 2020. B cell memory: building two walls of protection against pathogens. *Nature Reviews Immunology*, 20, 229-238.
- ALAGHEBAND BAHRAMI, A., AZARGOONJAHROMI, A., SADRAEI, S., AARABI, A., PAYANDEH, Z. & RAJABIBAZL, M. 2022. An overview of current drugs and prophylactic vaccines for coronavirus disease 2019 (COVID-19). *Cell Mol Biol Lett*, 27, 38.
- ALLAIN-DUPRÉ, D., CHATRY, I., KORNPROBST, A. & MICHALUN, M. 2020. The territorial impact of COVID-19: Managing the crisis across levels of government.
- ALLMAN, D. A.-O., WILMORE, J. A.-O. & GAUDETTE, B. T. 2019. The continuing story of T-cell independent antibodies. *Immunol Rev*.
- ALTENBURG, A. F., VAN TRIERUM, S. E., DE BRUIN, E., DE MEULDER, D., VAN DE SANDT, C. E., VAN DER KLIS, F. R. M., FOUCHIER, R. A. M., KOOPMANS, M. P. G., RIMMELZWAAN, G. F. & DE VRIES, R. D. 2018. Effects of pre-existing orthopoxvirus-specific immunity on the performance of Modified Vaccinia virus Ankara-based influenza vaccines. *Scientific Reports*, 8, 6474.
- ALTER, G., MALENFANT, J. M. & ALTFELD, M. 2004. CD107a as a functional marker for the identification of natural killer cell activity. *J Immunol Methods*, 294, 15-22.
- ALU, A., CHEN, L., LEI, H., WEI, Y., TIAN, X. & WEI, X. 2022. Intranasal COVID-19 vaccines: From bench to bed. *eBioMedicine*, 76.
- AMANAT, F., THAPA, M., LEI, T., AHMED, S. M. S., ADELSBERG, D. C., CARREÑO, J. M., STROHMEIER, S., SCHMITZ, A. J., ZAFAR, S., ZHOU, J. Q., RIJNINK, W., ALSHAMMARY, H., BORCHERDING, N.,

- REICHE, A. G., SRIVASTAVA, K., SORDILLO, E. M., VAN BAKEL, H., TURNER, J. S., BAJIC, G., SIMON, V., ELLEBEDY, A. H. & KRAMMER, F. 2021. SARS-CoV-2 mRNA vaccination induces functionally diverse antibodies to NTD, RBD, and S2. *Cell*, 184, 3936-3948.e10.
- AMANNA, I. J., CARLSON, N. E. & SLIFKA, M. K. 2007. Duration of humoral immunity to common viral and vaccine antigens. *N Engl J Med*, 357, 1903-15.
- AMERICO, J. L., COTTER, C. A., EARL, P. L., LIU, R. & MOSS, B. 2022. Intranasal inoculation of an MVA-based vaccine induces IgA and protects the respiratory tract of hACE2 mice from SARS-CoV-2 infection. *Proceedings of the National Academy of Sciences*, 119, e2202069119.
- ANGUM, F., KHAN, T., KALER, J., SIDDIQUI, L. & HUSSAIN, A. 2020. The Prevalence of Autoimmune Disorders in Women: A Narrative Review. *Cureus*, 12, e8094.
- ANTROBUS, R. D., LILLIE, P. J., BERTHOUD, T. K., SPENCER, A. J., MCLAREN, J. E., LADELL, K., LAMBE, T., MILICIC, A., PRICE, D. A., HILL, A. V. & GILBERT, S. C. 2012. A T cell-inducing influenza vaccine for the elderly: safety and immunogenicity of MVA-NP+M1 in adults aged over 50 years. *PLoS One*, 7, e48322.
- ANYWAINE, Z., WHITWORTH, H., KALEEBU, P., PRAYGOD, G., SHUKAREV, G., MANNO, D., KAPIGA, S., GROSSKURTH, H., KALLUVYA, S., BOCKSTAL, V., ANUMENDEM, D., LUHN, K., ROBINSON, C., DOUGUIH, M. & WATSON-JONES, D. 2019. Safety and Immunogenicity of a 2-Dose Heterologous Vaccination Regimen With Ad26.ZEBOV and MVA-BN-Filo Ebola Vaccines: 12-Month Data From a Phase 1 Randomized Clinical Trial in Uganda and Tanzania. *The Journal of Infectious Diseases*, 220, 46-56.
- AREVALO, C. P., BOLTON, M. J., LE SAGE, V., YE, N., FUREY, C., MURAMATSU, H., ALAMEH, M.-G., PARDI, N., DRAPEAU, E. M., PARKHOUSE, K., GARRETSON, T., MORRIS, J. S., MONCLA, L. H., TAM, Y. K., FAN, S. H. Y., LAKDAWALA, S. S., WEISSMAN, D. & HENSLEY, S. E. 2022. A multivalent nucleoside-modified mRNA vaccine against all known influenza virus subtypes. *Science*, 378, 899-904.
- ARNOLD, J. N., WORMALD MR FAU - SIM, R. B., SIM RB FAU - RUDD, P. M., RUDD PM FAU - DWEK, R. A. & DWEK, R. A. 2007. The impact of glycosylation on the biological function and structure of human immunoglobulins. *Annu Rev Immunol*.
- ARNOLD, K. B. & CHUNG, A. W. 2018. Prospects from systems serology research. *Immunology*, 153, 279-289.
- AZHAR, E. I., HUI, D. S., MCCLOSKEY, B., EL-KAFRAWY, S. A., SHARMA, A., MAEURER, M., LEE, S.-S. & ZUMLA, A. 2022. The Qatar FIFA World Cup 2022 and camel pageant championships increase risk of MERS-CoV transmission and global spread. *The Lancet Global Health*.
- BAHARON, S. & MEMISH, Z. A. 2019. MERS-CoV as an emerging respiratory illness: A review of prevention methods. *Travel Med Infect Dis*, 32, 101520.
- BAHRS, C. & HARRISON, N. 2022. Vaccine Response in the Immunocompromised Patient with Focus on Cellular Immunity. *Vaccines (Basel)*, 10.
- BARBEAU, D. J., MARTIN, J. M., CARNEY, E., DOUGHERTY, E., DOYLE, J. D., DERMODY, T. S., HOBERMAN, A., WILLIAMS, J. V., MICHAELS, M. G., ALCORN, J. F., PAUL DUPREX, W. & MCELROY, A. K. 2022. Comparative analysis of human immune responses following SARS-CoV-2 vaccination with BNT162b2, mRNA-1273, or Ad26.COV2.S. *NPJ Vaccines*, 7, 77.
- BARBER, D. L., WHERRY, E. J., MASOPUST, D., ZHU, B., ALLISON, J. P., SHARPE, A. H., FREEMAN, G. J. & AHMED, R. 2006. Restoring function in exhausted CD8 T cells during chronic viral infection. *Nature*, 439, 682-7.
- BAROUCH, D. H., KIK, S. V., WEVERLING, G. J., DILAN, R., KING, S. L., MAXFIELD, L. F., CLARK, S., NG'ANG'A, D., BRANDARIZ, K. L., ABBINK, P., SINANGIL, F., DE BRUYN, G., GRAY, G. E., ROUX, S., BEKKER, L. G., DILRAJ, A., KIBUUKA, H., ROBB, M. L., MICHAEL, N. L., ANZALA, O., AMORNKUL, P. N., GILMOUR, J., HURAL, J., BUCHBINDER, S. P., SEAMAN, M. S., DOLIN, R., BADEN, L. R., CARVILLE, A., MANSFIELD, K. G., PAU, M. G. & GOUDSMIT, J. 2011. International seroepidemiology of adenovirus serotypes 5, 26, 35, and 48 in pediatric and adult populations. *Vaccine*, 29, 5203-9.
- BARRETT, J. R., BELIJ-RAMMERSTORFER, S., DOLD, C., EWER, K. J., FOLEGATTI, P. M., GILBRIDE, C., HALKERSTON, R., HILL, J., JENKIN, D., STOCKDALE, L., VERHEUL, M. K., ALEY, P. K., ANGUS, B.,

- BELLAMY, D., BERRIE, E., BIBI, S., BITTAYE, M., CARROLL, M. W., CAVELL, B., CLUTTERBUCK, E. A., EDWARDS, N., FLAXMAN, A., FUSKOVA, M., GORRINGE, A., HALLIS, B., KERRIDGE, S., LAWRIE, A. M., LINDER, A., LIU, X., MADHAVAN, M., MAKINSON, R., MELLORS, J., MINASSIAN, A., MOORE, M., MUJADIDI, Y., PLESTED, E., POULTON, I., RAMASAMY, M. N., ROBINSON, H., ROLLIER, C. S., SONG, R., SNAPE, M. D., TARRANT, R., TAYLOR, S., THOMAS, K. M., VOYSEY, M., WATSON, M. E. E., WRIGHT, D., DOUGLAS, A. D., GREEN, C. M., HILL, A. V. S., LAMBE, T., GILBERT, S. & POLLARD, A. J. 2021. Phase 1/2 trial of SARS-CoV-2 vaccine ChAdOx1 nCoV-19 with a booster dose induces multifunctional antibody responses. *Nat Med*, 27, 279-288.
- BARROS-MARTINS, J., HAMMERSCHMIDT, S. I., COSSMANN, A., ODAK, I., STANKOV, M. V., MORILLAS RAMOS, G., DOPFER-JABLONKA, A., HEIDEMANN, A., RITTER, C., FRIEDRICHSEN, M., SCHULTZE-FLOREY, C., RAVENS, I., WILLENZON, S., BUBKE, A., RISTENPART, J., JANSSEN, A., SSEBYATIKA, G., BERNHARDT, G., MÜNCH, J., HOFFMANN, M., PÖHLMANN, S., KREY, T., BOŠNJAK, B., FÖRSTER, R. & BEHRENS, G. M. N. 2021. Immune responses against SARS-CoV-2 variants after heterologous and homologous ChAdOx1 nCoV-19/BNT162b2 vaccination. *Nat Med*, 27, 1525-1529.
- BARROW, G. I., HIGGINS, P. G., AL-NAKIB, W., SMITH, A. P., WENHAM, R. B. & TYRRELL, D. A. 1990. The effect of intranasal nedocromil sodium on viral upper respiratory tract infections in human volunteers. *Clin Exp Allergy*, 20, 45-51.
- BARTSCH, Y. C., CIZMECI, D., KANG, J., ZOHAR, T., PERIASAMY, S., MEHTA, N., TOLBOOM, J., VAN DER FITS, L., SADOFF, J., COMEAUX, C., CALLENDRET, B., BUKREYEV, A., LAUFFENBURGER, D. A., BASTIAN, A. R. & ALTER, G. 2022. Antibody effector functions are associated with protection from respiratory syncytial virus. *Cell*, 185, 4873-4886.e10.
- BATTEN, M., GROOM, J., CACHERO, T. G., QIAN, F., SCHNEIDER, P., TSCHOPP, J., BROWNING, J. L. & MACKAY, F. 2000. BAFF mediates survival of peripheral immature B lymphocytes. *J Exp Med*, 192, 1453-66.
- BELSHE, R. B., NEWMAN, F. K., WILKINS, K., GRAHAM, I. L., BABUSIS, E., EWELL, M. & FREY, S. E. 2007. Comparative immunogenicity of trivalent influenza vaccine administered by intradermal or intramuscular route in healthy adults. *Vaccine*, 25, 6755-63.
- BELYAKOV, I. M., HAMMOND, S. A., AHLERS, J. D., GLENN, G. M. & BERZOFSKY, J. A. 2004. Transcutaneous immunization induces mucosal CTLs and protective immunity by migration of primed skin dendritic cells. *J Clin Invest*, 113, 998-1007.
- BENDALL, SEAN C., DAVIS, KARA L., AMIR, E.-AD D., TADMOR, MICHELLE D., SIMONDS, ERIN F., CHEN, TIFFANY J., SHENFELD, DANIEL K., NOLAN, GARRY P. & PE'ER, D. 2014. Single-Cell Trajectory Detection Uncovers Progression and Regulatory Coordination in Human B Cell Development. *Cell*, 157, 714-725.
- BEŇOVÁ, K., HANCKOVÁ, M., KOČI, K., KÚDELOVÁ, M. & BETÁKOVÁ, T. 2020. T cells and their function in the immune response to viruses. *Acta Virol*, 64, 131-143.
- BERGER, I. & SCHAFFITZEL, C. 2020. The SARS-CoV-2 spike protein: balancing stability and infectivity. *Cell Res*, 30, 1059-1060.
- BERGTOLD, A., DESAI DD FAU - GAVHANE, A., GAVHANE A FAU - CLYNES, R. & CLYNES, R. 2015. Cell surface recycling of internalized antigen permits dendritic cell priming of B cells. *Immunity*.
- BEYERSTEDT, S., CASARO, E. B. & RANGEL É, B. 2021. COVID-19: angiotensin-converting enzyme 2 (ACE2) expression and tissue susceptibility to SARS-CoV-2 infection. *Eur J Clin Microbiol Infect Dis*, 40, 905-919.
- BIALEK, S. R., BOWER, W. A., NOVAK, R., HELGENBERGER, L., AUERBACH, S. B., WILLIAMS, I. T. & BELL, B. P. 2008. Persistence of protection against hepatitis B virus infection among adolescents vaccinated with recombinant hepatitis B vaccine beginning at birth: a 15-year follow-up study. *Pediatr Infect Dis J*, 27, 881-5.
- BLOOM, D. E., BLACK, S. & RAPPUOLI, R. 2017. Emerging infectious diseases: A proactive approach. *Proceedings of the National Academy of Sciences*, 114, 4055-4059.
- BOCKSTAL, V., SHUKAREV, G., MCLEAN, C., GOLDSTEIN, N., BART, S., GADDAH, A., ANUMENDEN, D., STOOP, J. N., MARIT DE GROOT, A., PAU, M. G., HENDRIKS, J., DE ROSA, S. C., COHEN, K. W., MCEL RATH, M. J., CALLENDRET, B., LUHN, K., DOUGUIH, M. & ROBINSON, C. 2022. First-in-

- human study to evaluate safety, tolerability, and immunogenicity of heterologous regimens using the multivalent filovirus vaccines Ad26.Filo and MVA-BN-Filo administered in different sequences and schedules: A randomized, controlled study. *PLoS One*, 17, e0274906.
- BONELLI, M. M., MRAK, D., PERKMANN, T., HASLACHER, H. & ALETAHA, D. 2021. SARS-CoV-2 vaccination in rituximab-treated patients: evidence for impaired humoral but inducible cellular immune response. *Ann Rheum Dis*, 80, 1355-1356.
- BORASCHI, D. & ITALIANI, P. 2014. Immunosenescence and vaccine failure in the elderly: Strategies for improving response. *Immunology Letters*, 162, 346-353.
- BOROSS, P., VAN MONTFOORT, N., STAPELS, D. A., VAN DER POEL, C. E., BERTENS, C., MEELDIJK, J., JANSEN, J. H., VERBEEK, J. S., OSSENDORP, F., WUBBOLTS, R. & LEUSEN, J. H. 2014. FcRγ-chain ITAM signaling is critically required for cross-presentation of soluble antibody-antigen complexes by dendritic cells. *J Immunol*.
- BORREGA, R., NELSON, D. K. S., KOVAL, A. P., BOND, N. G., HEINRICH, M. L., ROWLAND, M. M., LATHIGRA, R., BUSH, D. J., AIMUKANOVA, I., PHINNEY, W. N., KOVAL, S. A., HOFFMANN, A. R., SMITHER, A. R., BELL-KAREEM, A. R., MELNIK, L. I., GENEMARAS, K. J., CHAO, K., SNARSKI, P., MELTON, A. B., HARRELL, J. E., SMIRA, A. A., ELLIOTT, D. H., ROUELLE, J. A., SABINO-SANTOS, G., JR., DROUIN, A. C., MOMOH, M., SANDI, J. D., GOBA, A., SAMUELS, R. J., KANNEH, L., GBAKIE, M., BRANCO, Z. L., SHAFFER, J. G., SCHIEFFELIN, J. S., ROBINSON, J. E., FUSCO, D. N., SABETI, P. C., ANDERSEN, K. G., GRANT, D. S., BOISEN, M. L., BRANCO, L. M. & GARRY, R. F. 2021. Cross-Reactive Antibodies to SARS-CoV-2 and MERS-CoV in Pre-COVID-19 Blood Samples from Sierra Leoneans. *Viruses*, 13.
- BORTNICK, A. & ALLMAN, D. 2013. What is and what should always have been: long-lived plasma cells induced by T cell-independent antigens. *J Immunol*.
- BOS, R., RUTTEN, L., VAN DER LUBBE, J. E. M., BAKKERS, M. J. G., HARDENBERG, G., WEGMANN, F., ZUIJDEEST, D., DE WILDE, A. H., KOORNNEEF, A., VERWILLIGEN, A., VAN MANEN, D., KWAKS, T., VOGELS, R., DALEBOUT, T. J., MYENI, S. K., KIKKERT, M., SNIJDER, E. J., LI, Z., BAROUCH, D. H., VELLINGA, J., LANGEDIJK, J. P. M., ZAHN, R. C., CUSTERS, J. & SCHUITEMAKER, H. 2020. Ad26 vector-based COVID-19 vaccine encoding a prefusion-stabilized SARS-CoV-2 Spike immunogen induces potent humoral and cellular immune responses. *NPJ Vaccines*, 5, 91.
- BOSAEED, M., BALKHY, H. H., ALMAZIAD, S., ALJAMI, H. A., ALHATMI, H., ALANAZI, H., ALAHMADI, M., JAWHARY, A., ALENAZI, M. W., ALMASOUD, A., ALANAZI, R., BITTAYE, M., ABOAGYE, J., ALBAALHARITH, N., BATAWI, S., FOLEGATTI, P., RAMOS LOPEZ, F., EWER, K., ALMOAIKEL, K., ALJERAISY, M., ALOTHMAN, A., GILBERT, S. C. & KHALAF ALHARBI, N. 2022. Safety and immunogenicity of ChAdOx1 MERS vaccine candidate in healthy Middle Eastern adults (MERS002): an open-label, non-randomised, dose-escalation, phase 1b trial. *Lancet Microbe*, 3, e11-e20.
- BOŠNJAK, B., ODAK, I., BARROS-MARTINS, J., SANDROCK, I., HAMMERSCHMIDT, S. I., PERMANYER, M., PATZER, G. E., GREORGIEV, H., GUTIERREZ JAUREGUI, R., TSCHERNE, A., SCHWARZ, J. H., KALODIMOU, G., SSEBYATIKA, G., CIURKIEWICZ, M., WILLENZON, S., BUBKE, A., RISTENPART, J., RITTER, C., TUCHEL, T., MEYER ZU NATRUP, C., SHIN, D.-L., CLEVER, S., LIMPINSEL, L., BAUMGÄRTNER, W., KREY, T., VOLZ, A., SUTTER, G. & FÖRSTER, R. 2021. Intranasal Delivery of MVA Vector Vaccine Induces Effective Pulmonary Immunity Against SARS-CoV-2 in Rodents. *Frontiers in Immunology*, 12.
- BOURNAZOS, S., KLEIN, F., PIETZSCH, J., SEAMAN, M. S., NUSSENZWEIG, M. C. & RAVETCH, J. V. 2014. Broadly neutralizing anti-HIV-1 antibodies require Fc effector functions for in vivo activity. *Cell*.
- BOURNAZOS, S. & RAVETCH, J. V. 2017. Fcγ Receptor Function and the Design of Vaccination Strategies. *Immunity*, 47, 224-233.
- BOURNAZOS, S., WANG, T. T. & RAVETCH, J. V. 2016. The Role and Function of Fcγ Receptors on Myeloid Cells. LID - 10.1128/microbiolspec.MCHD-0045-2016 [doi]. *Microbiol Spectr*.
- BRADLEY, T., POLLARA, J., SANTRA, S., VANDERGRIFT, N., PITTALA, S., BAILEY-KELLOGG, C., SHEN, X., PARKS, R., GOODMAN, D., EATON, A., BALACHANDRAN, H., MACH, L. V., SAUNDERS, K. O., WEINER, J. A., SCEARCE, R., SUTHERLAND, L. L., PHOGAT, S., TARTAGLIA, J., REED, S. G., HU, S.-L., THEIS, J. F., PINTER, A., MONTEFIORI, D. C., KEPLER, T. B., PEACHMAN, K. K., RAO, M.,

- MICHAEL, N. L., SUSCOVICH, T. J., ALTER, G., ACKERMAN, M. E., MOODY, M. A., LIAO, H.-X., TOMARAS, G., FERRARI, G., KORBER, B. T. & HAYNES, B. F. 2017. Pentavalent HIV-1 vaccine protects against simian-human immunodeficiency virus challenge. *Nature Communications*, 8, 15711.
- BRISSE, M., VRBA, S. M., KIRK, N., LIANG, Y. & LY, H. 2020. Emerging Concepts and Technologies in Vaccine Development. *Front Immunol*, 11, 583077.
- BRYNJOLFSSON, S. F., MOHADDES, M., KÄRRHOLM, J. & WICK, M. J. 2017. Long-lived plasma cells in human bone marrow can be either CD19(+) or CD19(). *Blood Adv*.
- BUHRE, J. S., PONGRACZ, T., KÜNSTING, I., LIXENFELD, A. S., WANG, W., NOUTA, J., LEHRIAN, S., SCHMELTER, F., LUNDING, H. B., DÜHRING, L., KERN, C., PETRY, J., MARTIN, E. L., FÖH, B., STEINHAUS, M., VON KOPYLOW, V., SINA, C., GRAF, T., RAHMÖLLER, J., WUHRER, M. & EHLERS, M. 2023. mRNA vaccines against SARS-CoV-2 induce comparably low long-term IgG Fc galactosylation and sialylation levels but increasing long-term IgG4 responses compared to an adenovirus-based vaccine. *Frontiers in Immunology*, 13.
- BURTON, B. R., TENNANT, R. K., LOVE, J., TITBALL, R. W., WRAITH, D. C. & WHITE, H. N. 2018. Variant proteins stimulate more IgM+ GC B-cells revealing a mechanism of cross-reactive recognition by antibody memory. *eLife*, 7, e26832.
- CALLEGARO, A. & TIBALDI, F. 2019. Assessing correlates of protection in vaccine trials: statistical solutions in the context of high vaccine efficacy. *BMC Medical Research Methodology*, 19, 47.
- CALLOW, K. A. 1985. Effect of specific humoral immunity and some non-specific factors on resistance of volunteers to respiratory coronavirus infection. *J Hyg (Lond)*, 95, 173-89.
- CANETTI, M., BARDA, N., GILBOA, M., INDENBAUM, V., ASRAF, K., GONEN, T., WEISS-OTTOLENGHI, Y., AMIT, S., DOOLMAN, R., MENDELSON, E., FREEDMAN, L. S., KREISS, Y., LUSTIG, Y. & REGEV-YOCHAY, G. 2022. Six-Month Follow-up after a Fourth BNT162b2 Vaccine Dose. *New England Journal of Medicine*, 387, 2092-2094.
- CAUCHEMEZ, S., FRASER, C., VAN KERKHOVE, M. D., DONNELLY, C. A., RILEY, S., RAMBAUT, A., ENOUF, V., VAN DER WERF, S. & FERGUSON, N. M. 2013. Middle East respiratory syndrome coronavirus: quantification of the extent of the epidemic, surveillance biases, and transmissibility. *Lancet Infect Dis*.
- CEPI 2020. CEPI establishes global network of laboratories to centralise assessment of COVID-19 vaccine candidates.
- CERWENKA, A. & LANIER, L. L. 2001. Natural killer cells, viruses and cancer. *Nat Rev Immunol*, 1, 41-9.
- CHAN-YEUNG, M. & XU, R. H. 2003. SARS: epidemiology. *Respirology*, 8 Suppl, S9-14.
- CHAN, R. W. Y., CHAN, K. C. C., LUI, G. C. Y., TSUN, J. G. S., CHAN, K. Y. Y., YIP, J. S. K., LIU, S., YU, M. W. L., NG, R. W. Y., CHONG, K. K. L., WANG, M. H., CHAN, P. K. S., LI, A. M. & LAM, H. S. 2022. Mucosal Antibody Response to SARS-CoV-2 in Paediatric and Adult Patients: A Longitudinal Study. *Pathogens*, 11.
- CHAPLIN, D. D. 2010. Overview of the immune response. *J Allergy Clin Immunol*, 125, S3-23.
- CHEN, C. P., HUANG, K. A., SHIH, S. R., LIN, Y. C., CHENG, C. Y., HUANG, Y. C., LIN, T. Y. & CHENG, S. H. 2022a. Anti-Spike Antibody Response to Natural Infection with SARS-CoV-2 and Its Activity against Emerging Variants. *Microbiol Spectr*, 10, e0074322.
- CHEN, W., ZHANG, L., LI, J., BAI, S., WANG, Y., ZHANG, B., ZHENG, Q., CHEN, M., ZHAO, W. & WU, J. 2022b. The kinetics of IgG subclasses and contributions to neutralizing activity against SARS-CoV-2 wild-type strain and variants in healthy adults immunized with inactivated vaccine. *Immunology*, 167, 221-232.
- CHIU, M. L., GOULET, D. R., TEPLYAKOV, A. & GILLILAND, G. L. 2019. Antibody Structure and Function: The Basis for Engineering Therapeutics. *Antibodies*, 55.
- CHIUPPESI, F., SALAZAR, M. D., CONTRERAS, H., NGUYEN, V. H., MARTINEZ, J., PARK, Y., NGUYEN, J., KHA, M., INIGUEZ, A., ZHOU, Q., KALTICHEVA, T., LEVYTSKY, R., EBELT, N. D., KANG, T. H., WU, X., ROGERS, T. F., MANUEL, E. R., SHOSTAK, Y., DIAMOND, D. J. & WUSSOW, F. 2020. Development of a multi-antigenic SARS-CoV-2 vaccine candidate using a synthetic poxvirus platform. *Nat Commun*, 11, 6121.

- CHIUPPESI, F., ZAIA, J. A., FRANKEL, P. H., STAN, R., DRAKE, J., WILLIAMS, B., ACOSTA, A. M., FRANCIS, K., TAPLITZ, R. A., DICKTER, J. K., DADWAL, S., PUING, A. G., NANAYAKKARA, D. D., ASH, P., CUI, Y., CONTRERAS, H., LA ROSA, C., TIEMANN, K., PARK, Y., MEDINA, J., INIGUEZ, A., ZHOU, Q., KARPINSKI, V., JOHNSON, D., FAIRCLOTH, K., KALTICHEVA, T., NGUYEN, J., KHA, M., NGUYEN, V. H., FRANCISCO, S. O., GRIFONI, A., WONG, A., SETTE, A., WUSSOW, F. & DIAMOND, D. J. 2022. Safety and immunogenicity of a synthetic multiantigen modified vaccinia virus Ankara-based COVID-19 vaccine (COH04S1): an open-label and randomised, phase 1 trial. *Lancet Microbe*, 3, e252-e264.
- CHOI, J. A. & KIM, J. O. 2022. Middle East Respiratory Syndrome coronavirus vaccine development: updating clinical studies using platform technologies. *J Microbiol*, 60, 238-246.
- CHUNG, A. W., GHEBREMICHAEL M FAU - ROBINSON, H., ROBINSON H FAU - BROWN, E., BROWN E FAU - CHOI, I., CHOI I FAU - LANE, S., LANE S FAU - DUGAST, A.-S., DUGAST AS FAU - SCHOEN, M. K., SCHOEN MK FAU - ROLLAND, M., ROLLAND M FAU - SUSCOVICH, T. J., SUSCOVICH TJ FAU - MAHAN, A. E., MAHAN AE FAU - LIAO, L., LIAO L FAU - STREECK, H., STREECK H FAU - ANDREWS, C., ANDREWS C FAU - RERKS-NGARM, S., RERKS-NGARM S FAU - NITAYAPHAN, S., NITAYAPHAN S FAU - DE SOUZA, M. S., DE SOUZA MS FAU - KAEWKUNGWAL, J., KAEWKUNGWAL J FAU - PITISUTTITHUM, P., PITISUTTITHUM P FAU - FRANCIS, D., FRANCIS D FAU - MICHAEL, N. L., MICHAEL NL FAU - KIM, J. H., KIM JH FAU - BAILEY-KELLOGG, C., BAILEY-KELLOGG C FAU - ACKERMAN, M. E., ACKERMAN ME FAU - ALTER, G. & ALTER, G. 2014. Polyfunctional Fc-effector profiles mediated by IgG subclass selection distinguish RV144 and VAX003 vaccines. *Sci Transl Med*.
- CHUNG, A. W., KUMAR, M. P., ARNOLD, K. B., YU, W. H., SCHOEN, M. K., DUNPHY, L. J., SUSCOVICH, T. J., FRAHM, N., LINDE, C., MAHAN, A. E., HOFFNER, M., STREECK, H., ACKERMAN, M. E., MCEL RATH, M. J., SCHUITEMAKER, H., PAU, M. G., BADEN, L. R., KIM, J. H., MICHAEL, N. L., BAROUCH, D. H., LAUFFENBURGER, D. A. & ALTER, G. 2015. Dissecting Polyclonal Vaccine-Induced Humoral Immunity against HIV Using Systems Serology. *Cell*, 163, 988-98.
- CIABATTINI, A., PASTORE, G., FIORINO, F., POLVERE, J., LUCCHESI, S., PETTINI, E., AUDDINO, S., RANCAN, I., DURANTE, M., MISCIA, M., ROSSETTI, B., FABBIANI, M., MONTAGNANI, F. & MEDAGLINI, D. 2021. Evidence of SARS-CoV-2-Specific Memory B Cells Six Months After Vaccination With the BNT162b2 mRNA Vaccine. *Frontiers in Immunology*, 12.
- CLARKE, D. K., XU, R., MATASSOV, D., LATHAM, T. E., OTA-SETLIK, A., GERARDI, C. S., LUCKAY, A., WITKO, S. E., HERMIDA, L., HIGGINS, T., TREMBLAY, M., SCIOTTO-BROWN, S., CHEN, T., EGAN, M. A., RUSNAK, J. M., WARD, L. A. & ELDRIDGE, J. H. 2020. Safety and immunogenicity of a highly attenuated rVSVN4CT1-EBOVGP1 Ebola virus vaccine: a randomised, double-blind, placebo-controlled, phase 1 clinical trial. *Lancet Infect Dis*, 20, 455-466.
- COHEN, J. I. & BURBELO, P. D. 2021. Reinfection With SARS-CoV-2: Implications for Vaccines. *Clinical Infectious Diseases*, 73, e4223-e4228.
- COMBADIÈRE, B., VOGT, A., MAHÉ, B., COSTAGLIOLA, D., HADAM, S., BONDUELLE, O., STERRY, W., STASZEWSKI, S., SCHAEFER, H., VAN DER WERF, S., KATLAMA, C., AUTRAN, B. & BLUME-PEYTAVI, U. 2010. Preferential amplification of CD8 effector-T cells after transcutaneous application of an inactivated influenza vaccine: a randomized phase I trial. *PLoS One*, 5, e10818.
- COONEY, E. L., COLLIER, A. C., GREENBERG, P. D., COOMBS, R. W., ZARLING, J., ARDITTI, D. E., HOFFMAN, M. C., HU, S. L. & COREY, L. 1991. Safety of and immunological response to a recombinant vaccinia virus vaccine expressing HIV envelope glycoprotein. *Lancet*, 337, 567-72.
- COOPER, N. 1984. The role of antibody and complement in the control of viral infections. *J Invest Dermatol*.
- CORMAN, V. M., LIENAU, J. & WITZENRATH, M. 2019. [Coronaviruses as the cause of respiratory infections]. *Internist (Berl)*, 60, 1136-1145.
- CORTHÉSY, B. 2013. Multi-faceted functions of secretory IgA at mucosal surfaces. *Front Immunol*, 4, 185.
- CORTI, D., SUGUITAN, A. L., JR., PINNA, D., SILACCI, C., FERNANDEZ-RODRIGUEZ, B. M., VANZETTA, F., SANTOS, C., LUKE, C. J., TORRES-VELEZ, F. J., TEMPERTON, N. J., WEISS, R. A., SALLUSTO, F., SUBBARAO, K. & LANZAVECCHIA, A. 2010. Heterosubtypic neutralizing antibodies are

- produced by individuals immunized with a seasonal influenza vaccine. *J Clin Invest*, 120, 1663-73.
- COUGHLAN, L., SRIDHAR, S., PAYNE, R., EDMANS, M., MILICIC, A., VENKATRAMAN, N., LUGONJA, B., CLIFTON, L., QI, C., FOLEGATTI, P. M., LAWRIE, A. M., ROBERTS, R., DE GRAAF, H., SUKHTANKAR, P., FAUST, S. N., LEWIS, D. J. M., LAMBE, T., HILL, A. V. S. & GILBERT, S. C. 2018. Heterologous Two-Dose Vaccination with Simian Adenovirus and Poxvirus Vectors Elicits Long-Lasting Cellular Immunity to Influenza Virus A in Healthy Adults. *EBioMedicine*, 29, 146-154.
- COVID-19 VACCINE TRACKER. *VACCINE CANDIDATES IN CLINICAL TRIALS* [Online]. Available: <https://covid19.trackvaccines.org/vaccines/> [Accessed 21.12.2022].
- CROTTY, S. 2015. A brief history of T cell help to B cells. *Nat Rev Immunol*.
- CUSTERS, J., KIM, D., LEYSSEN, M., GURWITH, M., TOMAKA, F., ROBERTSON, J., HEIJNEN, E., CONDIT, R., SHUKAREV, G., HEERWEGH, D., VAN HEESBEEN, R., SCHUITEMAKER, H., DOUGUIH, M., EVANS, E., SMITH, E. R. & CHEN, R. T. 2021. Vaccines based on replication incompetent Ad26 viral vectors: Standardized template with key considerations for a risk/benefit assessment. *Vaccine*, 39, 3081-3101.
- CYSTER, J. G. & ALLEN, C. D. C. 2019. B Cell Responses: Cell Interaction Dynamics and Decisions. *Cell*, 177, 524-540.
- DAMELANG, T., AITKEN, E. H., HASANG, W., LOPEZ, E., KILLIAN, M., UNGER, H. W., SALANTI, A., SHUB, A., MCCARTHY, E., KEDZIERSKA, K., LAPPAS, M., KENT, S. J., ROGERSON, S. J. & CHUNG, A. W. 2021. Antibody mediated activation of natural killer cells in malaria exposed pregnant women. *Scientific Reports*, 11, 4130.
- DANGI, T., SANCHEZ, S., LEW, M. H., VISVABHARATHY, L., RICHNER, J., KORALNIK, I. J. & PENALOZA-MACMASTER, P. 2022. Pre-existing immunity modulates responses to mRNA boosters. *bioRxiv*.
- DAS, S., SINGH, J., SHAMAN, H., SINGH, B., ANANTHARAJ, A., SHARANABASAVA, P., PANDEY, R., LODHA, R., PANDEY, A. K. & MEDIGESHI, G. R. 2022. Pre-existing antibody levels negatively correlate with antibody titers after a single dose of BBV152 vaccination. *Nature Communications*, 13, 3451.
- DAVIES, J., JIANG, L., PAN, L. Z., LABARRE, M. J., ANDERSON, D. & REFF, M. 2001. Expression of GnTIII in a recombinant anti-CD20 CHO production cell line: Expression of antibodies with altered glycoforms leads to an increase in ADCC through higher affinity for FC gamma RIII. *Biotechnol Bioeng*, 74, 288-94.
- DAVIS, M. M. 2008. A prescription for human immunology. *Immunity*, 29, 835-8.
- DE SILVA, N. S. & KLEIN, U. 2015. Dynamics of B cells in germinal centres. *Nat Rev Immunol*.
- DE VRIES, R. D., ALTENBURG, A. F., NIEUWKOOP, N. J., DE BRUIN, E., VAN TRIERUM, S. E., PRONK, M. R., LAMERS, M. M., RICHARD, M., NIEUWENHUIJSE, D. F., KOOPMANS, M. P. G., KREIJTZ, J., FOUCHIER, R. A. M., OSTERHAUS, A., SUTTER, G. & RIMMELZWAAN, G. F. 2018. Induction of Cross-Clade Antibody and T-Cell Responses by a Modified Vaccinia Virus Ankara-Based Influenza A(H5N1) Vaccine in a Randomized Phase 1/2a Clinical Trial. *J Infect Dis*, 218, 614-623.
- DE WIT, E., VAN DOREMALEN, N., FALZARANO, D. & MUNSTER, V. J. 2016. SARS and MERS: recent insights into emerging coronaviruses. *Nat Rev Microbiol*.
- DELANY, I., RAPPUOLI, R. & DE GREGORIO, E. 2014. Vaccines for the 21st century. *EMBO Mol Med*, 6, 708-20.
- DEMING, M. E. & LYKE, K. E. 2021. A 'mix and match' approach to SARS-CoV-2 vaccination. *Nature Medicine*, 27, 1510-1511.
- DEMPSEY, P. W., VAIDYA, S. A. & CHENG, G. 2003. The art of war: Innate and adaptive immune responses. *Cell Mol Life Sci*, 60, 2604-21.
- DEVOLDERE, J., DEWITTE, H., DE SMEDT, S. C. & REMAUT, K. 2016. Evading innate immunity in nonviral mRNA delivery: don't shoot the messenger. *Drug Discov Today*, 21, 11-25.
- DI, S. A. P. A. 1950. Simultaneous immunization of newborn infants against diphtheria, tetanus, and pertussis; production of antibodies and duration of antibody levels in an eastern metropolitan area. *Am J Public Health Nations Health*, 40, 674-80.
- DOLGIN, E. 2021. The tangled history of mRNA vaccines. *Nature*, 597, 318-324.
- DOLGIN, E. 2022. Pan-coronavirus vaccine pipeline takes form. *Nat Rev Drug Discov*, 21, 324-326.

- DOLZHIKOVA, I. V., GROUSOVA, D. M., ZUBKOVA, O. V., TUKHVATULIN, A. I., KOVYRSHINA, A. V., LUBENETS, N. L., OZHAROVSKAIA, T. A., POPOVA, O., ESMAGAMBETOV, I. B., SHCHEBLYAKOV, D. V., EVGRAFOVA, I. M., NEDORUBOV, A. A., GORDEICHUK, I. V., GULYAEV, S. A., BOTIKOV, A. G., PANINA, L. V., MISHIN, D. V., LOGINOVA, S. Y., BORISEVICH, S. V., DERYABIN, P. G., NARODITSKY, B. S., LOGUNOV, D. Y. & GINTSBURG, A. L. 2020. Preclinical Studies of Immunogenicity, Protectivity, and Safety of the Combined Vector Vaccine for Prevention of the Middle East Respiratory Syndrome. *Acta Naturae*, 12, 114-123.
- DU, L., HE, Y., ZHOU, Y., LIU, S., ZHENG, B.-J. & JIANG, S. 2009. The spike protein of SARS-CoV — a target for vaccine and therapeutic development. *Nature Reviews Microbiology*, 7, 226-236.
- EARLE, K. A., AMBROSINO, D. M., FIORE-GARTLAND, A., GOLDBLATT, D., GILBERT, P. B., SIBER, G. R., DULL, P. & PLOTKIN, S. A. 2021. Evidence for antibody as a protective correlate for COVID-19 vaccines. *Vaccine*, 39, 4423-4428.
- EDWARDS, K. M. 2001. Development, acceptance, and use of immunologic correlates of protection in monitoring the effectiveness of combination vaccines. *Clin Infect Dis*, 33 Suppl 4, S274-7.
- EDWARDS, K. M. & NEUZIL, K. M. 2022. Understanding COVID-19 through human challenge models. *Nature Medicine*, 28, 903-904.
- EKIERT, D. C., BHABHA, G., ELSLIGER, M. A., FRIESEN, R. H., JONGENEELLEN, M., THROSBY, M., GOUDSMIT, J. & WILSON, I. A. 2009. Antibody recognition of a highly conserved influenza virus epitope. *Science*, 324, 246-51.
- EMA 2013. European Medicines Agency recommends approval of 44 medicines for human use and six medicines for veterinary use in first half 2013.
- EMA 2019. First vaccine to protect against Ebola.
- EMA 2020a. EMA recommends first COVID-19 vaccine for authorisation in the EU.
- EMA 2020b. New vaccine for prevention of Ebola virus disease recommended for approval in the European Union.
- EMA 2021a. EMA recommends COVID-19 Vaccine AstraZeneca for authorisation in the EU
- EMA 2021b. EMA recommends COVID-19 Vaccine Janssen for authorisation in the EU.
- EMA 2021c. EMA recommends COVID-19 Vaccine Moderna for authorisation in the EU.
- EMA 2022. EMA's Emergency Task Force advises on intradermal use of Imvanex / Jynneos against monkeypox.
- ERRICO, J. M., ADAMS, L. J. & FREMONT, D. H. 2022. Antibody-mediated immunity to SARS-CoV-2 spike. *Adv Immunol*, 154, 1-69.
- ESPESETH, A. S., CEJAS, P. J., CITRON, M. P., WANG, D., DISTEFANO, D. J., CALLAHAN, C., DONNELL, G. O., GALLI, J. D., SWOYER, R., TOUCH, S., WEN, Z., ANTONELLO, J., ZHANG, L., FLYNN, J. A., COX, K. S., FREED, D. C., VORA, K. A., BAHL, K., LATHAM, A. H., SMITH, J. S., GINDY, M. E., CIARAMELLA, G., HAZUDA, D., SHAW, C. A. & BETT, A. J. 2020. Modified mRNA/lipid nanoparticle-based vaccines expressing respiratory syncytial virus F protein variants are immunogenic and protective in rodent models of RSV infection. *NPJ Vaccines*, 5, 16.
- EWER, K., RAMPLING, T., VENKATRAMAN, N., BOWYER, G., WRIGHT, D., LAMBE, T., IMOUKHUEDE, E. B., PAYNE, R., FEHLING, S. K., STRECKER, T., BIEDENKOPF, N., KRÄHLING, V., TULLY, C. M., EDWARDS, N. J., BENTLEY, E. M., SAMUEL, D., LABBÉ, G., JIN, J., GIBANI, M., MINHINNICK, A., WILKIE, M., POULTON, I., LELLA, N., ROBERTS, R., HARTNELL, F., BLISS, C., SIERRA-DAVIDSON, K., POWLSON, J., BERRIE, E., TEDDER, R., ROMAN, F., DE RYCK, I., NICOSIA, A., SULLIVAN, N. J., STANLEY, D. A., MBAYA, O. T., LEDGERWOOD, J. E., SCHWARTZ, R. M., SIANI, L., COLLOCA, S., FOLGORI, A., DI MARCO, S., CORTESE, R., WRIGHT, E., BECKER, S., GRAHAM, B. S., KOUP, R. A., LEVINE, M. M., VOLKMANN, A., CHAPLIN, P., POLLARD, A. J., DRAPER, S. J., BALLOU, W. R., LAWRIE, A., GILBERT, S. C. & HILL, A. V. 2016a. A Monovalent Chimpanzee Adenovirus Ebola Vaccine Boosted with MVA. *N Engl J Med*, 374, 1635-46.
- EWER, K., SEBASTIAN, S., SPENCER, A. J., GILBERT, S., HILL, A. V. S. & LAMBE, T. 2017. Chimpanzee adenoviral vectors as vaccines for outbreak pathogens. *Human Vaccines & Immunotherapeutics*, 13, 3020-3032.
- EWER, K. J., LAMBE, T., ROLLIER, C. S., SPENCER, A. J., HILL, A. V. & DORRELL, L. 2016b. Viral vectors as vaccine platforms: from immunogenicity to impact. *Curr Opin Immunol*, 41, 47-54.

- FATHI, A., ADDO, M. M. & DAHLKE, C. 2020. Sex Differences in Immunity: Implications for the Development of Novel Vaccines Against Emerging Pathogens. *Front Immunol*, 11, 601170.
- FATHI, A., DAHLKE, C., KRAHLING, V., KUPKE, A., OKBA, N. M. A., RAADSEN, M. P., HEIDEPRIEM, J., MULLER, M. A., PARIS, G., LASSEN, S., KLUVER, M., VOLZ, A., KOCH, T., LY, M. L., FRIEDRICH, M., FUX, R., TSCHERNE, A., KALODIMOU, G., SCHMIEDEL, S., CORMAN, V. M., HESTERKAMP, T., DROSTEN, C., LOEFFLER, F. F., HAAGMANS, B. L., SUTTER, G., BECKER, S. & ADDO, M. M. 2022. Increased neutralization and IgG epitope identification after MVA-MERS-S booster vaccination against Middle East respiratory syndrome. *medRxiv*, 2022.02.14.22270168.
- FAUSTHER-BOVENDO, H. & KOBINGER, G. P. 2014. Pre-existing immunity against Ad vectors: humoral, cellular, and innate response, what's important? *Hum Vaccin Immunother*, 10, 2875-84.
- FDA 2019a. First FDA-approved vaccine for the prevention of Ebola virus disease, marking a critical milestone in public health preparedness and response.
- FDA. 2019b. *Summary Basis for Regulatory Action - JYNNEOS* [Online]. Available: <https://www.fda.gov/vaccines-blood-biologics/jynneos> [Accessed 22.12.2022].
- FDA 2020a. FDA Takes Additional Action in Fight Against COVID-19 By Issuing Emergency Use Authorization for Second COVID-19 Vaccine.
- FDA 2020b. FDA Takes Key Action in Fight Against COVID-19 By Issuing Emergency Use Authorization for First COVID-19 Vaccine.
- FDA 2021. FDA Issues Emergency Use Authorization for Third COVID-19 Vaccine.
- FEHERVARI, Z. 2019. Vaccine sex differences. *Nature Immunology*, 20, 111-111.
- FEHR, A. R. & PERLMAN, S. 2015. Coronaviruses: an overview of their replication and pathogenesis. *Methods Mol Biol*, 1282, 1-23.
- FELDMAN, R. A., FUHR, R., SMOLENOV, I., RIBEIRO, A., PANTHER, L., WATSON, M., SENN, J. J., SMITH, M., ALMARSSON, Ö., PUJAR, H. S., LASKA, M. E., THOMPSON, J., ZAKS, T. & CIARAMELLA, G. 2019. mRNA vaccines against H10N8 and H7N9 influenza viruses of pandemic potential are immunogenic and well tolerated in healthy adults in phase 1 randomized clinical trials. *Vaccine*, 37, 3326-3334.
- FENG, S., PHILLIPS, D. J., WHITE, T., SAYAL, H., ALEY, P. K., BIBI, S., DOLD, C., FUSKOVA, M., GILBERT, S. C., HIRSCH, I., HUMPHRIES, H. E., JEPSON, B., KELLY, E. J., PLESTED, E., SHOEMAKER, K., THOMAS, K. M., VEKEMANS, J., VILLAFANA, T. L., LAMBE, T., POLLARD, A. J. & VOYSEY, M. 2021. Correlates of protection against symptomatic and asymptomatic SARS-CoV-2 infection. *Nat Med*, 27, 2032-2040.
- FIOLET, T., KHERABI, Y., MACDONALD, C. J., GHOSN, J. & PEIFFER-SMADJA, N. 2022. Comparing COVID-19 vaccines for their characteristics, efficacy and effectiveness against SARS-CoV-2 and variants of concern: a narrative review. *Clin Microbiol Infect*, 28, 202-221.
- FIRAN, M., BAWDON R FAU - RADU, C., RADU C FAU - OBER, R. J., OBER RJ FAU - EAKEN, D., EAKEN D FAU - ANTOHE, F., ANTOHE F FAU - GHETIE, V., GHETIE V FAU - WARD, E. S. & WARD, E. S. 2001. The MHC class I-related receptor, FcRn, plays an essential role in the maternofetal transfer of gamma-globulin in humans. *Int Immunol*.
- FISCHINGER, S., BOUDREAU, C. M., BUTLER, A. L., STREECK, H. & ALTER, G. 2019. Sex differences in vaccine-induced humoral immunity. *Semin Immunopathol*, 41, 239-249.
- FISCHINGER, S., CIZMECI, D., DENG, D., GRANT, S. P., FRAHM, N., MCEL RATH, J., FUCHS, J., BART, P. A., PANTALEO, G., KEEFER, M., W, O. H., ROUPHAEL, N., CHURCHYARD, G., MOODIE, Z., DONASTORG, Y., STREECK, H. & ALTER, G. 2021. Sequence and vector shapes vaccine induced antibody effector functions in HIV vaccine trials. *PLoS Pathog*, 17, e1010016.
- FLACCO, M. E., SOLDATO, G., ACUTI MARTELLUCCI, C., DI MARTINO, G., CAROTA, R., CAPONETTI, A. & MANZOLI, L. 2022. Risk of SARS-CoV-2 Reinfection 18 Months After Primary Infection: Population-Level Observational Study. *Frontiers in Public Health*, 10.
- FLANAGAN, K. L., FINK, A. L., PLEBANSKI, M. & KLEIN, S. L. 2017. Sex and Gender Differences in the Outcomes of Vaccination over the Life Course. *Annual Review of Cell and Developmental Biology*, 33, 577-599.
- FLAXMAN, A., MARCHEVSKY, N. G., JENKIN, D., ABOAGYE, J., ALEY, P. K., ANGUS, B., BELIJ-RAMMERSTORFER, S., BIBI, S., BITTAYE, M., CAPPUCCINI, F., CICCIONI, P., CLUTTERBUCK, E. A.,

- DAVIES, S., DEJNIRATTISAI, W., DOLD, C., EWER, K. J., FOLEGATTI, P. M., FOWLER, J., HILL, A. V. S., KERRIDGE, S., MINASSIAN, A. M., MONGKOLSAPAYA, J., MUJADIDI, Y. F., PLESTED, E., RAMASAMY, M. N., ROBINSON, H., SANDERS, H., SHEEHAN, E., SMITH, H., SNAPE, M. D., SONG, R., WOODS, D., SCRETON, G., GILBERT, S. C., VOYSEY, M., POLLARD, A. J., LAMBE, T., ADLOU, S., ALEY, R., ALI, A., ANSLOW, R., BAKER, M., BAKER, P., BARRETT, J. R., BATES, L., BEADON, K., BECKLEY, R., BELL, J., BELLAMY, D., BEVERIDGE, A., BISSETT, C., BLACKWELL, L., BLETCHLY, H., BOYD, A., BRIDGES-WEBB, A., BROWN, C., BYARD, N., CAMARA, S., CIFUENTES GUTIERREZ, L., COLLINS, A. M., COOPER, R., CROCKER, W. E. M., DARTON, T. C., DAVIES, H., DAVIES, J., DEMISSIE, T., DI MASO, C., DINESH, T., DONNELLAN, F. R., DOUGLAS, A. D., DRAKE-BROCKMAN, R., DUNCAN, C. J. A., ELIAS, S. C., EMARY, K. R. W., GHULAM FAROOQ, M., FAUST, S. N., FELLE, S., FERREIRA, D., FERREIRA DA SILVA, C., FINN, A., FORD, K. J., FRANCIS, E., FURZE, J., FUSKOVA, M., GALIZA, E., GIBERTONI CRUZ, A., GODFREY, L., GOODMAN, A. L., GREEN, C., GREEN, C. A., GREENWOOD, N., HARRISON, D., HART, T. C., HAWKINS, S., HEATH, P. T., HILL, H., HILLSON, K., HORSINGTON, B., HOU, M. M., HOWE, E., et al. 2021. Reactogenicity and immunogenicity after a late second dose or a third dose of ChAdOx1 nCoV-19 in the UK: a substudy of two randomised controlled trials (COV001 and COV002). *The Lancet*, 398, 981-990.
- FOCOSI, D. & MAGGI, F. 2021. Neutralising antibody escape of SARS-CoV-2 spike protein: Risk assessment for antibody-based Covid-19 therapeutics and vaccines. *Rev Med Virol*, 31, e2231.
- FODOULIAN, L., TUBEROSA, J., ROSSIER, D., BOILLAT, M., KAN, C., PAULI, V., EGERVARI, K., LOBRINUS, J. A., LANDIS, B. N., CARLETON, A. & RODRIGUEZ, I. 2020. SARS-CoV-2 Receptors and Entry Genes Are Expressed in the Human Olfactory Neuroepithelium and Brain. *iScience*, 23, 101839.
- FOLEGATTI, P. M., BITTAYE, M., FLAXMAN, A., LOPEZ, F. R., BELLAMY, D., KUPKE, A., MAIR, C., MAKINSON, R., SHERIDAN, J., ROHDE, C., HALWE, S., JEONG, Y., PARK, Y. S., KIM, J. O., SONG, M., BOYD, A., TRAN, N., SILMAN, D., POULTON, I., DATOO, M., MARSHALL, J., THEMISTOCLEOUS, Y., LAWRIE, A., ROBERTS, R., BERRIE, E., BECKER, S., LAMBE, T., HILL, A., EWER, K. & GILBERT, S. 2020a. Safety and immunogenicity of a candidate Middle East respiratory syndrome coronavirus viral-vectored vaccine: a dose-escalation, open-label, non-randomised, uncontrolled, phase 1 trial. *Lancet Infect Dis*, 20, 816-826.
- FOLEGATTI, P. M., EWER, K. J., ALEY, P. K., ANGUS, B., BECKER, S., BELIJ-RAMMERSTORFER, S., BELLAMY, D., BIBI, S., BITTAYE, M., CLUTTERBUCK, E. A., DOLD, C., FAUST, S. N., FINN, A., FLAXMAN, A. L., HALLIS, B., HEATH, P., JENKIN, D., LAZARUS, R., MAKINSON, R., MINASSIAN, A. M., POLLOCK, K. M., RAMASAMY, M., ROBINSON, H., SNAPE, M., TARRANT, R., VOYSEY, M., GREEN, C., DOUGLAS, A. D., HILL, A. V. S., LAMBE, T., GILBERT, S. C., POLLARD, A. J., ABOAGYE, J., ADAMS, K., ALI, A., ALLEN, E., ALLISON, J. L., ANSLOW, R., ARBE-BARNES, E. H., BABBAGE, G., BAILLIE, K., BAKER, M., BAKER, N., BAKER, P., BALEANU, I., BALLAMINUT, J., BARNES, E., BARRETT, J., BATES, L., BATTEN, A., BEADON, K., BECKLEY, R., BERRIE, E., BERRY, L., BEVERIDGE, A., BEWLEY, K. R., BIJKER, E. M., BINGHAM, T., BLACKWELL, L., BLUNDELL, C. L., BOLAM, E., BOLAND, E., BORTHWICK, N., BOWER, T., BOYD, A., BRENNER, T., BRIGHT, P. D., BROWN-O'SULLIVAN, C., BRUNT, E., BURBAGE, J., BURGE, S., BUTTIGIEG, K. R., BYARD, N., CABERA PUIG, I., CALVERT, A., CAMARA, S., CAO, M., CAPPUCCINI, F., CARR, M., CARROLL, M. W., CARTER, V., CATHIE, K., CHALLIS, R. J., CHARLTON, S., CHELYSHEVA, I., CHO, J.-S., CICCONE, P., CIFUENTES, L., CLARK, H., CLARK, E., COLE, T., COLIN-JONES, R., CONLON, C. P., COOK, A., COOMBS, N. S., COOPER, R., COSGROVE, C. A., COY, K., CROCKER, W. E. M., CUNNINGHAM, C. J., et al. 2020b. Safety and immunogenicity of the ChAdOx1 nCoV-19 vaccine against SARS-CoV-2: a preliminary report of a phase 1/2, single-blind, randomised controlled trial. *The Lancet*, 396, 467-478.
- FÖRSTER, R., FLEIGE, H. & SUTTER, G. 2020. Combating COVID-19: MVA Vector Vaccines Applied to the Respiratory Tract as Promising Approach Toward Protective Immunity in the Lung. *Front Immunol*, 11, 1959.
- FRALEY, E., LEMASTER, C., GEANES, E., BANERJEE, D., KHANAL, S., GRUNDBERG, E., SELVARANGAN, R. & BRADLEY, T. 2021. Humoral immune responses during SARS-CoV-2 mRNA vaccine administration in seropositive and seronegative individuals. *BMC medicine*, 19, 169-169.

- GARBER, D. A., O'MARA, L. A., ZHAO, J., GANGADHARA, S., AN, I. & FEINBERG, M. B. 2009. Expanding the Repertoire of Modified Vaccinia Ankara-Based Vaccine Vectors via Genetic Complementation Strategies. *PLOS ONE*, 4, e5445.
- GARSIDE, P., INGULLI E FAU - MERICA, R. R., MERICA RR FAU - JOHNSON, J. G., JOHNSON JG FAU - NOELLE, R. J., NOELLE RJ FAU - JENKINS, M. K. & JENKINS, M. K. 1998. Visualization of specific B and T lymphocyte interactions in the lymph node. *Science*.
- GAVI, T. V. A. 2020. *Sustainable Development Goals* [Online]. Available: <https://www.gavi.org/our-alliance/global-health-development/sustainable-development-goals> [Accessed 27.12.2022].
- GEGINAT, J., PARONI, M., MAGLIE, S., ALFEN, J. S., KASTIRR, I., GRUARIN, P., DE SIMONE, M., PAGANI, M. & ABRIGNANI, S. 2014. Plasticity of human CD4 T cell subsets. *Front Immunol*.
- GILBERT, P. B., MONTEFIORI, D. C., MCDERMOTT, A. B., FONG, Y., BENKESER, D., DENG, W., ZHOU, H., HOUCHESS, C. R., MARTINS, K., JAYASHANKAR, L., CASTELLINO, F., FLACH, B., LIN, B. C., O'CONNELL, S., MCDANAL, C., EATON, A., SARZOTTI-KELSOE, M., LU, Y., YU, C., BORATE, B., VAN DER LAAN, L. W. P., HEJAZI, N. S., HUYNH, C., MILLER, J., EL SAHLY, H. M., BADEN, L. R., BARON, M., DE LA CRUZ, L., GAY, C., KALAMS, S., KELLEY, C. F., ANDRASIK, M. P., KUBLIN, J. G., COREY, L., NEUZIL, K. M., CARPP, L. N., PAJON, R., FOLLMANN, D., DONIS, R. O. & KOUP, R. A. 2022. Immune correlates analysis of the mRNA-1273 COVID-19 vaccine efficacy clinical trial. *Science*, 375, 43-50.
- GILBERT, S. C. 2012. T-cell-inducing vaccines – what's the future. *Immunology*, 135, 19-26.
- GILBERT, S. C. 2013. Clinical development of Modified Vaccinia virus Ankara vaccines. *Vaccine*, 31, 4241-4246.
- GOLDBLATT, D., ALTER, G., CROTTY, S. & PLOTKIN, S. A. 2022a. Correlates of protection against SARS-CoV-2 infection and COVID-19 disease. *Immunol Rev*, 310, 6-26.
- GOLDBLATT, D., FIORE-GARTLAND, A., JOHNSON, M., HUNT, A., BENGT, C., ZAVADSKA, D., SNIPE, H. D., BROWN, J. S., WORKMAN, L., ZAR, H. J., MONTEFIORI, D., SHEN, X., DULL, P., PLOTKIN, S., SIBER, G. & AMBROSINO, D. 2022b. Towards a population-based threshold of protection for COVID-19 vaccines. *Vaccine*, 40, 306-315.
- GONZALEZ, S. F., LUKACS-KORNEK V FAU - KULIGOWSKI, M. P., KULIGOWSKI MP FAU - PITCHER, L. A., PITCHER LA FAU - DEGN, S. E., DEGN SE FAU - TURLEY, S. J., TURLEY SJ FAU - CARROLL, M. C. & CARROLL, M. C. 2010. Complement-dependent transport of antigen into B cell follicles. *J Immunol*.
- GOOD-JACOBSON, K. L. & SHLOMCHIK, M. J. 2010. Plasticity and heterogeneity in the generation of memory B cells and long-lived plasma cells: the influence of germinal center interactions and dynamics. *J Immunol*.
- GOODNOW, C. C., VINUESA CG FAU - RANDALL, K. L., RANDALL KL FAU - MACKAY, F., MACKAY F FAU - BRINK, R. & BRINK, R. 2010. Control systems and decision making for antibody production. *Nat Immunol*.
- GORBALENYA, A. E., KOONIN, E. V., DONCHENKO, A. P. & BLINOV, V. M. 1989. Coronavirus genome: prediction of putative functional domains in the non-structural polyprotein by comparative amino acid sequence analysis. *Nucleic Acids Res*, 17, 4847-61.
- GOSSNER, C., DANIELSON, N., GERVELMEYER, A., BERTHE, F., FAYE, B., KAASIK AASLAV, K., ADLHOCH, C., ZELLER, H., PENTTINEN, P. & COULOMBIER, D. 2014. Human-Dromedary Camel Interactions and the Risk of Acquiring Zoonotic Middle East Respiratory Syndrome Coronavirus Infection. *Zoonoses Public Health*.
- GOUGLAS, D., CHRISTODOULOU, M., PLOTKIN, S. A. & HATCHETT, R. 2019. CEPI: Driving Progress Toward Epidemic Preparedness and Response. *Epidemiol Rev*, 41, 28-33.
- GRAHAM, B. A.-O. & SULLIVAN, N. J. 2018. Emerging viral diseases from a vaccinology perspective: preparing for the next pandemic. *Nat Immunol*.
- GRAM, M. A., EMBORG, H.-D., SCHELDE, A. B., FRIIS, N. U., NIELSEN, K. F., MOUSTSEN-HELMS, I. R., LEGARTH, R., LAM, J. U. H., CHAINE, M., MALIK, A. Z., RASMUSSEN, M., FONAGER, J., SIEBER, R. N., STEGGER, M., ETHELBERG, S., VALENTINER-BRANTH, P. & HANSEN, C. H. 2022. Vaccine effectiveness against SARS-CoV-2 infection or COVID-19 hospitalization with the Alpha, Delta,

- or Omicron SARS-CoV-2 variant: A nationwide Danish cohort study. *PLOS Medicine*, 19, e1003992.
- GRÄNICHER, G., TAPIA, F., BEHRENDT, I., JORDAN, I., GENZEL, Y. & REICHL, U. 2021. Production of Modified Vaccinia Ankara Virus by Intensified Cell Cultures: A Comparison of Platform Technologies for Viral Vector Production. *Biotechnol J*, 16, e2000024.
- GREVYS, A., FRICK, R., MESTER, S., FLEM-KARLSEN, K., NILSEN, J., FOSS, S., SAND, K. M. K., EMRICH, T., FISCHER, J. A. A., GREIFF, V., SANDLIE, I., SCHLOTHAUER, T. & ANDERSEN, J. T. 2022. Antibody variable sequences have a pronounced effect on cellular transport and plasma half-life. *iScience*, 25, 103746.
- GUDMUNDSDOTTER, L., NILSSON, C., BRAVE, A., HEJDEMAN, B., EARL, P., MOSS, B., ROBB, M., COX, J., MICHAEL, N., MAROVICH, M., BIBERFELD, G., SANDSTRÖM, E. & WAHREN, B. 2009. Recombinant Modified Vaccinia Ankara (MVA) effectively boosts DNA-primed HIV-specific immune responses in humans despite pre-existing vaccinia immunity. *Vaccine*, 27, 4468-74.
- GUNN, B. M. & ALTER, G. 2016. Modulating Antibody Functionality in Infectious Disease and Vaccination. *Trends in Molecular Medicine*, 22, 969-982.
- HAAGMANS, B. L., VAN DEN BRAND, J. M., RAJ, V. S., VOLZ, A., WOHLSEIN, P., SMITS, S. L., SCHIPPER, D., BESTEBROER, T. M., OKBA, N., FUX, R., BENSALD, A., SOLANES FOZ, D., KUIKEN, T., BAUMGÄRTNER, W., SEGALÉS, J., SUTTER, G. & OSTERHAUS, A. D. 2016. An orthopoxvirus-based vaccine reduces virus excretion after MERS-CoV infection in dromedary camels. *Science*, 351, 77-81.
- HAGEMANN, K. A.-O., RIECKEN, K. A.-O., JUNG, J. A.-O., HILDEBRANDT, H., MENZEL, S., BUNDERS, M. J., FEHSE, B. A.-O., KOCH-NOLTE, F. A.-O., HEINRICH, F. A.-O., PEINE, S., SCHULZE ZUR WIESCH, J., BREHM, T. T., ADDO, M. M., LÜTGEHETMANN, M. A.-O. & ALTFELD, M. A.-O. 2022. Natural killer cell-mediated ADCC in SARS-CoV-2-infected individuals and vaccine recipients. *Eur J Immunol*.
- HALL, V. G., FERREIRA, V. H., WOOD, H., IERULLO, M., MAJCHRZAK-KITA, B., MANGUIAT, K., ROBINSON, A., KULASINGAM, V., HUMAR, A. & KUMAR, D. 2022. Delayed-interval BNT162b2 mRNA COVID-19 vaccination enhances humoral immunity and induces robust T cell responses. *Nature Immunology*, 23, 380-385.
- HALSEY, N. & GALAZKA, A. 1985. The efficacy of DPT and oral poliomyelitis immunization schedules initiated from birth to 12 weeks of age. *Bull World Health Organ*, 63, 1151-69.
- HAMBLIN, A. D. & HAMBLIN, T. J. 2008. The immunodeficiency of chronic lymphocytic leukaemia. *Br Med Bull*, 87, 49-62.
- HAMRE, R., FARSTAD IN FAU - BRANDTZAEG, P., BRANDTZAEG P FAU - MORTON, H. C. & MORTON, H. C. 2003. Expression and modulation of the human immunoglobulin A Fc receptor (CD89) and the FcR gamma chain on myeloid cells in blood and tissue. *Scand J Immunol*.
- HARDT, K., VANDEBOSCH, A., SADOFF, J., LE GARS, M., TRUYERS, C., LOWSON, D., VAN DROMME, I., VINGERHOETS, J., KAMPHUIS, T., SCHEPER, G., RUIZ-GUIÑAZÚ, J., FAUST, S. N., SPINNER, C. D., SCHUITEMAKER, H., VAN HOOFF, J., DOUOGUIH, M. & STRUYF, F. 2022. Efficacy, safety, and immunogenicity of a booster regimen of Ad26.COVS vaccine against COVID-19 (ENSEMBLE2): results of a randomised, double-blind, placebo-controlled, phase 3 trial. *Lancet Infect Dis*, 22, 1703-1715.
- HATMAL, M. M. M., ALSHAER, W., AL-HATAMLEH, M. A. I., HATMAL, M., SMADI, O., TAHA, M. O., OWEIDA, A. J., BOER, J. C., MOHAMUD, R. & PLEBANSKI, M. 2020. Comprehensive Structural and Molecular Comparison of Spike Proteins of SARS-CoV-2, SARS-CoV and MERS-CoV, and Their Interactions with ACE2. *Cells* [Online], 9.
- HE, W., TAN, G. S., MULLARKEY, C. E., LEE, A. J., LAM, M. M., KRAMMER, F., HENRY, C., WILSON, P. C., ASHKAR, A. A., PALESE, P. & MILLER, M. S. 2016. Epitope specificity plays a critical role in regulating antibody-dependent cell-mediated cytotoxicity against influenza A virus. *Proc Natl Acad Sci USA*.
- HEIKKINEN, T. & JÄRVINEN, A. 2003. The common cold. *Lancet*, 361, 51-9.
- HENAO-RESTREPO, A. M., LONGINI, I. M., EGGER, M., DEAN, N. E., EDMUNDS, W. J., CAMACHO, A., CARROLL, M. W., DOUMBIA, M., DRAGUEZ, B., DURAFFOUR, S., ENWERE, G., GRAIS, R.,

- GUNTHER, S., HOSSMANN, S., KONDE, M. K., KONE, S., KUISMA, E., LEVINE, M. M., MANDAL, S., NORHEIM, G., RIVEROS, X., SOUMAH, A., TRELLE, S., VICARI, A. S., WATSON, C. H., KÉÏTA, S., KIENY, M. P. & RØTTINGEN, J.-A. 2015. Efficacy and effectiveness of an rVSV-vectored vaccine expressing Ebola surface glycoprotein: interim results from the Guinea ring vaccination cluster-randomised trial. *The Lancet*, 386, 857-866.
- HENNING, L., ENDT, K., STEIGERWALD, R., ANDERSON, M. & VOLKMANN, A. 2021. A Monovalent and Trivalent MVA-Based Vaccine Completely Protects Mice Against Lethal Venezuelan, Western, and Eastern Equine Encephalitis Virus Aerosol Challenge. *Frontiers in Immunology*, 11.
- HENNINGS, V., THÖRN, K., ALBINSSON, S., LINGBLOM, C., ANDERSSON, K., ANDERSSON, C., JÄRBUR, K., PULLERITS, R., IDORN, M., PALUDAN, S. R., ERIKSSON, K. & WENNERÅS, C. 2022. The presence of serum anti-SARS-CoV-2 IgA appears to protect primary health care workers from COVID-19. *Eur J Immunol*, 52, 800-809.
- HESSELL, A. J., HANGARTNER, L., HUNTER, M., HAVENITH, C. E. G., BEURSKENS, F. J., BAKKER, J. M., LANIGAN, C. M. S., LANDUCCI, G., FORTHAL, D. N., PARREN, P. W. H. I., MARX, P. A. & BURTON, D. R. 2007. Fc receptor but not complement binding is important in antibody protection against HIV. *Nature*, 449, 101-104.
- HOLMES, E. C., GOLDSTEIN, S. A., RASMUSSEN, A. L., ROBERTSON, D. L., CRITS-CHRISTOPH, A., WERTHEIM, J. O., ANTHONY, S. J., BARCLAY, W. S., BONI, M. F., DOHERTY, P. C., FARRAR, J., GEOGHEGAN, J. L., JIANG, X., LEIBOWITZ, J. L., NEIL, S. J. D., SKERN, T., WEISS, S. R., WOROBEY, M., ANDERSEN, K. G., GARRY, R. F. & RAMBAUT, A. 2021. The origins of SARS-CoV-2: A critical review. *Cell*, 184, 4848-4856.
- HU, B., GUO, H., ZHOU, P. & SHI, Z.-L. 2021. Characteristics of SARS-CoV-2 and COVID-19. *Nature Reviews Microbiology*, 19, 141-154.
- HUANG, A. T., GARCIA-CARRERAS, B., HITCHINGS, M. D. T., YANG, B., KATZELNICK, L. C., RATTIGAN, S. M., BORGERT, B. A., MORENO, C. A., SOLOMON, B. D., TRIMMER-SMITH, L., ETIENNE, V., RODRIGUEZ-BARRAQUER, I., LESSLER, J., SALJE, H., BURKE, D. S., WESOLOWSKI, A. & CUMMINGS, D. A. T. 2020. A systematic review of antibody mediated immunity to coronaviruses: kinetics, correlates of protection, and association with severity. *Nature Communications*, 11, 4704.
- HUI, D. S., AZHAR, E. I., KIM, Y. J., MEMISH, Z. A., OH, M. D. & ZUMLA, A. 2018. Middle East respiratory syndrome coronavirus: risk factors and determinants of primary, household, and nosocomial transmission. *Lancet Infect Dis*.
- HUMPHREYS, I. R. & SEBASTIAN, S. 2018. Novel viral vectors in infectious diseases. *Immunology*, 153, 1-9.
- HUNTER, J. C., NGUYEN, D., ADEN, B., AL BANDAR, Z., AL DHAHERI, W., ABU ELKHEIR, K., KHUDAIR, A., AL MULLA, M., EL SALEH, F., IMAMBACCUS, H., AL KAABI, N., SHEIKH, F. A., SASSE, J., TURNER, A., ABDEL WARETH, L., WEBER, S., AL AMERI, A., ABU AMER, W., ALAMI, N. N., BUNGA, S., HAYNES, L. M., HALL, A. J., KALLEN, A. J., KUCHAR, D., PHAM, H., PRINGLE, K., TONG, S., WHITAKER, B. L., GERBER, S. I. & AL HOSANI, F. I. 2016. Transmission of Middle East Respiratory Syndrome Coronavirus Infections in Healthcare Settings, Abu Dhabi. *Emerg Infect Dis*, 22, 647-56.
- IMAI, Y., KUBA, K., OHTO-NAKANISHI, T. & PENNINGER, J. M. 2010. Angiotensin-converting enzyme 2 (ACE2) in disease pathogenesis. *Circ J*, 74, 405-10.
- IRRGANG, P., GERLING, J., KOCHER, K., LAPUENTE, D., STEININGER, P., HABENICHT, K., WYTOPIL, M., BEILEKE, S., SCHÄFER, S., ZHONG, J., SSEBYATIKA, G., KREY, T., FALCONE, V., SCHÜLEIN, C., PETER, A. S., NGANOU-MAKAMDOP, K., HENGEL, H., HELD, J., BOGDAN, C., ÜBERLA, K., SCHOBER, K., WINKLER, T. H. & TENBUSCH, M. 2022. Class switch towards non-inflammatory, spike-specific IgG4 antibodies after repeated SARS-CoV-2 mRNA vaccination. *Sci Immunol*, eade2798.
- IRVINE, E. B. & ALTER, G. 2020. Understanding the role of antibody glycosylation through the lens of severe viral and bacterial diseases. *Glycobiology*, 30, 241-253.
- JACKSON, D. A., SYMONS, R. H. & BERG, P. 1972. Biochemical method for inserting new genetic information into DNA of Simian Virus 40: circular SV40 DNA molecules containing lambda

- phage genes and the galactose operon of *Escherichia coli*. *Proc Natl Acad Sci U S A*, 69, 2904-9.
- JACKSON, L. A., ANDERSON, E. J., ROUPHAEL, N. G., ROBERTS, P. C., MAKHENE, M., COLER, R. N., MCCULLOUGH, M. P., CHAPPELL, J. D., DENISON, M. R., STEVENS, L. J., PRUIJSSERS, A. J., MCDERMOTT, A., FLACH, B., DORIA-ROSE, N. A., CORBETT, K. S., MORABITO, K. M., O'DELL, S., SCHMIDT, S. D., SWANSON, P. A., 2ND, PADILLA, M., MASCOLA, J. R., NEUZIL, K. M., BENNETT, H., SUN, W., PETERS, E., MAKOWSKI, M., ALBERT, J., CROSS, K., BUCHANAN, W., PIKAART-TAUTGES, R., LEDGERWOOD, J. E., GRAHAM, B. S. & BEIGEL, J. H. 2020. An mRNA Vaccine against SARS-CoV-2 - Preliminary Report. *N Engl J Med*, 383, 1920-1931.
- JAIN, A. & PASARE, C. A.-O. 2017. Innate Control of Adaptive Immunity: Beyond the Three-Signal Paradigm.
- JANG, Y. H. & SEONG, B. L. 2021. Immune Responses Elicited by Live Attenuated Influenza Vaccines as Correlates of Universal Protection against Influenza Viruses. *Vaccines (Basel)*, 9.
- JENNEWEIN, M. F., KOSIKOVA, M., NOELETTE, F. J., RADVAK, P., BOUDREAU, C. M., CAMPBELL, J. D., CHEN, W. H., XIE, H., ALTER, G. & PASETTI, M. F. 2022. Functional and structural modifications of influenza antibodies during pregnancy. *iScience*, 25, 104088.
- JIN, P., LI, J., PAN, H., WU, Y. & ZHU, F. 2021. Immunological surrogate endpoints of COVID-2019 vaccines: the evidence we have versus the evidence we need. *Signal Transduction and Targeted Therapy*, 6, 48.
- JORDAN, E., LAWRENCE, S. J., MEYER, T. P. H., SCHMIDT, D., SCHULTZ, S., MUELLER, J., STROUKOVA, D., KOENEN, B., GRUENERT, R., SILBERNAGL, G., VIDOJKOVIC, S., CHEN, L. M., WEIDENTHALER, H., SAMY, N. & CHAPLIN, P. 2021. Broad Antibody and Cellular Immune Response From a Phase 2 Clinical Trial With a Novel Multivalent Poxvirus-Based Respiratory Syncytial Virus Vaccine. *J Infect Dis*, 223, 1062-1072.
- JU, B., ZHANG, Q., GE, J., WANG, R., SUN, J., GE, X., YU, J., SHAN, S., ZHOU, B., SONG, S., TANG, X., YU, J., LAN, J., YUAN, J., WANG, H., ZHAO, J., ZHANG, S., WANG, Y., SHI, X., LIU, L., ZHAO, J., WANG, X., ZHANG, Z. & ZHANG, L. 2020. Human neutralizing antibodies elicited by SARS-CoV-2 infection. *Nature*, 584, 115-119.
- KARIKÓ, K., MURAMATSU, H., WELSH, F. A., LUDWIG, J., KATO, H., AKIRA, S. & WEISSMAN, D. 2008. Incorporation of pseudouridine into mRNA yields superior nonimmunogenic vector with increased translational capacity and biological stability. *Mol Ther*, 16, 1833-40.
- KASTURI, S. P., SKOUNTZOU, I., ALBRECHT, R. A., KOUTSONANOS, D., HUA, T., NAKAYA, H. I., RAVINDRAN, R., STEWART, S., ALAM, M., KWISSA, M., VILLINGER, F., MURTHY, N., STEEL, J., JACOB, J., HOGAN, R. J., GARCÍA-SASTRE, A., COMPANS, R. & PULENDRAN, B. 2011. Programming the magnitude and persistence of antibody responses with innate immunity. *Nature*, 470, 543-7.
- KHAN, S., NAKAJIMA, R., JAIN, A., DE ASSIS, R. R., JASINSKAS, A., OBIERO, J. M., ADENAIYE, O., TAI, S., HONG, F., MILTON, D. K., DAVIES, H. & FELGNER, P. L. 2020. Analysis of Serologic Cross-Reactivity Between Common Human Coronaviruses and SARS-CoV-2 Using Coronavirus Antigen Microarray. *bioRxiv*.
- KHODADADI, L., CHENG, Q., RADBRUCH, A. & HIEPE, F. 2019. The Maintenance of Memory Plasma Cells. *Front Immunol*.
- KHOURY, D. S., CROMER, D., REYNALDI, A., SCHLUB, T. E., WHEATLEY, A. K., JUNO, J. A., SUBBARAO, K., KENT, S. J., TRICCAS, J. A. & DAVENPORT, M. P. 2021. Neutralizing antibody levels are highly predictive of immune protection from symptomatic SARS-CoV-2 infection. *Nature Medicine*, 27, 1205-1211.
- KILLINGLEY, B., MANN, A. J., KALINOVA, M., BOYERS, A., GOONAWARDANE, N., ZHOU, J., LINDSELL, K., HARE, S. S., BROWN, J., FRISE, R., SMITH, E., HOPKINS, C., NOULIN, N., LÖNDT, B., WILKINSON, T., HARDEN, S., MCSHANE, H., BAILLET, M., GILBERT, A., JACOBS, M., CHARMAN, C., MANDE, P., NGUYEN-VAN-TAM, J. S., SEMPLE, M. G., READ, R. C., FERGUSON, N. M., OPENSHAW, P. J., RAPEPORT, G., BARCLAY, W. S., CATCHPOLE, A. P. & CHIU, C. 2022. Safety, tolerability and viral kinetics during SARS-CoV-2 human challenge in young adults. *Nature Medicine*, 28, 1031-1041.

- KIM, K. H., TANDI, T. E., CHOI, J. W., MOON, J. M. & KIM, M. S. 2017. Middle East respiratory syndrome coronavirus (MERS-CoV) outbreak in South Korea, 2015: epidemiology, characteristics and public health implications. *J Hosp Infect*, 95, 207-213.
- KIM, W., ZHOU, J. Q., HORVATH, S. C., SCHMITZ, A. J., STURTZ, A. J., LEI, T., LIU, Z., KALAIKINA, E., THAPA, M., ALSOUSSI, W. B., HAILE, A., KLEBERT, M. K., SUESSEN, T., PARRA-RODRIGUEZ, L., MUDD, P. A., WHELAN, S. P. J., MIDDLETON, W. D., TEEFEY, S. A., PUSIC, I., O'HALLORAN, J. A., PRESTI, R. M., TURNER, J. S. & ELLEBEDY, A. H. 2022. Germinal centre-driven maturation of B cell response to mRNA vaccination. *Nature*, 604, 141-145.
- KIRCHDOERFER, R. N., COTTRELL, C. A., WANG, N., PALLESEN, J., YASSINE, H. M., TURNER, H. L., CORBETT, K. S., GRAHAM, B. S., MCLELLAN, J. S. & WARD, A. B. 2016. Pre-fusion structure of a human coronavirus spike protein. *Nature*, 531, 118-21.
- KIRCHDOERFER, R. N., WANG, N., PALLESEN, J., WRAPP, D., TURNER, H. L., COTTRELL, C. A., CORBETT, K. S., GRAHAM, B. S., MCLELLAN, J. S. & WARD, A. B. 2018. Stabilized coronavirus spikes are resistant to conformational changes induced by receptor recognition or proteolysis. *Sci Rep*, 8, 15701.
- KOCH, T., DAHLKE, C., FATHI, A., KUPKE, A., KRÄHLING, V., OKBA, N. M. A., HALWE, S., ROHDE, C., EICKMANN, M., VOLZ, A., HESTERKAMP, T., JAMBRECINA, A., BORREGAARD, S., LY, M. L., ZINSER, M. E., BARTELS, E., POETSCH, J. S. H., NEUMANN, R., FUX, R., SCHMIEDEL, S., LOHSE, A. W., HAAGMANS, B. L., SUTTER, G., BECKER, S. & ADDO, M. M. 2020. Safety and immunogenicity of a modified vaccinia virus Ankara vector vaccine candidate for Middle East respiratory syndrome: an open-label, phase 1 trial. *Lancet Infect Dis*, 20, 827-838.
- KOCH, T. A.-O., MELLINGHOFF, S. C., SHAMSRIZI, P. A.-O., ADDO, M. A.-O. & DAHLKE, C. A.-O. 2021. Correlates of Vaccine-Induced Protection against SARS-CoV-2. LID - 10.3390/vaccines9030238 [doi] LID - 238. *Vaccines*.
- KOENIG, P.-A. & SCHMIDT, F. I. 2021. Spike D614G — A Candidate Vaccine Antigen Against Covid-19. *New England Journal of Medicine*, 384, 2349-2351.
- KOTAKI, R., ADACHI, Y., MORIYAMA, S., ONODERA, T., FUKUSHI, S., NAGAKURA, T., TONOUCHE, K., TERAHARA, K., SUN, L., TAKANO, T., NISHIYAMA, A., SHINKAI, M., OBA, K., NAKAMURA-UCHIYAMA, F., SHIMIZU, H., SUZUKI, T., MATSUMURA, T., ISOGAWA, M. & TAKAHASHI, Y. 2022. SARS-CoV-2 Omicron-neutralizing memory B cells are elicited by two doses of BNT162b2 mRNA vaccine. *Science Immunology*, 7, eabn8590.
- KRACKER, S. & DURANDY, A. 2011. Insights into the B cell specific process of immunoglobulin class switch recombination. *Immunol Lett*.
- KRAMMER, F. 2021. A correlate of protection for SARS-CoV-2 vaccines is urgently needed. *Nature Medicine*, 27, 1147-1148.
- KREIJTZ, J. H., GOEIJENBIER, M., MOESKER, F. M., VAN DEN DRIES, L., GOEIJENBIER, S., DE GRUYTER, H. L., LEHMANN, M. H., MUTSERT, G., VAN DE VIJVER, D. A., VOLZ, A., FOUCHIER, R. A., VAN GORP, E. C., RIMMELZWAAN, G. F., SUTTER, G. & OSTERHAUS, A. D. 2014. Safety and immunogenicity of a modified-vaccinia-virus-Ankara-based influenza A H5N1 vaccine: a randomised, double-blind phase 1/2a clinical trial. *Lancet Infect Dis*, 14, 1196-207.
- KRONZER, V. L., BRIDGES, S. L., JR. & DAVIS, J. M., 3RD 2021. Why women have more autoimmune diseases than men: An evolutionary perspective. *Evol Appl*, 14, 629-633.
- KUMAVATH, R., BARH, D., ANDRADE, B. S., IMCHEN, M., ABURJAILE, F. F., CH, A., RODRIGUES, D. L. N., TIWARI, S., ALZHRANI, K. J., GÓES-NETO, A., WEENER, M. E., GHOSH, P. & AZEVEDO, V. 2021. The Spike of SARS-CoV-2: Uniqueness and Applications. *Front Immunol*, 12, 663912.
- KUROSAKI, T., KOMETANI, K. & ISE, W. 2015. Memory B cells. *Nature Reviews Immunology*, 15, 149-159.
- KWAK, K., AKKAYA, M. A.-O. & PIERCE, S. A.-O. 2019. B cell signaling in context. *Nat Immunol*.
- LA ROSA, C., LONGMATE, J., MARTINEZ, J., ZHOU, Q., KALTICHEVA, T. I., TSAI, W., DRAKE, J., CARROLL, M., WUSSOW, F., CHIUPPESI, F., HARDWICK, N., DADWAL, S., ALDOSS, I., NAKAMURA, R., ZAIA, J. A. & DIAMOND, D. J. 2017. MVA vaccine encoding CMV antigens safely induces durable expansion of CMV-specific T cells in healthy adults. *Blood*, 129, 114-125.

- LAMERTON, R. E., MARCIAL-JUAREZ, E., FAUSTINI, S. E., PEREZ-TOLEDO, M., GOODALL, M., JOSSI, S. E., NEWBY, M. L., CHAPPLE, I., DIETRICH, T., VEENITH, T., SHIELDS, A. M., HARPER, L., HENDERSON, I. R., RAYES, J., WRAITH, D. C., WATSON, S. P., CRISPIN, M., DRAYSON, M. T., RICHTER, A. G. & CUNNINGHAM, A. F. 2022. SARS-CoV-2 Spike- and Nucleoprotein-Specific Antibodies Induced After Vaccination or Infection Promote Classical Complement Activation. *Front Immunol*.
- LANGENMAYER, M. C., LÜLF-AVERHOFF, A. T., ADAM-NEUMAIR, S., FUX, R., SUTTER, G. & VOLZ, A. 2018. Distribution and absence of generalized lesions in mice following single dose intramuscular inoculation of the vaccine candidate MVA-MERS-S. *Biologicals*, 54, 58-62.
- LAUER KATHARINA, B., BORROW, R. & BLANCHARD THOMAS, J. 2017. Multivalent and Multipathogen Viral Vector Vaccines. *Clinical and Vaccine Immunology*, 24, e00298-16.
- LAURENT, P. E., BONNET, S., ALCHAS, P., REGOLINI, P., MIKSZTA, J. A., PETTIS, R. & HARVEY, N. G. 2007. Evaluation of the clinical performance of a new intradermal vaccine administration technique and associated delivery system. *Vaccine*, 25, 8833-42.
- LAVELLE, E. C. & WARD, R. W. 2022. Mucosal vaccines - fortifying the frontiers. *Nat Rev Immunol*, 22, 236-250.
- LEBIEN, T. W. 2000. Fates of human B-cell precursors. *Blood*, 96, 9-23.
- LEBIEN, T. W. & TEDDER, T. F. 2008. B lymphocytes: how they develop and function. *Blood*, 112, 1570-80.
- LEE, C. A.-O., ROMAIN, G., YAN, W. A.-O., WATANABE, M., CHARAB, W., TODOROVA, B., LEE, J., TRIPLETT, K., DONKOR, M., LUNGU, O. I., LUX, A., MARSHALL, N., LINDORFER, M. A., GOFF, O. R., BALBINO, B., KANG, T. H., TANNO, H., DELIDAKIS, G., ALFORD, C., TAYLOR, R. A.-O., NIMMERJAHN, F., VARADARAJAN, N., BRUHNS, P. A.-O., ZHANG, Y. J. & GEORGIU, G. 2017. IgG Fc domains that bind C1q but not effector Fcγ receptors delineate the importance of complement-mediated effector functions. *Nat Immunol*.
- LEFRANC, M. & LEFRANC, G. 2001. *The Immunoglobulin FactsBook*.
- LEVY, O. 2007. Innate immunity of the newborn: basic mechanisms and clinical correlates. *Nat Rev Immunol*, 7, 379-90.
- LI, F. 2016. Structure, Function, and Evolution of Coronavirus Spike Proteins. *Annu Rev Virol*, 3, 237-261.
- LI, G.-M., CHIU, C., WRAMMERT, J., MCCAUSLAND, M., ANDREWS, S. F., ZHENG, N.-Y., LEE, J.-H., HUANG, M., QU, X., EDUPUGANTI, S., MULLIGAN, M., DAS, S. R., YEWDELL, J. W., MEHTA, A. K., WILSON, P. C. & AHMED, R. 2012. Pandemic H1N1 influenza vaccine induces a recall response in humans that favors broadly cross-reactive memory B cells. *Proceedings of the National Academy of Sciences*, 109, 9047-9052.
- LI, J.-X., HOU, L.-H., MENG, F.-Y., WU, S.-P., HU, Y.-M., LIANG, Q., CHU, K., ZHANG, Z., XU, J.-J., TANG, R., WANG, W.-J., LIU, P., HU, J.-L., LUO, L., JIANG, R., ZHU, F.-C. & CHEN, W. 2017. Immunity duration of a recombinant adenovirus type-5 vector-based Ebola vaccine and a homologous prime-boost immunisation in healthy adults in China: final report of a randomised, double-blind, placebo-controlled, phase 1 trial. *The Lancet Global Health*, 5, e324-e334.
- LI, S. W. & LIN, C. W. 2013. Human coronaviruses: Clinical features and phylogenetic analysis. *Biomedicine (Taipei)*, 3, 43-50.
- LI, W., MOORE, M. J., VASILIEVA, N., SUI, J., WONG, S. K., BERNE, M. A., SOMASUNDARAN, M., SULLIVAN, J. L., LUZURIAGA, K., GREENOUGH, T. C., CHOE, H. & FARZAN, M. 2003. Angiotensin-converting enzyme 2 is a functional receptor for the SARS coronavirus. *Nature*, 426, 450-4.
- LINTERMAN, M. A. & VINUESA, C. G. 2010. T follicular helper cells during immunity and tolerance. *Prog Mol Biol Transl Sci*.
- LIU, C., ZHOU, Q., LI, Y., GARNER, L. V., WATKINS, S. P., CARTER, L. J., SMOOT, J., GREGG, A. C., DANIELS, A. D., JERVEY, S. & ALBAIU, D. 2020. Research and Development on Therapeutic Agents and Vaccines for COVID-19 and Related Human Coronavirus Diseases. *ASC Cent Sci*.
- LIU, D. X., LIANG, J. Q. & FUNG, T. S. 2021a. Human Coronavirus-229E, -OC43, -NL63, and -HKU1 (Coronaviridae). In: BAMFORD, D. H. & ZUCKERMAN, M. (eds.) *Encyclopedia of Virology (Fourth Edition)*. Oxford: Academic Press.

- LIU, J., CHANDRASHEKAR, A., SELLERS, D., BARRETT, J., LIFTON, M., MCMAHAN, K., SCIACCA, M., VANWYK, H., WU, C., YU, J., COLLIER, A. Y. & BAROUCH, D. H. 2022. Vaccines Elicit Highly Cross-Reactive Cellular Immunity to the SARS-CoV-2 Omicron Variant. *medRxiv*.
- LIU, J., WANG, Y., XIONG, E., HONG, R., LU, Q., OHNO, H. & WANG, J. Y. 2019. Role of the IgM Fc Receptor in Immunity and Tolerance. *Front Immunol*.
- LIU, M. A. 2019. A Comparison of Plasmid DNA and mRNA as Vaccine Technologies. *Vaccines (Basel)*, 7.
- LIU, Q., FAN, C., LI, Q., ZHOU, S., HUANG, W., WANG, L., SUN, C., WANG, M., WU, X., MA, J., LI, B., XIE, L. & WANG, Y. 2017. Antibody-dependent-cellular-cytotoxicity-inducing antibodies significantly affect the post-exposure treatment of Ebola virus infection. *Sci Rep*.
- LIU, Z., VANBLARGAN, L. A., BLOYET, L. M., ROTHLAUF, P. W., CHEN, R. E., STUMPF, S., ZHAO, H., ERRICO, J. M., THEEL, E. S., LIEBESKIND, M. J., ALFORD, B., BUCHSER, W. J., ELLEBEDY, A. H., FREMONT, D. H., DIAMOND, M. S. & WHELAN, S. P. J. 2021b. Identification of SARS-CoV-2 spike mutations that attenuate monoclonal and serum antibody neutralization. *Cell Host Microbe*, 29, 477-488.e4.
- LJUNGMAN, P. 2012. Vaccination of immunocompromised patients. *Clinical Microbiology and Infection*, 18, 93-99.
- LU, G., HU, Y., WANG, Q., QI, J., GAO, F., LI, Y., ZHANG, Y., ZHANG, W., YUAN, Y., BAO, J., ZHANG, B., SHI, Y., YAN, J. & GAO, G. F. 2013. Molecular basis of binding between novel human coronavirus MERS-CoV and its receptor CD26. *Nature*, 500, 227-31.
- LU, L., LIU, Q., ZHU, Y., CHAN, K. H., QIN, L., LI, Y., WANG, Q., CHAN, J. F., DU, L., YU, F., MA, C., YE, S., YUEN, K. Y., ZHANG, R. & JIANG, S. 2014. Structure-based discovery of Middle East respiratory syndrome coronavirus fusion inhibitor. *Nat Commun*, 5, 3067.
- LU, L. L., SUSCOVICH, T. J., FORTUNE, S. M. & ALTER, G. 2018. Beyond binding: antibody effector functions in infectious diseases. *Nat Rev Immunol*.
- LU, R., ZHAO, X., LI, J., NIU, P., YANG, B., WU, H., WANG, W., SONG, H., HUANG, B., ZHU, N., BI, Y., MA, X., ZHAN, F., WANG, L., HU, T., ZHOU, H., HU, Z., ZHOU, W., ZHAO, L., CHEN, J., MENG, Y., WANG, J., LIN, Y., YUAN, J., XIE, Z., MA, J., LIU, W. J., WANG, D., XU, W., HOLMES, E. C., GAO, G. F., WU, G., CHEN, W., SHI, W. & TAN, W. 2020. Genomic characterisation and epidemiology of 2019 novel coronavirus: implications for virus origins and receptor binding. *Lancet*, 395, 565-574.
- LU, X. & YAMASAKI, S. 2022. Current understanding of T cell immunity against SARS-CoV-2. *Inflammation and Regeneration*, 42, 51.
- LUSTIG, Y., SAPIR, E., REGEV-YOCHAY, G., COHEN, C., FLUSS, R., OLMER, L., INDENBAUM, V., MANDELBOIM, M., DOOLMAN, R., AMIT, S., MENDELSON, E., ZIV, A., HUPPERT, A., RUBIN, C., FREEDMAN, L. & KREISS, Y. 2021. BNT162b2 COVID-19 vaccine and correlates of humoral immune responses and dynamics: a prospective, single-centre, longitudinal cohort study in health-care workers. *Lancet Respir Med*, 9, 999-1009.
- LV, J., WU, H., XU, J. & LIU, J. 2022. Immunogenicity and safety of heterologous versus homologous prime-boost schedules with an adenoviral vectored and mRNA COVID-19 vaccine: a systematic review. *Infect Dis Poverty*, 11, 53.
- MACLENNAN, I. C. 1994. Germinal centers. *Annu Rev Immunol*, 12, 117-39.
- MACLENNAN, I. C., TOELLNER KM FAU - CUNNINGHAM, A. F., CUNNINGHAM AF FAU - SERRE, K., SERRE K FAU - SZE, D. M. Y., SZE DM FAU - ZÚÑIGA, E., ZÚÑIGA E FAU - COOK, M. C., COOK MC FAU - VINUESA, C. G. & VINUESA, C. G. 2003. Extrafollicular antibody responses. *Immunol Rev*.
- MADHAVAN, M., RITCHIE, A. J., ABOAGYE, J., JENKIN, D., PROVSTGAAD-MORYS, S., TARBET, I., WOODS, D., DAVIES, S., BAKER, M., PLATT, A., FLAXMAN, A., SMITH, H., BELIJ-RAMMERSTORFER, S., WILKINS, D., KELLY, E. J., VILLAFANA, T., GREEN, J. A., POULTON, I., LAMBE, T., HILL, A. V. S., EWER, K. J. & DOUGLAS, A. D. 2022. Tolerability and immunogenicity of an intranasally-administered adenovirus-vectored COVID-19 vaccine: An open-label partially-randomised ascending dose phase I trial. *eBioMedicine*, 85.
- MAHAN, A. E., JENNEWEIN, M. F., SUSCOVICH, T., DIONNE, K., TEDESCO, J., CHUNG, A. W., STREECK, H., PAU, M., SCHUITEMAKER, H., FRANCIS, D., FAST, P., LAUFER, D., WALKER, B. D., BADEN, L.,

- BAROUCH, D. H. & ALTER, G. 2016. Antigen-Specific Antibody Glycosylation Is Regulated via Vaccination. *PLoS Pathog*, 12, e1005456.
- MAO, H. H. & CHAO, S. 2020. Advances in Vaccines. *Adv Biochem Eng Biotechnol*, 171, 155-188.
- MARTIN, V. G., WU, Y.-C. B., TOWNSEND, C. L., LU, G. H. C., O'HARE, J. S., MOZEIKA, A., COOLEN, A. C. C., KIPLING, D., FRATERNALI, F. & DUNN-WALTERS, D. K. 2016. Transitional B Cells in Early Human B Cell Development – Time to Revisit the Paradigm? *Frontiers in Immunology*, 7.
- MASLINSKA, M., DMOWSKA-CHALABA, J. & JAKUBASZEK, M. 2022. The Role of IgG4 in Autoimmunity and Rheumatic Diseases. *Front Immunol*.
- MASLOW, J. N. 2017. Vaccine development for emerging virulent infectious diseases. *Vaccine*, 35, 5437-5443.
- MASTRANGELO, M. J., EISENLOHR, L. C., GOMELLA, L. & LATTIME, E. C. 2000. Poxvirus vectors: orphaned and underappreciated. *J Clin Invest*, 105, 1031-4.
- MAYER, L., WESKAMM, L. M., FATHI, A., KONO, M., HEIDEPRIEM, J., MELLINGHOFF, S. C., LY, M. L., FRIEDRICH, M., HARDTKE, S., BORREGAARD, S., HESTERKAMP, T., LOEFFLER, F. F., VOLZ, A., SUTTER, G., BECKER, S., DAHLKE, C. & ADDO, M. M. submitted to Nature Communications. Humoral and cellular immunogenicity of two MVA-based COVID-19 vaccine candidates compared to ChAd and mRNA platforms.
- MCELHANEY, J. E., ZHOU, X., TALBOT, H. K., SOETHOUT, E., BLEACKLEY, R. C., GRANVILLE, D. J. & PAWELEC, G. 2012. The unmet need in the elderly: how immunosenescence, CMV infection, co-morbidities and frailty are a challenge for the development of more effective influenza vaccines. *Vaccine*, 30, 2060-7.
- MEDETGUL-ERNAR, K. & DAVIS, M. M. 2022. Standing on the shoulders of mice. *Immunity*, 55, 1343-1353.
- MEDINA-ENRÍQUEZ, M. M., LOPEZ-LEÓN, S., CARLOS-ESCALANTE, J. A., APONTE-TORRES, Z., CUAPIO, A. & WEGMAN-OSTROSKY, T. 2020. ACE2: the molecular doorway to SARS-CoV-2. *Cell & Bioscience*, 10, 148.
- MEDZHITOV, R. & JANEWAY, C., JR. 2000. Innate immune recognition: mechanisms and pathways.
- MEHAND, M. S., AL-SHORBAJI, F., MILLETT, P. & MURGUE, B. 2018. The WHO R&D Blueprint: 2018 review of emerging infectious diseases requiring urgent research and development efforts. *Antiviral Res*.
- MELLINGHOFF, S. C., MAYER, L., ROBRECHT, S., WESKAMM, L. M., DAHLKE, C., GRUELL, H., SCHLOTZ, M., VANSHYLLA, K., SCHLOSER, H. A., THELEN, M., FINK, A. M., FISCHER, K., KLEIN, F., ADDO, M. M., EICHHORST, B., HALLEK, M. & LANGERBEINS, P. 2022a. SARS-CoV-2-specific cellular response following third COVID-19 vaccination in patients with chronic lymphocytic leukemia. *Haematologica*, 107, 2480-2484.
- MELLINGHOFF, S. C., ROBRECHT, S., MAYER, L., WESKAMM, L. M., DAHLKE, C., GRUELL, H., VANSHYLLA, K., SCHLÖSSER, H. A., THELEN, M., FINK, A. M., FISCHER, K., KLEIN, F., ADDO, M. M., EICHHORST, B., HALLEK, M. & LANGERBEINS, P. 2022b. SARS-CoV-2 specific cellular response following COVID-19 vaccination in patients with chronic lymphocytic leukemia. *Leukemia*, 36, 562-565.
- MEMISH, Z. A., PERLMAN, S., VAN KERKHOVE, M. D. & ZUMLA, A. 2020. Middle East respiratory syndrome. *Lancet*, 395, 1063-1077.
- MEO, S. A., ALHOWIKAN, A. M., AL-KHLAIWI, T., MEO, I. M., HALEPOTO, D. M., IQBAL, M., USMANI, A. M., HAJJAR, W. & AHMED, N. 2020. Novel coronavirus 2019-nCoV: prevalence, biological and clinical characteristics comparison with SARS-CoV and MERS-CoV. *Eur Rev Med Pharmacol Sci*, 24, 2012-2019.
- MERLE, N. S., CHURCH, S. E., FREMEAUX-BACCHI, V. & ROUMENINA, L. T. 2015a. Complement System Part I - Molecular Mechanisms of Activation and Regulation. *Front Immunol*, 6.
- MERLE, N. S., NOE, R., HALBWACHS-MECARELLI, L., FREMEAUX-BACCHI, V. & ROUMENINA, L. T. 2015b. Complement System Part II: Role in Immunity. *Front Immunol*, 6.
- METTELMAN, R. C., ALLEN, E. K. & THOMAS, P. G. 2022. Mucosal immune responses to infection and vaccination in the respiratory tract. *Immunity*, 55, 749-780.
- MEYER, M., GUNN, B. M., MALHERBE, D. C., GANGAVARAPU, K., YOSHIDA, A., PIETZSCH, C., KUZMINA, N. A., SAPHIRE, E. O., COLLINS, P. L., CROWE, J. E., JR., ZHU, J. J., SUCHARD, M. A., BRINING, D.

- L., MIRE, C. E., CROSS, R. W., GEISBERT, J. B., SAMAL, S. K., ANDERSEN, K. G., ALTER, G., GEISBERT, T. W. & BUKREYEV, A. 2021. Ebola vaccine-induced protection in nonhuman primates correlates with antibody specificity and Fc-mediated effects. *Sci Transl Med*, 13.
- MEYER ZU NATRUP, C., TSCHERNE, A., DAHLKE, C., CIURKIEWICZ, M., SHIN, D. L., FATHI, A., ROHDE, C., KALODIMOU, G., HALWE, S., LIMPINSEL, L., SCHWARZ, J. H., KLUG, M., ESEN, M., SCHNEIDERHAN-MARRA, N., DULOVIC, A., KUPKE, A., BROSINSKI, K., CLEVER, S., SCHÜNEMANN, L. M., BEYTHIEN, G., ARMANDO, F., MAYER, L., WESKAMM, L. M., JANY, S., FREUDENSTEIN, A., TUCHEL, T., BAUMGÄRTNER, W., KREMSNER, P., FENDEL, R., ADDO, M. M., BECKER, S., SUTTER, G. & VOLZ, A. 2022. Stabilized recombinant SARS-CoV-2 spike antigen enhances vaccine immunogenicity and protective capacity. *J Clin Invest*.
- MINASSIAN, A. M., ROWLAND, R., BEVERIDGE, N. E. R., POULTON, I. D., SATTI, I., HARRIS, S., POYNTZ, H., HAMILL, M., GRIFFITHS, K., SANDER, C. R., AMBROZAK, D. R., PRICE, D. A., HILL, B. J., CASAZZA, J. P., DOUEK, D. C., KOUP, R. A., ROEDERER, M., WINSTON, A., ROSS, J., SHERRARD, J., ROONEY, G., WILLIAMS, N., LAWRIE, A. M., FLETCHER, H. A., PATHAN, A. A. & MCSHANE, H. 2011. A Phase I study evaluating the safety and immunogenicity of MVA85A, a candidate TB vaccine, in HIV-infected adults. *BMJ Open*, 1, e000223.
- MODJARRAD, K., ROBERTS, C. C., MILLS, K. T., CASTELLANO, A. R., PAOLINO, K., MUTHUMANI, K., REUSCHEL, E. L., ROBB, M. L., RACINE, T., OH, M. D., LAMARRE, C., ZAIDI, F. I., BOYER, J., KUDCHODKAR, S. B., JEONG, M., DARDEN, J. M., PARK, Y. K., SCOTT, P. T., REMIGIO, C., PARIKH, A. P., WISE, M. C., PATEL, A., DUPERRET, E. K., KIM, K. Y., CHOI, H., WHITE, S., BAGARAZZI, M., MAY, J. M., KANE, D., LEE, H., KOBINGER, G., MICHAEL, N. L., WEINER, D. B., THOMAS, S. J. & MASLOW, J. N. 2019. Safety and immunogenicity of an anti-Middle East respiratory syndrome coronavirus DNA vaccine: a phase 1, open-label, single-arm, dose-escalation trial. *Lancet Infect Dis*, 19, 1013-1022.
- MOKHORT, H., KOVALCHUK, A., SOKOLOVSKA, O. & HIGGS, S. 2018. Contribution of Vaccination to the Reduction of Infectious Mortality in Ukraine in the Second Half of the 20(th) and Early 21(st) Century: A Comparative Population-Based Study of the Dynamics and Structure of Infectious Mortality and Incidence. *Viral Immunol*, 31, 695-707.
- MOLDOVEANU, Z., CLEMENTS, M. L., PRINCE, S. J., MURPHY, B. R. & MESTECKY, J. 1995. Human immune responses to influenza virus vaccines administered by systemic or mucosal routes. *Vaccine*, 13, 1006-1012.
- MOLINO, D., DURIER, C., RADENNE, A., DESAINT, C., ROPERS, J., COURCIER, S., VIEILLARD, L. V., REKACEWICZ, C., PARFAIT, B., APPAY, V., BATTEUX, F., BARILLOT, E., COGNÉ, M., COMBADIÈRE, B., EBERHARDT, C. S., GOROCHOV, G., HUPÉ, P., NINOVE, L., PAUL, S., PELLEGRIN, I., VAN DER WERF, S., LEFEBVRE, M., BOTELHO-NEVERS, E., ORTEGA-PEREZ, I., JASPARD, M., SOW, S., LELIÈVRE, J. D., DE LAMBALLERIE, X., KIENY, M. P., TARTOUR, E. & LAUNAY, O. 2022. A comparison of Sars-Cov-2 vaccine platforms: the CoviCompare project. *Nature Medicine*, 28, 882-884.
- MONTEIRO, R. C. & VAN DE WINKEL, J. G. 2001. IgA Fc receptors. *Annu Rev Immunol*.
- MORELL, A., TERRY, W. D. & WALDMANN, T. A. 1970. Metabolic properties of IgG subclasses in man. *The Journal of Clinical Investigation*, 49, 673-680.
- MORENS, D. M. & FAUCI, A. S. 2013. Emerging Infectious Diseases: Threats to Human Health and Global Stability. *PLOS Pathogens*, 9, e1003467.
- MORENS, D. M. & FAUCI, A. S. 2020. Emerging Pandemic Diseases: How We Got to COVID-19. *Cell*, 182, 1077-1092.
- MORGAN, D. & TERGAONKAR, V. 2022. Unraveling B cell trajectories at single cell resolution. *Trends in Immunology*, 43, 210-229.
- MORIYAMA, S., ADACHI, Y., SATO, T., TONOUCHE, K., SUN, L., FUKUSHI, S., YAMADA, S., KINOSHITA, H., NOJIMA, K., KANNO, T., TOBIUME, M., ISHIJIMA, K., KURODA, Y., PARK, E. S., ONODERA, T., MATSUMURA, T., TAKANO, T., TERAHARA, K., ISOGAWA, M., NISHIYAMA, A., KAWANA-TACHIKAWA, A., SHINKAI, M., TACHIKAWA, N., NAKAMURA, S., OKAI, T., OKUMA, K., MATANO, T., FUJIMOTO, T., MAEDA, K., OHNISHI, M., WAKITA, T., SUZUKI, T. & TAKAHASHI, Y. 2021. Temporal maturation of neutralizing antibodies in COVID-19 convalescent individuals

- improves potency and breadth to circulating SARS-CoV-2 variants. *Immunity*, 54, 1841-1852.e4.
- MORRISON, B. J., ROMAN, J. A., LUKE, T. C., NAGABHUSHANA, N., RAVIPRAKASH, K., WILLIAMS, M. & SUN, P. 2017. Antibody-dependent NK cell degranulation as a marker for assessing antibody-dependent cytotoxicity against pandemic 2009 influenza A(H1N1) infection in human plasma and influenza-vaccinated transchromosomal bovine intravenous immunoglobulin therapy. *J Virol Methods*, 248, 7-18.
- MUNRO, A. P. S., JANANI, L., CORNELIUS, V., ALEY, P. K., BABBAGE, G., BAXTER, D., BULA, M., CATHIE, K., CHATTERJEE, K., DODD, K., ENEVER, Y., GOKANI, K., GOODMAN, A. L., GREEN, C. A., HARND AHL, L., HAUGHNEY, J., HICKS, A., VAN DER KLA AUW, A. A., KWOK, J., LAMBE, T., LIBRI, V., LLEWELYN, M. J., MCGREGOR, A. C., MINASSIAN, A. M., MOORE, P., MUGHAL, M., MUJADIDI, Y. F., MURIRA, J., OSANLOU, O., OSANLOU, R., OWENS, D. R., PACURAR, M., PALFREEMAN, A., PAN, D., RAMPLING, T., REGAN, K., SAICH, S., SALKELD, J., SARALAYA, D., SHARMA, S., SHERIDAN, R., STURDY, A., THOMSON, E. C., TODD, S., TWELVES, C., READ, R. C., CHARLTON, S., HALLIS, B., RAMSAY, M., ANDREWS, N., NGUYEN-VAN-TAM, J. S., SNAPE, M. D., LIU, X., FAUST, S. N., RIORDAN, A., USTIANOWSKI, A., ROGERS, C. A., HUGHES, S., LONGSHAW, L., STOCKPORT, J., HUGHES, R., GRUNDY, L., TUDOR JONES, L., GUHA, A., SNASHALL, E., EADSFORTH, T., REEDER, S., STORTON, K., MUNUSAMY, M., TANDY, B., EGBO, A., COX, S., AHMED, N. N., SHENOY, A., BOUSFIELD, R., WIXTED, D., GUTTERIDGE, H., MANSFIELD, B., HERBERT, C., HOLLIDAY, K., CALDERWOOD, J., BARKER, D., BRANDON, J., TULLOCH, H., COLQUHOUN, S., THORP, H., RADFORD, H., EVANS, J., BAKER, H., THORPE, J., BATHAM, S., HAILSTONE, J., PHILLIPS, R., KUMAR, D., WESTWELL, F., MAKIA, F., HOPKINS, N., BARCELLA, L., MPELEMBUE, M., DABAGH, M., et al. 2021. Safety and immunogenicity of seven COVID-19 vaccines as a third dose (booster) following two doses of ChAdOx1 nCov-19 or BNT162b2 in the UK (COV-BOOST): a blinded, multicentre, randomised, controlled, phase 2 trial. *The Lancet*, 398, 2258-2276.
- MURPHY, K. 2012. *Janeway's Immunobiology, 8th Edition*.
- MUTUA, G., ANZALA, O., LUHN, K., ROBINSON, C., BOCKSTAL, V., ANUMENDEM, D. & DOUGUIH, M. 2019. Safety and Immunogenicity of a 2-Dose Heterologous Vaccine Regimen With Ad26.ZEBOV and MVA-BN-Filo Ebola Vaccines: 12-Month Data From a Phase 1 Randomized Clinical Trial in Nairobi, Kenya. *The Journal of Infectious Diseases*, 220, 57-67.
- NACHBAGAUER, R., FESER, J., NAFICY, A., BERNSTEIN, D. I., GUPTILL, J., WALTER, E. B., BERLANDA-SCORZA, F., STADLBAUER, D., WILSON, P. C., AYDILLO, T., BEHZADI, M. A., BHAVSAR, D., BLISS, C., CAPUANO, C., CARREÑO, J. M., CHROMIKOVA, V., CLAEYS, C., COUGHLAN, L., FREYN, A. W., GAST, C., JAVIER, A., JIANG, K., MARIOTTINI, C., MCMAHON, M., MCNEAL, M., SOLÓRZANO, A., STROHMEIER, S., SUN, W., VAN DER WIELEN, M., INNIS, B. L., GARCÍA-SASTRE, A., PALESE, P. & KRAMMER, F. 2021. A chimeric hemagglutinin-based universal influenza virus vaccine approach induces broad and long-lasting immunity in a randomized, placebo-controlled phase I trial. *Nat Med*, 27, 106-114.
- NAGASAWA, T. 2006. Microenvironmental niches in the bone marrow required for B-cell development. *Nature Reviews Immunology*, 6, 107-116.
- NAKAYA, H. I., HAGAN, T., DURAISINGHAM, S. S., LEE, E. K., KWISSA, M., ROUPHAEL, N., FRASCA, D., GERSTEN, M., MEHTA, A. K., GAUJOUX, R., LI, G. M., GUPTA, S., AHMED, R., MULLIGAN, M. J., SHEN-ORR, S., BLOMBERG, B. B., SUBRAMANIAM, S. & PULENDRAN, B. 2015. Systems Analysis of Immunity to Influenza Vaccination across Multiple Years and in Diverse Populations Reveals Shared Molecular Signatures. *Immunity*, 43, 1186-98.
- NAKAYA, H. I., WRAMMERT, J., LEE, E. K., RACIOPPI, L., MARIE-KUNZE, S., HAINING, W. N., MEANS, A. R., KASTURI, S. P., KHAN, N., LI, G. M., MCCAUSLAND, M., KANCHAN, V., KOKKO, K. E., LI, S., ELBEIN, R., MEHTA, A. K., ADEREM, A., SUBBARAO, K., AHMED, R. & PULENDRAN, B. 2011. Systems biology of vaccination for seasonal influenza in humans. *Nat Immunol*, 12, 786-95.
- NAQVI, A. A. T., FATIMA, K., MOHAMMAD, T., FATIMA, U., SINGH, I. K., SINGH, A., ATIF, S. M., HARIPRASAD, G., HASAN, G. M. & HASSAN, M. I. 2020. Insights into SARS-CoV-2 genome,

- structure, evolution, pathogenesis and therapies: Structural genomics approach. *Biochim Biophys Acta Mol Basis Dis*, 1866, 165878.
- NDIAYE, B. P., THIENEMANN, F., OTA, M., LANDRY, B. S., CAMARA, M., DIÈYE, S., DIEYE, T. N., ESMAIL, H., GOLIATH, R., HUYGEN, K., JANUARY, V., NDIAYE, I., ONI, T., RAINE, M., ROMANO, M., SATTI, I., SUTTON, S., THIAM, A., WILKINSON, K. A., MBOUP, S., WILKINSON, R. J. & MCSHANE, H. 2015. Safety, immunogenicity, and efficacy of the candidate tuberculosis vaccine MVA85A in healthy adults infected with HIV-1: a randomised, placebo-controlled, phase 2 trial. *The Lancet Respiratory Medicine*, 3, 190-200.
- NG, K. W., FAULKNER, N., FINSTERBUSCH, K., WU, M., HARVEY, R., HUSSAIN, S., GRECO, M., LIU, Y., KJAER, S., SWANTON, C., GANDHI, S., BEALE, R., GAMBLIN, S. J., CHEREPANOV, P., MCCAULEY, J., DANIELS, R., HOWELL, M., ARASE, H., WACK, A., BAUER, D. L. V. & KASSIOTIS, G. 2022. SARS-CoV-2 S2-targeted vaccination elicits broadly neutralizing antibodies. *Sci Transl Med*, 14, eabn3715.
- NGUIPDOP-DJOMO, THOMAS & FINE 2013. Correlates of vaccine-induced protection: methods and implications. *WHO/IVB*, 181, 1-55.
- NGUYEN-CONTANT, P., EMBONG, A. K., KANAGAIH, P., CHAVES FRANCISCO, A., YANG, H., BRANCHE ANGELA, R., TOPHAM DAVID, J. & SANGSTER MARK, Y. 2020. S Protein-Reactive IgG and Memory B Cell Production after Human SARS-CoV-2 Infection Includes Broad Reactivity to the S2 Subunit. *mBio*, 11, e01991-20.
- NGUYEN, A. V. & SOULIKA, A. M. 2019. The Dynamics of the Skin's Immune System. *Int J Mol Sci*, 20.
- NIC LOCHLAINN, L., GIER, B., MAAS, N., ROTS, N., BINNENDIJK, R., MELKER, H. & HAHNÉ, S. 2015. *Measles vaccination below 9 months of age: Systematic literature review and meta-analyses of effects and safety*.
- NIMMERJAHN, F. & RAVETCH, J. V. 2008. Fcγ receptors as regulators of immune responses. *Nat Rev Immunol*, 8, 34-47.
- NISHIO, A., HASAN, S., PARK, H., PARK, N., SALAS, J. H., SALINAS, E., KARDAVA, L., JUNEAU, P., FRUMENTO, N., MASSACCESI, G., MOIR, S., BAILEY, J. R., GRAKOU, A., GHANY, M. G. & REHERMANN, B. 2022. Serum neutralization activity declines but memory B cells persist after cure of chronic hepatitis C. *Nature Communications*, 13, 5446.
- NOHO-KONTEH, F., ADETIFA, J., COX, M., FORSTER, T., DRAMMEH, A., NJIE-JOBE, J., JEFFRIES, D., PLEBANSKI, M., GHAZAL, P., DICKINSON, P., WHITTLE, H., ROWLAND-JONES, S., SUTHERLAND, J. & FLANAGAN, K. 2014. Sex differences in immune responses to vaccines. *International Journal of Infectious Diseases*, 21, 65.
- OBUKHANYCH, T. V. & NUSSENZWEIG, M. C. 2006. T-independent type II immune responses generate memory B cells. *J Exp Med*, 203, 305-10.
- ODENDAHL, M., MEI, H., HOYER, B. F., JACOBI, A. M., HANSEN, A., MUEHLINGHAUS, G., BEREK, C., HIEPE, F., MANZ, R., RADBRUCH, A. & DÖRNER, T. 2005. Generation of migratory antigen-specific plasma blasts and mobilization of resident plasma cells in a secondary immune response. *Blood*, 105, 1614-1621.
- OKBA, N. M. A., MÜLLER, M. A., LI, W., WANG, C., GEURTSVANKESSEL, C. H., CORMAN, V. M., LAMERS, M. M., SIKKEMA, R. S., DE BRUIN, E., CHANDLER, F. D., YAZDANPANA, Y., LE HINGRAT, Q., DESCAMPS, D., HOUHOU-FIDOUH, N., REUSKEN, C., BOSCH, B. J., DROSTEN, C., KOOPMANS, M. P. G. & HAAGMANS, B. L. 2020. Severe Acute Respiratory Syndrome Coronavirus 2-Specific Antibody Responses in Coronavirus Disease Patients. *Emerg Infect Dis*, 26, 1478-1488.
- ORLOVA, O. V., GLAZKOVA, D. V., BOGOSLOVSKAYA, E. V., SHIPULIN, G. A. & YUDIN, S. M. 2022. Development of Modified Vaccinia Virus Ankara-Based Vaccines: Advantages and Applications. *Vaccines (Basel)*, 10.
- OU, X., LIU, Y., LEI, X., LI, P., MI, D., REN, L., GUO, L., GUO, R., CHEN, T., HU, J., XIANG, Z., MU, Z., CHEN, X., CHEN, J., HU, K., JIN, Q., WANG, J. & QIAN, Z. 2020. Characterization of spike glycoprotein of SARS-CoV-2 on virus entry and its immune cross-reactivity with SARS-CoV. *Nat Commun*, 11, 1620.
- OVERTON, E. T., STAPLETON, J., FRANK, I., HASSLER, S., GOEPFERT, P. A., BARKER, D., WAGNER, E., VON KREMPELHUBER, A., VIRGIN, G., MEYER, T. P., MÜLLER, J., BÄDEKER, N., GRÜNERT, R., YOUNG,

- P., RÖSCH, S., MACLENNAN, J., ARNDTZ-WIEDEMANN, N. & CHAPLIN, P. 2015. Safety and Immunogenicity of Modified Vaccinia Ankara-Bavarian Nordic Smallpox Vaccine in Vaccinia-Naive and Experienced Human Immunodeficiency Virus-Infected Individuals: An Open-Label, Controlled Clinical Phase II Trial. *Open Forum Infect Dis*, 2, ofv040.
- OZHAROVSKAIA, T. A., ZUBKOVA, O. V., DOLZHIKOVA, I. V., GROMOVA, A. S., GROUSOVA, D. M., TUKHVATULIN, A. I., POPOVA, O., SHCHEBLYAKOV, D. V., SCHERBININ, D. N., DZHARULLAEVA, A. S., EROKHOVA, A. S., SHMAROV, M. M., LOGINOVA, S. Y., BORISEVICH, S. V., NARODITSKY, B. S., LOGUNOV, D. Y. & GINTSBURG, A. L. 2019. Immunogenicity of Different Forms of Middle East Respiratory Syndrome S Glycoprotein. *Acta Naturae*, 11, 38-47.
- PALGEN, J. L., TCHITCHEK, N., RODRIGUEZ-POZO, A., JOUHAULT, Q., ABDELHOUAHAB, H., DEREUDDRE-BOSQUET, N., CONTRERAS, V., MARTINON, F., COSMA, A., LEVY, Y., LE GRAND, R. & BEIGNON, A. S. 2020. Innate and secondary humoral responses are improved by increasing the time between MVA vaccine immunizations. *NPJ Vaccines*, 5, 24.
- PALLESEN, J., WANG, N., CORBETT, K. S., WRAPP, D., KIRCHDOERFER, R. N., TURNER, H. L., COTTRELL, C. A., BECKER, M. M., WANG, L., SHI, W., KONG, W. P., ANDRES, E. L., KETTENBACH, A. N., DENISON, M. R., CHAPPELL, J. D., GRAHAM, B. S., WARD, A. B. & MCLELLAN, J. S. 2017. Immunogenicity and structures of a rationally designed prefusion MERS-CoV spike antigen. *Proc Natl Acad Sci U S A*, 114, E7348-e7357.
- PALM, A. E. & HENRY, C. 2019. Remembrance of Things Past: Long-Term B Cell Memory After Infection and Vaccination. *Front Immunol*, 10.
- PARDI, N., HOGAN, M. J., PORTER, F. W. & WEISSMAN, D. 2018. mRNA vaccines — a new era in vaccinology. *Nature Reviews Drug Discovery*, 17, 261-279.
- PASCHOLD, L., KLEE, B., GOTTSCHICK, C., WILLSCHER, E., DIEXER, S., SCHULTHEIß, C., SIMNICA, D., SEDDING, D., GIRNDT, M., GEKLE, M., MIKOLAJCZYK, R. & BINDER, M. 2022. Rapid Hypermutation B Cell Trajectory Recruits Previously Primed B Cells Upon Third SARS-Cov-2 mRNA Vaccination. *Front Immunol*, 13, 876306.
- PEIRIS, J. S. 2003. Severe Acute Respiratory Syndrome (SARS). *J Clin Virol*, 28, 245-7.
- PHAN, T. G., GRAY EE FAU - CYSTER, J. G. & CYSTER, J. G. 2009. The microanatomy of B cell activation. *Curr Opin Immunol*.
- PICCOLI, L., PARK, Y. J., TORTORICI, M. A., CZUDNOCHOWSKI, N., WALLS, A. C., BELTRAMELLO, M., SILACCI-FREGNI, C., PINTO, D., ROSEN, L. E., BOWEN, J. E., ACTON, O. J., JACONI, S., GUARINO, B., MINOLA, A., ZATTA, F., SPRUGASCI, N., BASSI, J., PETER, A., DE MARCO, A., NIX, J. C., MELE, F., JOVIC, S., RODRIGUEZ, B. F., GUPTA, S. V., JIN, F., PIUMATTI, G., LO PRESTI, G., PELLANDA, A. F., BIGGIOGERO, M., TARKOWSKI, M., PIZZUTO, M. S., CAMERONI, E., HAVENAR-DAUGHTON, C., SMITHEY, M., HONG, D., LEPORI, V., ALBANESE, E., CESCHI, A., BERNASCONI, E., ELZI, L., FERRARI, P., GARZONI, C., RIVA, A., SNELL, G., SALLUSTO, F., FINK, K., VIRGIN, H. W., LANZAVECCHIA, A., CORTI, D. & VEESLER, D. 2020. Mapping Neutralizing and Immunodominant Sites on the SARS-CoV-2 Spike Receptor-Binding Domain by Structure-Guided High-Resolution Serology. *Cell*, 183, 1024-1042.e21.
- PIECHOTTA, V., MELLINGHOFF, S. C., HIRSCH, C., BRINKMANN, A., IANNIZZI, C., KREUZBERGER, N., ADAMS, A., MONSEF, I., STEMLER, J., CORNELY, O. A., BRÖCKELMANN, P. J. & SKOETZ, N. 2022. Effectiveness, immunogenicity, and safety of COVID-19 vaccines for individuals with hematological malignancies: a systematic review. *Blood Cancer J*, 12, 86.
- PINCETIC, A., BOURNAZOS, S., DILILLO, D. J., MAAMARY, J., WANG, T. T., DAHAN, R., FIEBIGER, B. M. & RAVETCH, J. V. 2014. Type I and type II Fc receptors regulate innate and adaptive immunity. *Nat Immunol*, 15, 707-16.
- PITISUTTITHUM, P., NITAYAPHAN, S., CHARİYALERTSAK, S., KAEWKUNGWAL, J., DAWSON, P., DHITAVAT, J., PHONRAT, B., AKAPIRAT, S., KARASAVVAS, N., WIECZOREK, L., POLONIS, V., ELLER, M. A., PEGU, P., KIM, D., SCHUETZ, A., JONGRAKTHAITAE, S., ZHOU, Y., SINANGIL, F., PHOGAT, S., DIAZGRANADOS, C. A., TARTAGLIA, J., HEGER, E., SMITH, K., MICHAEL, N. L., EXCLER, J. L., ROBB, M. L., KIM, J. H., O'CONNELL, R. J., VASAN, S. & GROUP, R. V. S. 2020. Late boosting of the RV144 regimen with AIDS-VAX B/E and ALVAC-HIV in HIV-uninfected Thai volunteers: a double-blind, randomised controlled trial. *Lancet HIV*, 7, e238-e248.

- PLANAS, D., VEYER, D., BAIDALIUK, A., STAROPOLI, I., GUIVEL-BENHASSINE, F., RAJAH, M. M., PLANCHAIS, C., PORROT, F., ROBILLARD, N., PUECH, J., PROT, M., GALLAIS, F., GANTNER, P., VELAY, A., LE GUEN, J., KASSIS-CHIKHANI, N., EDRISS, D., BELEC, L., SEVE, A., COURTELLEMONT, L., PÉRE, H., HOCQUELOUX, L., FAFI-KREMER, S., PRAZUCK, T., MOUQUET, H., BRUEL, T., SIMON-LORIÈRE, E., REY, F. A. & SCHWARTZ, O. 2021. Reduced sensitivity of SARS-CoV-2 variant Delta to antibody neutralization. *Nature*, 596, 276-280.
- PLOTKIN, S. A. 2001. Immunologic correlates of protection induced by vaccination. *Pediatr Infect Dis J*.
- PLOTKIN, S. A. 2008. Vaccines: correlates of vaccine-induced immunity. *Clin Infect Dis*.
- PLOTKIN, S. A. 2010. Correlates of protection induced by vaccination. *Clin Vaccine Immunol*.
- PLOTKIN, S. A. 2017. Vaccines for epidemic infections and the role of CEPI. *Hum Vaccin Immunother*.
- PLOTKIN, S. A. & GILBERT, P. B. 2012. Nomenclature for Immune Correlates of Protection After Vaccination. *Clinical Infectious Diseases*, 54, 1615-1617.
- PLOTKIN, S. A., MAHMOUD AA FAU - FARRAR, J. & FARRAR, J. 2015. Establishing a Global Vaccine-Development Fund. *N Engl J Med*.
- POLLARD, A. J. & BIJKER, E. M. 2021. A guide to vaccinology: from basic principles to new developments. *Nature Reviews Immunology*, 21, 83-100.
- POTTER, C. W. 2001. A history of influenza. *J Appl Microbiol*, 91, 572-9.
- POZZETTO, B., LEGROS, V., DJEBALI, S., BARATEAU, V., GUIBERT, N., VILLARD, M., PEYROT, L., ALLATIF, O., FASSIER, J.-B., MASSARDIER-PILONCHÉRY, A., BRENGEL-PESCE, K., YAUGEL-NOVOA, M., DENOLLY, S., BOSON, B., BOURLET, T., BAL, A., VALETTE, M., ANDRIEU, T., LINA, B., SAKER, K., COMPAGNON, C., MOKDAD, B., D'AUBAREDE, C., PITIOT, V., ESCURET, V., MORFIN, F., TRABAUD, M.-A., PRIEUX, M., DUBOIS, V., JOSSET, L., DANIEL, S., COSSET, F.-L., PAUL, S., DEFRANCE, T., MARVEL, J., WALZER, T., TROUILLET-ASSANT, S. & COVID-SER STUDY, G. 2021. Immunogenicity and efficacy of heterologous ChAdOx1–BNT162b2 vaccination. *Nature*, 600, 701-706.
- PRABAKARAN, M., LEYRER, S., HE, F., AUER, S., KUMAR, S. R., KINDSMUELLER, K., MYTLE, N., SCHNEIDER, J., LOCKHART, S. & KWANG, J. 2014. Progress toward a universal H5N1 vaccine: a recombinant modified vaccinia virus Ankara-expressing trivalent hemagglutinin vaccine. *PLoS One*, 9, e107316.
- PRICE, P. J., TORRES-DOMÍNGUEZ, L. E., BRANDMÜLLER, C., SUTTER, G. & LEHMANN, M. H. 2013. Modified Vaccinia virus Ankara: innate immune activation and induction of cellular signalling. *Vaccine*, 31, 4231-4.
- PULENDRAN, B. & AHMED, R. 2011. Immunological mechanisms of vaccination. *Nat Immunol*, 12, 509-17.
- PULENDRAN, B., LI, S. & NAKAYA, H. I. 2010. Systems vaccinology. *Immunity*, 33, 516-29.
- PULENDRAN, B., OH, J. Z., NAKAYA, H. I., RAVINDRAN, R. & KAZMIN, D. A. 2013. Immunity to viruses: learning from successful human vaccines. *Immunol Rev*, 255, 243-55.
- PURTHA, W. E., TEDDER TF FAU - JOHNSON, S., JOHNSON S FAU - BHATTACHARYA, D., BHATTACHARYA D FAU - DIAMOND, M. S. & DIAMOND, M. S. 2011. Memory B cells, but not long-lived plasma cells, possess antigen specificities for viral escape mutants. *J Exp Med*.
- QIN, L., GILBERT, P. B., COREY, L., MCEL RATH, M. J. & SELF, S. G. 2007. A framework for assessing immunological correlates of protection in vaccine trials. *J Infect Dis*, 196, 1304-12.
- QUARESMA JUAREZ ANTONIO, S. 2019. Organization of the Skin Immune System and Compartmentalized Immune Responses in Infectious Diseases. *Clinical Microbiology Reviews*, 32, e00034-18.
- QUEREC, T. D., AKONDY, R. S., LEE, E. K., CAO, W., NAKAYA, H. I., TEUWEN, D., PIRANI, A., GERNERT, K., DENG, J., MARZOLF, B., KENNEDY, K., WU, H., BENNOUNA, S., OLUOCH, H., MILLER, J., VENCIO, R. Z., MULLIGAN, M., ADEREM, A., AHMED, R. & PULENDRAN, B. 2009. Systems biology approach predicts immunogenicity of the yellow fever vaccine in humans. *Nat Immunol*, 10, 116-125.

- RABAAN, A. A., AL-AHMED, S. H., HAQUE, S., SAH, R., TIWARI, R., MALIK, Y. S., DHAMA, K., YATOO, M. I., BONILLA-ALDANA, D. K. & RODRIGUEZ-MORALES, A. J. 2020. SARS-CoV-2, SARS-CoV, and MERS-COV: A comparative overview. *Infez Med*, 28, 174-184.
- RABAAN, A. A., AL-AHMED, S. H., SAH, R., ALQUMBER, M. A., HAQUE, S., PATEL, S. K., PATHAK, M., TIWARI, R., YATOO, M. I., HAQ, A. U., BILAL, M., DHAMA, K. & RODRIGUEZ-MORALES, A. J. 2021. MERS-CoV: epidemiology, molecular dynamics, therapeutics, and future challenges. *Annals of Clinical Microbiology and Antimicrobials*, 20, 8.
- RADBRUCH, A., MUEHLINGHAUS, G., LUGER, E. O., INAMINE, A., SMITH, K. G., DÖRNER, T. & HIEPE, F. 2006. Competence and competition: the challenge of becoming a long-lived plasma cell. *Nat Rev Immunol*, 6, 741-50.
- RAJ, V. S., MOU, H., SMITS, S. L., DEKKERS, D. H., MÜLLER, M. A., DIJKMAN, R., MUTH, D., DEMMERS, J. A., ZAKI, A., FOUCHIER, R. A., THIEL, V., DROSTEN, C., ROTTIER, P. J., OSTERHAUS, A. D., BOSCH, B. J. & HAAGMANS, B. L. 2013. Dipeptidyl peptidase 4 is a functional receptor for the emerging human coronavirus-EMC. *Nature*, 495, 251-4.
- RAMEZANPOUR, B., HAAN, I., OSTERHAUS, A. & CLAASSEN, E. 2016. Vector-based genetically modified vaccines: Exploiting Jenner's legacy. *Vaccine*, 34, 6436-6448.
- RAUCH, S., JASNY, E., SCHMIDT, K. E. & PETSCH, B. 2018. New Vaccine Technologies to Combat Outbreak Situations. *Frontiers in Immunology*, 9.
- RAVANDI, F. & O'BRIEN, S. 2006. Immune defects in patients with chronic lymphocytic leukemia. *Cancer Immunol Immunother*, 55, 197-209.
- REIF, K., EKLAND EH FAU - OHL, L., OHL L FAU - NAKANO, H., NAKANO H FAU - LIPP, M., LIPP M FAU - FÖRSTER, R., FÖRSTER R FAU - CYSTER, J. G. & CYSTER, J. G. 2002. Balanced responsiveness to chemoattractants from adjacent zones determines B-cell position. *Nature*.
- REUSCH, D. & TEJADA, M. L. 2015. Fc glycans of therapeutic antibodies as critical quality attributes. *Glycobiology*.
- ROLLIER, C. S., REYES-SANDOVAL, A., COTTINGHAM, M. G., EWER, K. & HILL, A. V. 2011. Viral vectors as vaccine platforms: deployment in sight. *Curr Opin Immunol*, 23, 377-82.
- ROOZBEH, J., MOINI, M., LANKARANI, K. B., SAGHEB, M. M., SHAHPOORI, S. & BASTANI, B. 2005. Low dose intradermal versus high dose intramuscular hepatitis B vaccination in patients on chronic hemodialysis. *Asaio j*, 51, 242-5.
- ROSENBAUM, P., TCHITCHEK, N., JOLY, C., POZO, A., STIMMER, L., LANGLOIS, S., HOCINI, H., GOSSE, L., PEJOSKI, D., COSMA, A., BEIGNON, A.-S., DEREUDDRE-BOSQUET, N., LEVY, Y., GRAND, R. & MARTINON, F. 2020. Vaccine Inoculation Route Modulates Early Immunity and Consequently Antigen-Specific Immune Response. *SSRN Electronic Journal*.
- RØTTINGEN, J.-A., GOUGLAS, D., FEINBERG, M., PLOTKIN, S., RAGHAVAN, K. V., WITTY, A., DRAGHIA-AKLI, R., STOFFELS, P. & PIOT, P. 2017. New Vaccines against Epidemic Infectious Diseases. *New England Journal of Medicine*, 376, 610-613.
- ROUSH, S. W. & MURPHY, T. V. 2007. Historical comparisons of morbidity and mortality for vaccine-preventable diseases in the United States. *Jama*, 298, 2155-63.
- ROUTHU, N. K., CHEEDARLA, N., GANGADHARA, S., BOLLIMPELLI, V. S., BODDAPATI, A. K., SHIFERAW, A., RAHMAN, S. A., SAHOO, A., EDARA, V. V., LAI, L., FLOYD, K., WANG, S., FISCHINGER, S., ATYEO, C., SHIN, S. A., GUMBER, S., KIREJCZYK, S., COHEN, J., JEAN, S. M., WOOD, J. S., CONNOR-STROUD, F., STAMMEN, R. L., UPADHYAY, A. A., PELLEGRINI, K., MONTEFIORI, D., SHI, P. Y., MENACHERY, V. D., ALTER, G., VANDERFORD, T. H., BOSINGER, S. E., SUTHAR, M. S. & AMARA, R. R. 2021. A modified vaccinia Ankara vector-based vaccine protects macaques from SARS-CoV-2 infection, immune pathology, and dysfunction in the lungs. *Immunity*, 54, 542-556.e9.
- ROUTHU, N. K., GANGADHARA, S., LAI, L., DAVIS-GARDNER, M. E., FLOYD, K., SHIFERAW, A., BARTSCH, Y. C., FISCHINGER, S., KHOURY, G., RAHMAN, S. A., STAMPFER, S. D., SCHÄFER, A., JEAN, S. M., WALLACE, C., STAMMEN, R. L., WOOD, J., JOYCE, C., NAGY, T., PARSONS, M. S., GRALINSKI, L., KOZŁOWSKI, P. A., ALTER, G., SUTHAR, M. S. & AMARA, R. R. 2022. A modified vaccinia Ankara vaccine expressing spike and nucleocapsid protects rhesus macaques against SARS-CoV-2 Delta infection. *Sci Immunol*, 7, eabo0226.

- RUSSELL, M. W. 2007. Biological Functions of IgA. *Mucosal Immunology*.
- RUSSELL, M. W., MOLDOVEANU, Z., OGRA, P. L. & MESTECKY, J. 2020. Mucosal Immunity in COVID-19: A Neglected but Critical Aspect of SARS-CoV-2 Infection. *Front Immunol*, 11, 611337.
- RÜTHRICH, M. M., GIESEN, N., MELLINGHOFF, S. C., RIEGER, C. T. & VON LILIENFELD-TOAL, M. 2022. Cellular Immune Response after Vaccination in Patients with Cancer-Review on Past and Present Experiences. *Vaccines (Basel)*, 10.
- SALLARD, E., HALLOY, J., CASANE, D., DECROLY, E. & VAN HELDEN, J. 2021. Tracing the origins of SARS-CoV-2 in coronavirus phylogenies: a review. *Environmental Chemistry Letters*, 19, 769-785.
- SALLEH, M. Z., DERRICK, J. P. & DERIS, Z. Z. 2021. Structural Evaluation of the Spike Glycoprotein Variants on SARS-CoV-2 Transmission and Immune Evasion. *Int J Mol Sci*, 22.
- SALLUSTO, F., LANZAVECCHIA A FAU - ARAKI, K., ARAKI K FAU - AHMED, R. & AHMED, R. 2010. From vaccines to memory and back. *Immunity*.
- SAMARASEKERA, U. 2021. CEPI prepares for future pandemics and epidemics. *Lancet Infect Dis*, 21, 608.
- SANDS, P., MUNDACA-SHAH, C. & DZAU, V. J. 2016. The Neglected Dimension of Global Security — A Framework for Countering Infectious-Disease Crises. *New England Journal of Medicine*, 374, 1281-1287.
- SANO, K., BHAVSAR, D., SINGH, G., FLODA, D., SRIVASTAVA, K., GLEASON, C., AMOAKO, A. A., ANDRE, D., BEACH, K. F., BERMÚDEZ-GONZÁLEZ, M. C., CAI, G., COGNIGNI, C., KAWABATA, H., KLEINER, G., LYTTLE, N., MENDEZ, W., MULDER, L. C. F., OOSTENINK, A., RASKIN, A., ROOKER, A., RUSSO, K. T., SALIMBANGON, A. B. T., SAKSENA, M., SOMINSKY, L. A., TCHEOU, J., WAJNBERG, A., CARREÑO, J. M., SIMON, V., KRAMMER, F. & GROUP, P. S. 2022. SARS-CoV-2 vaccination induces mucosal antibody responses in previously infected individuals. *Nature Communications*, 13, 5135.
- SANZ, I., WEI, C., JENKS, S. A., CASHMAN, K. S., TIPTON, C., WOODRUFF, M. C., HOM, J. & LEE, F. E. 2019. Challenges and Opportunities for Consistent Classification of Human B Cell and Plasma Cell Populations. *Front Immunol*, 10.
- SASAKI, S., HE, X. S., HOLMES, T. H., DEKKER, C. L., KEMBLE, G. W., ARVIN, A. M. & GREENBERG, H. B. 2008. Influence of prior influenza vaccination on antibody and B-cell responses. *PLoS One*, 3, e2975.
- SASSO, E., D'ALISE, A. M., ZAMBRANO, N., SCARSELLI, E., FOLGORI, A. & NICOSIA, A. 2020. New viral vectors for infectious diseases and cancer. *Semin Immunol*, 50, 101430.
- SAXENA, M., VAN, T. T. H., BAIRD, F. J., COLOE, P. J. & SMOOKER, P. M. 2013. Pre-existing immunity against vaccine vectors--friend or foe? *Microbiology (Reading)*, 159, 1-11.
- SCHMIDT, T., KLEMIS, V., SCHUB, D., MIHM, J., HIELSCHER, F., MARX, S., ABU-OMAR, A., ZIEGLER, L., GUCKELMUS, C., URSCHEL, R., SCHNEITLER, S., BECKER, S. L., GÄRTNER, B. C., SESTER, U. & SESTER, M. 2021a. Immunogenicity and reactogenicity of heterologous ChAdOx1 nCoV-19/mRNA vaccination. *Nat Med*, 27, 1530-1535.
- SCHMIDT, T., KLEMIS, V., SCHUB, D., SCHNEITLER, S., REICHERT, M. C., WILKENS, H., SESTER, U., SESTER, M. & MIHM, J. 2021b. Cellular immunity predominates over humoral immunity after homologous and heterologous mRNA and vector-based COVID-19 vaccine regimens in solid organ transplant recipients. *Am J Transplant*, 21, 3990-4002.
- SCHROEDER, H. W., JR. & CAVACINI, L. 2013. Structure and function of immunoglobulins. *J Allergy Clin Immunol*.
- SCRIBA, T. J., TAMERIS, M., MANSOOR, N., SMIT, E., VAN DER MERWE, L., ISAACS, F., KEYSER, A., MOYO, S., BRITAIN, N., LAWRIE, A., GELDERBLOEM, S., VELDSMAN, A., HATHERILL, M., HAWKRIDGE, A., HILL, A. V. S., HUSSEY, G. D., MAHOMED, H., MCSHANE, H. & HANEKOM, W. A. 2010. Modified vaccinia Ankara-expressing Ag85A, a novel tuberculosis vaccine, is safe in adolescents and children, and induces polyfunctional CD4+ T cells. *European Journal of Immunology*, 40, 279-290.
- SETTE, A. & CROTTY, S. 2021. Adaptive immunity to SARS-CoV-2 and COVID-19. *Cell*, 184, 861-880.

- SHARMA, A., AHMAD FAROUK, I. A.-O. X. & LAL, S. A.-O. 2021. COVID-19: A Review on the Novel Coronavirus Disease Evolution, Transmission, Detection, Control and Prevention. LID - 10.3390/v13020202 [doi] LID - 202. *Viruses*.
- SHAW, R. H., LIU, X., STUART, A. S. V., GREENLAND, M., ALEY, P. K., ANDREWS, N. J., CAMERON, J. C., CHARLTON, S., CLUTTERBUCK, E. A., COLLINS, A. M., DEJNIRATTISAI, W., DINESH, T., FAUST, S. N., FERREIRA, D. M., FINN, A., GREEN, C. A., HALLIS, B., HEATH, P. T., HILL, H., LAMBE, T., LAZARUS, R., LIBRI, V., LONG, F., MUJADIDI, Y. F., PLESTED, E. L., MOREY, E. R., PROVSTGAARD-MORYS, S., RAMASAMY, M. N., RAMSAY, M., READ, R. C., ROBINSON, H., SCREATON, G. R., SINGH, N., TURNER, D. P. J., TURNER, P. J., VICHOS, I., WALKER, L. L., WHITE, R., NGUYEN-VANTAM, J. S., SNAPE, M. D., MUNRO, A. P. S., BARTHOLOMEW, J., PRESLAND, L., HORSWILL, S., WARREN, S., VARKONYI-CLIFFORD, S., SAICH, S., ADAMS, K., RICAMARA, M., TURNER, N., YEE TING, N. Y., WHITTLEY, S., RAMPLING, T., DESAI, A., BROWN, C. H., QURESHI, E., GOKANI, K., NAKER, K., KELLETT WRIGHT, J. K., WILLIAMS, R. L., RIAZ, T., PENCIU, F. D., CARSON, A., DI MASO, C., MEAD, G., HOWE, E. G., VICHOS, I., GHULAM FAROOQ, M., NORISTANI, R., YAO, X. L., OLDFIELD, N. J., HAMMERSLEY, D., BELTON, S., ROYAL, S., SAN FRANCISCO RAMOS, A., HULTIN, C., GALIZA, E. P., CROOK, R., BULA, M., FYLES, F., BURHAN, H., MAELIN, F., HUGHES, E. & OKENYI, E. 2022. Effect of priming interval on reactogenicity, peak immunological response, and waning after homologous and heterologous COVID-19 vaccine schedules: exploratory analyses of Com-COV, a randomised control trial. *The Lancet Respiratory Medicine*, 10, 1049-1060.
- SIEGRIST, C.-A. 2018. 2 - Vaccine Immunology. In: PLOTKIN, S. A., ORENSTEIN, W. A., OFFIT, P. A. & EDWARDS, K. M. (eds.) *Plotkin's Vaccines (Seventh Edition)*. Elsevier.
- SIEGRIST, C. A. 2001. Neonatal and early life vaccinology. *Vaccine*, 19, 3331-46.
- SIEGRIST, C. A. 2007. The challenges of vaccine responses in early life: selected examples. *J Comp Pathol*, 137 Suppl 1, S4-9.
- SIEGRIST, C. A. & ASPINALL, R. 2009. B-cell responses to vaccination at the extremes of age. *Nat Rev Immunol*, 9, 185-94.
- SLÜTTER, B., PEWE, L. L., KAECH, S. M. & HARTY, J. T. 2013. Lung airway-surveilling CXCR3(hi) memory CD8(+) T cells are critical for protection against influenza A virus. *Immunity*, 39, 939-48.
- SMITH, G. L. & MOSS, B. 1983. Infectious poxvirus vectors have capacity for at least 25 000 base pairs of foreign DNA. *Gene*, 25, 21-8.
- SON, Y. M., CHEON, I. S., WU, Y., LI, C., WANG, Z., GAO, X., CHEN, Y., TAKAHASHI, Y., FU, Y. X., DENT, A. L., KAPLAN, M. H., TAYLOR, J. J., CUI, W. & SUN, J. 2021. Tissue-resident CD4(+) T helper cells assist the development of protective respiratory B and CD8(+) T cell memory responses. *Sci Immunol*, 6.
- SONG, F., FUX, R., PROVACIA, L. B., VOLZ, A., EICKMANN, M., BECKER, S., OSTERHAUS, A. D., HAAGMANS, B. L. & SUTTER, G. 2013. Middle East respiratory syndrome coronavirus spike protein delivered by modified vaccinia virus Ankara efficiently induces virus-neutralizing antibodies. *J Virol*, 87, 11950-4.
- STARR, T. N., GREANEY, A. J., HILTON, S. K., ELLIS, D., CRAWFORD, K. H. D., DINGENS, A. S., NAVARRO, M. J., BOWEN, J. E., TORTORICI, M. A., WALLS, A. C., KING, N. P., VEESLER, D. & BLOOM, J. D. 2020. Deep Mutational Scanning of SARS-CoV-2 Receptor Binding Domain Reveals Constraints on Folding and ACE2 Binding. *Cell*, 182, 1295-1310.e20.
- STEEL, J., LOWEN, A. C., WANG, T. T., YONDOLA, M., GAO, Q., HAYE, K., GARCÍA-SASTRE, A. & PALESE, P. 2010. Influenza virus vaccine based on the conserved hemagglutinin stalk domain. *mBio*, 1.
- STEFFEN, T. L., STONE, E. T., HASSERT, M., GEERLING, E., GRIMBERG, B. T., ESPINO, A. M., PANTOJA, P., CLIMENT, C., HOFT, D. F., GEORGE, S. L., SARIOL, C. A., PINTO, A. K. & BRIEN, J. D. 2020. The receptor binding domain of SARS-CoV-2 spike is the key target of neutralizing antibody in human polyclonal sera. *bioRxiv*, 2020.08.21.261727.
- STICKL, H., HOCHSTEIN-MINTZEL, V., MAYR, A., HUBER, H. C., SCHÄFER, H. & HOLZNER, A. 1974. [MVA vaccination against smallpox: clinical tests with an attenuated live vaccinia virus strain (MVA) (author's transl)]. *Dtsch Med Wochenschr*, 99, 2386-92.

- STIKO 2022a. Beschluss der STIKO für die Empfehlung zur Impfung gegen Affenpocken mit Imvanex (MVA-Impfstoff)
- STIKO. 2022b. *Empfehlungen der Ständigen Impfkommission beim Robert Koch-Institut 2022* [Online]. Available: [https://www.rki.de/DE/Content/Infekt/EpidBull/Archiv/2022/Ausgaben/04_22.pdf? blob=publicationFile](https://www.rki.de/DE/Content/Infekt/EpidBull/Archiv/2022/Ausgaben/04_22.pdf?blob=publicationFile) [Accessed 22.12.2022].
- STROHL, W. R., KU, Z., AN, Z., CARROLL, S. F., KEYT, B. A. & STROHL, L. M. 2022. Passive Immunotherapy Against SARS-CoV-2: From Plasma-Based Therapy to Single Potent Antibodies in the Race to Stay Ahead of the Variants. *BioDrugs*, 36, 231-323.
- STRUGNELL, R. A. & WIJBURG, O. L. C. 2010. The role of secretory antibodies in infection immunity. *Nature Reviews Microbiology*, 8, 656-667.
- SUAN, D., NGUYEN, A., MORAN, I., BOURNE, K., HERMES, J. R., ARSHI, M., HAMPTON, H. R., TOMURA, M., MIWA, Y., KELLEHER, A. D., KAPLAN, W., DEENICK, E. K., TANGYE, S. G., BRINK, R., CHTANOVA, T. & PHAN, T. G. 2015. T follicular helper cells have distinct modes of migration and molecular signatures in naive and memory immune responses. *Immunity*.
- SUN, X., YI, C., ZHU, Y., DING, L., XIA, S., CHEN, X., LIU, M., GU, C., LU, X., FU, Y., CHEN, S., ZHANG, T., ZHANG, Y., YANG, Z., MA, L., GU, W., HU, G., DU, S., YAN, R., FU, W., YUAN, S., QIU, C., ZHAO, C., ZHANG, X., HE, Y., QU, A., ZHOU, X., LI, X., WONG, G., DENG, Q., ZHOU, Q., LU, H., LING, Z., DING, J., LU, L., XU, J., XIE, Y. & SUN, B. 2022. Neutralization mechanism of a human antibody with pan-coronavirus reactivity including SARS-CoV-2. *Nat Microbiol*, 7, 1063-1074.
- SUTTER, G. & STAIB, C. 2003. Vaccinia vectors as candidate vaccines: the development of modified vaccinia virus Ankara for antigen delivery. *Curr Drug Targets Infect Disord*, 3, 263-71.
- SWARNALEKHA, N., SCHREINER, D., LITZLER, L. C., IFTIKHAR, S., KIRCHMEIER, D., KÜNZLI, M., SON, Y. M., SUN, J., MOREIRA, E. A. & KING, C. G. 2021. T resident helper cells promote humoral responses in the lung. *Sci Immunol*, 6.
- SZABÓ, G. T., MAHINY, A. J. & VLATKOVIC, I. 2022. COVID-19 mRNA vaccines: Platforms and current developments. *Molecular Therapy*, 30, 1850-1868.
- TAI, W., ZHANG, X., YANG, Y., ZHU, J. & DU, L. 2022. Advances in mRNA and other vaccines against MERS-CoV. *Translational Research*, 242, 20-37.
- TAMERIS, M. D., HATHERILL, M., LANDRY, B. S., SCRIBA, T. J., SNOWDEN, M. A., LOCKHART, S., SHEA, J. E., MCCLAIN, J. B., HUSSEY, G. D., HANEKOM, W. A., MAHOMED, H. & MCSHANE, H. 2013. Safety and efficacy of MVA85A, a new tuberculosis vaccine, in infants previously vaccinated with BCG: a randomised, placebo-controlled phase 2b trial. *Lancet*, 381, 1021-8.
- TANGYE, S. & MACKAY, F. 2006. CHAPTER 11 - B Cells and Autoimmunity. In: ROSE, N. R. & MACKAY, I. R. (eds.) *The Autoimmune Diseases (Fourth Edition)*. St. Louis: Academic Press.
- TARKOWSKI, M., DE JAGER, W., SCHIUMA, M., COVIZZI, A., LAI, A., GABRIELI, A., CORBELLINO, M., BERGNA, A., VENTURA, C. D., GALLI, M., RIVA, A. & ANTINORI, S. 2021. Anti-SARS-CoV-2 Immunoglobulin Isotypes, and Neutralization Activity Against Viral Variants, According to BNT162b2-Vaccination and Infection History. *Front Immunol*, 12, 793191.
- TAY, M. Z., WIEHE, K. & POLLARA, J. 2019. Antibody-Dependent Cellular Phagocytosis in Antiviral Immune Responses. *Front Immunol*.
- TAYLOR, J. J., PAPE KA FAU - JENKINS, M. K. & JENKINS, M. K. 2012. A germinal center-independent pathway generates unswitched memory B cells early in the primary response. *J Exp Med*.
- TONG, P., GAUTAM, A., WINDSOR, I., TRAVERS, M., CHEN, Y., GARCIA, N., WHITEMAN, N. B., MCKAY, L. G. A., LELIS, F. J. N., HABIBI, S., CAI, Y., RENNICK, L. J., DUPREX, W. P., MCCARTHY, K. R., LAVINE, C. L., ZUO, T., LIN, J., ZUIANI, A., FELDMAN, J., MACDONALD, E. A., HAUSER, B. M., GRIFFITHS, A., SEAMAN, M. S., SCHMIDT, A. G., CHEN, B., NEUBERG, D., BAJIC, G., HARRISON, S. C. & WESEMANN, D. R. 2021. Memory B cell repertoire for recognition of evolving SARS-CoV-2 spike. *bioRxiv*.
- TORRES, M. & CASADEVALL, A. 2008. The immunoglobulin constant region contributes to affinity and specificity. *Trends Immunol.*, 29, 91-97.
- TRAPANI, J. A. & SMYTH, M. J. 2002. Functional significance of the perforin/granzyme cell death pathway. *Nat Rev Immunol*.

- TRAVIESO, T., LI, J., MAHESH, S., MELLO, J. D. F. R. E. & BLASI, M. 2022. The use of viral vectors in vaccine development. *npj Vaccines*, 7, 75.
- TROVATO, M., SARTORIUS, R., D'APICE, L., MANCO, R. & DE BERARDINIS, P. 2020. Viral Emerging Diseases: Challenges in Developing Vaccination Strategies. *Front Immunol*, 11, 2130.
- TSCHERNE, A., SCHWARZ, J. H., ROHDE, C., KUPKE, A., KALODIMOU, G., LIMPINSEL, L., OKBA, N. M. A., BOŠNJAK, B., SANDROCK, I., ODAK, I., HALWE, S., SAUERHERING, L., BROSINSKI, K., LIANGLIANG, N., DUELL, E., JANY, S., FREUDENSTEIN, A., SCHMIDT, J., WERNER, A., GELLHORN SERRA, M., KLÜVER, M., GUGGEMOS, W., SEILMAIER, M., WENDTNER, C. M., FÖRSTER, R., HAAGMANS, B. L., BECKER, S., SUTTER, G. & VOLZ, A. 2021. Immunogenicity and efficacy of the COVID-19 candidate vector vaccine MVA-SARS-2-S in preclinical vaccination. *Proc Natl Acad Sci U S A*, 118.
- TUAILLON, E., TABAA, Y. A., PETITJEAN, G., HUGUET, M.-F., PAJEAUX, G., FONDERE, J.-M., PONSEILLE, B., DUCOS, J., BLANC, P. & VENDRELL, J. P. 2006. Detection of memory B lymphocytes specific to hepatitis B virus (HBV) surface antigen (HBsAg) from HBsAg-vaccinated or HBV-immunized subjects by ELISPOT assay. *Journal of Immunological Methods*, 315, 144-152.
- TURNER, J. S., O'HALLORAN, J. A., KALADINA, E., KIM, W., SCHMITZ, A. J., ZHOU, J. Q., LEI, T., THAPA, M., CHEN, R. E., CASE, J. B., AMANAT, F., RAUSEO, A. M., HAILE, A., XIE, X., KLEBERT, M. K., SUESSEN, T., MIDDLETON, W. D., SHI, P. Y., KRAMMER, F., TEEFEY, S. A., DIAMOND, M. S., PRESTI, R. M. & ELLEBEDY, A. H. 2021. SARS-CoV-2 mRNA vaccines induce persistent human germinal centre responses. *Nature*, 596, 109-113.
- TURVEY, S. E. & BROIDE, D. H. 2010. Innate immunity.
- UN. 2015. *Resolution adopted by the General Assembly on 25 September 2015* [Online]. Available: https://www.un.org/en/development/desa/population/migration/generalassembly/docs/globalcompact/A_RES_70_1_E.pdf [Accessed 20.12.2022].
- URA, T., OKUDA, K. & SHIMADA, M. 2014. Developments in Viral Vector-Based Vaccines. *Vaccines (Basel)*, 2, 624-41.
- URA, T., TAKEUCHI, M., KAWAGOE, T., MIZUKI, N., OKUDA, K. & SHIMADA, M. 2022. Current Vaccine Platforms in Enhancing T-Cell Response. *Vaccines* [Online], 10.
- URA, T., YAMASHITA, A., MIZUKI, N., OKUDA, K. & SHIMADA, M. 2021. New vaccine production platforms used in developing SARS-CoV-2 vaccine candidates. *Vaccine*, 39, 197-201.
- VAN EGMOND, M., VIDARSSON, G. & BAKEMA, J. E. 2015. Cross-talk between pathogen recognizing Toll-like receptors and immunoglobulin Fc receptors in immunity. *Immunol Rev*.
- VAN LINT, S., RENMANS, D., BROOS, K., DEWITTE, H., LENTACKER, I., HEIRMAN, C., BRECKPOT, K. & THIELEMANS, K. 2015. The ReNAissanCe of mRNA-based cancer therapy. *Expert Rev Vaccines*, 14, 235-51.
- VÁZQUEZ-RAMÍREZ, D., JORDAN, I., SANDIG, V., GENZEL, Y. & REICHL, U. 2019. High titer MVA and influenza A virus production using a hybrid fed-batch/perfusion strategy with an ATF system. *Appl Microbiol Biotechnol*, 103, 3025-3035.
- VENKATRAMAN, N., NDIAYE, B. P., BOWYER, G., WADE, D., SRIDHAR, S., WRIGHT, D., POWLSON, J., NDIAYE, I., DIÈYE, S., THOMPSON, C., BAKHOUM, M., MORTER, R., CAPONE, S., DEL SORBO, M., JAMIESON, S., RAMPLING, T., DATOO, M., ROBERTS, R., POULTON, I., GRIFFITHS, O., BALLOU, W. R., ROMAN, F., LEWIS, D. J. M., LAWRIE, A., IMOUKHUEDE, E., GILBERT, S. C., DIEYE, T. N., EWER, K. J., MBOUP, S. & HILL, A. V. S. 2019. Safety and Immunogenicity of a Heterologous Prime-Boost Ebola Virus Vaccine Regimen in Healthy Adults in the United Kingdom and Senegal. *J Infect Dis*, 219, 1187-1197.
- VIDARSSON, G., DEKKERS, G. & RISPENS, T. 2014. IgG subclasses and allotypes: from structure to effector functions. *Front Immunol*.
- VIRGIN, H. W., WHERRY, E. J. & AHMED, R. 2009. Redefining chronic viral infection. *Cell*, 138, 30-50.
- VIVIER, E., RAULET DH FAU - MORETTA, A., MORETTA A FAU - CALIGIURI, M. A., CALIGIURI MA FAU - ZITVOGEL, L., ZITVOGEL L FAU - LANIER, L. L., LANIER LL FAU - YOKOYAMA, W. M., YOKOYAMA WM FAU - UGOLINI, S. & UGOLINI, S. 2011. Innate or adaptive immunity? The example of natural killer cells. *Science*.

- VOLKMANN, A., WILLIAMSON, A. L., WEIDENTHALER, H., MEYER, T. P. H., ROBERTSON, J. S., EXCLER, J. L., CONDIT, R. C., EVANS, E., SMITH, E. R., KIM, D. & CHEN, R. T. 2021. The Brighton Collaboration standardized template for collection of key information for risk/benefit assessment of a Modified Vaccinia Ankara (MVA) vaccine platform. *Vaccine*, 39, 3067-3080.
- VOLZ, A., KUPKE, A., SONG, F., JANY, S., FUX, R., SHAMS-ELDIN, H., SCHMIDT, J., BECKER, C., EICKMANN, M., BECKER, S. & SUTTER, G. 2015. Protective Efficacy of Recombinant Modified Vaccinia Virus Ankara Delivering Middle East Respiratory Syndrome Coronavirus Spike Glycoprotein. *J Virol*, 89, 8651-6.
- VOLZ, A. & SUTTER, G. 2017. Modified Vaccinia Virus Ankara: History, Value in Basic Research, and Current Perspectives for Vaccine Development. *Adv Virus Res*, 97, 187-243.
- VON HOLLE, T. A. & MOODY, M. A. 2019. Influenza and Antibody-Dependent Cellular Cytotoxicity. *Front Immunol*.
- VONO, M., HUTTNER, A., LEMEILLE, S., MARTINEZ-MURILLO, P., MEYER, B., BAGGIO, S., SHARMA, S., THIRIARD, A., MARCHANT, A., GODEKE, G. J., REUSKEN, C., ALVAREZ, C., PEREZ-RODRIGUEZ, F., ECKERLE, I., KAISER, L., LOEVY, N., EBERHARDT, C. S., BLANCHARD-ROHNER, G., SIEGRIST, C. A. & DIDIERLAURENT, A. M. 2021. Robust innate responses to SARS-CoV-2 in children resolve faster than in adults without compromising adaptive immunity. *Cell Rep*, 37, 109773.
- VOYSEY, M., COSTA CLEMENS, S. A., MADHI, S. A., WECKX, L. Y., FOLEGATTI, P. M., ALEY, P. K., ANGUS, B., BAILLIE, V. L., BARNABAS, S. L., BHORAT, Q. E., BIBI, S., BRINER, C., CICONI, P., CLUTTERBUCK, E. A., COLLINS, A. M., CUTLAND, C. L., DARTON, T. C., DHEDA, K., DOLD, C., DUNCAN, C. J. A., EMARY, K. R. W., EWER, K. J., FLAXMAN, A., FAIRLIE, L., FAUST, S. N., FENG, S., FERREIRA, D. M., FINN, A., GALIZA, E., GOODMAN, A. L., GREEN, C. M., GREEN, C. A., GREENLAND, M., HILL, C., HILL, H. C., HIRSCH, I., IZU, A., JENKIN, D., JOE, C. C. D., KERRIDGE, S., KOEN, A., KWATRA, G., LAZARUS, R., LIBRI, V., LILLIE, P. J., MARCHEVSKY, N. G., MARSHALL, R. P., MENDES, A. V. A., MILAN, E. P., MINASSIAN, A. M., MCGREGOR, A., MUJADIDI, Y. F., NANA, A., PADAYACHEE, S. D., PHILLIPS, D. J., PITTELLA, A., PLESTED, E., POLLOCK, K. M., RAMASAMY, M. N., RITCHIE, A. J., ROBINSON, H., SCHWARZBOLD, A. V., SMITH, A., SONG, R., SNAPE, M. D., SPRINZ, E., SUTHERLAND, R. K., THOMSON, E. C., TOROK, M. E., TOSNER, M., TURNER, D. P. J., VEKEMANS, J., VILLAFANA, T. L., WHITE, T., WILLIAMS, C. J., DOUGLAS, A. D., HILL, A. V. S., LAMBE, T., GILBERT, S. C., POLLARD, A. J. & OXFORD, C. V. T. G. 2021. Single-dose administration and the influence of the timing of the booster dose on immunogenicity and efficacy of ChAdOx1 nCoV-19 (AZD1222) vaccine: a pooled analysis of four randomised trials. *Lancet*, 397, 881-891.
- VOYSEY, M., KELLY, D. F., FANSHAW, T. R., SADARANGANI, M., O'BRIEN, K. L., PERERA, R. & POLLARD, A. J. 2017. The Influence of Maternally Derived Antibody and Infant Age at Vaccination on Infant Vaccine Responses : An Individual Participant Meta-analysis. *JAMA Pediatr*, 171, 637-646.
- VOYSEY, M. & POLLARD, A. J. 2021. ChAdOx1 nCoV-19 vaccine: asymptomatic efficacy estimates - Authors' reply. *Lancet*, 397, 2248.
- VUOLA, J. M., KEATING, S., WEBSTER, D. P., BERTHOUD, T., DUNACHIE, S., GILBERT, S. C. & HILL, A. V. 2005. Differential immunogenicity of various heterologous prime-boost vaccine regimens using DNA and viral vectors in healthy volunteers. *J Immunol*, 174, 449-55.
- WALSH, E. E., FRENCK, R. W., JR., FALSEY, A. R., KITCHIN, N., ABSALON, J., GURTMAN, A., LOCKHART, S., NEUZIL, K., MULLIGAN, M. J., BAILEY, R., SWANSON, K. A., LI, P., KOURY, K., KALINA, W., COOPER, D., FONTES-GARFIAS, C., SHI, P. Y., TÜRECI, Ö., TOMPKINS, K. R., LYKE, K. E., RAABE, V., DORMITZER, P. R., JANSEN, K. U., ŞAHIN, U. & GRUBER, W. C. 2020. Safety and Immunogenicity of Two RNA-Based Covid-19 Vaccine Candidates. *N Engl J Med*, 383, 2439-2450.
- WALSH, S. R., SEAMAN, M. S., GRANDPRE, L. E., CHARBONNEAU, C., YANOSICK, K. E., METCH, B., KEEFER, M. C., DOLIN, R. & BADEN, L. R. 2012. Impact of anti-orthopoxvirus neutralizing antibodies induced by a heterologous prime-boost HIV-1 vaccine on insert-specific immune responses. *Vaccine*, 31, 114-9.

- WALSH, S. R., WILCK, M. B., DOMINGUEZ, D. J., ZABLOWSKY, E., BAJIMAYA, S., GAGNE, L. S., VERRILL, K. A., KLEINJAN, J. A., PATEL, A., ZHANG, Y., HILL, H., ACHARYYA, A., FISHER, D. C., ANTIN, J. H., SEAMAN, M. S., DOLIN, R. & BADEN, L. R. 2013. Safety and immunogenicity of modified vaccinia Ankara in hematopoietic stem cell transplant recipients: a randomized, controlled trial. *J Infect Dis*, 207, 1888-97.
- WALTARI, E., MCGEEVER, A., FRIEDLAND, N., KIM, P. S. & MCCUTCHEON, K. M. 2019. Functional Enrichment and Analysis of Antigen-Specific Memory B Cell Antibody Repertoires in PBMCs. *Front Immunol*, 10, 1452.
- WAN, Z., ZHOU, Z., LIU, Y., LAI, Y., LUO, Y., PENG, X. & ZOU, W. 2020. Regulatory T cells and T helper 17 cells in viral infection. *Scand J Immunol*, 91, e12873.
- WANG, C., HORBY, P. W., HAYDEN, F. G. & GAO, G. F. 2020. A novel coronavirus outbreak of global health concern. *The Lancet*, 395, 470-473.
- WANG, C., VAN HAPEREN, R., GUTIÉRREZ-ÁLVAREZ, J., LI, W., OKBA, N. M. A., ALBULESCU, I., WIDJAJA, I., VAN DIEREN, B., FERNANDEZ-DELGADO, R., SOLA, I., HURDISS, D. L., DARAMOLA, O., GROSVELD, F., VAN KUPPEVELD, F. J. M., HAAGMANS, B. L., ENJUANES, L., DRABEK, D. & BOSCH, B.-J. 2021. A conserved immunogenic and vulnerable site on the coronavirus spike protein delineated by cross-reactive monoclonal antibodies. *Nature Communications*, 12, 1715.
- WANG, N., SHI, X., JIANG, L., ZHANG, S., WANG, D., TONG, P., GUO, D., FU, L., CUI, Y., LIU, X., ARLEDGE, K. C., CHEN, Y.-H., ZHANG, L. & WANG, X. 2013. Structure of MERS-CoV spike receptor-binding domain complexed with human receptor DPP4. *Cell Research*, 23, 986-993.
- WANG, S., LIU, H., ZHANG, X. & QIAN, F. 2015. Intranasal and oral vaccination with protein-based antigens: advantages, challenges and formulation strategies. *Protein Cell*, 6, 480-503.
- WEISBLUM, Y., SCHMIDT, F., ZHANG, F., DASILVA, J., POSTON, D., LORENZI, J. C., MUECKSCH, F., RUTKOWSKA, M., HOFFMANN, H. H., MICHAILIDIS, E., GAEBLER, C., AGUDELO, M., CHO, A., WANG, Z., GAZUMYAN, A., CIPOLLA, M., LUCHSINGER, L., HILLYER, C. D., CASKEY, M., ROBBIANI, D. F., RICE, C. M., NUSSENZWEIG, M. C., HATZIOANNOU, T. & BIENIASZ, P. D. 2020. Escape from neutralizing antibodies by SARS-CoV-2 spike protein variants. *Elife*, 9.
- WESKAMM, L. M., DAHLKE, C. & ADDO, M. M. 2022a. Flow cytometric protocol to characterize human memory B cells directed against SARS-CoV-2 spike protein antigens. *STAR Protoc*, 3.
- WESKAMM, L. M., FATHI, A., RAADSEN, M. P., MYKYTYN, A. Z., KOCH, T., SPOHN, M., FRIEDRICH, M., HAAGMANS, B. L., BECKER, S., SUTTER, G., DAHLKE, C. & ADDO, M. M. 2022b. Persistence of MERS-CoV-spike-specific B cells and antibodies after late third immunization with the MVA-MERS-S vaccine. *Cell Rep Med*, 3(7).
- WEST, D. J. & CALANDRA, G. B. 1996. Vaccine induced immunologic memory for hepatitis B surface antigen: implications for policy on booster vaccination. *Vaccine*, 14, 1019-27.
- WHERRY, E. J., HA, S. J., KAECH, S. M., HAINING, W. N., SARKAR, S., KALIA, V., SUBRAMANIAM, S., BLATTMAN, J. N., BARBER, D. L. & AHMED, R. 2007. Molecular signature of CD8+ T cell exhaustion during chronic viral infection. *Immunity*, 27, 670-84.
- WHITE, H. N. 2021. B-Cell Memory Responses to Variant Viral Antigens. *Viruses*, 13.
- WHO 2016. AN R&D BLUEPRINT FOR ACTION TO PREVENT EPIDEMICS.
- WHO. 2020a. *COVID 19: Public Health Emergency of International Concern (PHEIC)* [Online]. [Accessed 19.12.2022].
- WHO. 2020b. *Immunization Agenda 2030: A Global Strategy to Leave No One Behind* [Online]. Available: <https://www.who.int/teams/immunization-vaccines-and-biologicals/strategies/ia-2030#:~:text=Immunization%20is%20playing%20a%20critical,driver%20toward%20universal%20health%20coverage> [Accessed 20.12.2022].
- WHO. 2020c. *WHO Director-General's Opening Remarks at the Media Briefing on COVID-19–11 March 2020* [Online]. [Accessed 23.09.2022].
- WHO. 2022a. *Fact Sheet: Middle East respiratory syndrome coronavirus* [Online]. Available: [https://www.who.int/news-room/fact-sheets/detail/middle-east-respiratory-syndrome-coronavirus-\(mers-cov\)](https://www.who.int/news-room/fact-sheets/detail/middle-east-respiratory-syndrome-coronavirus-(mers-cov)) [Accessed 22.12.2022].
- WHO 2022b. Health Topics: Covid-19.

- WHO. 2022c. *MERS Situation Update* [Online]. Available: <http://www.emro.who.int/health-topics/mers-cov/mers-outbreaks.html> [Accessed 15.01.2023].
- WHO. 2022d. *WHO Coronavirus (COVID-19) Dashboard* [Online]. [Accessed 23.09.2022].
- WIECZOREK, M., ABUALROUS, E. T., STICHT, J., ÁLVARO-BENITO, M., STOLZENBERG, S., NOÉ, F. & FREUND, C. 2017. Major Histocompatibility Complex (MHC) Class I and MHC Class II Proteins: Conformational Plasticity in Antigen Presentation.
- WIENDL, H., HOHLFELD, R. & KIESEIER, B. C. 2005. Immunobiology of muscle: advances in understanding an immunological microenvironment. *Trends Immunol*, 26, 373-80.
- WILCK, M. B., SEAMAN, M. S., BADEN, L. R., WALSH, S. R., GRANDPRE, L. E., DEVOY, C., GIRI, A., KLEINJAN, J. A., NOBLE, L. C., STEVENSON, K. E., KIM, H. T. & DOLIN, R. 2010. Safety and immunogenicity of modified vaccinia Ankara (ACAM3000): effect of dose and route of administration. *J Infect Dis*, 201, 1361-70.
- WISHNIE, A. J., CHWAT-EDELSTEIN, T., ATTAWAY, M. & VUONG, B. Q. 2021. BCR Affinity Influences T-B Interactions and B Cell Development in Secondary Lymphoid Organs. *Frontiers in Immunology*, 12.
- WOOF, J. M. & MESTECKY, J. 2005. Mucosal immunoglobulins. *Immunol Rev*.
- WOOLHOUSE, M. E. & GOWTAGE-SEQUERIA, S. 2005. Host range and emerging and reemerging pathogens. *Emerg Infect Dis*, 11, 1842-7.
- WOOLHOUSE, M. E. J., HAYDON, D. T. & ANTIA, R. 2005. Emerging pathogens: the epidemiology and evolution of species jumps. *Trends in Ecology & Evolution*, 20, 238-244.
- XU, S., CARPENTER, M. C., SPRENG, R. L., NEIDICH, S. D., SARKAR, S., TENNEY, D., GOODMAN, D., SAWANT, S., JHA, S., DUNN, B., JULIANA MCEL RATH, M., BEKKER, V., MUDRAK, S. V., FLINKO, R., LEWIS, G. K., FERRARI, G., TOMARAS, G. D., SHEN, X. & ACKERMAN, M. E. 2022. Impact of adjuvants on the biophysical and functional characteristics of HIV vaccine-elicited antibodies in humans. *npj Vaccines*, 7, 90.
- YONG, C. Y., ONG, H. K., YEAP, S. K., HO, K. L. & TAN, W. S. 2019. Recent Advances in the Vaccine Development Against Middle East Respiratory Syndrome-Coronavirus. *Front Microbiol*, 10, 1781.
- YOSHIKAWA, T. 2021. Third-generation smallpox vaccine strain-based recombinant vaccines for viral hemorrhagic fevers. *Vaccine*, 39, 6174-6181.
- YUAN, M., LIU, H., WU, N. C. & WILSON, I. A. 2021. Recognition of the SARS-CoV-2 receptor binding domain by neutralizing antibodies. *Biochem Biophys Res Commun*, 538, 192-203.
- ZAECK, L. M., LAMERS, M. M., VERSTREPEN, B. E., BESTEBROER, T. M., VAN ROYEN, M. E., GÖTZ, H., SHAMIER, M. C., VAN LEEUWEN, L. P. M., SCHMITZ, K. S., ALBLAS, K., VAN EFFEREN, S., BOGERS, S., SCHERBEIJN, S., RIMMELZWAAN, G. F., VAN GORP, E. C. M., KOOPMANS, M. P. G., HAAGMANS, B. L., GEURTSVANKESSEL, C. H. & DE VRIES, R. D. 2022. Low levels of monkeypox virus-neutralizing antibodies after MVA-BN vaccination in healthy individuals. *Nature Medicine*.
- ZAKI, A. M., VAN BOHEEMEN S FAU - BESTEBROER, T. M., BESTEBROER TM FAU - OSTERHAUS, A. D. M. E., OSTERHAUS AD FAU - FOUCHIER, R. A. M. & FOUCHIER, R. A. 2012. Isolation of a novel coronavirus from a man with pneumonia in Saudi Arabia. *N Engl J Med*.
- ZHAND, S., SAGHAEIAN JAZI, M., MOHAMMADI, S., TARIGHATI RASEKHI, R., ROSTAMIAN, G., KALANI, M. R., ROSTAMIAN, A., GEORGE, J. & DOUGLAS, M. W. 2020. COVID-19: The Immune Responses and Clinical Therapy Candidates. *International Journal of Molecular Sciences* [Online], 21.
- ZHANG, A., STACEY, H. D., D'AGOSTINO, M. R., TUGG, Y., MARZOK, A. & MILLER, M. S. 2022a. Beyond neutralization: Fc-dependent antibody effector functions in SARS-CoV-2 infection. *Nature Reviews Immunology*.
- ZHANG, C., MARUGGI, G., SHAN, H. & LI, J. 2019. Advances in mRNA Vaccines for Infectious Diseases. *Front Immunol*, 10, 594.
- ZHANG, N., SHANG, J., LI, C., ZHOU, K. & DU, L. 2020. An overview of Middle East respiratory syndrome coronavirus vaccines in preclinical studies. *Expert Rev Vaccines*, 19, 817-829.

- ZHANG, Z., MATEUS, J., COELHO, C. H., DAN, J. M., MODERBACHER, C. R., GÁLVEZ, R. I., CORTES, F. H., GRIFONI, A., TARKE, A., CHANG, J., ESCARREGA, E. A., KIM, C., GOODWIN, B., BLOOM, N. I., FRAZIER, A., WEISKOPF, D., SETTE, A. & CROTTY, S. 2022b. Humoral and cellular immune memory to four COVID-19 vaccines. *bioRxiv*.
- ZHANG, Z., SHEN, Q. & CHANG, H. 2022c. Vaccines for COVID-19: A Systematic Review of Immunogenicity, Current Development, and Future Prospects. *Front Immunol*, 13, 843928.
- ZHONG, C., LIU, F., HAJNIK, R. J., YAO, L., CHEN, K., WANG, M., LIANG, Y., SUN, J., SOONG, L., HOU, W. & HU, H. 2021. Type I Interferon Promotes Humoral Immunity in Viral Vector Vaccination. *J Virol*, 95, e0092521.
- ZHOU, P., SONG, G., HE, W. T., BEUTLER, N., TSE, L. V., MARTINEZ, D. R., SCHÄFER, A., ANZANELLO, F., YONG, P., PENG, L., DUEKER, K., MUSHARRAFIEH, R., CALLAGHAN, S., CAPOZZOLA, T., YUAN, M., LIU, H., LIMBO, O., PARREN, M., GARCIA, E., RAWLINGS, S. A., SMITH, D. M., NEMAZEE, D., JARDINE, J. G., WILSON, I. A., SAFONOVA, Y., ROGERS, T. F., BARIC, R. S., GRALINSKI, L. E., BURTON, D. R. & ANDRABI, R. 2022. Broadly neutralizing anti-S2 antibodies protect against all three human betacoronaviruses that cause severe disease. *bioRxiv*.
- ZHU, J., MARTINEZ, J., HUANG, X. & YANG, Y. 2007. Innate immunity against vaccinia virus is mediated by TLR2 and requires TLR-independent production of IFN-beta. *Blood*, 109, 619-25.
- ZHU, Z., LIAN, X., SU, X., WU, W., MARRARO, G. A. & ZENG, Y. 2020. From SARS and MERS to COVID-19: a brief summary and comparison of severe acute respiratory infections caused by three highly pathogenic human coronaviruses. *Respiratory Research*, 21, 224.
- ZIEBUHR, J. 2004. Molecular biology of severe acute respiratory syndrome coronavirus. *Curr Opin Microbiol*, 7, 412-9.
- ZIMMERMANN, P. & CURTIS, N. 2019. Factors That Influence the Immune Response to Vaccination. *Clin Microbiol Rev*, 32.
- ZOHAR, T., LOOS, C., FISCHINGER, S., ATYEO, C., WANG, C., SLEIN, M. D., BURKE, J., YU, J., FELDMAN, J., HAUSER, B. M., CARADONNA, T., SCHMIDT, A. G., CAI, Y., STREECK, H., RYAN, E. T., BAROUCH, D. H., CHARLES, R. C., LAUFFENBURGER, D. A. & ALTER, G. 2020. Compromised Humoral Functional Evolution Tracks with SARS-CoV-2 Mortality. *Cell*.
- ZOTOS, D., COQUET JM FAU - ZHANG, Y., ZHANG Y FAU - LIGHT, A., LIGHT A FAU - D'COSTA, K., D'COSTA K FAU - KALLIES, A., KALLIES A FAU - CORCORAN, L. M., CORCORAN LM FAU - GODFREY, D. I., GODFREY DI FAU - TOELLNER, K.-M., TOELLNER KM FAU - SMYTH, M. J., SMYTH MJ FAU - NUTT, S. L., NUTT SL FAU - TARLINTON, D. M. & TARLINTON, D. M. 2010. IL-21 regulates germinal center B cell differentiation and proliferation through a B cell-intrinsic mechanism. *J Exp Med*.

6 Abbreviations

| | |
|----------------|---|
| ACE2 | angiotensin-converting enzyme 2 |
| Ad26 | adenovirus type 26 |
| Ad5 | adenovirus type 5 |
| ADCC | antibody-dependent cellular cytotoxicity |
| ADCD | antibody-dependent complement deposition |
| ADCP | antibody-dependent cellular phagocytosis |
| ADNP | antibody-dependent neutrophil phagocytosis |
| BCR | B cell receptor |
| BNITM | Bernhard Nocht Institute for Tropical Medicine |
| CCR7 | C-C chemokine receptor type 7 |
| CD | cluster of differentiation |
| CD40L | CD40 ligand |
| CEF | chicken embryo fibroblasts |
| CEPI | Coalition for Epidemic Preparedness Innovations |
| CFR | case fatality rate |
| C _H | heavy chain constant region |
| ChAd | chimpanzee adenovirus Y25 |
| C _L | light chain constant region |
| CLL | chronic lymphocytic leukemia |
| CoP | correlate of protection |
| CoV | coronavirus |
| COVID-19 | Coronavirus Disease-2019 |
| CSR | class switch recombination |
| CXCL13 | C-X-C motif ligand 13 |
| CXCR5 | C-X-C chemokine receptor type 5 |
| D0 | day 0 |
| D28 | day 28 |
| DAMP | damage-associated molecular pattern |
| DC | dendritic cell |
| DPP4 | dipeptidyl peptidase 4 |
| E | envelope |
| EMA | European Medicines Agency |
| EVD | Ebola virus disease |
| Fab | fragment antigen binding |
| Fc | fragment crystallizable |
| Fc μ R | Fc receptor for IgM |

| | |
|---------------|--|
| Fc α R | Fc receptor for IgA |
| Fc γ R | Fc receptor for IgG |
| FDA | U.S. Food and Drug Administration |
| FDC | follicular dendritic cell |
| FITC | fluorescein isothiocyanate |
| FP9 | fowlpox virus 9 |
| Gavi | Gavi, the Vaccine Alliance |
| GC | germinal center |
| HC | heavy chain |
| HCoV | human coronavirus |
| HIV | human immunodeficiency virus |
| HSC | hematopoietic stem cell |
| ICOS | inducible T-cell costimulator |
| ID | intra-dermal |
| IFN- γ | interferon γ |
| Ig | immunoglobulin |
| IgA | immunoglobulin A |
| IgD | immunoglobulin D |
| IgE | immunoglobulin E |
| IgG | immunoglobulin G |
| IL | interleukin |
| IM | intramuscular |
| ITAM | immunoreceptor tyrosine-based activation motif |
| ITIM | immunoreceptor tyrosine-based inhibitory motif |
| LC | light chain |
| LLPC | long-lived plasma cells |
| M | membrane |
| M12 | month 12 |
| MALT | mucosa-associated lymphoid tissue |
| MBC | memory B cell |
| MERS | Middle East respiratory syndrome |
| MFI | mean fluorescence intensity |
| MHC | major histocompatibility complex |
| MIP-1 β | macrophage inflammatory protein 1 β |
| MVA | Modified Vaccinia virus Ankara |
| N | nucleocapsid |
| NK cell | natural killer cell |
| nsp | non-structural protein |

| | |
|----------------|---|
| ORF | open reading frame |
| PAMP | pathogen-associated molecular pattern |
| PRR | pattern recognition receptor |
| R&D | research and development |
| RBD | receptor binding domain |
| rMVA | recombinant Modified Vaccinia virus Ankara |
| RSV | <i>Respiratory syncytial virus</i> |
| S | spike |
| S1 | spike protein subunit S1 |
| S2 | spike protein subunit S2 |
| SARS | severe acute respiratory syndrome |
| SC | subcutaneous |
| SDG | Sustainable Development Goal |
| SHM | somatic hypermutation |
| sIgA | secretory IgA |
| SLO | secondary lymphoid organ |
| STIKO | Ständige Impfkommission |
| SV40 | simian virus 40 |
| T1 | transitional state 1 |
| T2 | transitional state 2 |
| TCR | T cell receptor |
| Tfh cell | T follicular helper cell |
| TLR | Toll-like receptor |
| TRM cell | resident memory T cell |
| UKE | University Medical Center Hamburg-Eppendorf |
| UN | United Nations |
| V1 | first vaccination |
| V2 | second vaccination |
| V3 | third vaccination |
| V _H | heavy chain variable region |
| V _L | light chain variable region |
| VSV | vesicular stomatitis virus |
| WHO | World Health Organization |

7 Acknowledgements

I would like to express my gratitude to Prof. Dr. med. Marylyn Addo, for giving me the opportunity to do my doctoral studies at the Institute for Infection Research and Vaccine Development (IIRVD) at the University Medical Center Hamburg-Eppendorf. Besides supervising the project and providing laboratory and scientific infrastructure, she encouraged me to participate in conferences, seminars, and workshops. Without her expertise and her encouragement to pursue my own ideas, the realization of this project would not have been possible. I would also like to especially thank Prof. Dr. Thomas Dobner for supervising and evaluating my doctoral thesis.

I would like to thank Dr. Christine Dahlke for her constant support and mentoring during all stages of my doctoral thesis, including fruitful discussions about ongoing and future experiments and projects, as well as critical revisions of manuscripts and this thesis. I really appreciate that she always made time for me, no matter how many other things were on her agenda. I am also grateful to Dr. med. Anahita Fathi, who initiated the follow-up for the MVA-MERS-S study and was involved in the clinical management and the proposals for ethical approval of all study cohorts, Dr. Svenja Hardtke for coordination of the clinical trials, as well as Dr. med Sibylle Mellinghoff, who initiated the joint projects on the CLL patients and was involved in establishing the control cohorts for the COVID-19 vaccine studies. Additionally, I would like to thank Leonie Mayer for thorough discussions of experiments and data, as well as for the critical revision of my thesis. I really enjoyed the joint work on different projects and the respective manuscripts.

A special thanks also goes to My Linh Ly, Monika Friedrich, and Cordula Grüttner for managing the whole lab, providing technical support for experiments, and substantially contributing to establish all study cohorts. Especially, I would like to thank Monika Friedrich, who supported me beyond laboratory work. I also would like to thank Dr. Maya Kono who contributed to the work on the COVID-19 vaccine cohorts, and Paulina Tarnow who was involved in the analysis of non-neutralizing antibody functions.

I also would like to thank all other members of the IIRVD team who contributed to this work: Alena Sendzik, Claudia Schlesner, Dr. Etienne Bartels, Dr. med. Hanna-Marie Weichel, Maher Almahfoud, Maren Sandkuhl, Monika Rottstegge, PD Dr. med. Robin Kobbe, Ruben Baumann, Stephanie Petereit, Dr. Susanne Ziegler, and Dr. Tamara Zoran. Thanks for contributing to scientific discussions, coordination, laboratory work and documentation of the clinical studies, as well as for the nice working atmosphere, great team events, and non-work-related conversations.

At the Bernhard Nocht Institute for Tropical Medicine, I would like to thank the FACS facility and especially Dr. Johannes Brandi for sharing his expertise on the Cytex Aurora. Additionally, thanks goes to Prof. Dr. Minka Breloer for organizing the weekly immunology seminars, thus providing the opportunity to exchange ideas and discuss projects and data with other research groups.

I would like to thank everyone involved in the pre-clinical and clinical evaluation of the different rMVA-based vaccine candidates, including the German Center for Infection Research, the CTC North and all study participants as well as our collaboration partners at the Ludwig Maximilian University of Munich, the University of Veterinary Medicine Hannover, the Philipps University of Marburg, and the Erasmus Medical Center Rotterdam.

Lastly, I would like to thank my friends and family, especially my parents, for constant support during the whole process of my doctoral studies.